

NITROGEN-CONTAINING HETEROCYCLES: THEIR APPLICATION IN TOTAL
SYNTHESIS OF BIS- AND TRIS-INDOLE NATURAL PRODUCTS AND 20S
PROTEASOME MODULATION

By

Kyra Rose Dvorak

A THESIS

Submitted to
Michigan State University
in partial fulfillment of the requirements
for the degree of

Chemistry – Master of Science

2024

ABSTRACT

Herein, the syntheses of nitrogen-containing heterocycles are applied to the areas of total synthesis and small molecule design for proteasome modulation. Indole alkaloids have been shown to display diverse biological activities. Moreover, it has been reported that the vast majority of biologically active compounds bear one or more nitrogen-containing heterocyclic moieties. Therefore, the synthesis of indole alkaloids bearing nitrogen-containing heterocycles are of particular interest. Progress toward the first total synthesis of Tulongicin and its related natural product analogues is described. Particular emphasis is placed on the exploration and optimization of the key imidazoline cyclization and Friedel-Crafts alkylation steps. In addition, the design and synthesis of small molecule acyl Astemizole analogues containing various *N*-heterocyclic cores is discussed. These acyl Astemizole analogues were explored for their use in proteasome modulation and several active scaffolds were identified.

ACKNOWLEDGEMENTS

First, I would like to thank my advisor Dr. Jetze Tepe. Thank you for supporting me and allowing me to follow my research passions. Additionally, your patience in teaching me, yet allowing me the freedom to explore my own ideas along the way has helped me build my confidence and provided me the tools to become an independent scientist. Thank you for fostering a great lab environment.

I would also like to thank my committee members, Dr. Huang, Dr. Borhan, and Dr. Draths for your guidance, feedback, and willingness to answer all my questions along the way. I would especially like to thank Dr. Draths. I am grateful to have had such a welcoming and encouraging fellow Belle as a mentor.

To my labmates, thank you for providing such a fun, supportive, and encouraging work environment. Grace, Konika, and Dare, thank you for guiding me as I started graduate school and always being there along the way whenever I had questions. Thank you to my co-workers and friends Sophie, Allison, Konika, Dare, Charles, Daniel, Evan, Bahareh, Shannon, Sydney, and Miracle. I truly felt as if I was working with my best friends every day and I couldn't have made it through the tumultuous life of graduate school without you. I especially would like to thank Daniel and Evan. Ever since we found each other during recruitment weekend, we have been through every step of graduate school together and your support, countless discussions, and friendship have meant the world.

I would also like to thank my friend, roommate, and fellow graduate student, Elizabeth. I will always be grateful for our countless chats after long days in lab and weekend brunches at Anna's House.

Lastly, I would like to thank my family. To my parents and my brother, thank you for your endless love and support. I would not be where I am today without you. You all inspire me every day. To my girlfriend, Hannah, thank you for your love and support. Thank you for always being there to celebrate the wins and bounce back from the losses. I could not have made it through the highs and lows of graduate school without you.

TABLE OF CONTENTS

LIST OF ABBREVIATIONS.....	vi
Chapter 1: Recent Advances in the Total Synthesis of Bis- and Tris-Indole Alkaloids Containing <i>N</i> -Heterocyclic Linker Moieties ^{1*}	1
REFERENCES.....	77
Chapter 2: Efforts Toward the Total Synthesis of Tulongicin and Its Related Natural Product Analogues	88
REFERENCES	175
APPENDIX.....	179
Chapter 3: Synthesis of Small Molecule Acyl-Astemizole Analogues as Activators of the 20S Proteasome	216
REFERENCES	268
APPENDIX.....	270
Chapter 4: Conclusions and Future Works.....	296

LIST OF ABBREVIATIONS

AcOH	Acetic acid
AIBN	Azobisisobutyronitrile
Aq	Aqueous
AMC	7-amino-4-methylcoumarin
Ar	Aryl
BBB	Blood brain barrier
BBN	Borabicyclo[3.3.1]nonane
BEMP	1,3,2-Diazaphosphorin-2-amine
Bn	Benzyl
Boc	Tert-butyloxycarbonyl
Bop	Benzotriazole-1-yl-oxy-tris-(dimethylamino)-phosphonium hexafluorophosphate
Bpin	Bis(pinacolato)diboron
Bu	Butyl-
°C	Degrees Celsius
Casp-L	Caspase-like
CD	Circular dichroism
CDI	Carbonyldiimidazole
CT-L	Chymotrypsin-like
dba	Dibenzylideneacetone
DBU	1,8-Diazabicyclo[5.4.0]undec-7-ene
DCC	<i>N,N'</i> -Dicyclohexylcarbodiimide
DCM	Dichloromethane

DDQ	2,3-Dichloro-5,6-dicyano-1,4-benzoquinone
DEAD	Diethyl azodicarboxylate
DIBAL-H	Diisobutylaluminum hydride
DIPEA	<i>N,N</i> -Diisopropylethylamine
DMA	Dimethylacetamide
DMAP	4-Dimethylaminopyridine
DMF	Dimethylformamide
DMP	Dess-Martin periodinane
DMSO	Dimethylsulfoxide
DPPA	Diphenylphosphoryl azide
dppp	1,3-Bis(diphenylphosphino)propane
EC ₂₀₀	200% efficacy concentration
EA	Ethyl acetate
Equiv	Equivalents
Et	Ethyl-
IBX	2-iodoxybenzoic acid
IDP	Intrinsically disordered proteins
IPA	Isopropyl alcohol
iPr	Isopropyl-
LDA	Lithium diisopropylamide
LiHMDS	Lithium bis(trimethylsilyl)amide
mCPBA	m-chlorobenzoic acid
Me	Methyl-

MeCN	Acetonitrile
MP	Melting point
MS	Mass spectrometry
NBS	<i>N</i> -bromosuccinimide
NCS	<i>N</i> -chlorosuccinimide
NMR	Nuclear magnetic resonance
Ph	Phenyl-
PIDA	(Diacetoxyiodo)benzene
Pr	Propyl-
rt	Room temperature
Sat.	Saturated
Soln.	Solution
TBAB	Tetrabutylammonium bromide
TBAF	Tetrabutylammonium fluoride
TBAI	Tetrabutylammonium iodide
TBS	<i>Tert</i> -butyldimethylsilyl chloride
<i>t</i> Bu	<i>Tert</i> -butyl
TCDI	1,1'-thiocarbonyldiimidazole
TFA	Trifluoroacetic acid
THF	Tetrahydrofuran
T-L	Trypsin-like
TLC	Thin layer chromatography
TMG	1,1,3,3-Tetramethylguanidine

TMS	Tetramethylsilane
Ts	Tosyl-
VioB	Violacein biosynthesis protein

Chapter 1: Advances in the Total Synthesis of Bis- and Tris-Indole Alkaloids Containing *N*-Heterocyclic Linker Moieties^{1*}

1.1 Introduction

As their name suggests, indole alkaloids are natural products that contain one or more indole structural moieties. They are commonly isolated from a variety of marine sources, including sponges, tunicates, red algae, acorn worms, and symbiotic bacteria, and they represent the largest, and among the most complicated, class of the marine alkaloids.¹ Indole alkaloids have been shown to display diverse biological activities, including cytotoxic, antitumor, antiviral, antibacterial, and anti-inflammatory activities.² The structure, activity, and synthesis of indole alkaloids have been discussed in several reviews over the years.³ The goal of this review is to provide a detailed overview on recent advances in isolation and total synthesis of bis- and tris-indole alkaloid natural products that contain *N*-heterocyclic linker moieties. These heterocyclic moieties are of particular interest as it has been reported that more than 85% of biologically active compounds contain one or more heterocyclic moieties with *N*-heterocycles being the most prevalent.⁴ These heterocyclic moieties are of particular interest as it has been reported that more than 85% of biologically active compounds contain one or more heterocyclic moieties.⁵ The biological activities of these natural products will also be discussed.

¹ * This chapter was reproduced from the recently published review with permission from the Royal Society of Chemistry (RSC), Natural Product Reports. (Dvorak, K.; Tepe, J., Advances in the Synthesis of Bis- and Tris-Indole Alkaloids containing *N*-Heterocyclic Linker Moieties, *Natural Product Reports*, **2024**, DOI: 10.1039/D4NP0).

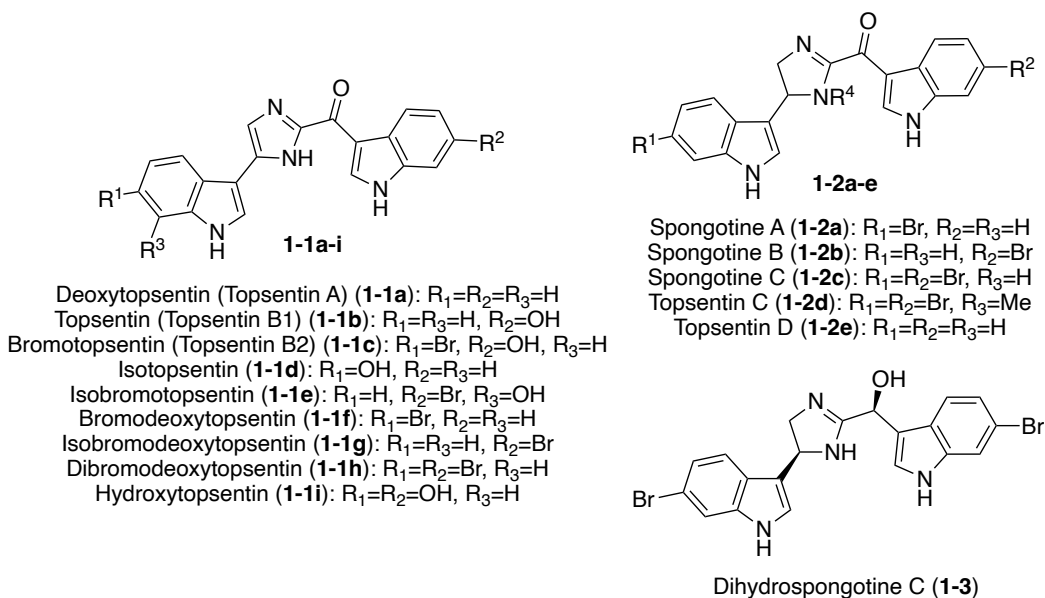
1.2 Bis-indole alkaloids

1.2.1. Imidazole and imidazoline linker moieties

1.2.1.1. Topsentins and Spongotines

Topsentins and Spongotines are classes of marine alkaloid bis-indole natural products that contain characteristic 2-carbonylimidazole or 2-carbonylimidazoline linker moieties between their two indole fragments. The first few natural products that were discovered in these classes were Deoxytopsentin (Topsentin A) (**1-1a**), Topsentin (Topsentin B1) (**1-1b**), and Bromotopsentin (Topsentin B2) (**1-1c**). These three natural products were first isolated from Mediterranean marine sponge *Topsentia Genitrix*.⁶ The structures of these natural products were elucidated via spectroscopic methods, as shown in **Scheme 1.1**, and **1-1a**, **1-1b**, and **1-1c** were identified as weakly cytotoxic for fish and for dissociated cells of the freshwater sponge *Ephydatia Fluviatilis*.⁵ After these initial discoveries, the structurally related analogues **1-1d-h** and **1-2a-e**, were isolated from various marine sponges, including *Spongosorites*,^{2,5,7,8} *Hexadella*,^{9,10} *Discodermia Calyx*,¹¹ *Rhaphisia Lacezie*,¹² and *Topsentia*.^{5,13} Natural products of the Topsentin and Spongotine classes have been shown to possess cytotoxic, anticancer, antibacterial, antiviral, antifungal and anti-inflammatory activities.^{3,14}

Scheme 1.1. Chemical structures of Topsentin and Spongotine natural products (**1-1a-h**, **1-2a-e**, **3**) and the synthetic analogue Hydroxytopsentin (**1-1i**).

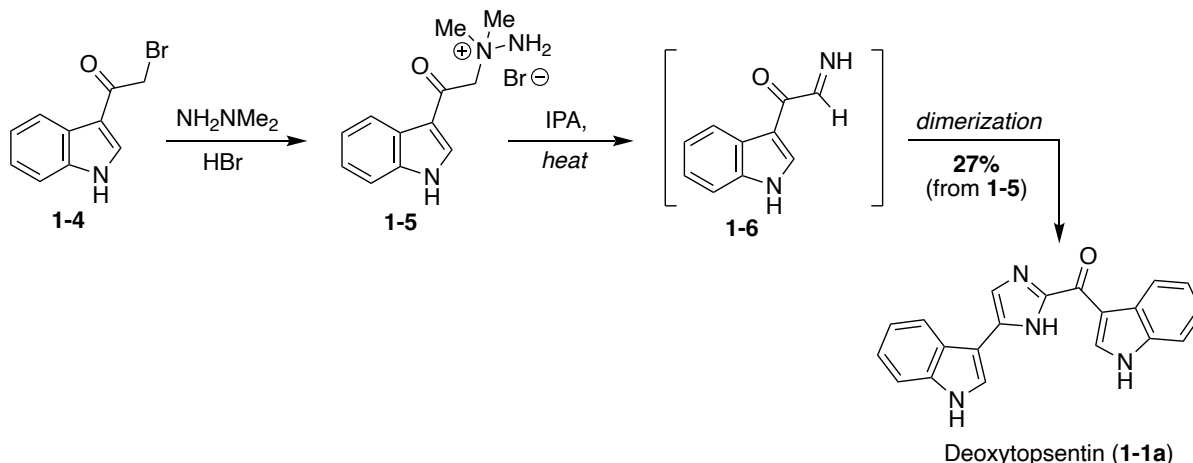


In addition to these previously discussed natural products, the most recently isolated natural product in the Spongotine class was Dihydrospogotine C (**1-3**), which was isolated as a single enantiomer in 2017 from the *Topsentia sp.* marine sponge. Its structure was elucidated via spectroscopic methods. Both stereocenters were determined to have the *S*-stereochemistry configurations consistent with experimental and calculated circular dichroism (CD) data (MPW1PW91/6-31G(d,p)).¹³ In addition, **1-3** displayed antibacterial activity toward *S. aureus* (MIC: 3.7 $\mu\text{g/mL}$), anti-HIV activity (IC₅₀ (YU2): 3.5 μM ; IC₅₀ (HxB2): 4.5 μM), and displayed no evidence of cytotoxic activity toward mammalian cells.¹³ Dihydrospogotine C (**1-3**) has yet to be accessed via total synthesis.

The first natural product of the Topsentin and Spongotine classes to be accessed via total synthesis was Deoxytopsentin (Topsentin A) (**1-1a**) by Braekman, J., *et. al.* in 1988.¹⁵ As shown in **Scheme 1.2**, 3-(bromoacetyl)indole (**1-4**) was reacted with 1,1-dimethylhydrazine in acidic conditions to afford the amine salt (**1-5**). Then, **1-5** was refluxed in isopropanol (IPA) to prompt

migration of the methyl groups and elimination of dimethylamine to afford the imine intermediate **1-6**, which immediately dimerized to afford **1-1a** in 27% yield from **1-5**.¹⁵

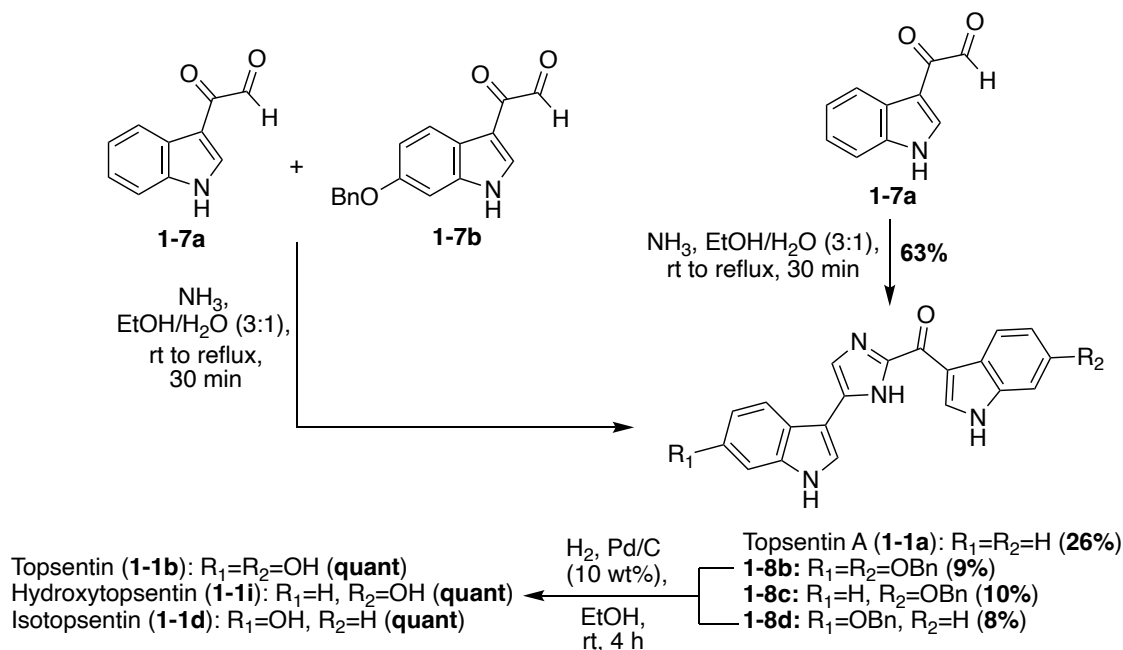
Scheme 1.2. The first total synthesis of Deoxytopsentin (**1-1a**).



Additional progress was then made toward the synthesis of the Topsentin natural products **1-1a**, **1-1b**, **1-1d**, and the natural product analogue **1-1i**. The synthetic route began with the synthesis of key indole-3-keto-aldehyde fragments **1-7a** and **1-7b** via a subsequent oxidative step that was carried out on the indole-3- α -chloro-ketone starting material. The penultimate step of this synthesis was the condensation and cyclization of **1-7a** and **1-7b** to ideally afford Topsentin (**1b**), as shown in **Scheme 1.3**. However, this cyclization proved to be unselective, affording a mixture of **1-1a** (26%), **1-8b** (9%), **1-8c** (10%), and **1-8d** (8%). Each of these intermediates were isolated before undergoing quantitative hydrogenolysis to remove the benzyl group, affording **1-1b**, **1-1d**, and the natural product analogue **1-1i**. The same condensation/cyclization reaction was carried out to dimerize and condense two equivalents of **1-7a**, rather than the mixed keto-aldehyde intermediates, and the desired product **1-1a** was accessed in 63% yield. This emphasized that the selectivity was the major issue with this approach.¹⁶ Over the years, additional dimerization-cyclization approaches toward the total synthesis of **1-1a** have also been completed, such as the dimerization of an indolic α -amino-ketone fragment by Miyake *et. al.*¹⁷

Scheme 1.3. Total synthesis of Topsentins **1-1a**, **1-1b**, **1-1d**, and the natural product analogue **1-**

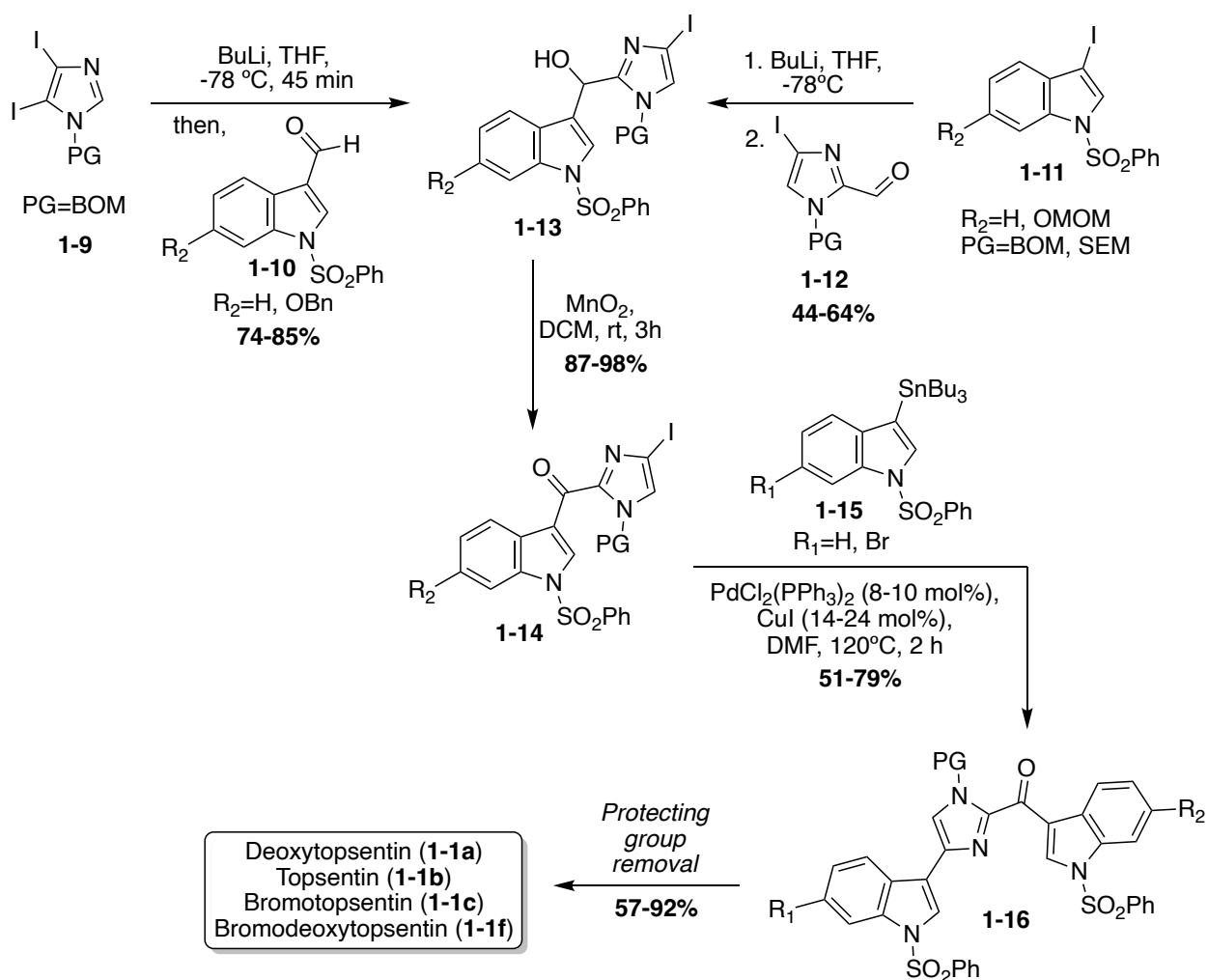
1i.



Considering the selectivity issues of these dimerization-like approaches toward the Topsentin natural products, additional synthetic approaches toward these scaffolds were developed to improve this selectivity, such as the use of lithiation and subsequent cross coupling reactions. For example, in this approach, the imidazole core was the starting point, and the indole-3-aldehyde and indole moieties were subsequently added to the imidazole ring (**Scheme 1.4**).^{18,19} There were two lithiation and subsequent nucleophilic addition approaches to access the key imidazoline intermediate (**1-13**). In the first synthetic strategy, di-iodo-imidazole (**1-9**) was first lithiated with *n*BuLi, which subsequently underwent nucleophilic addition to indole-3-aldehydes (**1-10**) to access **1-11** in high yields. In the second approach, the electronics of the reaction were reversed in which the 3-iodo-indoles (**1-11**) underwent lithium-halogen exchange and were subsequently added to the imidazole-2-aldehydes (**1-12**) to afford the key intermediate **1-13** in good yield. To access the Topsentin natural products **1-1a**, **1-1b**, **1-1c**, and **1-1f**, the

alcohol **1-13** was oxidized to the ketone **1-14** using MnO_2 and coupled with the tributyltin indole **1-15** via the Stille method in high yield. After removal of protecting groups, the desired products **1-1a**, **1-1b**, **1-1c**, and **1-1f** were isolated in 57-92% yield.^{18,19} This approach proved to be a much more efficient and highly selective approach toward installing two indole fragments on the imidazole core that bear different substituents.

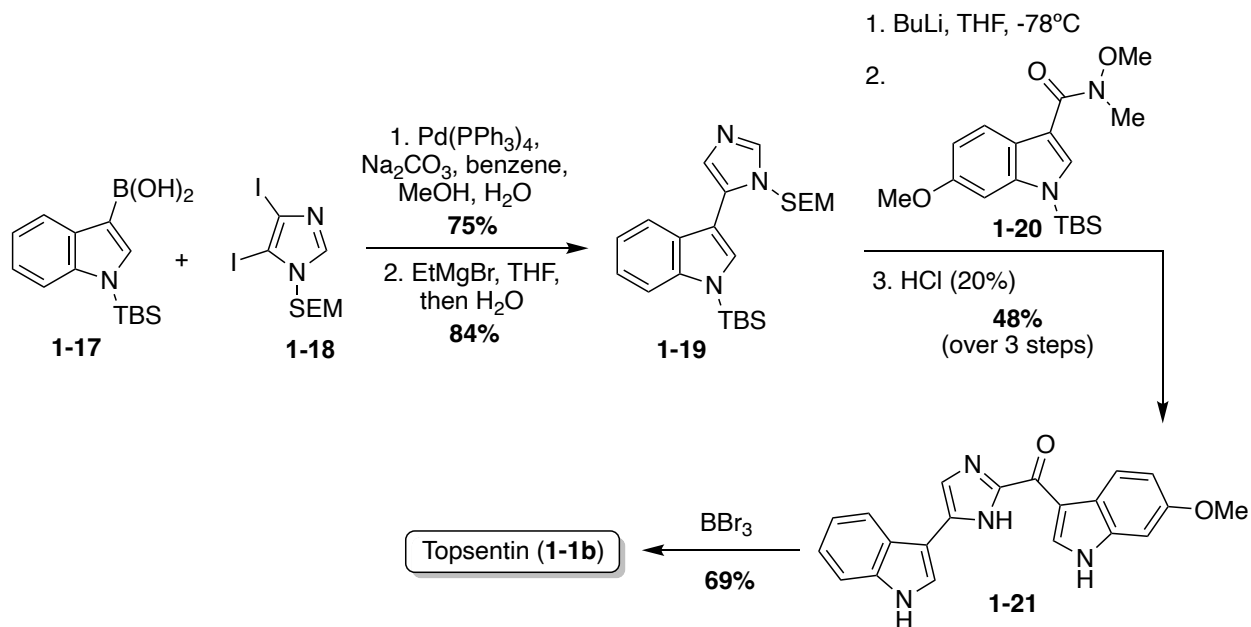
Scheme 1.4. Lithiation and cross-coupling synthetic approaches toward **1-1a**, **1-1b**, **1-1c**, and **1-1f**.



Considering the efficiency of cross-coupling, additional cross-coupling approaches toward these natural products were completed. For example, Kawasaki *et al.* coupled a borylated

indole **1-17** with *N*-SEM-di-iodoimidazole **1-18** and subsequently de-iodinated to afford the imidazole intermediate **1-19** in high yields (**Scheme 1.5**). A late-stage lithiation of **1-19** was then carried out and subsequently reacted with the indole-3-amide intermediate **1-20**. Lastly, the protecting groups were removed using BBr_3 , to render Topsentin (**1-1b**) in 69% yield.²⁰

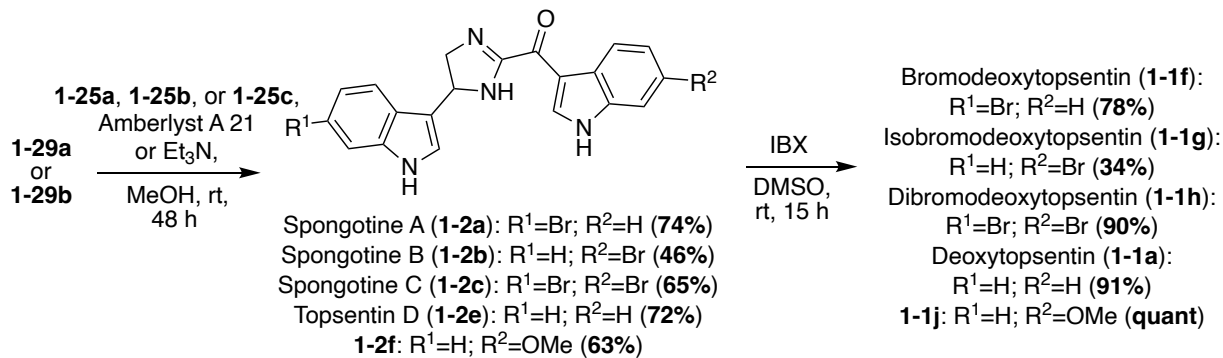
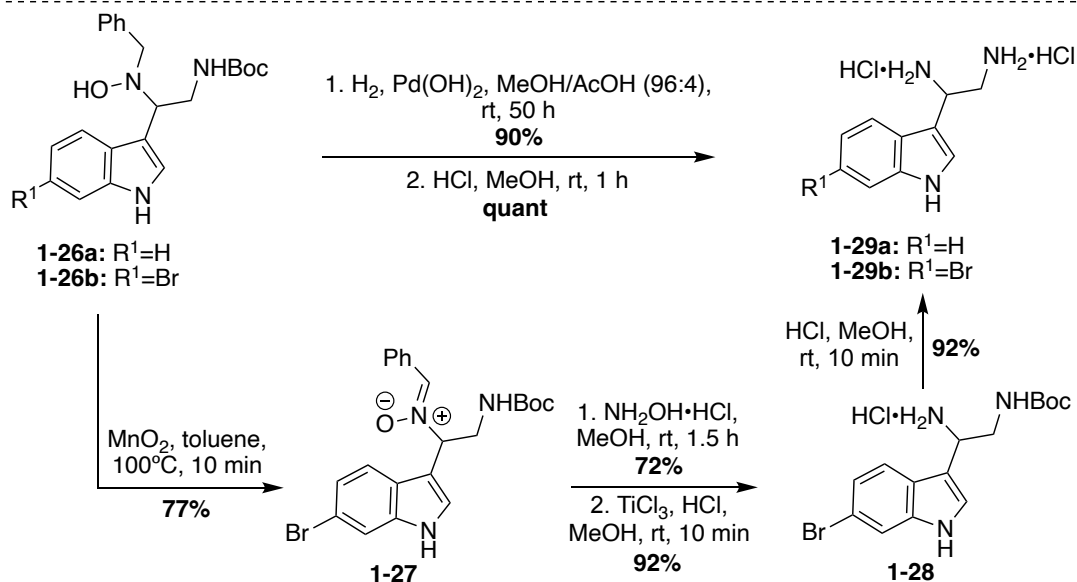
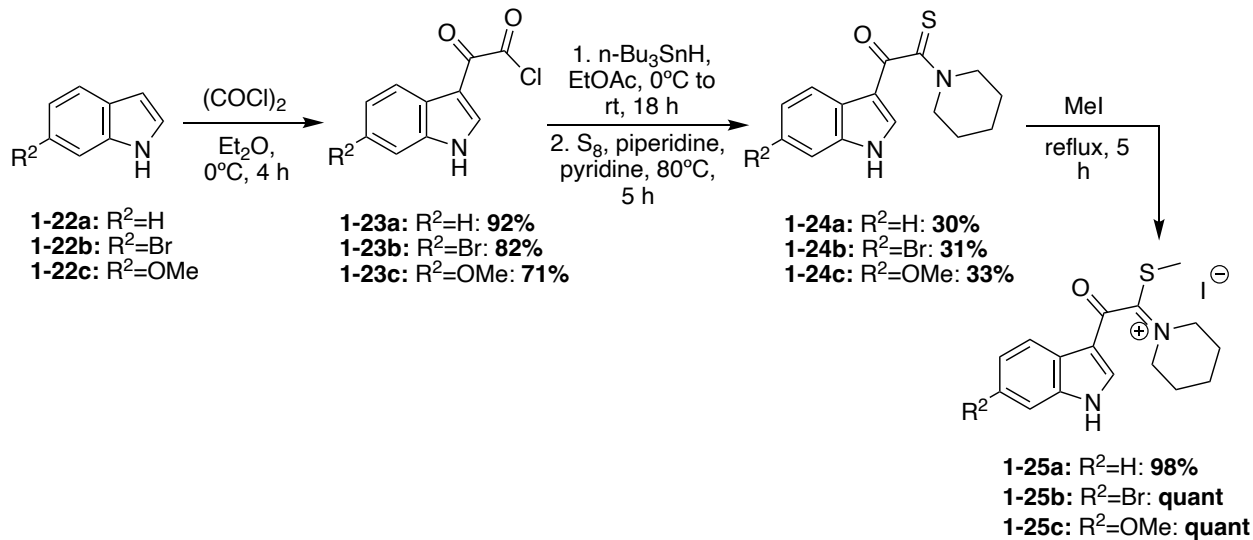
Scheme 1.5. Cross-coupling and late-stage lithiation approach to Topsentin (**1-1b**).



The newer isolated Spongotone natural products were accessed via total synthesis more recently. The first total syntheses of several Spongotone and Topsentin natural products were achieved via a common key cyclization approach toward the imidazoline core, in which a keto-thioimide (**1-25a-c**) fragment and diamine (**1-29a-b**) fragment were cyclized.^{21,22} Intermediates **1-25a-c** were synthesized in four steps from commercially available indole starting materials (**1-22a-c**) in good yields (**Scheme 1.6**). There were two different approaches for accessing the indolic diamine fragments (**1-29a** and **1-29b**). The first approach was used to synthesize the indolic diamine (**1-29a**). In this approach, an indolic hydroxylamine intermediate (**1-26a**) underwent reductions and hydrogenolysis via hydrogen and Pearlman's catalyst to access the

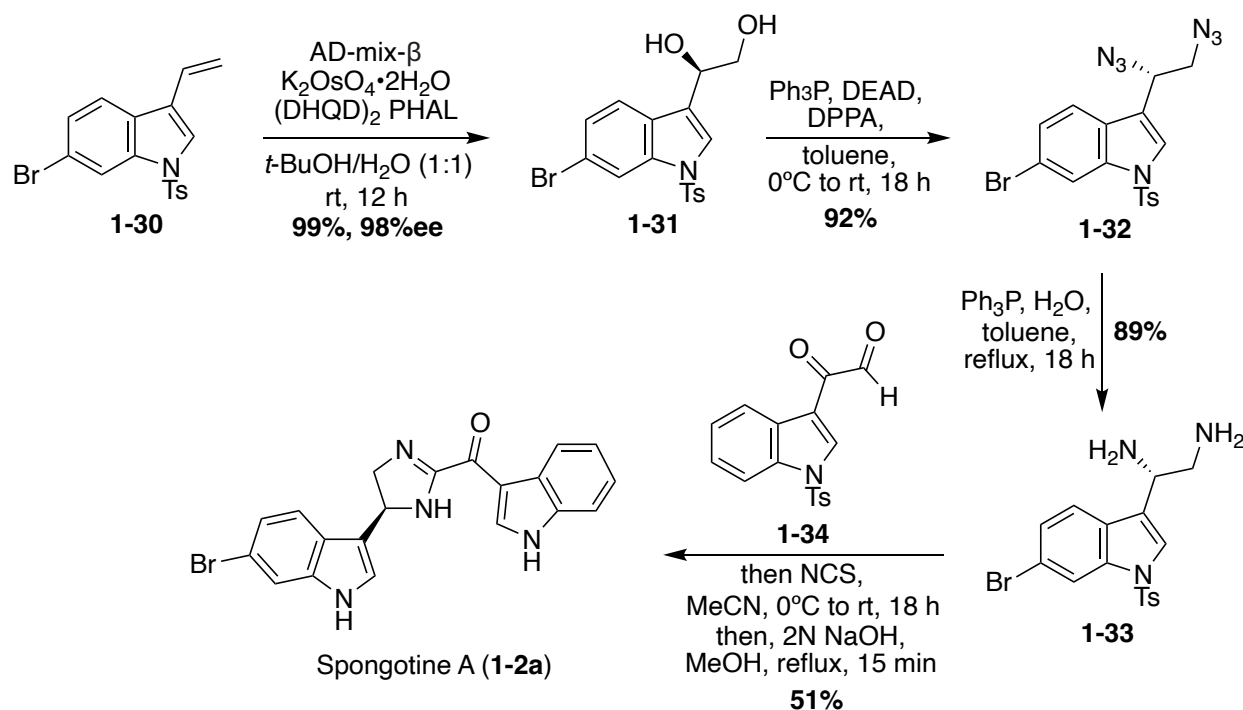
debenzylated intermediate in 90% yield. Then, the Boc protecting group was quantitatively removed under acidic conditions to access **1-29a**.²³ The second approach was a little more step-intensive to access the indolic diamine intermediate **1-29b** as it could not be synthesized via the hydrogenative method of **1-29a** due to problematic dehydrohalogenation of indoles under hydrogenative conditions.²³ In order to avoid hydrogenation conditions, the 6-bromo-indolic hydroxylamine intermediate **1-26b** was oxidized to **1-27** via MnO₂ and subsequently reacted with hydroxylamine hydrochloride to remove the benzyl group and reduced via TiCl₃ to achieve **1-28** in high yields. From there, **1-28** was subjected to acidic conditions to remove the Boc group and access **1-29b** in 99% yield.²² The desired natural products were then accessed via the key base-catalyzed imidazoline cyclization between **1-25a-c** and **1-29a-b**. This cyclization was carried out with either Et₃N or Amberlyst A21 resin to access the desired natural products (**1-2a** (74%), **1-2b** (46%), **1-2c** (65%), **1-2e** (72%)) and the natural product analogue (**1-2f** (63%)) in good yields. Then, the imidazoline cores of **1-2a-c**, **1-2e**, and **1-2f** were oxidized via IBX to the imidazole of Topsentins **1-1f** (78%), **1-1g** (34%), **1-1h** (90%), **1-1a** (91%), and Topsentin analogue **1-1j** (quant). This was the first total synthesis of Spongotine A-C (**1-2a-c**), Bromodeoxytopsentin (**1-1f**), Isobromodeoxytopsentin (**1-1g**), and Dibromodeoxytopsentin (**1-1h**).^{21,22} The natural product analogue **1-1j** was also synthesized and could be de-methylated in the future with BBr₃ to access Hydroxytopsentin (**Scheme 1.6**).

Scheme 1.6. Total synthesis of **1-1a**, **1-1f-h**, **1-2a-c**, and **1-2e**.



The first enantioselective total synthesis of Spongotine A (**1-2a**) was achieved via a key imidazoline cyclization between a keto-aldehyde fragment (**1-34**) and an optically active diamine fragment (**1-33**), as shown in **Scheme 1.7**.²⁴ First, **1-34** was synthesized in three steps from 1*H*-indole, via a keto-acyl chloride intermediate, according to literature procedures.²⁵ Fragment **1-33** was synthesized via Sharpless dihydroxylation of a 3-vinyl indole intermediate (**1-30**) to access (*R*)-**1-31** in high yield and enantioselectivity. Then, (*R*)-**1-31** underwent a stereospecific Mitsunobu reaction to access the diazide intermediate (*S*)-**1-32** in 95% yield, in which the (*S*)-stereochemistry was set via inversion of the chiral center. The diazide (*S*)-**1-32** was then reduced to access the optically active indolic diamine intermediate (*S*)-**1-33** in high yields with 98% *ee*. To synthesize the imidazoline core and achieve Spongotine A (**1-2a**), (*S*)-**1-33** and **1-34** underwent condensation, cyclization, and oxidation to the imidazoline via NCS. Subsequent removal of the tosyl protecting group with base achieved Spongotine A (**1-2a**) in 51% yield. Through these final steps, the stereochemistry was retained, allowing for the first enantioselective total synthesis of Spongotine A (**1-2a**).²⁴ In addition, the specific optical rotation of the synthesized (*S*)-Spongotine A (**1-2a**) matched that of the natural Spongotine A (**1-2a**), allowing for the establishment of its previously unknown absolute configuration as (*S*)-Spongotine A.

Scheme 1.7. The first enantioselective total synthesis of (*S*)-Spongotine A (**1-2a**).

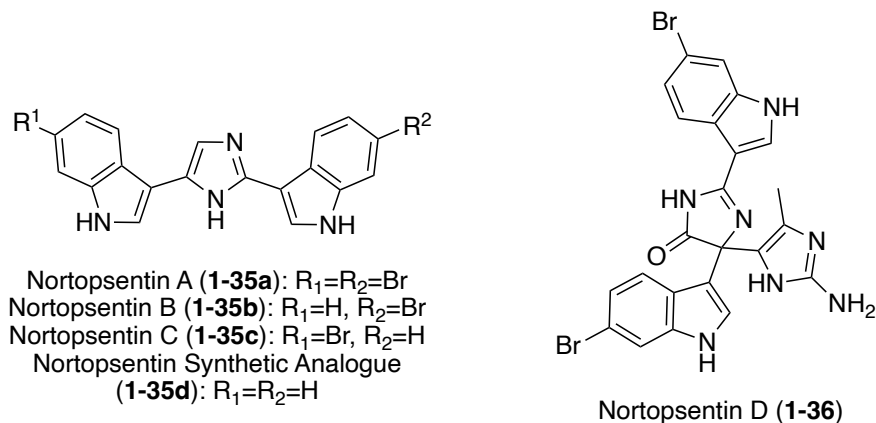


1.2.1.2. Nortopsentins

The Nortopsentin class of bis-indole natural products are structurally similar to those of the Topsentin class, however, they lack a carbonyl moiety on the imidazole linker moiety, as shown in **Scheme 1.8**, Nortopsentin A (**1-35a**), B (**1-35b**), and C (**1-35c**) were first isolated from *Spongosorites ruetzleri* in 1987.²⁶ Nortopsentins A-C (**1-35a-c**) were found to possess cytotoxic and antifungal activities. Interestingly, the methylated derivatives of **1-35a-c** also displayed enhanced cytotoxic activity in P388 cells compared to the isolated natural products.²⁶ In addition, the unnatural synthetic Nortopsentin analogue **1-35d**, unfortunately also referred to as *Nortopsentin D* in several early literature reports, was accessed via hydrogenation of **1-35a-c**, as indole readily undergo de-halogenation under hydrogenation conditions.²⁷ Several years later, in 1996, the more complex structural variant of this class, Nortopsentin D (**1-36**), composed of a tri-substituted imidazolinone ((4*H*)-imidazol-4-one) core, was first isolated from the axinellid

sponge, *Dragmacidon sp.*²⁸ Later, **1-36** was also isolated from the sponge *Agelas dendromorpha*.²⁹ It is interesting to mention that the methylated derivative of **1-36** was also shown to have antifungal activity against yeast and high cytotoxicity toward tumoral cells.^{28,30}

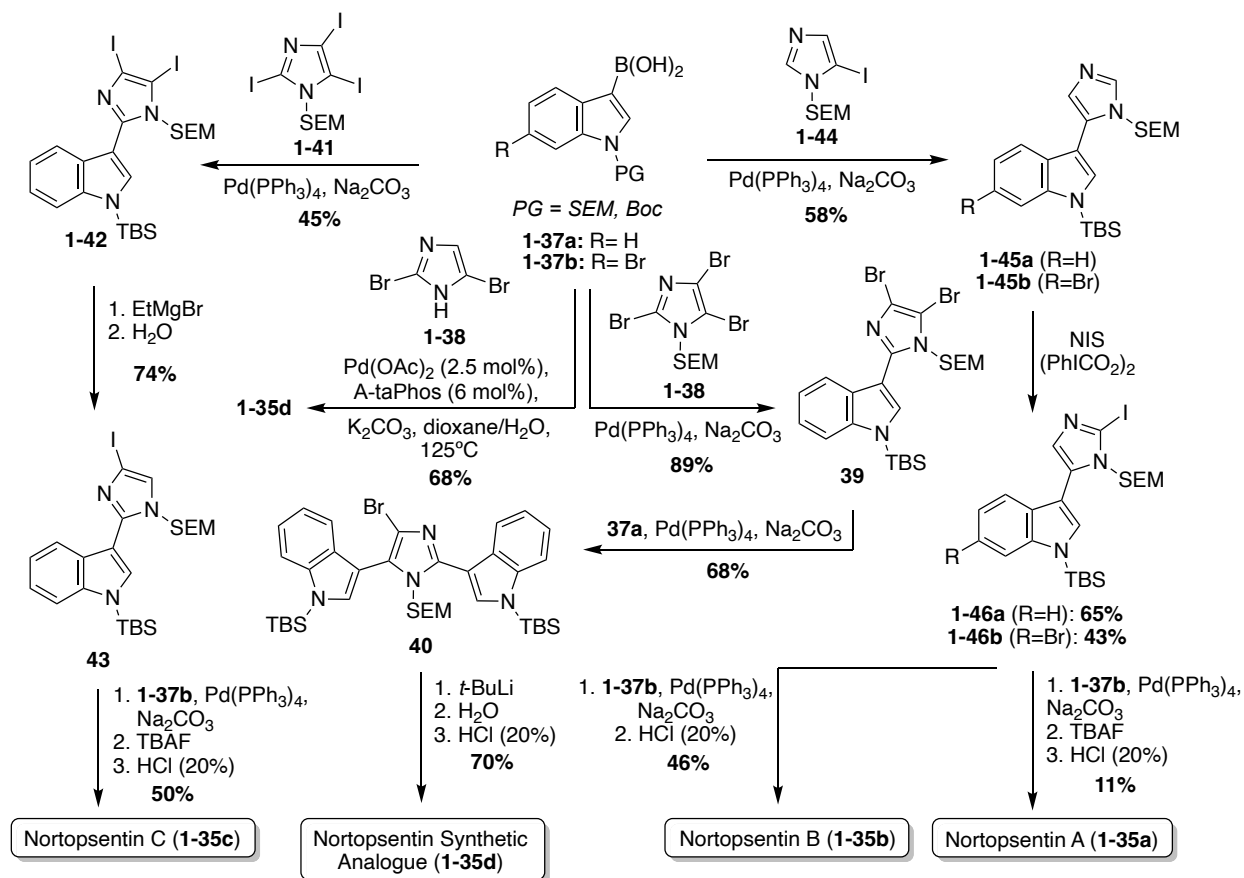
Scheme 1.8. Chemical structures of Nortopsentins A-D (**1-35a-c**, **1-36**) and Nortopsentin synthetic analogue (**1-35d**).



The first total syntheses of Nortopsentins A-C (**1-35a-c**), as well as the synthetic analogue **1-35d**, were achieved via a successive Pd-catalyzed cross-couplings of indole fragments to the imidazole core, as shown in **Scheme 1.9**.³⁰ The synthetic analogue **1-35d** was the first of these to be accessed via successive cross coupling reactions of a tri-brominated imidazole (**1-38**) with an *N*-TBS-protected indole-3-boronic acid (**1-37a**), using $Pd(PPh_3)_4$ as a catalyst. The protecting groups and remaining bromide were then removed to access **1-35d** in high yields. During route development, SEM- and MOM-protecting groups were also explored for **1-37a**, yet the TBS-protecting group resulted in the highest yield of the coupling reaction.³⁰ More recently, an adapted method for palladium-catalyzed cross coupling of unprotected imidazoles was developed and utilized in the synthesis of **1-35d**, as shown in **Scheme 1.9**.³¹ This Suzuki-Miyaura cross-coupling method allowed for a significantly expedited approach toward **1-35d**, as compared to previous reports. However, this method is likely only efficient for natural products bearing

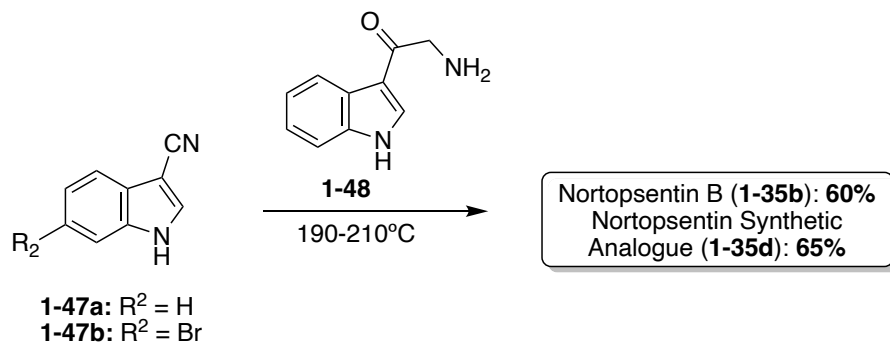
symmetrical indole moieties. In a similar manner, the first total syntheses of Nortopsentin A (**1-35a**) and C (**1-35c**) were achieved, as shown in **Scheme 1.9**. The efficient synthesis of **1-35c** was very similar to that of **1-35d**. Iodide was utilized as a coupling partner here, rather than bromide. Iodide was likely used here to prevent potential selectivity issues given the bromide substituents on the boronic acid coupling partners. The other major difference was the removal of the additional iodide before the second indole coupling (**Scheme 1.9**, synthesis of **1-35c**). It is noteworthy to mention that the selective de-iodination to access intermediate **1-43** was confirmed via a NOESY correlation between the SEM group on the nitrogen and the C5-H of the imidazole.³⁰ The approach toward the first total synthesis of Nortopsentin A (**1-35a**) and Nortopsentin B (**1-35b**), which also bear bromide substituents on their indoles, implemented a later stage iodination approach in the synthesis of **1-46** before the second cross coupling reaction to access **1-35a** and **1-35b** in moderate and good yield, respectively (**Scheme 1.9**).³⁰

Scheme 1.9. The first total synthesis of Nortopsentin A-C (**1-35a-c**) and the Nortopsentin synthetic analogue (**1-35d**).



In addition to these cross-coupling approaches, a different non-cross-coupling approach was used to access the Nortopsentin natural products **1-35b** and **1-35d**. This method utilized the condensation of a nitrile with an α -amino-ketone fragment and subsequent cyclization and aromatization of the imidazole at high temperatures to achieve Nortopsentin B (**1-35b**) and the Nortopsentin D synthetic analogue **1-35d** in good yields (Scheme 1.10).¹⁷ This method was not viable for the total synthesis of Nortopsentins A (**1-35a**) and C (**1-35c**). This was likely due to the necessary hydrogenation step for the synthesis of intermediate **1-48**, which would not tolerate a bromide substituent on the indole (**1-48**), as has been previously discussed.

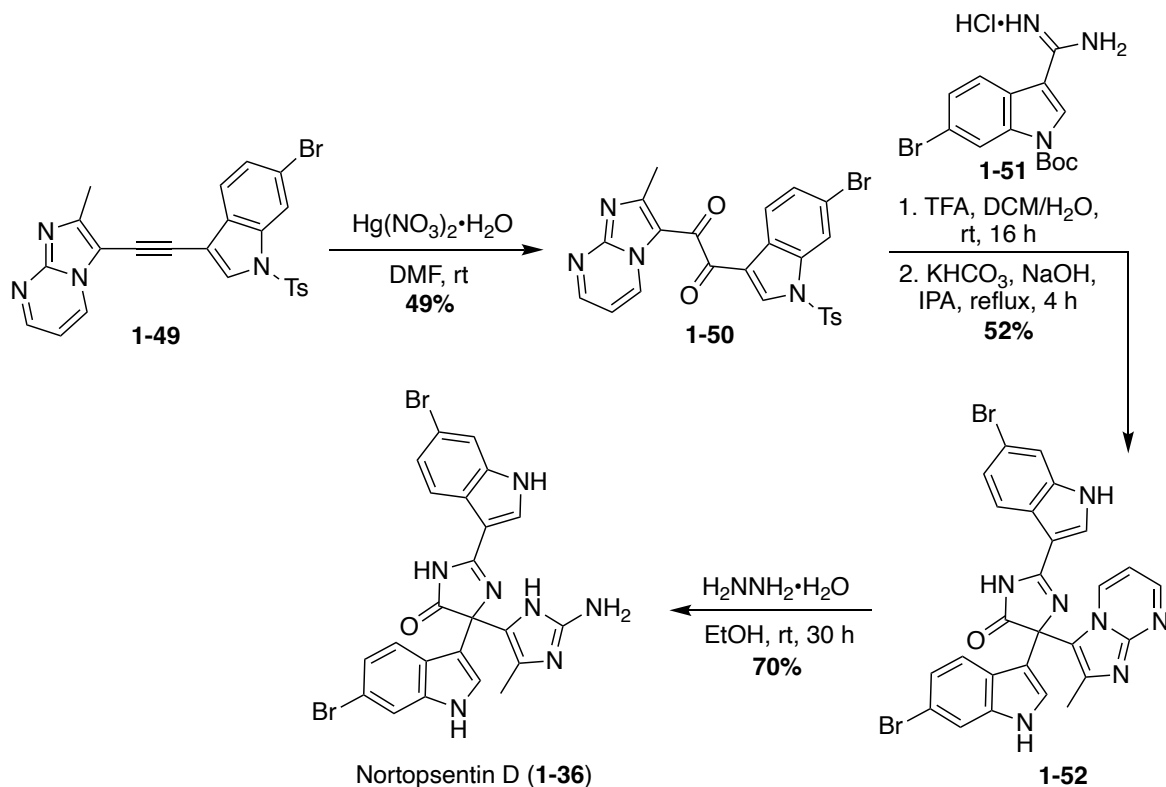
Scheme 1.10. Synthesis of Nortopsentin B (**1-35b**) and its synthetic analogue (**1-35d**) via thermal cyclization.



The first total synthesis of the more structurally complex Nortopsentin D (**1-36**) was completed by K. Keel, *et. al.*, in 2021, as shown in **Scheme 1.11**.³² The complex tri-substituted imidazolinone ((4*H*)-imidazol-4-one) core was constructed via a late-stage Pinacol-like rearrangement. Two key fragments were utilized in this approach; an alkyne fragment (**1-49**) and amidine fragment (**1-51**). The alkyne (**1-49**) and amidine (**1-51**) were accessed in two and five steps, respectively from the commercially available 6-bromo-1*H*-indole.³² The alkyne fragment (**1-49**) was oxidized to the di-ketone intermediate (**1-50**) via mercuric nitrate monohydrate. The key condensation-cyclization and subsequent Pinacol-like rearrangement steps were then carried out to form the tri-substituted imidazolinone core of Nortopsentin D (**1-36**), accessing **1-52** in 52% yield. The *N*-tosyl and *N*-boc protecting groups were deprotected during this reaction. Precise deprotection was key for optimization, as successful cyclization was dependent upon electronics. It was found that the *N*-boc protecting group of **1-51** had to first be deprotected to allow for sufficient nucleophilicity of the amidine (**1-51**) to condense and cyclize with the di-ketone (**1-50**). The presence of the *N*-tosyl protecting group of **1-50** was also found to contribute to increased electrophilicity of the ketone. Therefore, initial acidic conditions were implemented to remove the *N*-boc group of **1-51**, followed by the strategic use of a mildly nucleophilic base

and solvent to allow for cyclization to occur prior to de-tosylation of **1-50** (**Scheme 1.11**). After removal of the remaining protecting group to access the 2-amino-imidazole substituent, Nortopsentin D (**1-36**) was accessed in 70% yield.³²

Scheme 1.11. First total synthesis of Nortopsentin D (**1-36**).



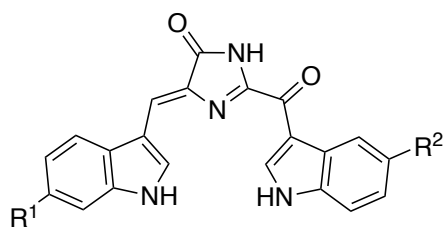
1.2.2. Imidazolinone linker moieties

1.2.2.1. Rhopaladins

Natural products of the Rhopaladin class are bis-indole alkaloids comprised of two indole fragments connected by an imidazolinone ((4*H*)-imidazol-4-one) linker moiety, similar to Nortopsentin D (**1-36**). In addition, the indolylcarbonyl substitution at the C-2 position of the imidazolinone core is similar to the Spongotine and Topsentin natural product classes (**Scheme 1.12**). However, unlike any of the previously discussed natural product classes, the second indole moiety is connected at the 5-position of the imidazolinone core by a unique vinyl chain.

Rhopaladins A-D (**1-53a-d**) were first isolated in 1998 by Sato *et. al.* from the marine tunicate *Rhopalaea sp.*³³ The geometry of the alkene present in these natural products (**1-53a-d**) was identified as (*Z*) by a NOESY experiment that was run on Rhopaladin C (**1-53d**). The studies identified various NOESY correlations, such as a NOESY correlation between the two C-2 hydrogens of the indole moieties, indicating a (*Z*) geometry of the alkene. In terms of biological activities, these natural products were reported to demonstrate antibacterial activity against *Sarcina lutea* and *Corynebacterium xerosis* and inhibitory activity against cyclin dependent kinase 4 and *c-erbB-2* kinase. However, their broader biological activity has yet to be explored.³³

Scheme 1.12. Chemical structure of Rhopaladins A-D (**1-53a-d**).

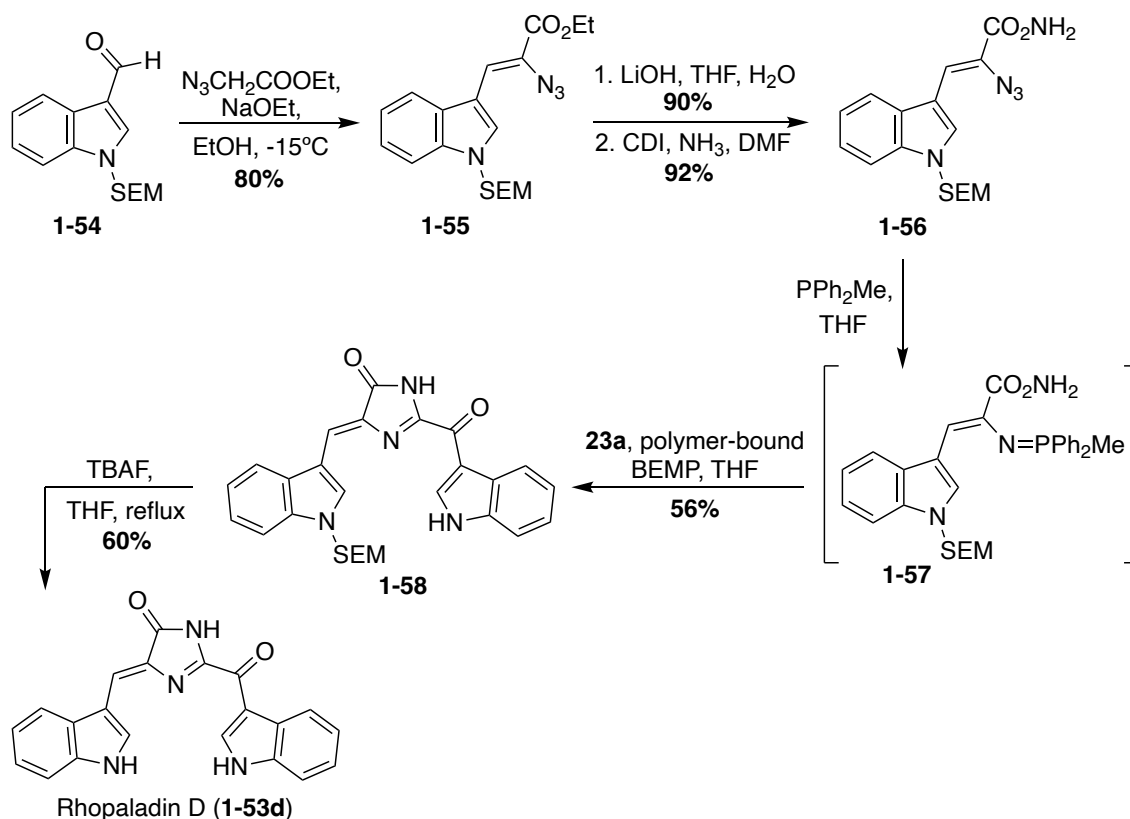


Rhopaladin A (**1-53a**): R¹=OH, R²=Br
 Rhopaladin B (**1-53b**): R¹=OH, R²=H
 Rhopaladin C (**1-53c**): R¹=H, R²=Br
 Rhopaladin D (**1-53d**): R¹=H, R²=H

The first total synthesis of Rhopaladin D (**1-53d**) was reported in 2000, in which a key intermolecular aza-Wittig reaction was utilized, followed by subsequent condensation and cyclization to form the imidazolinone core of **1-53d**.³⁴ To perform the aza-Wittig reaction, the azide intermediate (**1-56**) was first accessed in three steps in high yields from indolyl-3-aldehyde **1-54** (**Scheme 1.13**). Then, the aza-Wittig reaction was performed on azide intermediate **1-56** to access intermediate **1-57**, which was immediately condensed and cyclized with keto-acyl chloride **1-23a** to access imidazolinone **1-58** in 56% yield over two steps. Lastly, the protecting group was removed to afford Rhopaladin D (**1-53d**) in 60% yield. However, **1-58** was isolated as a 6:4 mixture of *E/Z* isomers and after chromatographic separation, the (*Z*) isomer isomerized to

the (*E*) isomer upon sunlight irradiation. Therefore, after the last step, Rhopaladin D (**1-53d**) was also isolated as a mixture of *E/Z* isomers.³⁴

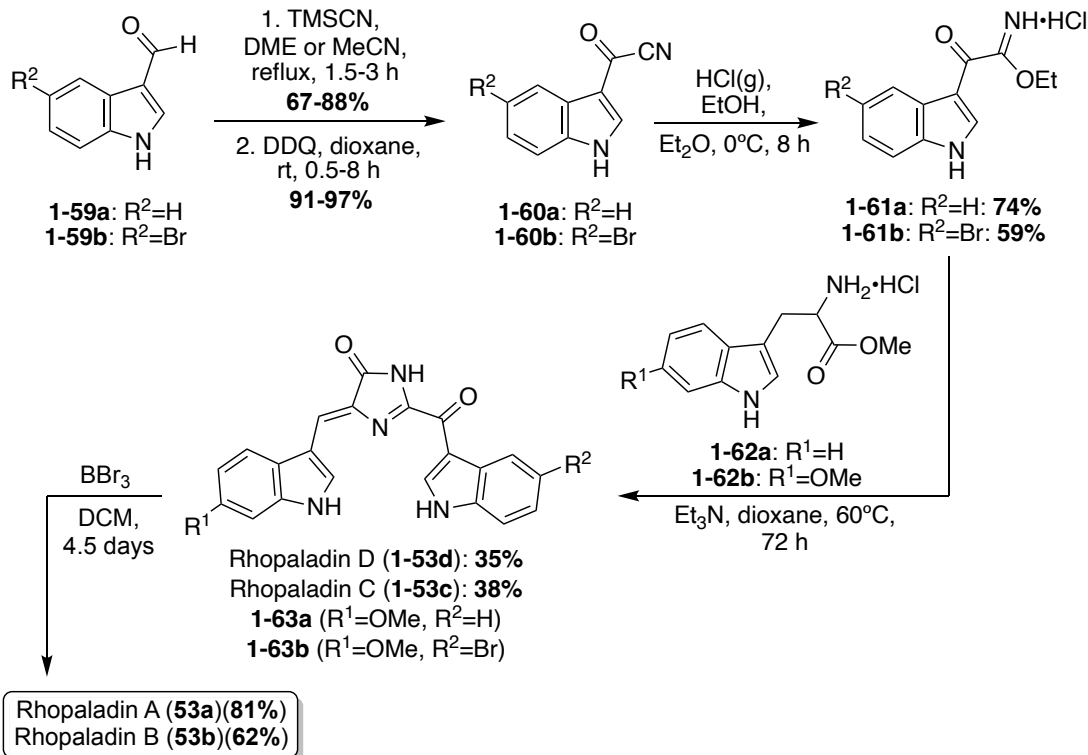
Scheme 1.13. First total synthesis of Rhopaladin D (**53d**).



A couple years later, the total syntheses of all four Rhopaladins A-D (**1-53a-d**) were achieved via a key imidate-based cyclization with tryptophan esters to form the imidazolinone core of these natural products, as shown in **Scheme 1.14**.³⁵ First, the carbonyl nitrile intermediate (**1-60a-b**) was synthesized via a TMS-cyanohydrin intermediate from aldehyde **1-59a-b**, followed by subsequent oxidation to the carbonyl nitrile **1-60a-b** in high yields. Then, **1-60a-b** underwent a Pinner reaction with gaseous hydrochloric acid and ethanol to form the imidate intermediate (**1-61a-b**). Compounds **1-61a-b** were immediately condensed and cyclized with tryptophan methyl ester hydrochloride (**1-62a**) in the presence of triethylamine to access Rhopaladin C (**1-53b**) and D (**1-53d**) in 38% and 35% yield, respectively. Interestingly, the

dehydrogenation to form the alkene of the Rhopaladins occurs spontaneously after the cyclization has occurred. This is likely due to the highly conjugated nature of the Rhopaladins, contributing to high stability. Interestingly, this cyclization and spontaneous dehydrogenation specifically produced (*Z*)-isomers of the Rhopaladins, as was confirmed via NOESY correlations, including a NOESY correlation between the C2-H's of the indole moieties. The presence of the (*E*)-isomers could not be detected.³⁵ Thus, this method was proven to be very selective to the (*Z*)-isomer, which is a major advantage compared to the previous synthesis of Rhopaladin D (**1-53d**). Rhopaladins A and B (**1-53a** and **1-53b**) were synthesized in the same manner as Rhopaladin C and D (**1-53c** and **1-53d**), as shown in **Scheme 1.14**. The only difference was the identity of the tryptophan methyl ester (**1-62b**). In addition, after the key cyclization reaction and spontaneous dehydrogenation to access **1-63a** and **1-63b**, an additional de-methylation step via BBr₃ was required to access Rhopaladins A (**1-53a**) and B (**1-53b**) in 81% and 62% yields, respectively. In addition, similarly to **1-53c** and **1-53d**, the Rhopaladins A (**1-53a**) and B (**1-53b**) were confirmed with NOESY as the desired (*Z*)-isomer.³⁵

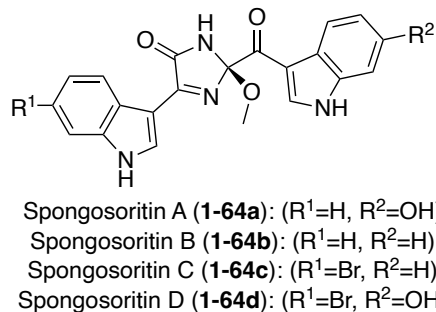
Scheme 1.14. Total synthesis of Rhopaladins A-D (**1-53a-d**).



1.2.2.2. Spongositins

Recently, the first of the Spongositins were isolated, which marks another natural product class to contain an imidazolinone (2,3-dihydro-4*H*-imidazol-4-one) core. Spongositins A-D (**1-64a-d**) were first isolated in 2021 from *Spongosorites sp.* by Park, *et. al.*³⁶ As shown in **Scheme 1.15**, the chemical structure of the Spongositins contains one indole moiety and one indolyl-3-ketone moiety connected by a 2-methoxy-1-imidazole-5-one linker. These chemical structures were elucidated via spectroscopic methods. In addition, these Spongositins (**1-64a-d**) contain one stereocenter at the C-2 position of the imidazolinone. The absolute configuration of this position was determined via a density functional theory (DFT)-based computational method and electronic circular dichroism (ECD). Comparing measured data with the calculated data, the stereochemistry was assigned as a (2*R*) configuration.³⁶

Scheme 1.15. Chemical structures of Spongisoritins A-D (**1-64a-d**).



Initial biological activity exploration of the Spongisoritins (**1-64a-d**) was conducted and it was found that they exhibited moderate inhibition against transpeptidase sortase A and weak inhibition against human pathogenic bacteria and A549 and K562 cancer cell lines. The biological activity findings are detailed in **Table 1.1**, including the known antibiotic, ampicillin, for comparison.³⁶ Though some information is now known, much of the Spongisoritins' biological activities remain elusive. Furthermore, Spongisoritins A-D (**1-64a-d**) have yet to be accessed via total synthesis.

Table 1.1. Biological activity of Spongisoritins A-D (**1-64a-d**).³⁶

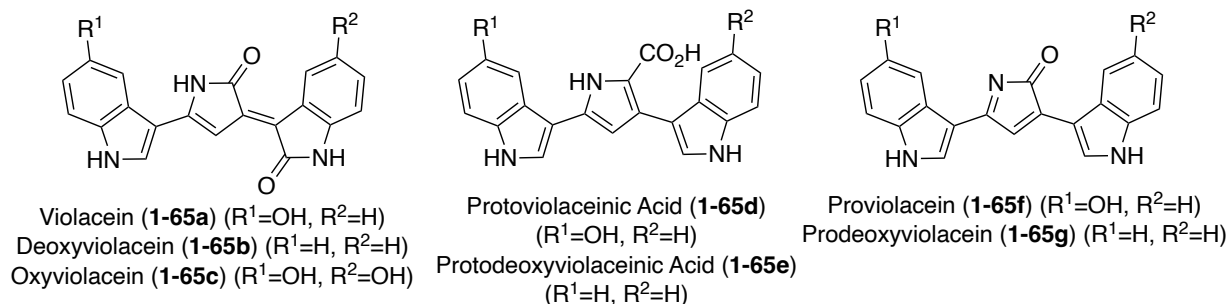
#	Gram (+) MIC (µg/mL)			Gram (-) MIC (µg/mL)			IC ₅₀ (µM)		
	<i>S. aureus</i>	<i>Enterococcus faecalis</i>	<i>Enterococcus faecium</i>	<i>Klebsiella pneumoniae</i>	<i>Salmonella enterica</i>	<i>E. coli</i>	Srt A	A549	K562
1-64a	>128	>128	>128	>128	>128	>128	>329.8	77.3	24.2
1-64b	64	>128	>128	128	128	>128	62.7	55.7	28.2
1-64c	32	128	>128	>128	64	>128	43.9	61.2	37.7
1-64d	16	120	120	>128	64	>128	>274.7	70.9	54.2
ampicillin	0.13	0.5	1	---	0.25	8	---	---	---

1.2.2.3. Violaceins

Natural products of the Violacein class are purple-blue pigments produced from bacteria, unlike many other bis-indole natural products which come from marine sponges and tunicates. Violacein (**1-65a**) was first discovered in 1882 by Boisbaudran, *et. al.*³⁷ Natural products of the Violacein class (**1-65a-g**) have been isolated from several Gram-negative bacteria, including

Chromobacterium violaceum, *Janthionobacterium lividum*, *Pseudoalteromonas luteoviolacea*, *Psudomonas* sp., *Collimonas* sp., *Dunganella*. etc.^{38,39,40,41,42} As shown in **Scheme 1.16**, the structure of the Violacein natural products consist of three main sub-classes, the Violaceins (**1-65a-c**), whose two indole moieties are connected by a 1,3-dihydro-2*H*-pyrrol-2-one core linker, the Protoviolaceinic Acids (**1-65d-e**), whose two indole moieties are connected by a pyrrole-2-carboxylic acid linker, and the Proviolaceins (**1-65f-g**), which contain a 2*H*-pyrrol-2-one core. These various sub-classes are produced from the same biosynthetic pathway, either as related paths or as intermediates toward one another.⁴³ In addition, these natural products exhibit significant biological activity, such as antibacterial, antifungal, anticancer, antiviral, and antiparasitic activity.⁴⁴

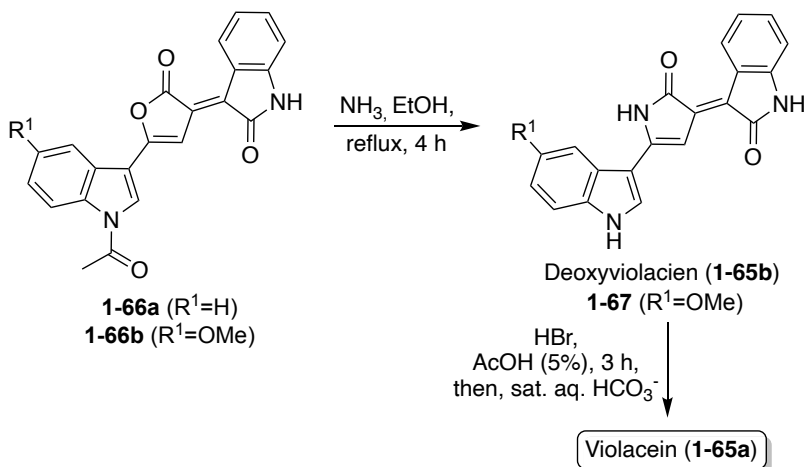
Scheme 1.16. Chemical structures of Violacein (**1-65a**) and related natural product analogues (**1-65b-g**).



Natural products of the Violacein class (**1-65a-g**) have been most widely accessed via exploration of biosynthetic pathways.⁴³ However, these biosynthetic pathways fall outside the scope of this review. Progress has also been made toward the total synthesis of these compounds. The first total synthesis of Violacein and Deoxyviolacein was achieved by Ballantine, *et. al.*⁴⁵ via a key reaction of the lactone intermediates **1-66a** or **1-66b** with ammonia under heating to replace the oxygen atom of the lactone with a nitrogen atom to afford the desired 1,3-dihydro-2*H*-pyrrol-2-one core of Deoxyviolacein (**1-65b**) and imidazolinone intermediate (**1-67**) in good

yields, as is shown in **Scheme 1.17**. Violacein was then accessed after an additional demethylation step of **1-67** to complete the first total synthesis of Violacein (**1-65a**).⁴⁵

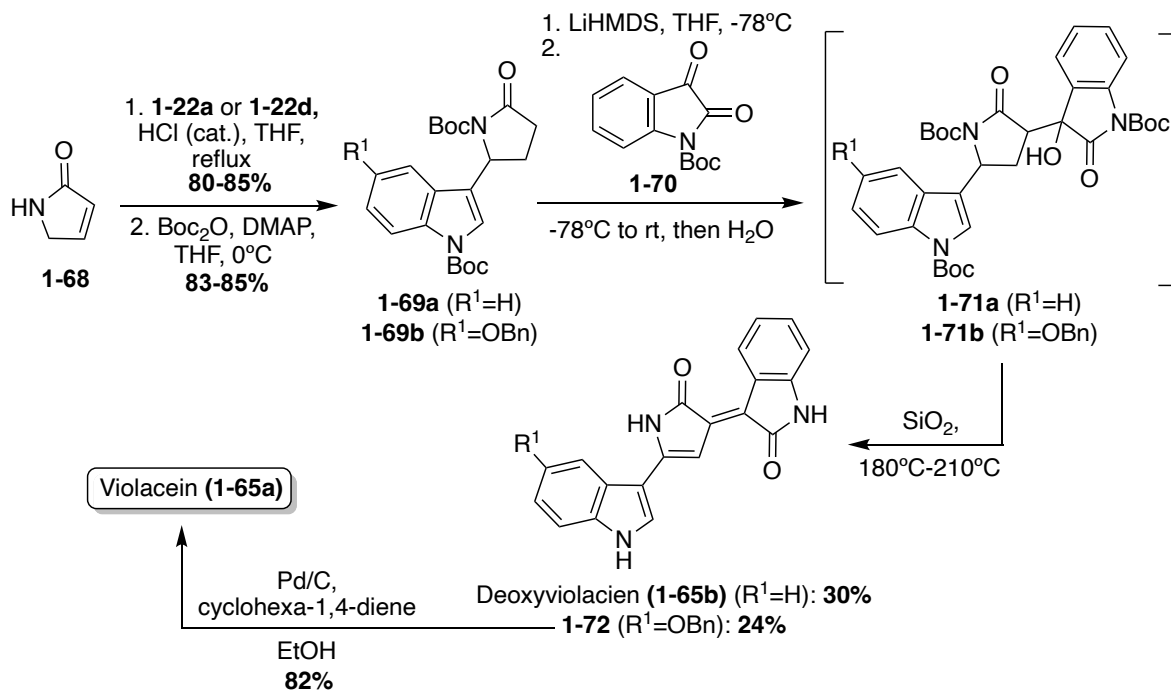
Scheme 1.17. Total synthesis of Violacein (**1-65a**) and Deoxyviolacein (**1-65b**).



Violacein and Deoxyviolacein were also accessed via total synthesis in 2001, in which Steglich, *et. al.* implemented a strategy where the two indole groups were attached stepwise to an already formed pyrrolinone core, as shown in **Scheme 1.18**.⁴⁶ First, pyrrolinone **1-68** underwent an acid-catalyzed reaction with **1-22a** or **1-22d**, and subsequent protection of both the nitrogens via Boc-anhydride, to access intermediates **1-69a-b** in high yields. Then, **1-69a-b** were converted to their corresponding enolates using LiHMDS as the base, followed by subsequent reaction with *N*-Boc-isatin (**1-70**) to afford the aldol condensation intermediates (**1-71a-b**). Then, **1-71a-b** were immediately heated to afford Deoxyviolacein (**1-65b**) and intermediate **1-72** in 30% and 24%, respectively. It is noteworthy to mention that upon adsorption to silica gel and heating for 15-20 minutes, dehydration, dehydrogenation, and cleavage of the Boc-protecting groups all occurred simultaneously. Lastly, **1-72** underwent debenzoylation to access Violacein (**1-65a**) in 82% yield. The configurations of **1-65a-b** were confirmed as (*E*)-isomers via NMR.⁴⁶ This

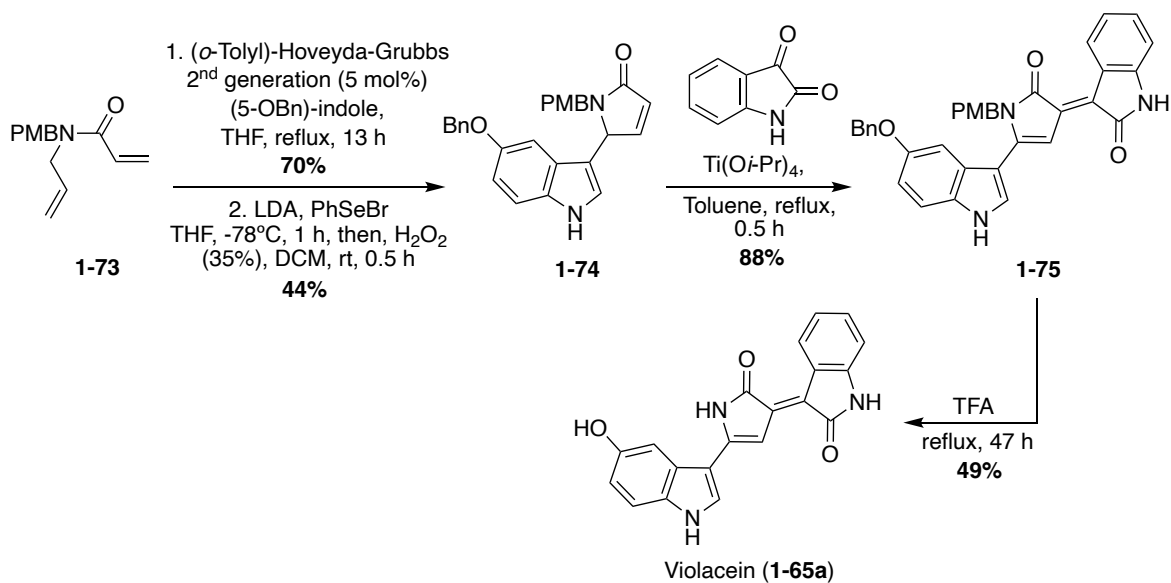
approach was advantageous as it was significantly higher yielding than the first reported total synthesis of these natural products (**1-65a-b**).

Scheme 1.18. Total synthesis of Violacein (**1-65a**) and Deoxyviolacein (**1-65b**).



A more recent approach used a tandem ring-closing metathesis (RCM)/ isomerization/ nucleophilic addition sequence toward the total synthesis of Violacein, as shown in **Scheme 1.19**.⁴⁷ This tandem RCM/ isomerization/ nucleophilic addition was the first step used in the total synthesis, followed by elimination to intermediate **1-74** in good yields. The oxindole moiety was then attached via a Ti-catalyzed tautomerization/aldol condensation with isatin to access **1-75** in high yield. After acid-mediated removal of protecting groups, Violacein (**1-65a**) was achieved in 49% yield. The authors mentioned that the final product **1-65a** was very difficult to handle and had very minimal solubility in common solvents. Therefore, it was suspected that the crude yield was significantly higher than the isolated yield.⁴⁷

Scheme 1.19. Total synthesis of Violacein (**1-65a**) via a tandem RCM/isomerization/nucleophilic addition sequence.



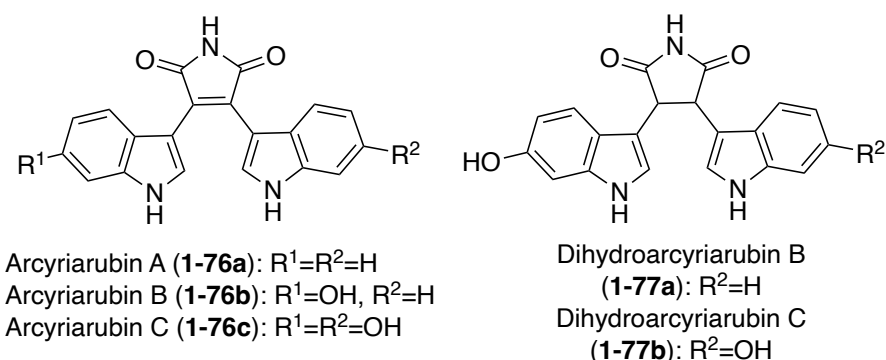
1.2.3. Pyrrole and pyrrole-dione linker moieties

1.2.3.1. Arcyriarubins

Arcyriarubins A-C (**1-76a-c**) are bisindolylmaleimides first isolated by Steglich, *et. al.* in 1980 from the red sporangia of the slime mold *Arcyria denudate*.⁴⁸ Arcyriarubins B (**1-76b**) and C (**1-76c**) were also isolated from *Tubifera casparyi* in 2003 by Ishibashi, *et. al.*⁴⁹ The chemical structure (**Scheme 1.20**) of these compounds was elucidated by spectroscopic means.

Arcyriarubins A-C (**1-76a-c**) contain two indole moieties linked by a pyrrole-2,5-dione (maleimide) core. These natural products display moderate antibiotic, antifungal, cytotoxic, and kinase inhibition activities.^{48,49} These natural products are also of great interest, as many structurally related bisindolylmaleimides are selective protein kinase C (PKC) inhibitors, which show promise as novel potential therapeutics for autoimmune diseases.^{50,51}

Scheme 1.20. Chemical structures of Arcyriarubins A-C (**1-76a-c**) and Dihydroarcyriarubins A-B (**1-77a-b**).

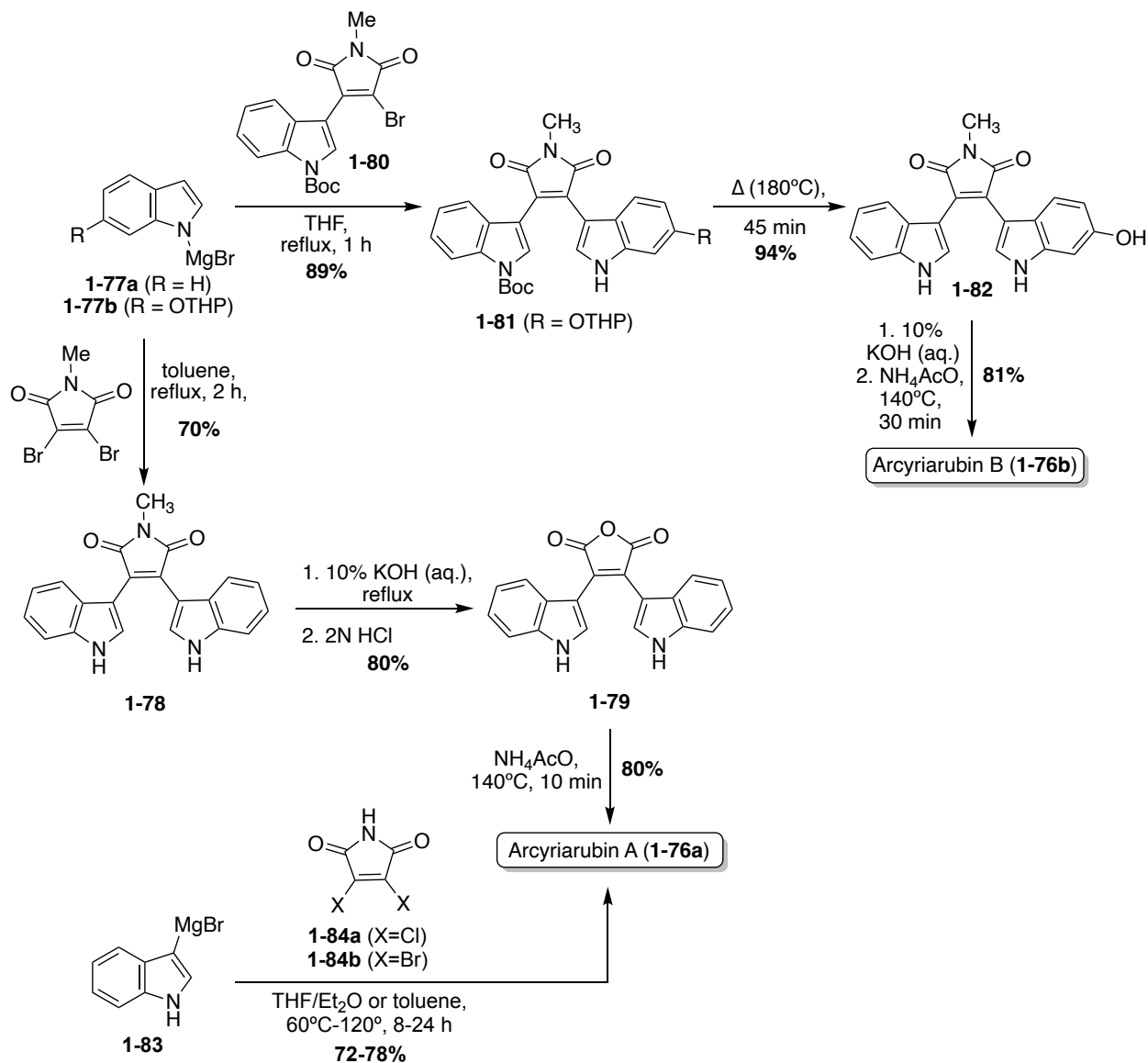


In addition, two structurally related natural products that have also been isolated include Dihydroarcyriarubins B (**1-77a**) and C (**1-77b**). As shown in **Scheme 1.20**, these natural products are incredibly similar to the Arcyriarubins (**1-76a-c**), however, the reduced pyrrolidine-2,5-dione (succinimide) core of the Dihydroarcyriarubins (**1-77a-b**) sets them apart. Dihydroarcyriarubin B (**1-77a**) was first isolated by Steglich, *et. al.* from the slime mold, *Arcyria denudate*, alongside the Arcyriarubins (**1-76a-b**).⁴⁸ Dihydroarcyriarubin C (**1-77b**) was first isolated in 2003 by Ishibashi, *et. al.* from *Arcyria ferruginae*, alongside Arcyriarubin C (**1-76b**).⁴⁹ The biological activities of the Dihydroarcyriarubins B (**1-77a**) and C (**1-77b**) are very similar to that of **1-76a-c**, including antibiotic, antifungal, cytotoxic, and kinase inhibition activities.^{48,49,52}

The first natural products of the Arcyriarubin class to be accessed via total synthesis were Arcyriarubin A (**1-76a**) and Arcyriarubin B (**1-76b**) in 1988 by Steglich, *et. al.*⁵³ These total syntheses were accomplished using Grignard reactions to install the indole moieties on the maleimide core, as shown in **Scheme 1.21**. In the first total synthesis of Arcyriarubin A (**1-76a**), a Grignard reaction was carried out via an indole Grignard reagent and 3,4-dibromo-*N*-methylmaleimide to access bisindolylmaleimide intermediate (**1-78**) in high yield. To remove the methyl group of **1-78**, a maleic anhydride intermediate (**1-79**) was accessed and then

subsequently reacted with ammonium acetate at high temperatures to access Arcyriarubin A (**1-76a**) in high yields.⁵³

Scheme 1.21. Total syntheses of Arcyriarubins A-B (**1-76a-b**).



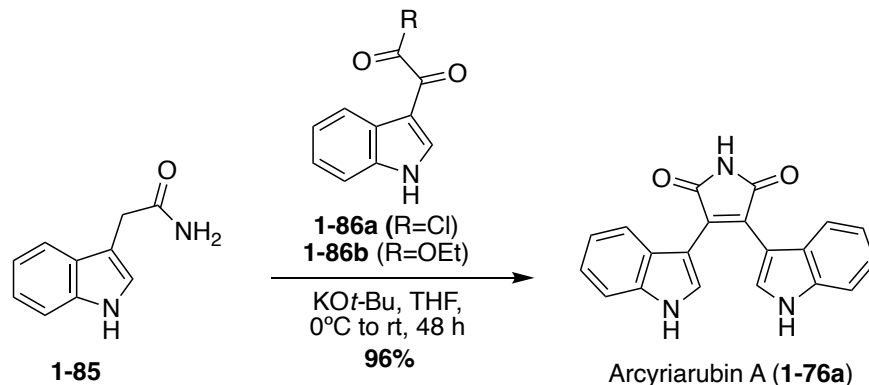
Due to the asymmetric nature of the indole moieties in Arcyriarubin B (**1-76b**), the synthetic approach to this natural product was slightly different. As shown in **Scheme 1.21**, the first total synthesis of **1-76b** was achieved via a reaction of an indole Grignard reagent (**1-77b**) with a mono-indolic maleimide intermediate (**1-80**) to access intermediate **1-81** in 89% yield.

This approach allowed for the synthesis of a maleimide intermediate with asymmetric indole moieties (**1-81**) in a stepwise manner. After de-methylation and removal of protecting groups, Arcyriarubin B (**1-76b**) was accessed in high yield.⁵³

Several years later, a similar Grignard approach to the total synthesis of Arcyriarubin A (**1-76a**) was utilized in 1995 (**Scheme 1.21**).⁵⁴ Here, an indole Grignard (**1-83**) was reacted with 3,4-dichloromaleimide (**1-84a**) at high temperature to access Arcyriarubin A (**1-76a**) in 72% yield. This approach was advantageous in that it allowed for the synthesis of Arcyriarubin A (**1-76a**) without the need for protecting groups, which greatly expediting its synthesis.⁵⁴ However, the intolerance for asymmetric indole moieties in this method makes it unsuitable for application to other Arcyriarubins. This Grignard strategy was again slightly improved upon in 2017 for the total synthesis of Arcyriarubin A (**1-76a**), as shown in **Scheme 1.21**.⁵⁵ Utilizing the same indole Grignard (**1-83**) and 3,4-dibromomaleimide (**1-84b**) at a higher temperature, for a shorter reaction time, Arcyriarubin A (**1-76a**) was synthesized in 78% yield.⁵⁵ It is also noteworthy to mention that Arcyriarubin C (**1-76c**) has yet to be accessed via total synthesis.

In addition to this Grignard approach, a more biomimetic approach has also been explored toward the total synthesis of Arcyriarubin A (**1-76a**), as shown in **Scheme 1.22**. This approach consisted of a base-mediated condensation-cyclization reaction between an indole-3-acetamide intermediate (**1-85**) and an indole-3-oxo-acyl chloride intermediate (**1-86a**) to access Arcyriarubin A (**1-76a**), although in a low 11% yield. Recently, an adapted and improved biomimetic total synthesis of Arcyriarubin A (**1-76a**) was developed, as shown in **Scheme 1.22**. For this approach, intermediate **1-85** was condensed and cyclized with an indole-3-oxo-ester intermediate (**1-86b**) to access Arcyriarubin A (**1-76a**) in an excellent 96% yield.⁵⁶

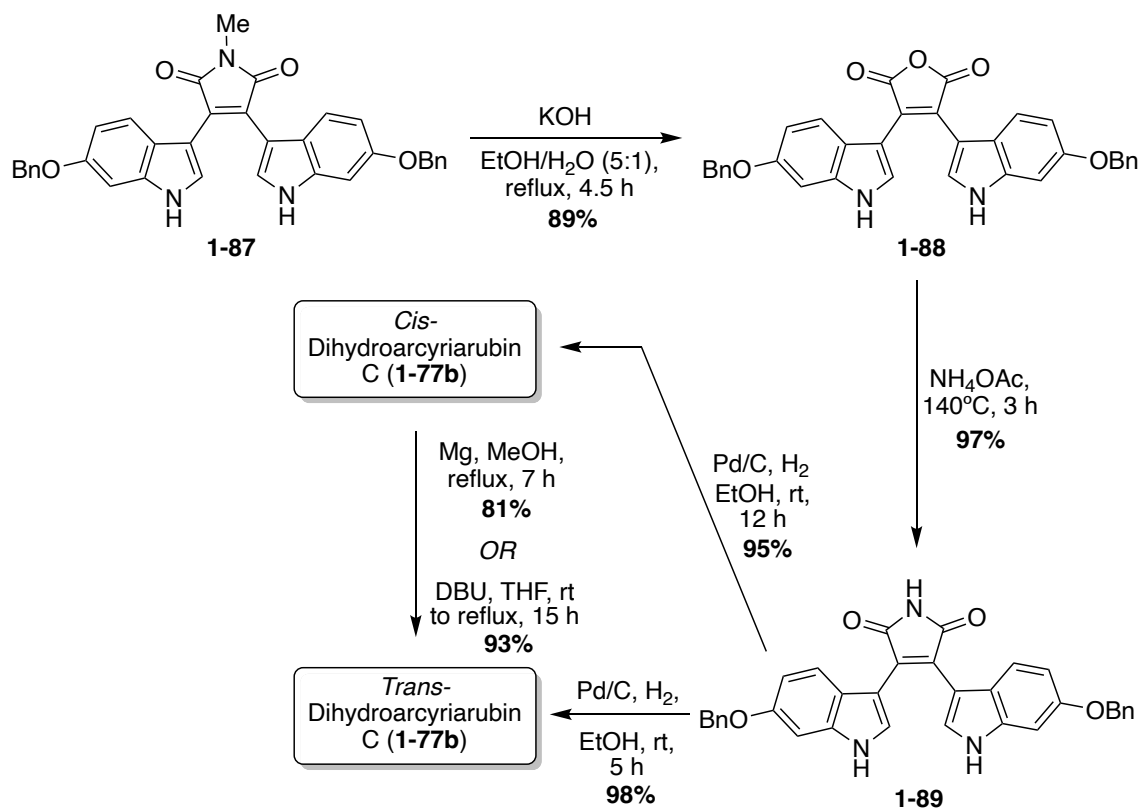
Scheme 1.22. Total synthesis of Arcyriarubin A (**1-76a**).



In terms of the Dihydroarcyriarubins (**1-77a-b**), Dihydroarcyriarubin B (**1-77a**) has yet to be accessed via total synthesis. On the other hand, the first total synthesis of Dihydroarcyriarubin C (**1-77b**) was completed in 2007 by Ishibashi, *et. al.*, as shown below in **Scheme 1.23**.⁵² First, the bis-indolyl-*N*-methylmaleimide intermediate (**1-87**) was synthesized in four steps from 3,4-dibromomaleimide and 6-benzyloxyindole, following the same Grignard approach as was previously published by Steglich, *et. al.*⁵³ To remove the *N*-methyl group, intermediate **1-87** was converted to the maleic anhydride intermediate (**1-88**), which was subsequently reacted with ammonium acetate at high temperatures to access the bis-indolylmaleimide intermediate (**1-89**) in very high yields. Then, **1-89** underwent hydrogenation to reduce the maleimide core of **1-89** to the succinimide core of Dihydroarcyriarubin C (**77b**). In addition to the desired reduction of **1-89**, both benzyl groups were also removed. While this was beneficial for the total synthesis of Dihydroarcyriarubin C (**1-77b**); it was also the reason why this approach was not viable for synthesizing Arcyriarubin C (**1-76c**). It is noteworthy to mention that at a 12-hour hydrogenation reaction time, *cis*- Dihydroarcyriarubin C (**1-77b**) was accessed in 95% yield, but at a 5-hour reaction time, *trans*- Dihydroarcyriarubin C (**1-77b**) was accessed in 98% yield. In addition, *cis*- Dihydroarcyriarubin C (**1-77b**) could be isomerized to *trans*- Dihydroarcyriarubin C (**1-77b**) either by magnesium in methanol or DBU in tetrahydrofuran in 81% and 93% yield, respectively.

To accomplish the first total synthesis of Dihydroarcyriarubin C (**1-77b**), both the *cis*-(**1-77b**) and *trans*-(**1-77b**) isomers were synthesized to allow for the stereochemical determination of the isolated Dihydroarcyriarubin C (**1-77b**). Comparison of their NMR data allowed for confirmation of the isolated **1-77b** as *trans*-Dihydroarcyriarubin C (**1-77b**).⁵²

Scheme 1.23. Total synthesis of Dihydroarcyriarubin C (**1-77b**).

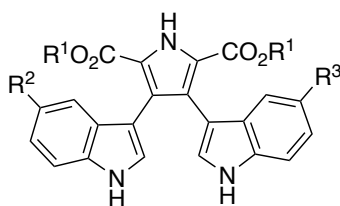


1.2.3.2. Lycogarubins

Lycogarubins A-C (**1-90a-c**) and Lycagolic acid (**1-90d**) were first isolated independently by Steglich, *et. al.* and Asakawa, *et. al.* from *Lycogala epidendrum*, a slime mold (Myxomycetes).^{57,58} Lycagolic Acid (**1-90d**) has also been referred to as chromopyrrolic acid (CPA). The chemical structures of these natural products were elucidated via spectroscopic analysis. As shown below in **Scheme 1.24**, the two indole moieties of these bis-indole natural products are linked by a pyrrole-2,5-methyl ester core in Lycogarubins A-C (**1-90a-c**) or a

pyrrole-2,5-carboxylic acid core in Lycagolic acid (**1-90d**). These natural products closely resemble the previously discussed Arcyriarubin natural products (**1-76a-c**), differing mainly in the aromatic pyrrole core of **1-90a-d** rather than the maleimide core of **1-76a-c**. Much of the biological activity of these natural products is unexplored, though Lycogarubin C displayed moderate anti-HSV-I virus activity.⁵⁸ In addition, these compounds are of interest due to their structural similarity to potent kinase inhibitors.⁵²

Scheme 1.24. Chemical structures of Lycogarubins A-C (**1-90a-c**).



Lycogarubin A (**1-90a**): $R^1=Me$, $R^2=OH$, $R^3=OH$

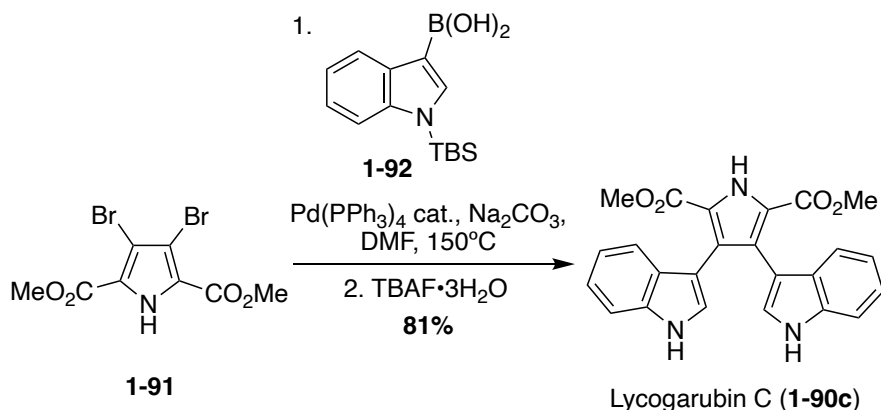
Lycogarubin B (**1-90b**): $R^1=Me$, $R^2=H$, $R^3=OH$

Lycogarubin C (**1-90c**): $R^1=Me$, $R^2=R^3=H$

Lycagolic Acid (**1-90d**): $R^1=R^2=R^3=H$

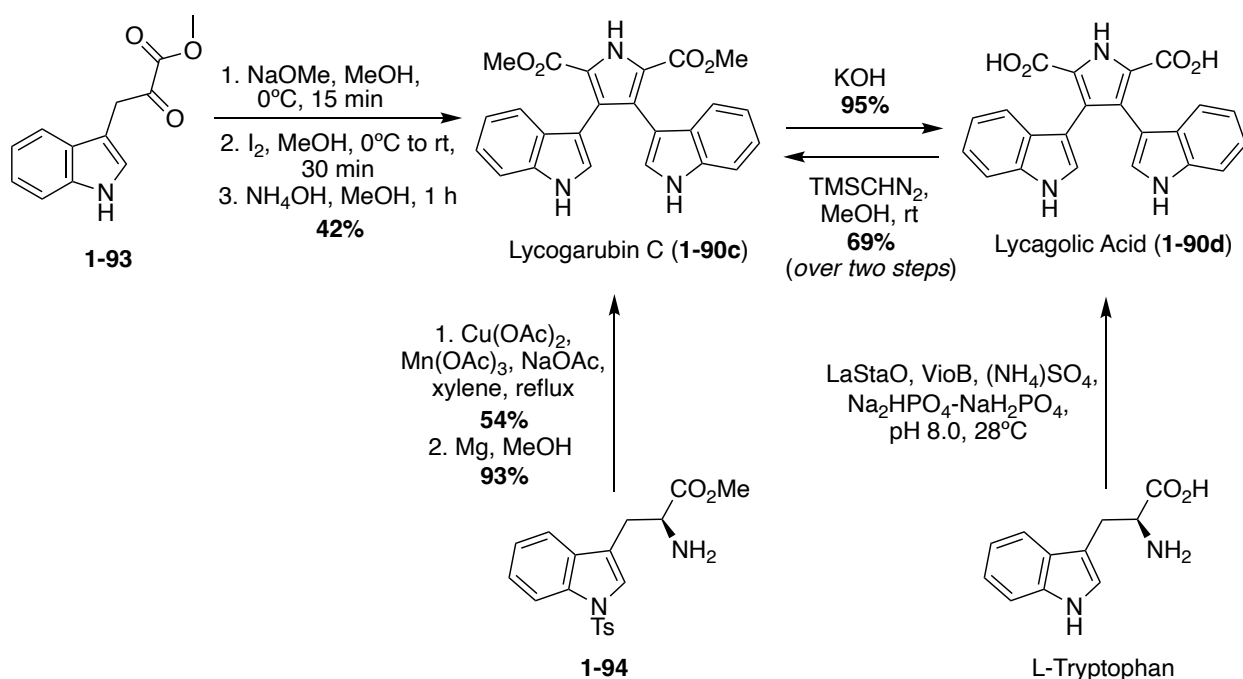
Many of the early syntheses of the Lycogarubins (**1-90a-c**) and Lycagolic acid (**1-90d**) were carried out via the exploration of the biosynthetic pathway to these natural products.⁵⁹ However, the first of these natural products to be accessed via total synthesis was Lycogarubin C (**1-90c**) using a palladium-catalyzed Suzuki coupling reaction of dimethyl 3,4-dibromo-1*H*-pyrrole-2,5-dicarboxylate (**1-91**) with an indole-3-boronic acid (**1-92**) and subsequent removal of the protecting group via TBAF to access Lycogarubin C (**1-90c**) in 81% yield, as shown in **Scheme 1.25**.³⁵

Scheme 1.25. Total synthesis of Lycogarubin C (**1-90c**).



This Suzuki method has been implemented in recent literature as well in the synthesis of **1-90c** and similar structures.⁶⁰ Considering the ongoing study of the biosynthesis of the Lycogarubin natural products, several biomimetic syntheses have been developed as well. One of the earliest of these was completed in 2006 in which a methyl 3-(1*H*-indol-3-yl)-2-oxopropanoate intermediate (**1-93**) underwent a dimerization/cyclization sequence over three steps to access Lycogarubin C (**1-90c**) in 42% yield (Scheme 1.26).^{59,61}

Scheme 1.26. Biomimetic total syntheses of Lycogarubin C (**1-90c**) and Lycagolic acid (**1-90d**).

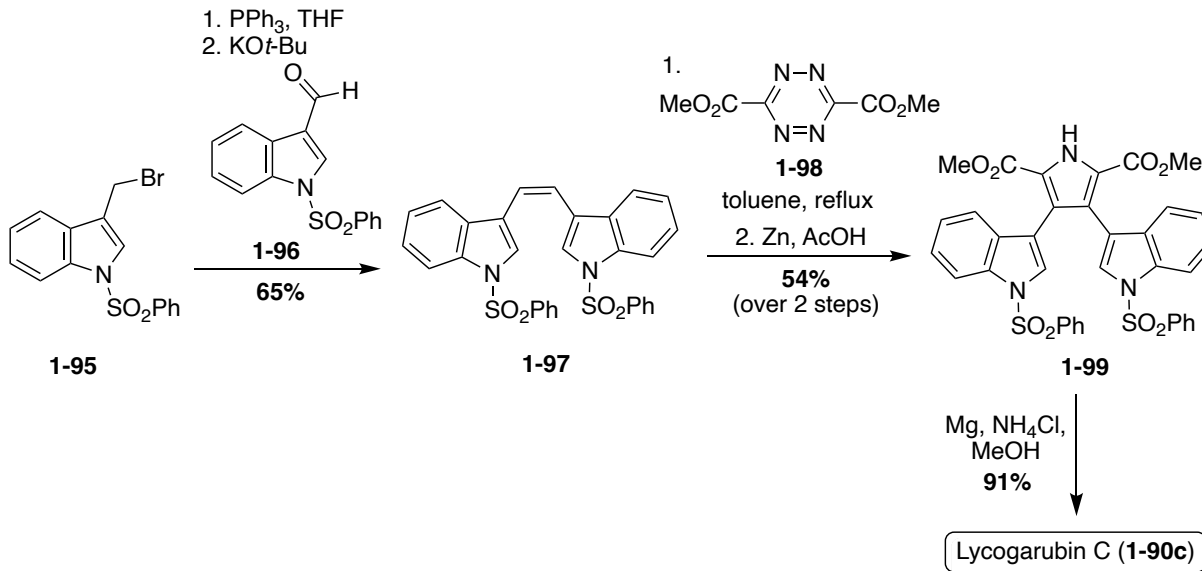


Another biomimetic synthesis of Lycogarubin C (**1-90c**), as well as Lycagolic acid (**1-90d**), was carried out via a Cu/Mn co-oxidized dimerization/cyclization of a Tosyl-tryptophan methyl ester (**1-94**) with another molecule of itself (**Scheme 1.26**). It is noteworthy to mention that biosynthesis of the Lycogarubins also begins with tryptophan starting materials. After removal of the protecting groups, Lycogarubin C (**1-90c**) was accessed in high yields. Lycogarubin C (**1-90c**) was then converted to Lycagolic acid (**1-90d**) in 95% yield via base-catalyzed ester hydrolysis.⁶²

Recently, a semi-total synthesis of Lycogarubin C (**1-90c**) was completed via Lycagolic acid (**1-90d**) as an intermediate (**Scheme 1.26**). First, enzymatic biological reactions were conducted to accomplish the dimerization/cyclization of the L-Tryptophan (L-Trp) starting material (**1-94**) to access Lycagolic acid (**1-90d**). Then, **1-90d** was immediately reacted with TMSCHN₂ in methanol to access Lycogarubin C (**1-90c**) in 69% over two steps from the simple and readily accessible L-Trp (**1-94**) starting material.⁶³

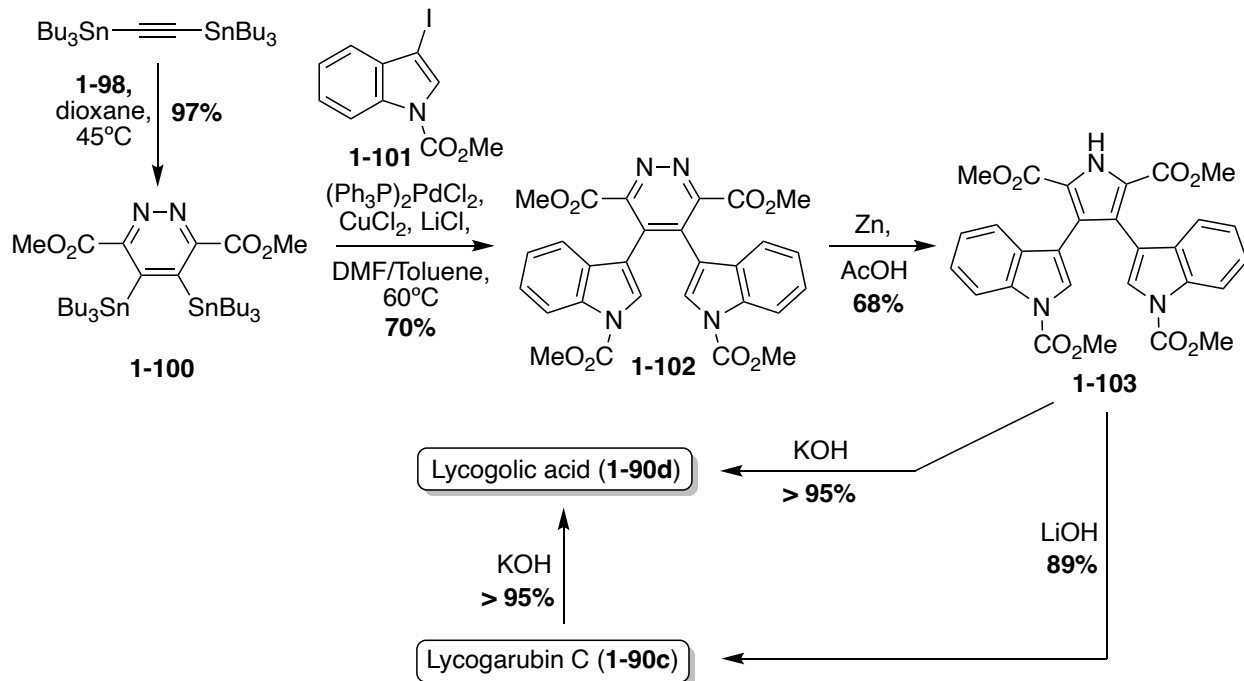
Another synthetic method that has been used to synthesize Lycogarubin C (**1-90c**) and Lycagolic acid (**1-90d**) was the use of key Diels-Alder and Kornfeld-Boger ring contraction reactions. One example utilizing this method, as shown in **Scheme 1.27**, began with the synthesis of the di-protected-bis-indole alkene intermediate (**1-97**) via a Wittig reaction between the bromide intermediate (**1-95**) and the aldehyde intermediate (**1-96**). Then, **1-97** underwent a Diels-Alder reaction with the tetrazine intermediate (**1-98**), followed by a subsequent Kornfeld-Boger ring contraction to access the pyrrole intermediate (**1-99**) in 54% yield over two steps. After removal of the protecting groups, Lycogarubin C (**1-90c**) was accessed in 91% yield. Protection of both indole moieties was necessary to access intermediate **1-99** in good yields and to avoid side product formation via the Diels-Alder/ Kornfeld-Boger reaction sequence.⁶⁴

Scheme 1.27. Total synthesis of Lycogarubin C (**1-90c**).



Another example in which this method was implemented, as shown in **Scheme 1.28**, began with the Diels-Alder reaction between **1-98** and 1,2-bis-(tributylstannyl)-acetylene to access diazine intermediate (**1-100**) in very high yield. Stille coupling of **1-100** with the 3-iodo-indole intermediate (**1-101**) and a subsequent Kornfeld-Boger ring contraction of the diazine core led to the desired pyrrole core of **1-103** in good yields. Then, **1-103** could be subjected to LiOH or KOH to access Lycogarubin C (**1-90c**) or Lycagolic acid (**1-90d**), respectively, in very high yields. Furthermore, Lycogarubin C (**1-90c**) could also be converted to Lycagolic acid (**1-90d**) via KOH in very high yields.⁶⁵ This approach (**Scheme 1.28**) is favorable in comparison to the previously discussed Diels-Alder/Kornfeld Boger approach (**Scheme 1.27**), as it not only allowed for the total synthesis of Lycogarubin C (**1-90c**) in good yields, but also allowed for the total synthesis of Lycagolic acid (**1-90d**) in good yields.

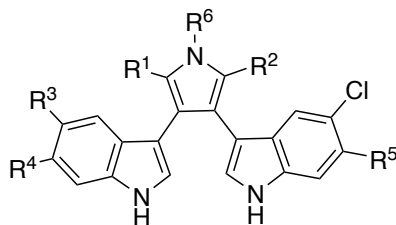
Scheme 1.28. Total syntheses of Lycogarubin C (**1-90c**) and Lycagolic acid (**1-90d**).



1.2.3.3. Lynamincins

More recently, a class of natural products that is structurally related to the Lycogarubins (**1-90a-d**) was discovered. In 2008, Lynamincins A-E (**1-104a-e**) were isolated by Potts, *et al.* from a novel marine actinomycete of the proposed genus *Marinispora*. The chlorinated bis-indole chemical structures linked by a pyrrole moiety, as shown in **Scheme 1.29**, was confirmed in these natural products via spectroscopic methods.⁶⁶ Not only were these natural products (**1-104a-e**) the first examples of bis-indole pyrrole alkaloids bearing chloride substituents, but the Lynamincins A-E (**1-104a-e**) have also been found to display broad-spectrum antibiotic activity against both Gram-positive and Gram-negative bacteria, such as *Staphylococcus aureus* and *Enterococcus faecium*.⁶⁶ The Lynamincins have also been shown to possess anticancer and kinase inhibition activity.⁶⁷

Scheme 1.29. Chemical structures of Lynamycins A-G (**1-104a-g**).



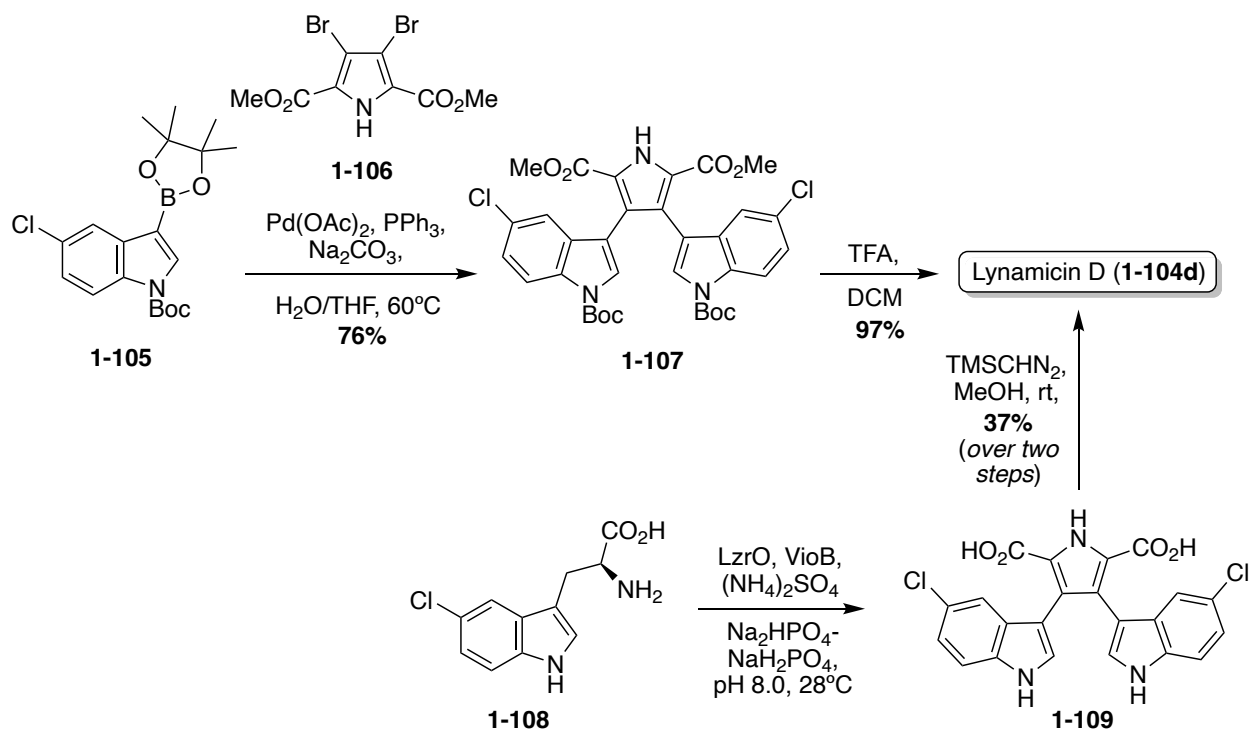
Lynamycin A (**1-104a**): R¹=H, R²=COOMe, R³=Cl, R⁴=H, R⁵=H
Lynamycin B (**1-104b**): R¹=H, R²=COOMe, R³=Cl, R⁴=Cl, R⁵=H
Lynamycin C (**1-104c**): R¹=H, R²=H, R³=Cl, R⁴=Cl, R⁵=Cl
Lynamycin D (**1-104d**): R¹=COOMe, R²=COOMe, R³=Cl, R⁴=H, R⁵=H
Lynamycin E (**1-104e**): R¹=COOMe, R²=COOMe, R³=H, R⁴=H, R⁵=Cl
Lynamycin F (**1-104f**): R¹=H, R²=COOMe, R³=Cl, R⁴=H, R⁵=H, R⁶=Me
Lynamycin G (**1-104g**): R¹=R²=COOMe, R³=Cl, R⁴=H, R⁵=H, R⁶=Me

Two additional natural products of the Lynamycin class, Lynamycin F (**1-104f**) and Lynamycin G (**1-104g**), were isolated in 2014 by Zhang, *et. al.*⁶⁸ from the deep-sea-derived actinomycete, *Streptomyces* sp. The chemical structures of Lynamycin F (**1-104f**) and Lynamycin G (**1-104g**), as shown in **Scheme 1.29**, were elucidated via spectroscopic methods. The characteristic *N*-methyl group in **1-104f** and **1-104g** was confirmed via key HMBC correlations between the hydrogens on the methyl group and the C-2 and C-5 carbons of the pyrrole ring. Interestingly, the presence of this methyl group seems to have a significant effect on biological activity because, unlike Lynamycins A-E (**1-104a-e**), Lynamycin F (**1-104f**) and Lynamycin G (**1-104g**) showed no significant antibiotic activity against *Staphylococcus aureus*, *Escherichia coli*, etc. and no significant cytotoxic activity toward cancer cell lines.⁶⁸

The first of the Lycogarubin class to be accessed via total synthesis was Lynamycin D (**1-104d**) by Nikolakaki, *et. al.* in 2017, which utilized a Suzuki coupling approach to install the two indole moieties to the pyrrole core.⁶⁸ As shown in **Scheme 1.30**, first, the 3,4-dibromopyrrole intermediate **1-106** was initially synthesized in two steps from the corresponding pyrrole-2-methylester in good yields. An indolic boronic ester intermediate (**1-105**) then underwent a

palladium-catalyzed Suzuki reaction with **1-106** to access intermediate **1-107** in 76% yield. After removal of the Boc protecting groups via acidic conditions, Lynamycin D (**1-104d**) was achieved in 97% yield.⁶⁸ Recently, a semi-total synthesis of Lynamycin D (**1-104d**), resembling that of Lycogarubin C (**1-90c**), was also completed (**Scheme 1.30**).⁶³ First, enzymatic biological reactions were conducted to accomplish the dimerization/cyclization of the 5-chloro-L-Tryptophan (5-Cl-L-Trp) starting material (**1-108**), following the biosynthetic path, to access the carboxylic acid analogue of Lynamycin D (**1-109**). Then, **1-109** was immediately reacted with TMSCHN₂ in MeOH to access Lynamycin D (**1-104d**) in 37% over two steps from the simple 5-Cl-L-Trp (**1-108**) starting material.⁶³

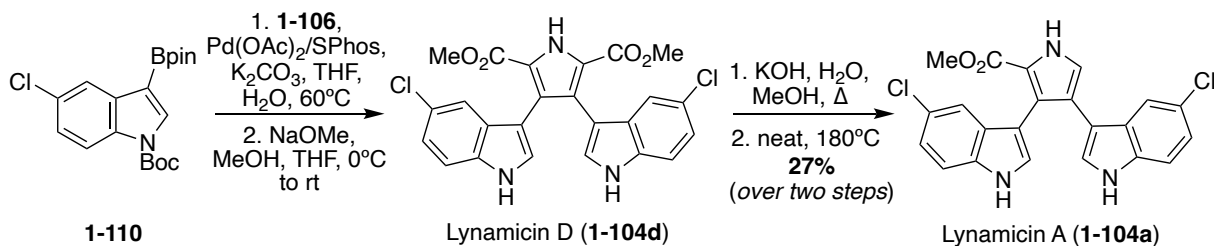
Scheme 1.30. Total synthesis of Lynamycin D (**1-104d**).



The first total synthesis of Lynamycin A (**1-104a**) was completed in 2021 by Smith, *et. al.*, as well as a slightly adapted total synthesis of Lynamycin D (**1-104d**).⁶⁹ As shown in **Scheme**

1.31, these total syntheses follow a very similar Suzuki cross-coupling to that of Nikolakaki's previously discussed method to install the indole moieties onto the pyrrole core of these natural products.⁶⁷ However, the Suzuki cross coupling step between the boronic ester intermediate (**1-110**) and the 3,4-dibromo pyrrole intermediate (**1-106**) utilized different palladium catalysts, as shown in **Scheme 1.31**, and featured a subsequent deprotection of the protecting groups to access Lynamycin D (**1-104d**) in 67% yield. Then, Lynamycin D (**1-104d**) was subjected to a basic environment, at high temperatures, which led to the removal of one of the ester groups on the pyrrole ring, accessing Lynamycin A (**1-104a**) in 67% yield.⁶⁹ Lynamycins B, C, and E-G (**1-104b, c, e-g**) have yet to be accessed via total synthesis.

Scheme 1.31. Total synthesis of Lynamycin A (**1-104a**).



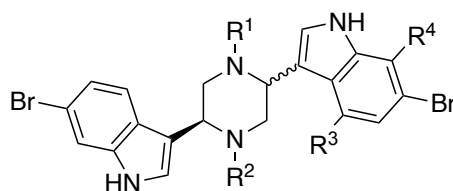
1.2.4. Piperazine, piperazinone, and pyridine linker moieties

1.2.4.1. Dragmacidins

The Dragmacidin class of natural products consists of two main structural sub-classes. The first sub-class consists of Dragmacidin (**1-111**) and Dragmacidins A-C (**1-111a-c**), which are bis-indole alkaloids whose two indole moieties are linked by a piperazine core, as shown in **Scheme 1.32**. Dragmacidin was first isolated in 1988, by Koehn *et. al.*, from *Dragmacidon* marine sponge.⁷⁰ A couple years later, Dragmacidin A (**1-111a**) and Dragmacidin B (**1-111b**) were isolated from *Hexadella* marine sponge.¹⁰ The chemical structure of these natural products was elucidated via spectroscopic methods. Dragmacidin (**1-111**) and Dragmacidins A-B (**1-111a-**

b) were confirmed to have *trans* configurations.^{10,71} Dragmacidin C (**1-111c**) was the last of this sub-class to be discovered and was first isolated in 1991, by Smith, *et. al.*, from the sea squirt *Didenium candidum*.⁷¹ Dragmacidin C (**1-111c**) was initially thought to have *trans* configuration, but it was later shown to be of *cis* configuration.⁷² The biological activities of Dragmacidin (**1-111**) and Dragmacidins A-C (**1-111a-c**) are relatively unexplored; however, Dragmacidin (**1-111**) and Dragmacidin A (**1-111a**) have been found to display significant cytotoxicity against a variety of cancer cell lines.⁷⁰

Scheme 1.32. Chemical structures of Dragmacidin (**1-111**) and Dragmacidins A-C (**1-111a-c**).

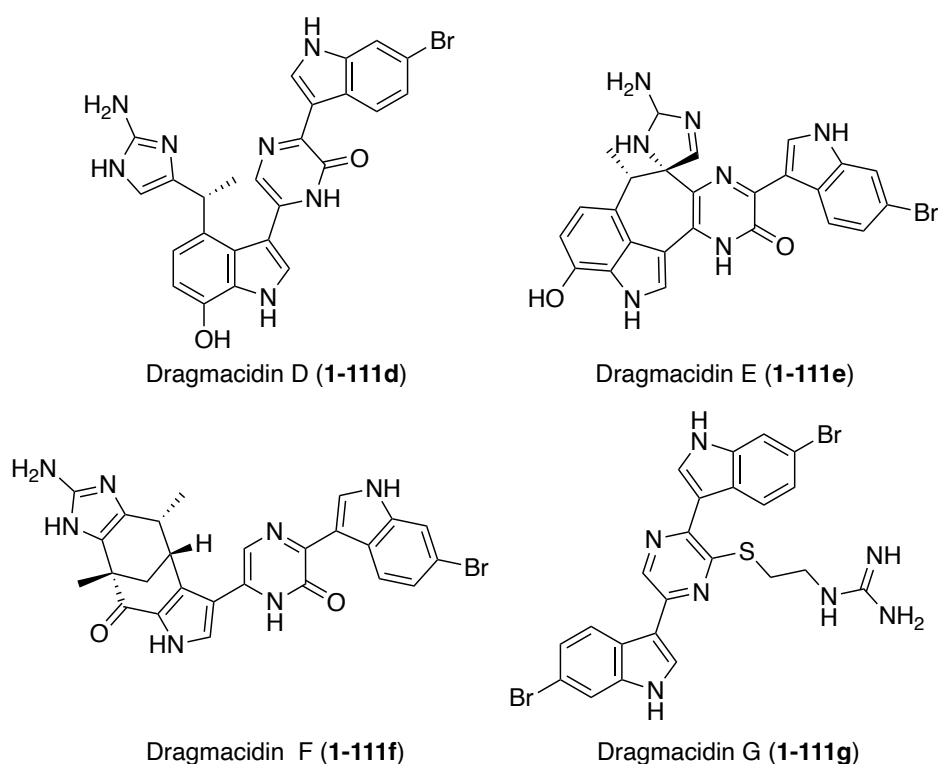


(*Cis*)-Dragmacidin (**1-111**): R¹=H, R²=Me, R³=OH, R⁴=Br
Trans-Dragmacidin A (**1-111a**): R¹=Me, R²=R³=R⁴=H
Trans-Dragmacidin B (**1-111b**): R¹=R²=Me, R³=R⁴=H
Cis-Dragmacidin C (**1-111c**): R¹=R²=R³=R⁴=H

The second sub-class of the Dragmacidins is comprised of more structurally complex natural products, including Dragmacidins D (**1-111d**), E, (**1-111e**), and F (**1-111f**). These bis-indole natural products (**1-111d-f**) contain a 2-pyridone core that links their two indole, or modified indole, moieties, as shown in **Scheme 1.33**. Another structural distinction of this sub-class is the presence of a guanidine moiety. Dragmacidin D (**1-111d**) and Dragmacidin E (**1-111e**) were isolated in 1988 by Carroll, *et. al.* from *Spongosorites* and *Hexadella* marine sponges and their structures were elucidated via spectroscopic means.⁷³ In addition, Dragmacidin D (**1-111d**) and Dragmacidin E (**1-111e**) were found to be potent inhibitors of serine-threonine protein phosphatases.⁷³ Dragmacidin F (**1-111f**) was isolated a couple years later, in 2000, by Riccio, *et. al.* from a *Halicortex* marine sponge. The complex ring structure of Dragmacidin F (**1-111f**) was

elucidated via extensive spectroscopic analysis and its unprecedented carbon skeleton was proposed to result from the cyclization of a partially oxidized form of Dragmacidin D (**1-111d**). Dragmacidin F (**1-111f**) was found to display antiviral activity against HSV-1 and HIV-1.⁷⁴ Dragmacidin E (**1-111e**) and Dragmacidin F (**1-111f**) have both been accessed via total synthesis; however, these syntheses will not be discussed in detail as these chemical structures fall outside the scope of this review.^{75,76}

Scheme 1.33. Chemical structures of Dragmacidins D-G (**1-111d-g**).

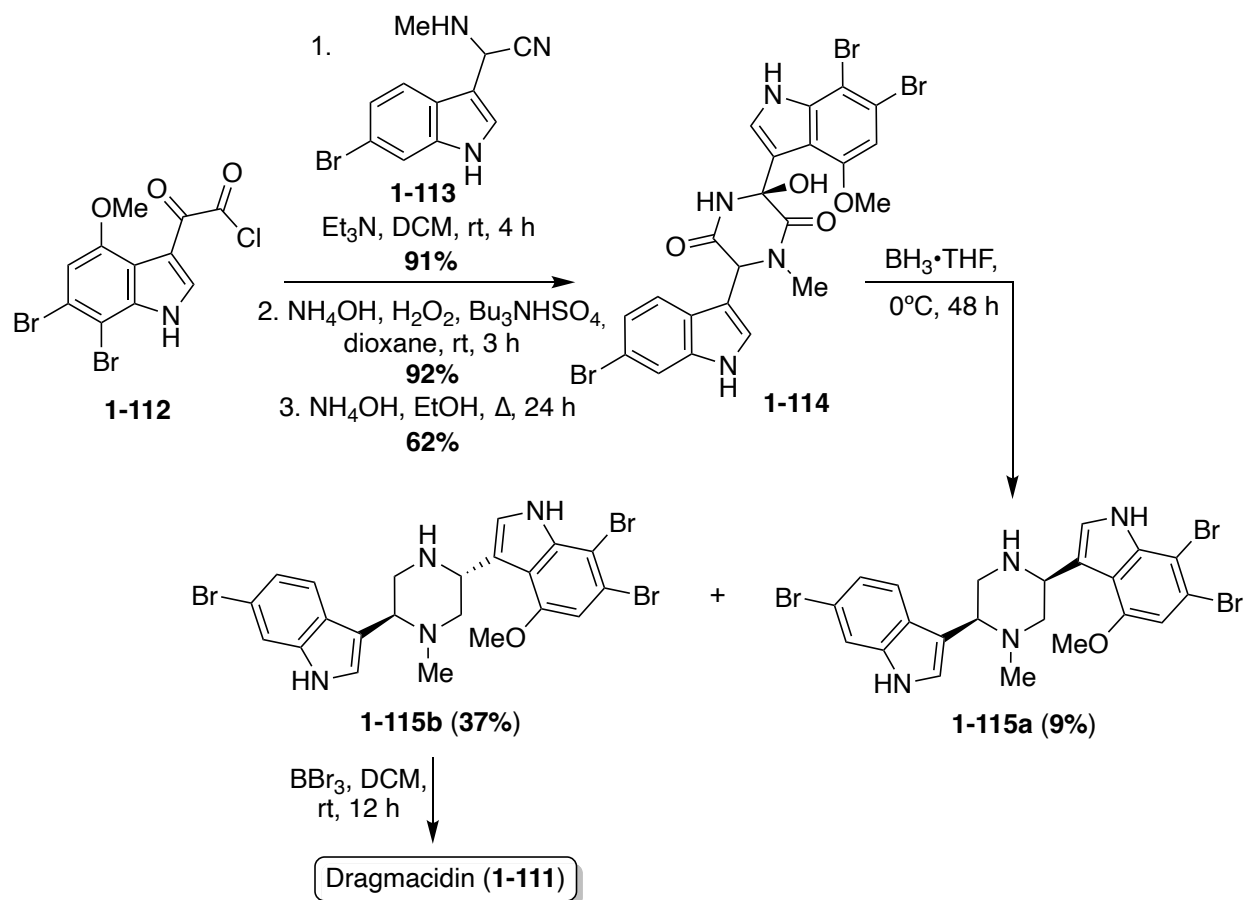


Recently, Dragmacidin G (**1-111g**) was isolated by Wright, *et. al.* from *Spongosorites* marine sponge. As is shown in **Scheme 1.33**, the chemical structure of Dragmacidin G (**1-111g**) does not exactly fit into the second sub-class of the Dragmacidins, as it is the only natural product in its class to contain a piperazine (1,4-diazine) core linking the two indole moieties. However, Dragmacidin G (**1-111g**) does contain a characteristic guanidine moiety, thus enabling it to still be considered part of the second structural sub-class of the Dragmacidins. In addition,

Dragmacidin G (**1-111g**) was found to exhibit antibacterial activity against *Staphylococcus aureus*, *Mycobacterium tuberculosis*, *Plasmodium falciparum*, etc., and cytotoxic activity against a panel of pancreatic cell lines.⁷⁷ Dragmacidin G (**1-111g**) has yet to be accessed via total synthesis.

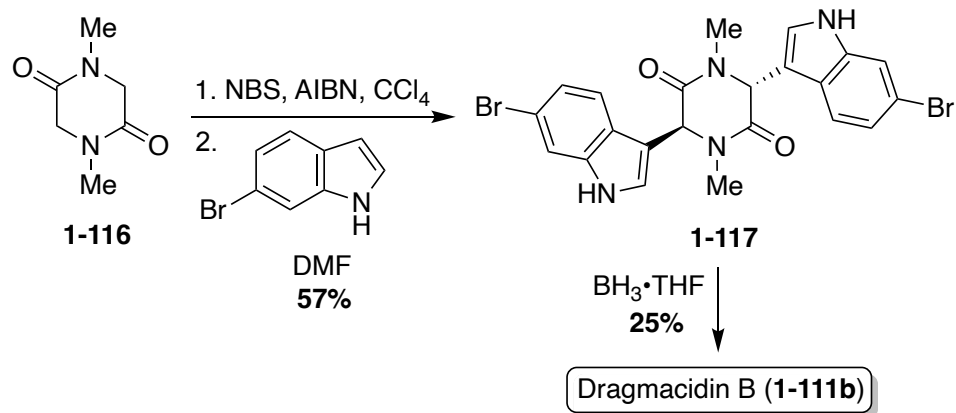
Dragmacidin (**1-111**) was the first natural product of this class to be accessed via total synthesis. In 1994, Wuonola *et. al.* completed the first racemic total synthesis of Dragmacidin (**1-111**) via an initial condensation of an oxo-acyl chloride (**1-112**) and an amino nitrile (**1-113**) (synthesized via a Strecker method), followed by subsequent oxidation and cyclization, as shown in **Scheme 1.34**. These transformations proceeded in high yields. The cyclized intermediate was then subjected to reductive conditions to access **1-115a** and **1-115b**. This reduction, specifically the loss of the hydroxyl group, was not stereoselective at room temperature, resulting in a ratio of (**1-115a**:**1-115b** = 1:1). However, significant selectivity in favor of the desired *trans* isomer (**1-115b**) was achieved by lowering the temperature to 0°C for this reduction reaction, as shown in **Scheme 1.34**, resulting in 37% of the *trans* isomer (**1-115b**) compared to 9% of the undesired *cis* isomer (**1-115a**). Then, **1-115b** was de-methylated to afford Dragmacidin (**1-111**).⁷⁸

Scheme 1.34. First total synthesis of Dragmacidin (**1-111**).



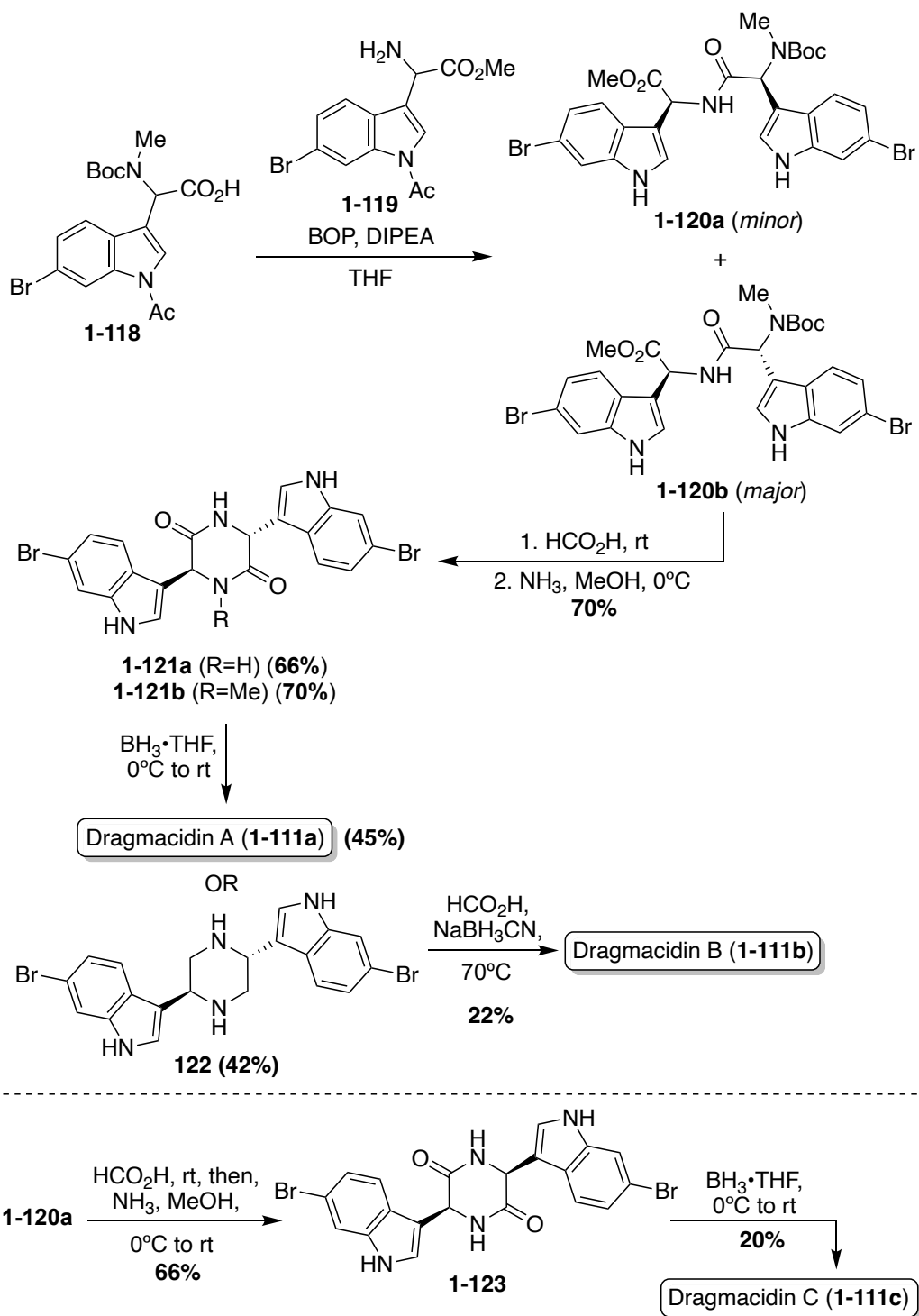
The first total synthesis of Dragmacidin B (**1-111b**) was achieved in the same year as Dragmacidin (**1-111**). However, considering its less substituted indole moieties, the approach toward Dragmacidin B (**1-111b**) was less step intensive, as shown in **Scheme 1.35**. First, an *N*-dimethylated piperazinedione (**1-116**) was brominated before undergoing a double nucleophilic attack with 6-bromo-1*H*-indole to access intermediate **1-117** in 57% yield. The bromination and nucleophilic attacks were conducted in a one-pot manner and no acid or base was necessary for the nucleophilic step. Then, **1-117** was reduced to access Dragmacidin B (**1-111b**) in moderate yield. This made for a very expeditious two-step approach to complete the total synthesis of Dragmacidin B (**1-111b**) in 14% yield overall (**Scheme 1.35**).⁷⁹

Scheme 1.35. First total synthesis of Dragmacidin B (**1-111b**).



The first total synthesis of Dragmacidin A (**1-111a**) was completed in 2000 via a condensation/cyclization sequence of methylated (**1-118**) and free (**1-119**) indolic α -amino carboxylic acids to access the piperazinedione intermediate (**1-121**) in good yields, as shown in **Scheme 1.36**. The condensation step was diastereoselective and the desired isomer (**1-120b**) predominated. After the cyclization, the carbonyl groups of intermediate (**1-121a**) were removed via reductive conditions to access Dragmacidin A (**1-111a**) in 45% yield. The total yield of Dragmacidin A (**1-111a**) after this efficient three-step approach was 21% overall.⁸⁰

Scheme 1.36. Total syntheses of Dragmacidins A-C (**1-11a-c**).

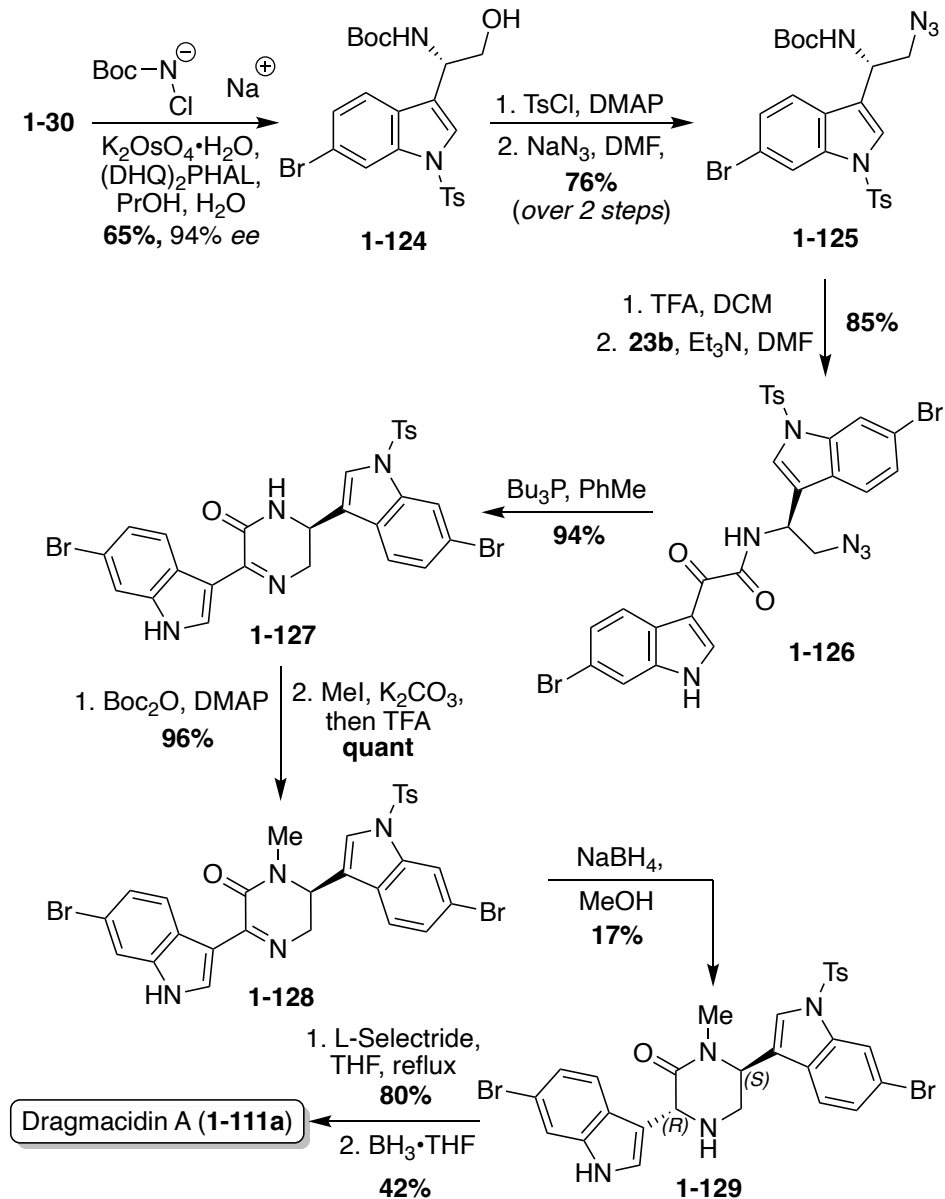


The first total synthesis of Dragmacidin C (**1-111c**) was completed in 2002 via the same three step method (condensation/cyclization/oxidation) that was previously discussed for the first

total synthesis of Dragmacidin A (**1-111a**), and the relative *cis* configuration of Dragmacidin C (**1-111c**) was confirmed (**Scheme 1.36**). As shown in **Scheme 1.36**, Dragmacidin B (**1-111b**) was also synthesized using this method, though incomplete reduction of **1-121b** resulted in a prominent side product in which one carbonyl remained on the ring. This accounts for the lower yield of **1-122**. In the synthesis of Dragmacidin B (**1-111b**) a late-stage methylation step was carried out on the piperazine intermediate (**1-122**) to install the two methyl groups on the piperazine ring of Dragmacidin B (**1-111b**).⁷²

Optically active Dragmacidin A (**1-111a**) was synthesized via a Sharpless asymmetric aminohydroxylation of 6-bromo-3-vinylindole (**1-30**) to access **1-124** in 65% yield and 94% enantiomeric excess, as shown in **Scheme 1.37**. The hydroxyl group of **1-124** was then tosylated and subsequently substituted by an azido group in high yield over two steps. The resulting amino azide intermediate (**1-125**) was then deprotected and acylated with **1-23b**, followed by reduction of the azide and subsequent cyclization to afford **1-127**. After Boc-protection, **1-127** was selectively and quantitatively methylated and subsequently deprotected to afford **1-128**. The reduction of intermediate **1-128** proved to be problematic, as it was nonselective. In fact, the desired isomer (**1-129**) was the minor product in just 17% isolated yield (82% of *cis* isomer isolated). Despite this low yield, **1-129** was de-tosylated via L-selectride and the piperazinone was reduced to the desired piperazine core to access (*2S*, *5R*)-Dragmacidin A (**1-111a**) in 42% yield over two steps.⁸¹

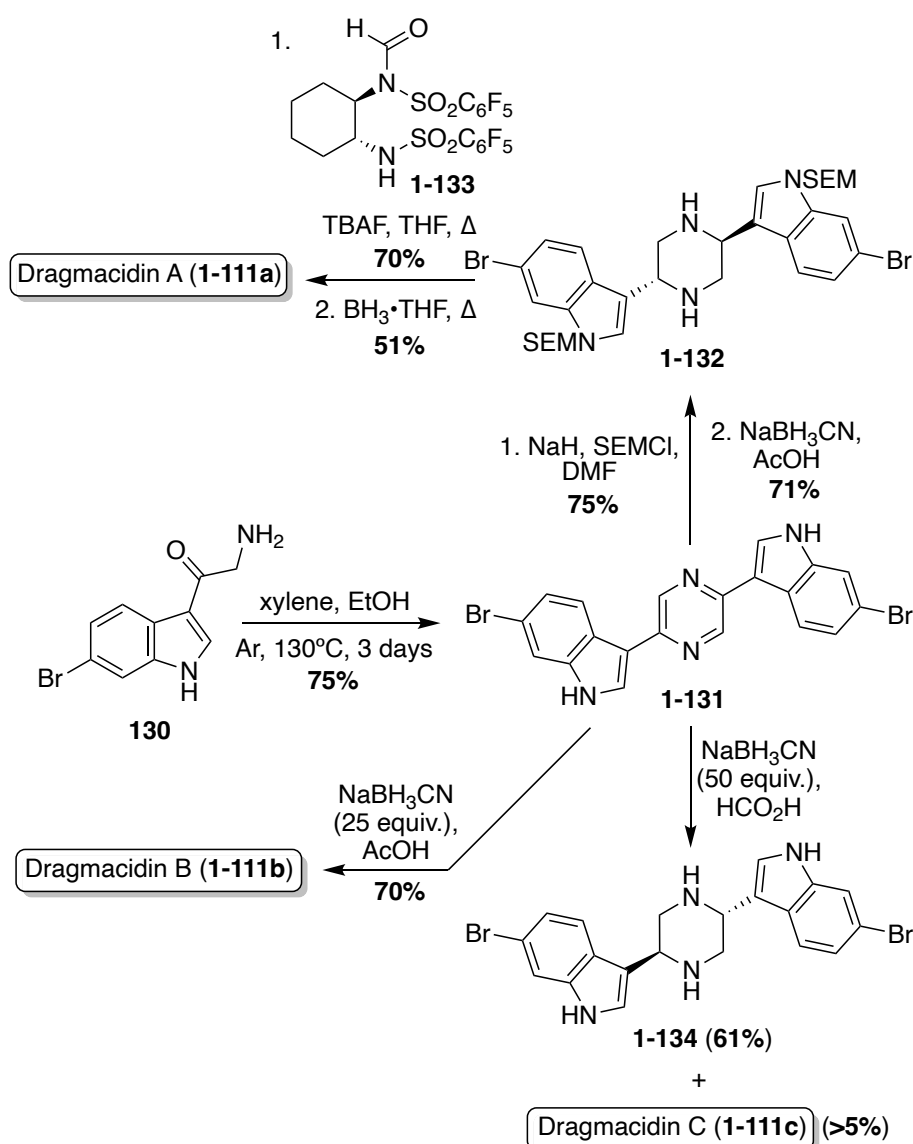
Scheme 1.37. First total synthesis of optically active Dragmacidin (**1-111**).



An expedited method of synthesizing optically active Dragmacidin A (**1-111a**) was developed in which a bis-indolylpyrazine intermediate (**1-131**) was protected and subsequently reduced to the corresponding piperazine intermediate (**1-132**) in high yields, as shown in **Scheme 1.38**. Then, de-symmetrization of the piperazine (**1-132**) was completed via enantioselective formylation using a chiral formylating reagent. This method ultimately proved to be only moderately stereoselective, affording the dextrorotatory isomer of Dragmacidin A (**1-111a**) in

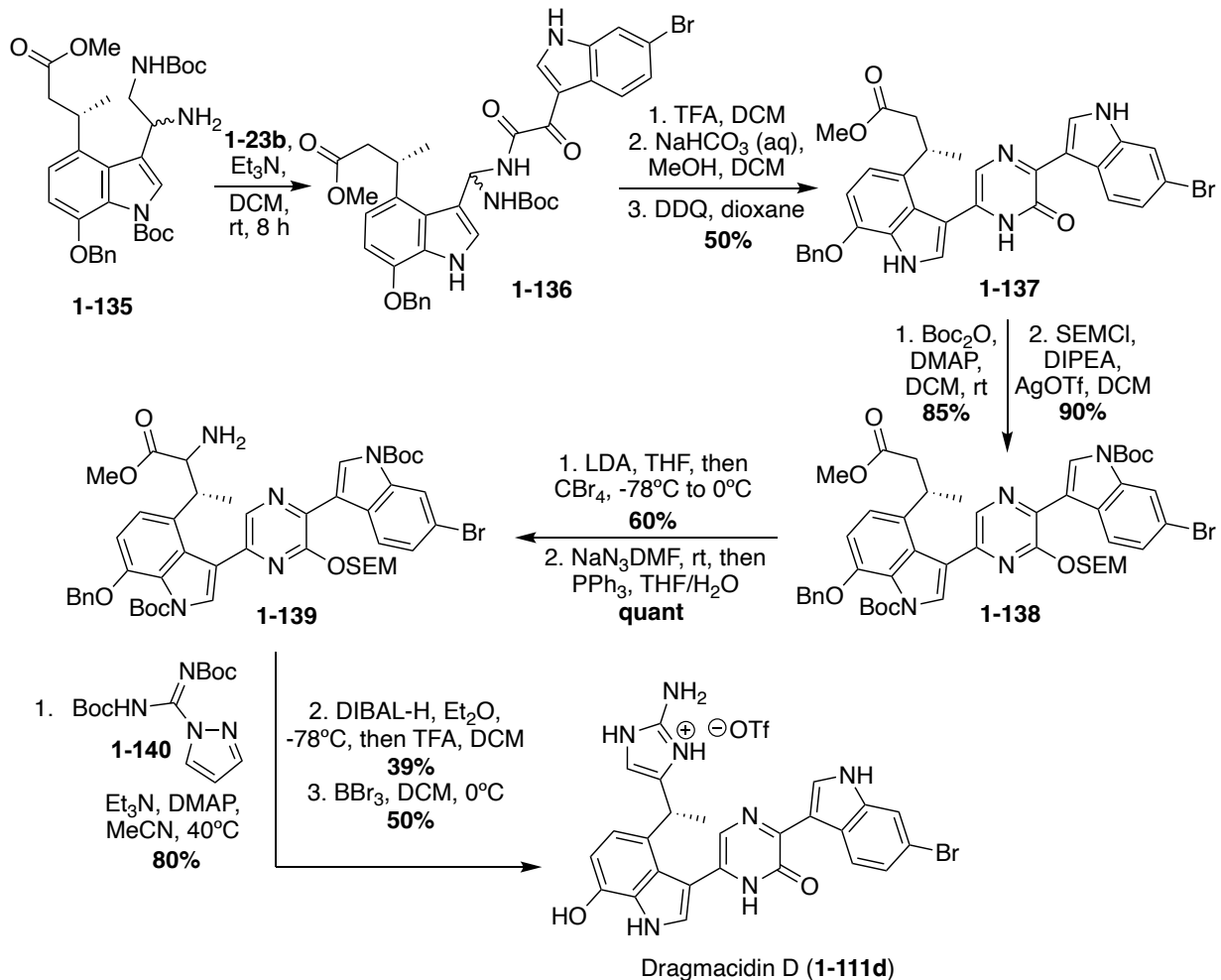
44% enantiomeric excess after transformation of the aldehyde to a methyl group and subsequent deprotection.⁸² Using a similar reductive approach to that used on the bis-indolylpyrazine intermediate (**1-131**), an efficient synthesis of Dragmacidin B (**1-111b**) was achieved in 53% overall yield over two steps, as shown in **Scheme 1.38**. It should be noted that this was not an efficient method for synthesizing Dragmacidin C (**1-111c**), as the undesired isomer predominated and less than 5% yield of Dragmacidin C (**1-111c**) was isolated.^{83,84}

Scheme 1.38. Total synthesis of Dragmacidin A-C (**1-111a-c**).



Recently, the first total synthesis of the more structurally complex Dragmacidin D (**111d**) was completed, as shown in **Scheme 1.39**.⁸⁵ First, the iodinated indolic diamine intermediate (**1-135**) was synthesized in 11 linear steps from commercially available starting materials. Here, the desired stereoisomer of **1-135** was accessed via the use of Evan's oxazolidinone chiral auxiliary ((*S*)-3-acryloyl-4-phenyloxazolidin-2-one) and column chromatography.⁸⁵ After the key diamine intermediate (**1-135**) was synthesized, it was condensed with 6-bromo-1*H*-indole-3-oxo-acyl chloride and subsequently cyclized and oxidized to access 2-piperazinone intermediate (**1-137**) in 50% yield over multiple steps, as shown in **Scheme 1.39**. Then, **1-137** was protected to allow for selective α -bromination, followed by a Staudinger reaction to access the α -amino ester (**1-139**) in high yields. Treatment of this α -amino ester (**1-139**) with pyrazole-1-carboxamide afforded a guanidine intermediate, which underwent subsequent reduction and cyclization to construct the 2-aminoimidazole moiety of Dragmacidin D in good yields. Deprotection then afforded Dragmacidin D (**1-111d**) in 50% yield. This synthesis revised the earlier stereochemical assignment that was based on biosynthetic considerations, assigning the absolute configuration as (*R*)-(+)-Dregmacidin D (**1-111d**). Furthermore, chiral HPLC-DAD methodology was developed and utilized to confirm, for the first time, that naturally occurring Dragmacidin D (**1-111d**) was isolated as either a racemate or a scalemic mixture (39% ee), which has prompted questions regarding the absolute configurations of Dragmacidins D-F (**1-111d-f**).⁸⁵

Scheme 1.39. First total synthesis of Dragmacidin D (**1-111d**).



1.2.4.2. Hamacanthins

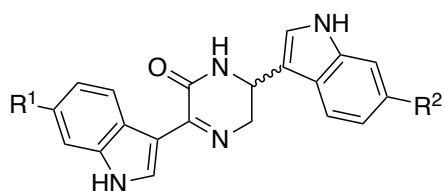
Another class of bis-indole alkaloids that are structurally related to the Dragmacidins are the Hamacanthins (**1-141a-d**, **1-142a-d**, **1-143a-d**, **1-144a-d**), which contain a 5,6-dihydro-2-pyridone or 2-piperazinone core connecting the two indole moieties, as shown in **Scheme 1.40**.

The first of these natural products to be isolated were Hamacanthin A (**1-141a**) and Hamacanthin B (**1-143a**), which were isolated from *Hamacantha* marine sponge in 1994 by Gunasekera, *et. al.*

These natural products were found to display antifungal activity.⁸⁶

Scheme 1.40. Chemical structures of Hamacanthins A-B (**1-141a** and **143a**),

Dihydrohamacanthins A-B (**142a** and **144a**) and related Debrominated natural products.

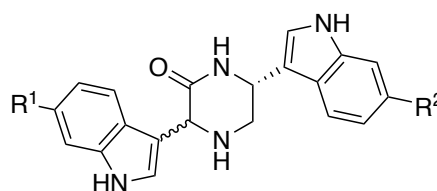


Hamacanthin A (**1-141a**):
(R¹ = R² = Br)

6'-Debromohamacanthin A (**1-141b**):
(R¹ = H, R² = Br)

6''-Debromohamacanthin A (**1-141c**):
(R¹ = Br, R² = H)

6',6''-Debromohamacanthin A (**1-141d**):
(R¹ = R² = H)

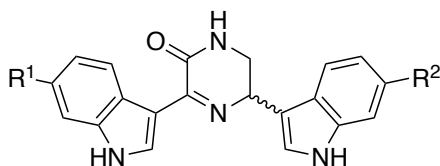


cis-3,4-dihydroamacanthin A (**1-142a**):
(R¹ = R² = Br)

trans-3,4-dihydroamacanthin A (**1-142b**):
(R¹ = R² = Br)

6'-Debromo-*trans*-3,4-dihydroamacanthin A (**1-142c**):
(R¹ = H, R² = Br)

6''-Debromo-*trans*-3,4-dihydroamacanthin A (**1-142d**):
(R¹ = Br, R² = H)

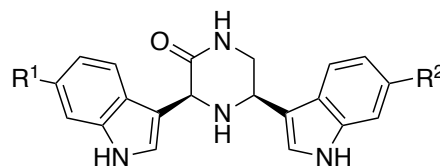


Hamacanthin B (**1-143a**):
(R¹ = R² = Br)

6'-Debromohamacanthin B (**1-143b**):
(R¹ = H, R² = Br)

6''-Debromohamacanthin B (**1-143c**):
(R¹ = Br, R² = H)

6',6''-Debromohamacanthin B (**143d**):
(R¹ = R² = H)



cis-3,4-dihydroamacanthin B (**1-144a**):
(R¹ = R² = Br)

6'-Debromo-*cis*-3,4-dihydroamacanthin A (**1-144b**):
(R¹ = H, R² = Br)

6''-Debromo-*cis*-3,4-dihydroamacanthin A (**1-144c**):
(R¹ = Br, R² = H)

6',6''-Debromo-*cis*-3,4-dihydroamacanthin A (**1-144d**):
(R¹ = H, R² = H)

In more recent years, the de-bromo and dihydro Hamacanthin analogues (**1-141b-d**, **1-142a-d**, **1-143b-d**, **1-144a-d**) have been isolated from various natural marine sources, as shown in **Table 1.2**. The configurations of these natural products are also indicated in Table 2, and many were later confirmed via total syntheses. Despite their structural similarities, the configurations of these Hamacanthins vary. For example, Hamacanthin A (**1-141a**) exists as the (*S*)-isomer, while its analogous mono de-bromo natural products (**1-141b** and **1-141c**) exist as the (*R*)-isomers, and its bis de-bromo analogue (**1-141d**) exists as the (*S*)-isomer (**Table 1.2**). Overall,

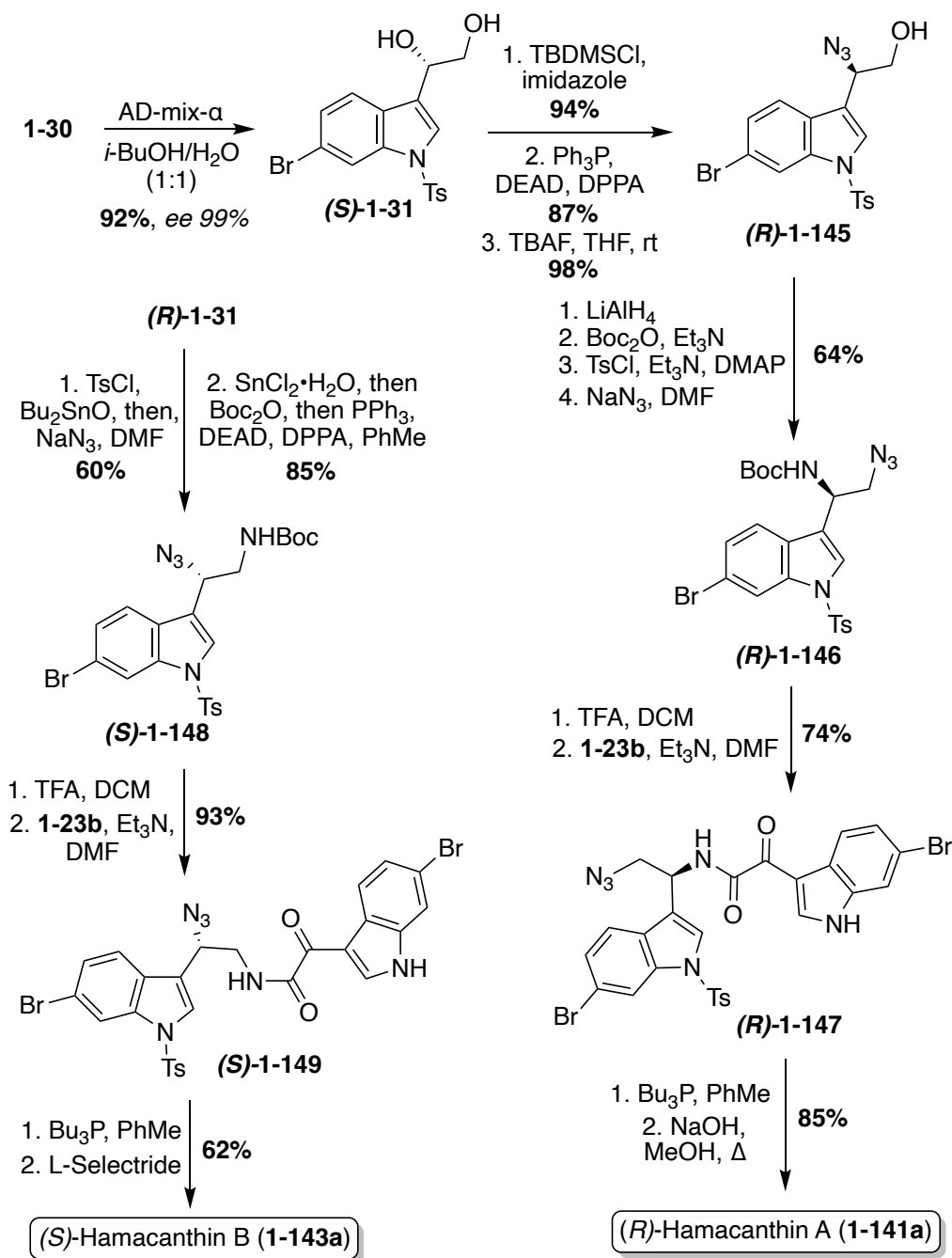
natural products of the Hamacanthin class (**1-141a-d**, **1-142a-d**, **1-143a-d**, **1-143a-d**) have been shown to display antifungal, antibacterial, and cytotoxic activity.⁸⁶

Table 1.2. Hamacanthin natural products – Isolation data.^{2, 7, 8, 12, 86, 11}

Compound	Configuration	Natural Source
1-141a	<i>S</i>	<i>Hamacantha, Spongosorites, Discodermia calyx</i>
1-141b	<i>R</i>	<i>Spongosorites</i>
1-141c	<i>R</i>	<i>Spongosorites, Discodermia calyx</i>
1-141d	<i>S</i>	<i>Spongosorites</i>
1-143a	<i>S</i>	<i>Hamacantha, Spongosorites, Discodermia calyx</i>
1-143b	<i>R</i>	<i>Spongosorites, Discodermia calyx</i>
1-143c	<i>R</i>	<i>Spongosorites</i>
1-143d	<i>R</i>	<i>Spongosorites</i>
1-142a	<i>3R, 6R</i>	<i>Rhaphizia lacazei</i>
1-142b	<i>3S, 6R</i>	<i>Rhaphizia lacazei, Spongosorites</i>
1-142c	<i>3S, 6R</i>	<i>Rhaphizia lacazei, Spongosorites</i>
1-142d	<i>3S, 6R</i>	<i>Rhaphizia lacazei, Spongosorites</i>
1-144a	<i>3S, 5R</i>	<i>Rhaphizia lacazei, Spongosorites, Discodermia calyx</i>
1-144b	<i>3S, 5R</i>	<i>Rhaphizia lacazei, Spongosorites</i>
1-144c	<i>3S, 5R</i>	<i>Rhaphizia lacazei, Spongosorites</i>
1-144d	<i>3S, 5R</i>	<i>Spongosorites</i>

The first enantioselective total synthesis of the unnatural (*R*)-Hamacanthin A (**1-141a**) was completed in 2001 by Jiang, *et. al.* via the coupling of a 3-indolyl- α -oxo-acetyl chloride intermediate (**1-23b**) and 3-indolyl azidoethylamine intermediate (*R*)-(**1-146**), prior to an intramolecular aza-Wittig type cyclization to access (*R*)-Hamacanthin A (**1-141a**) in high yields, as shown in **Scheme 1.41**.⁸⁷ The 3-indolyl azidoethylamine intermediate was synthesized in four steps from *N*-tosylated-6-bromo-3-vinyl indole in high yields. The stereocenter of (**1-141a**) was established via a Sharpless asymmetric dihydroxylation reaction, followed by a stereospecific azidation. In spectroscopic comparison of the naturally isolated Hamacanthin A (**1-141a**) and the synthesized (*R*)-Hamacanthin A (**141a**), it was confirmed that the natural Hamacanthin A (**1-141a**) existed as the (*S*)-isomer.^{87, 88}

Scheme 1.41. Enantioselective total syntheses of Hamacanthins A and B (**141a** and **143a**).

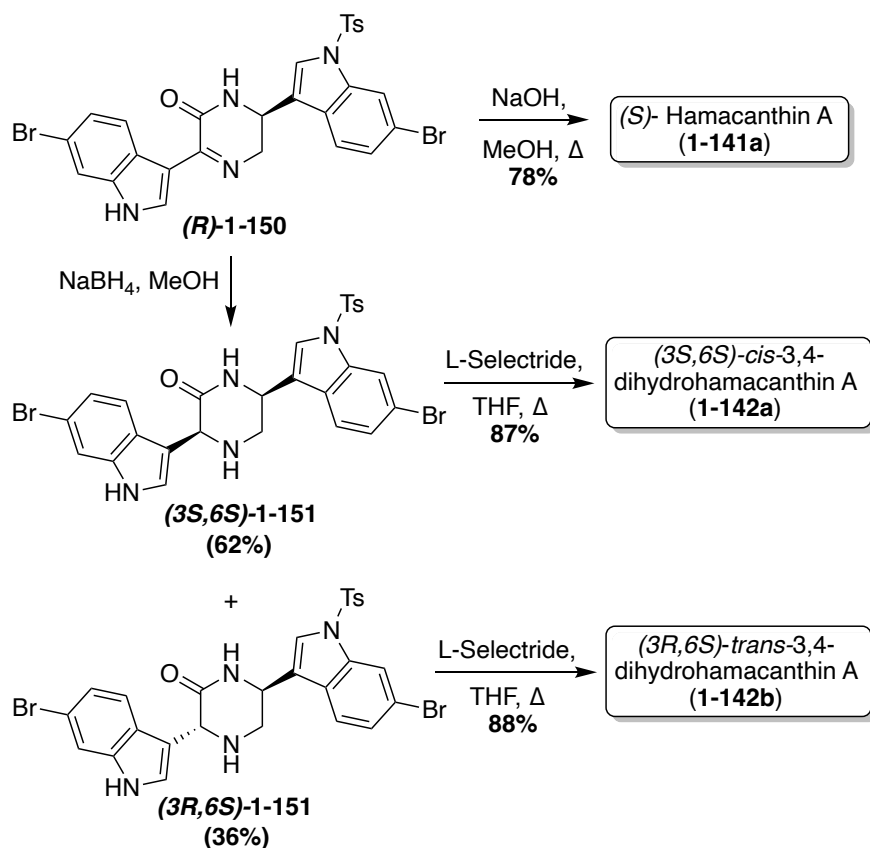


A year later, the same research team completed the first enantioselective total synthesis of Hamacanthin B (**1-143a**). As shown in **Scheme 1.41**, this synthesis was completed via a similar approach as was previously discussed for (*R*)-Hamacanthin A (**1-141a**). Considering the established (*S*)-configuration of (**1-141a**), (*S*)-Hamacanthin B (**1-143a**) was synthesized. When

compared to the naturally isolated Hamacanthin B (**1-143a**), the synthesized (*S*)- **1-143a** confirmed the configuration of the natural **1-143a** as the (*S*)- isomer.⁸⁸

With the elucidation of the absolute configuration of (*S*)-Hamacanthin A (**1-141a**), the first enantioselective total synthesis of the desired (*S*)-Hamacanthin A (**1-141a**) was completed via deprotection and simultaneous inversion of the stereocenter of (*R*)-**1-150** to access (*S*)-**1-141a** in 78% yield, as shown in **Scheme 1.42**. This allowed for additional confirmation that this was the correct configuration of the naturally occurring (*S*)-Hamacanthin A (**1-141a**). The synthetic approach toward (*R*)-**1-150** was previously discussed in the Dragmacidin section (**Scheme 1.37**).⁸² Also, using intermediate (*R*)-**1-150**, the first total syntheses of the unnatural (*3S, 6S*)-*cis*-3,4-dihydrohamacanthin A (**1-142a**) and (*3R, 6S*)-*trans*-3,4-dihydrohamacanthin A (**1-142b**) were both completed. The reduction of (*R*)-**1-150** afforded 62% yield of (*3S, 6S*)-*cis*-**1-151** and 36% yield of (*3R, 6S*)-*trans*-**1-151**. These 2-piperidone intermediates (**1-151**) were then deprotected via L-selectride to access (*3S, 6S*)-*cis*-3,4-dihydrohamacanthin A (**1-142a**) and (*3R, 6S*)-*trans*-3,4-dihydrohamacanthin A (**1-142b**) in 87% and 88% yields, respectively (**Scheme 1.42**). Via comparison of the naturally isolated *cis*-3,4-dihydrohamacanthin A (**1-142a**) and *trans*-3,4-dihydrohamacanthin A (**1-142b**) with the synthesized (*3S, 6S*)-*cis*-**1-142a** and (*3S, 6S*)-*trans*-**1-142b**, it was found that the configurations of these synthesized natural products did not match that of the isolated optical rotation data. Therefore, it was concluded that the absolute configurations of *cis*-3,4-dihydrohamacanthin A (**1-142a**) and *cis*-3,4-dihydrohamacanthin A (**1-142a**) are (*3R, 6R*) and (*3S, 6R*), respectively.⁸¹ Additionally, racemic *cis*- and *trans*-3,4-dihydrohamacanthins can be accessed, albeit in low yields, via partial reduction of cyclized dipeptides (**121** and **123**), as was also discussed in the Dragmacidin section (**Scheme 1.36**).⁷¹

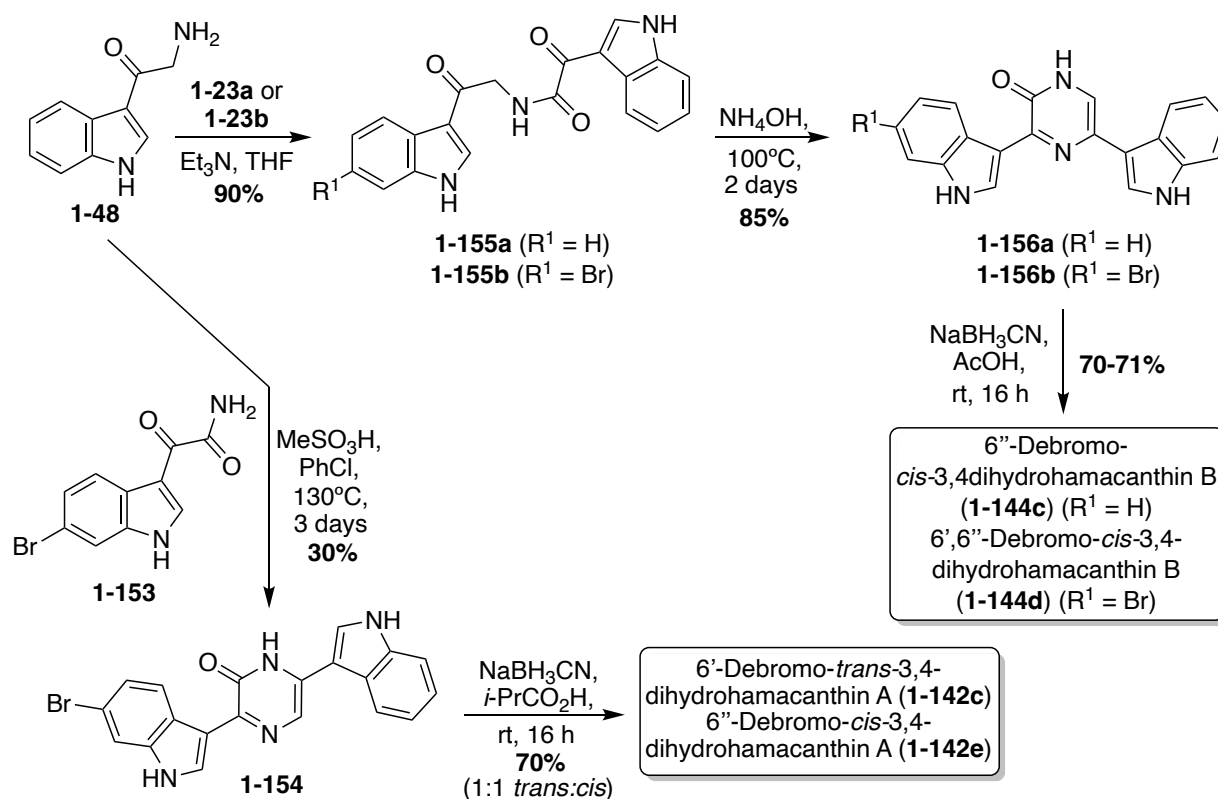
Scheme 1.42. Enantioselective total syntheses of Hamacanthin A (**1-141a**) and Dihydrohamacanthin A-B (**1-141a-b**).



The first total syntheses of racemic 6'-debromo-*trans*-3,4-dihydrohamacanthin A (**1-142c**) and the unnatural 6''-debromo-*cis*-3,4-dihydrohamacanthin A (**1-142e**) were carried out via the condensation and subsequent cyclization of an indolic α -amino ketone intermediate (**1-48**) with an indolic keto-amide intermediate (**1-153**). After formation of this bis-indolylpyrazinone intermediate, it underwent reduction to access 6'-debromo-*trans*-3,4-dihydrohamacanthin A (**1-142c**) and the unnatural 6''-debromo-*cis*-3,4-dihydrohamacanthin A (**1-142e**) in 70% yield as a 1:1 mixture (**Scheme 1.43**). While it was not enantioselective, this method proved to be a very expeditious synthesis of these natural products.⁸⁹ This method also allowed for the first racemic total synthesis of 6''-debromo-*cis*-3,4-dihydrohamacanthin B (**1-**

144c) and 6',6''-debromo-*cis*-3,4-dihydrohamacanthin B (**1-144d**). As shown in **Scheme 1.43**, this method was adapted to achieve the 3,5-disubstituted cyclized product by condensing and cyclizing an indolic oxo-acyl chloride intermediate (**1-23a-b**) with an indolic α -amino ketone intermediate (**1-48**). In addition to being an efficient and high yielding route, this method was selective for the desired *cis*-isomers of 6''-debromo-*cis*-3,4-dihydrohamacanthin B (**1-144c**) and 6',6''-debromo-*cis*-3,4-dihydrohamacanthin B (**1-144d**), respectively.⁸⁹

Scheme 1.43. Enantioselective total syntheses of Debromo-Dihydrohamacanthins (**1-142c** and **1-141c-d**).



A similar bio-mimetic cyclization of a ketoamide (**1-157**) was proven efficient for the synthesis of both racemic Hamacanthin A (**1-141a**) and Hamacanthin B (**1-143a**). As shown in **Scheme 1.44**, to access Hamacanthin B (**1-143a**), nucleophilic attack of the primary amine on the indolic (C3) ketone and subsequent dehydration led to intermediate (**II**), which was

Through mechanistic study, it was determined that the ratio of **1-141a**:**1-143a** was heavily dependent on the identity of the solvent, and the protecting groups (R' and R''), as indicated by the results shown in **Table 1.3**. In this case, more polar, protic solvents, such as ethanol, led to predominant formation of intermediate (**II**) while more non-polar solvents, such as dichloroethane (DCE), led to predominant formation of intermediate (**V**). In addition, the presence of stronger electron-withdrawing groups, such as a tosyl group, on the indole nitrogen led to predominant formation of intermediate (**II**) over intermediate (**V**) due to the resulting increased electrophilicity of the carbonyl group adjacent to the indole, making nucleophilic attack on this carbonyl preferable.⁸⁹

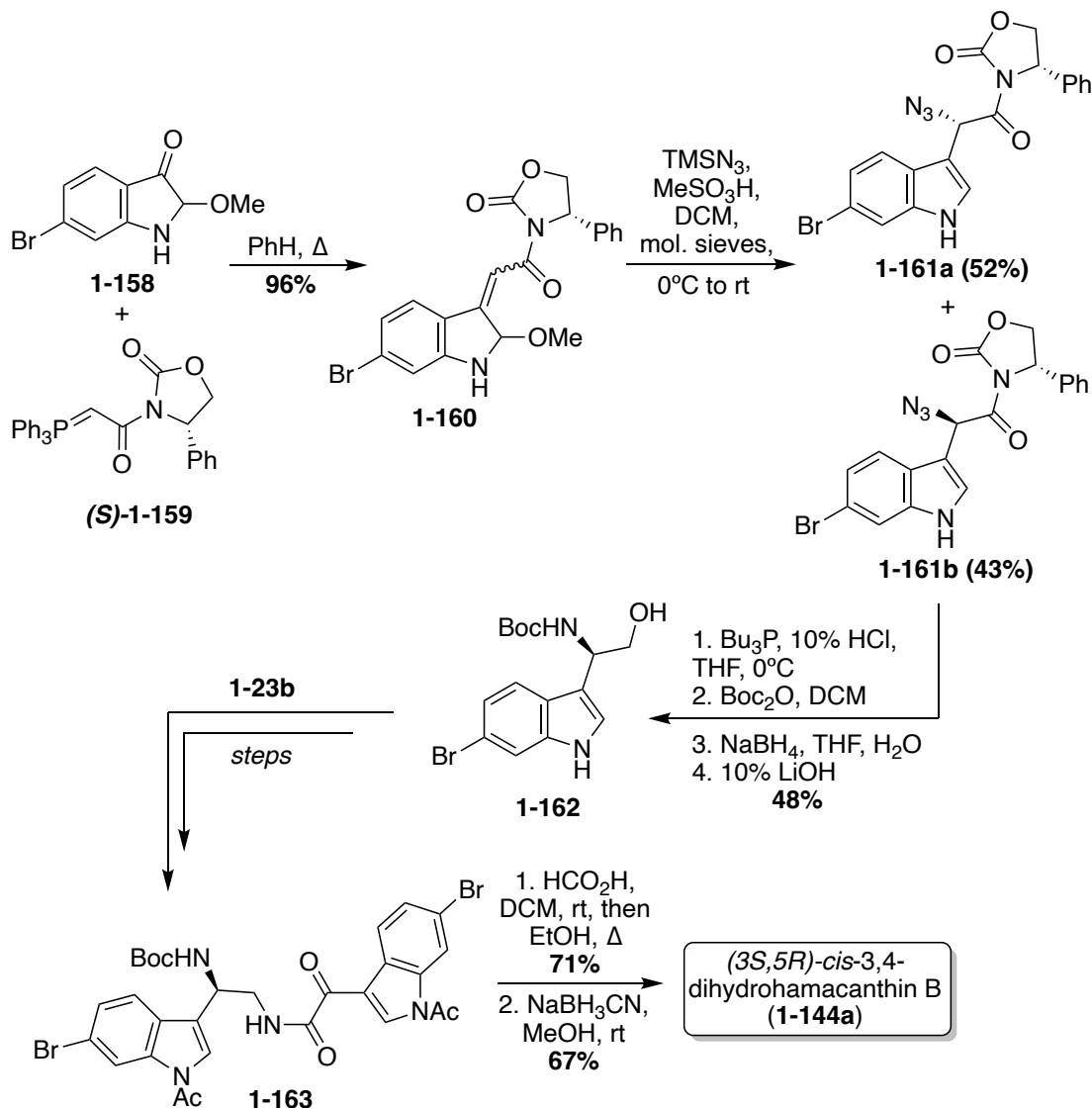
Table 1.3. Cyclization conditions of keto-amide (**1-157**).

R'	R''	Solvent	Yield (V)	Yield (II)
Ts	H	DCE	42%	35%
Ts	H	1,4-Dioxane	30%	38%
Ts	H	EtOH	15%	75%
Ts	H	DMF	7%	46%
Ts	Ac	DCE	42%	55%
Ts	Ts	DCE	18%	68%

In 2007, along with enantioselective total synthesis of (*S*)-Hamacanthins A and B (**1-141a** and **1-143a**), the first enantioselective total synthesis of *cis*-3,4-dihydrohamacanthin B (**1-144a**) was also completed.⁹⁰ As shown in **Scheme 1.45**, this synthesis proceeded via the condensation of an indolic amino- alcohol intermediate (**1-162**) and an indolic oxo-acyl chloride intermediate (**1-23b**) to access a similar keto-amide intermediate (**1-163**), as was previously discussed. Subsequent cyclization of the keto-amide intermediate (**1-163**) and stereospecific reduction afforded (*3S*-,*5R*)-*cis*-3,4-dihydrohamacanthin B (**1-144a**) in high yields. Here, the

stereochemistry was set via the installation of an (*S*)-phenyloxazolidone chiral auxiliary (*S*)-**1-159**).⁹⁰

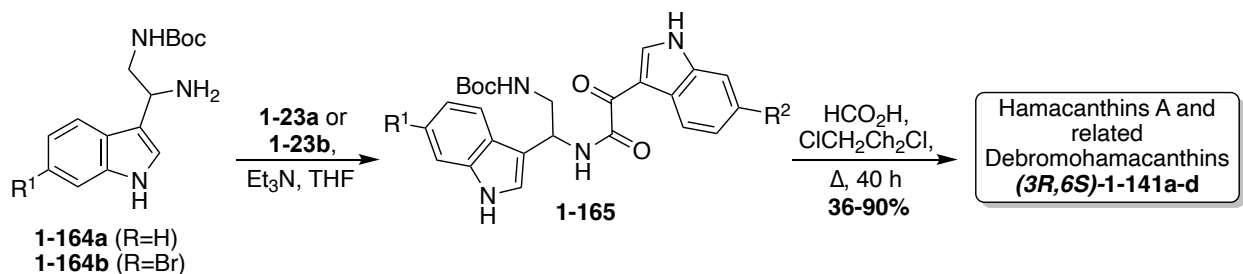
Scheme 1.45. First enantioselective total synthesis of Dihydrohamacanthin B (**1-144a**).



In a slightly adapted, but very similar condensation of an indolic diamine intermediate (**1-164**) and an indolic oxo-acyl chloride intermediate (**1-23a-b**) and following cyclization, racemic Hamacanthin A (**1-141a**) and its related Debromohamacanthins (**1-141b-d**) were accessed in moderate to high yields, as shown in **Scheme 1.46**.²² The indolic diamine intermediates (**164a-b**) were synthesized using the same method discussed previously in the Spongotine Section

(Scheme 5). At present, several debromo analogues of Hamacanthin B and Dihydrohamacanthin B have yet to be accessed via total synthesis.

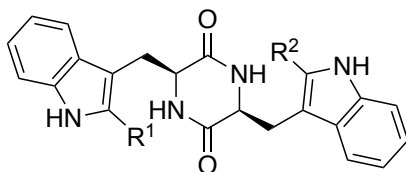
Scheme 1.46. Total synthesis of Hamacanthin A (**1-141a**) and related Debromohamacanthins (**1-141b-d**).



1.2.4.3. Fellutanines

Fellutanines A-C (**1-166a-c**) were first isolated in 2000 by Kozlovsky *et. al.* from the fungi *Penicillium fellutanum*. The 3,6-di-substituted-bis-indolyl-piperazine-2,5-dione structures of these natural products was elucidated via spectroscopic methods (**Scheme 1.47**). In addition, it was discovered that Fellutanine B (**1-166b**) contained an isopentenyl group on the 2-position of one of the indole moieties and Fellutanine C (**1-166c**) contained two isopentenyl substituents, one on the 2-position of each indole moiety.⁹¹ The configuration of these Fellutanines A-C (**1-166a-c**) was initially reported as the *cis*-isomer, but this structure was later revised to the correct *trans*-isomer of the piperazine-2,5-dione core.⁹¹ Much of the biological activity of these compounds is unknown, though some studies have shown they possess antibacterial activity, but no significant cytotoxic activity.^{91, 92}

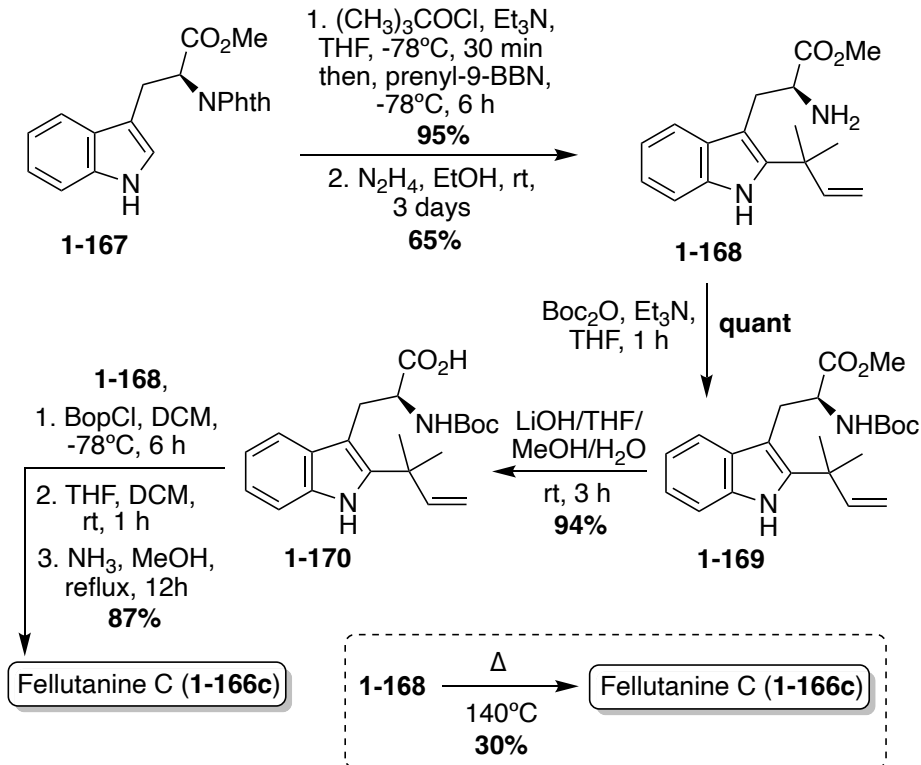
Scheme 1.47. Chemical structures of Fellutanines A-C (**1-166a-c**).



Fellutanine A (**1-166a**): $R^1=R^2=H$
Fellutanine B (**1-166b**): $R^1=3\text{-isopentenyl}$, $R^2=H$
Fellutanine C (**1-166c**): $R^1=R^2=3\text{-isopentenyl}$

Interestingly, the first total synthesis of Fellutanine C (**1-166c**) was completed before its first isolation, as it was an intermediate that was accessed in the 1995 total synthesis of another related fused bicyclic natural product, Gypsetin.⁹³ As is shown in **Scheme 1.48**, this total synthesis began with indolic C-2 reverse prenylation of *N*-phthaloyl-L-tryptophan methyl ester (**1-167**) via prenyl-9-BBN in high yield, followed by hydrazinolysis and subsequent Boc-protection and saponification to access intermediate (**1-170**) in high yields. Then, **1-170** and **1-168** were coupled to access the desired *cis*-Fellutanine C (**1-166c**) in a very high 87% yield over three steps.⁹³

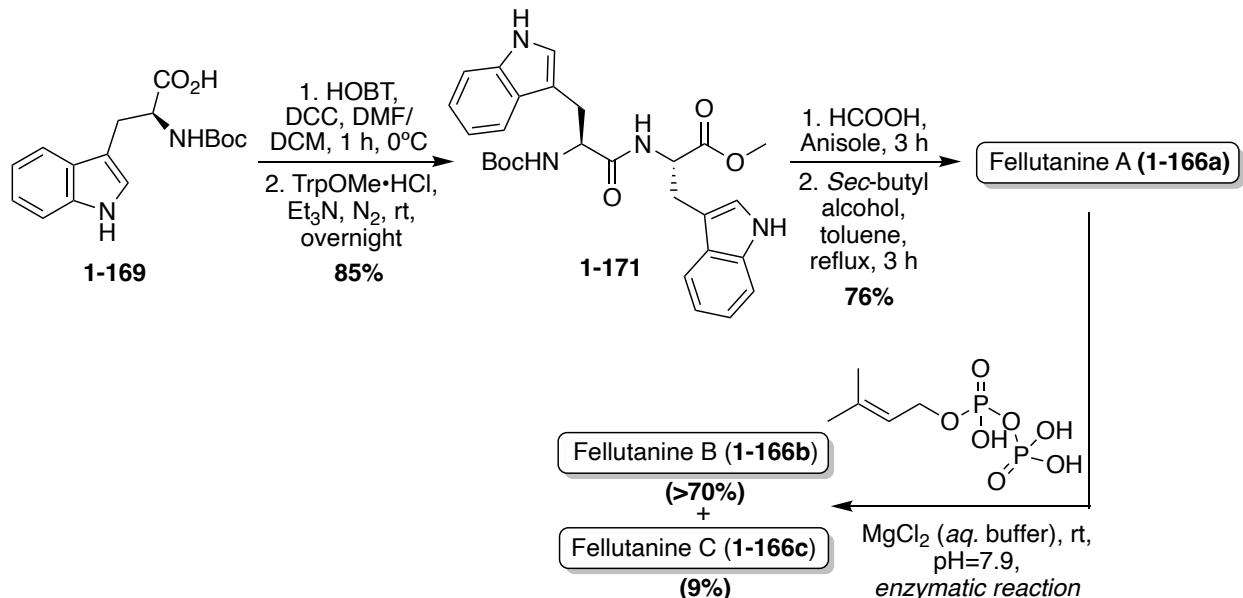
Scheme 1.48. First total synthesis of Fellutanine C (**1-166c**).



In a similar approach using L-tryptophan analogues as starting materials, Fellutanine C (**1-166c**) was synthesized via the same intermediate (**1-168**) used previously, though here undergoing an expeditious dimerization and cyclization via pyrolysis conditions to access *cis*-Fellutanine C (**1-166c**) in 30% yield.⁹⁴ This proved to be an advantageous process in terms of step count by saving four steps compared to the previous synthesis, yet the yield decreased significantly in spite of this.

The first total synthesis of Fellutanine A (**1-166a**) was completed in 2008 in a similar method to that of Fellutanine C (**1-166c**). Here, a tryptophan analogue (**1-169**) and TrpOMe•HCl were condensed and subsequently cyclized to access the desired *cis*-Fellutanine A (**1-166a**) in 76% yield (Scheme 1.49).⁹⁵

Scheme 1.49. First total synthesis of Fellutanine A-B (**1-166a-b**).



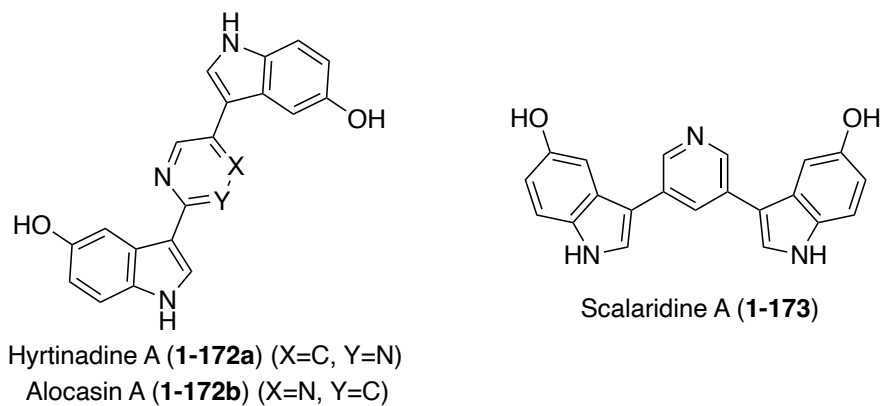
In addition to the previously discussed synthetic methods of accessing these Fellutanine natural products, many enzymatic biosynthetic methods have also been utilized over the years, using L-tryptophan as the starting material to access these molecules.^{96, 97} Recently, a semi-total synthesis was developed and conducted to achieve all three natural products, Fellutanines A-C (**166a-c**), via the same route. As shown in **Scheme 1.49**, the same condensation and subsequent cyclization of tryptophan derivatives (**1-169**) and TrpOMe•HCl was conducted to access *cis*-Fellutanine A (**1-166a**) in 76% yield. Then, the enzymatic C2-reverse-prenylation of indole was performed via DMAPP prenyltransferase and aqueous MgCl₂ under slightly basic conditions, to access the mono-reverse prenylated *cis*-Fellutanine B (**1-166b**) as the major product in >70% yield. It is noteworthy to mention that, while not the major product, *cis*-Fellutanine C (**1-166c**) was also accessed via this method in 9% yield. The most significant achievement of this work was the first total synthesis of Fellutanine B (**1-166b**) and the development of a late stage selective reverse prenylation methodology of indole. It was also a significant that all three Fellutanines A-C (**1-166a-c**) could be accessed via this same route (**Scheme 1.49**).⁹⁸

1.2.5. Pyridine and diazine linker moieties

1.2.5.1. Hyrtinadine/Alocasin/Scalaridine

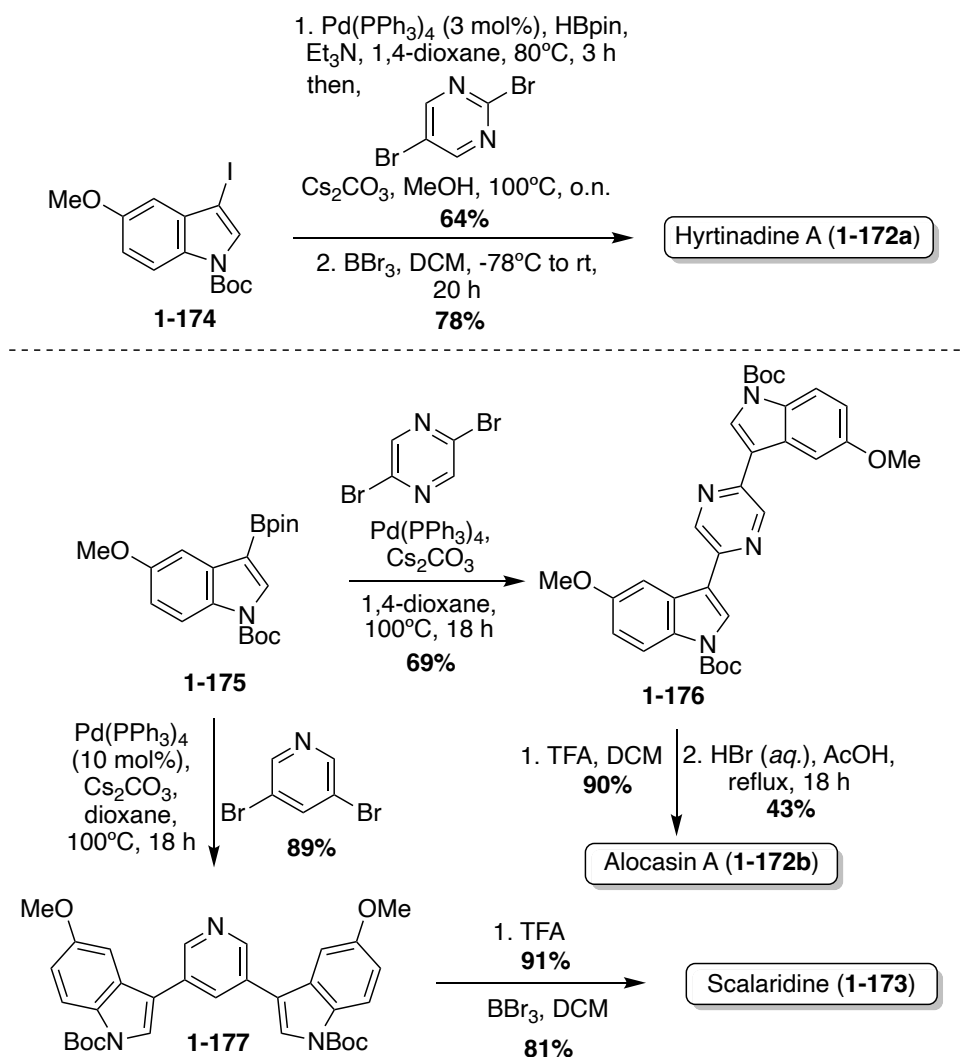
Three structurally related bis-indole natural products with heterocyclic aromatic linker moieties were discovered between 2007 and 2013. The first of these was Hyrtinadine, A (**1-172a**), which was isolated in 2007 by Endo, *et. al.* from the Okinawan marine sponge *Hyrtios* sp.⁹⁹ This bis-indolyl-2,5-di-substituted pyrimidine structure was elucidated via spectroscopic methods (**Scheme 1.50**). Hyrtinadine A (**1-172a**) was also found to be highly cytotoxic towards murine Leukemia L1210 and human epidermoid carcinoma KB cell lines.⁹⁹ The next of these related natural products to be discovered was Alocasin A (**1-172b**), which was isolated in 2012 by Zhu, *et. al.* from the dried rhizomes of the herbaceous plant *Alocasia macrorrhiza*.¹⁰⁰ Alocasin A (**1-172b**) was reportedly the first heterocycle-linked bis-indole alkaloid isolated from a terrestrial source. As shown in **Scheme 1.50**, the chemical structure of (**1-172b**) has remarkable structural similarity to that of Hyrtinadine A (**1-172a**). However, the two indole moieties of Alocasin A (**1-172b**) are connected by a pyrazine linker moiety, rather than the pyrimidine of (**1-172a**). Much is unknown regarding the biological activity of Alocasin A (**1-172b**); however, it has been shown to display weak antiproliferative activity against Hep-2 and Hep-G2 cell lines.¹⁰⁰ The most recent of these to be discovered was Scalaridine A (**1-173**), which was isolated in 2013 by Lee *et. al.* from the marine sponge *Scalarispongia* sp., along with the previously discussed Hyrtinadine A (**1-172a**).¹⁰¹ This natural product (**1-173**) was determined to have a bis-indolyl-2,5-di-substituted pyridine structure. Interestingly, this is the only bis-indole alkaloid of its kind to contain a pyridine linker moiety. Much is also unknown regarding the biological activity of Scalaridine A (**1-173**), but much like its two aforementioned structural relatives, it also displayed significant cytotoxicity.¹⁰¹

Scheme 1.50. Chemical structures of Hyrtinidine A (**1-172a**), Alocasin A (**1-172b**) and Scalaridine A (**1-173**).



The first of these natural products to be accessed via total synthesis was Hyrtinidine A (**1-172b**) in 2011, by Müller, *et. al.* As shown in **Scheme 1.51**, the first total synthesis of Hyrtinidine A (**1-173**) was achieved via sequential palladium-catalyzed Masuda borylation and double Suzuki cross-coupling reactions to install the two indole moieties on the 2- and 5-positions of the pyrimidine core. Subsequent de-methylathylation via BBr_3 achieved Hyrtinidine A (**1-172a**) in 78% yield.¹⁰²

Scheme 1.51. First total synthesis of Hyrtinadine A (**1-172a**), Alocasin (**1-172b**), and Scalaridine A (**1-173**).

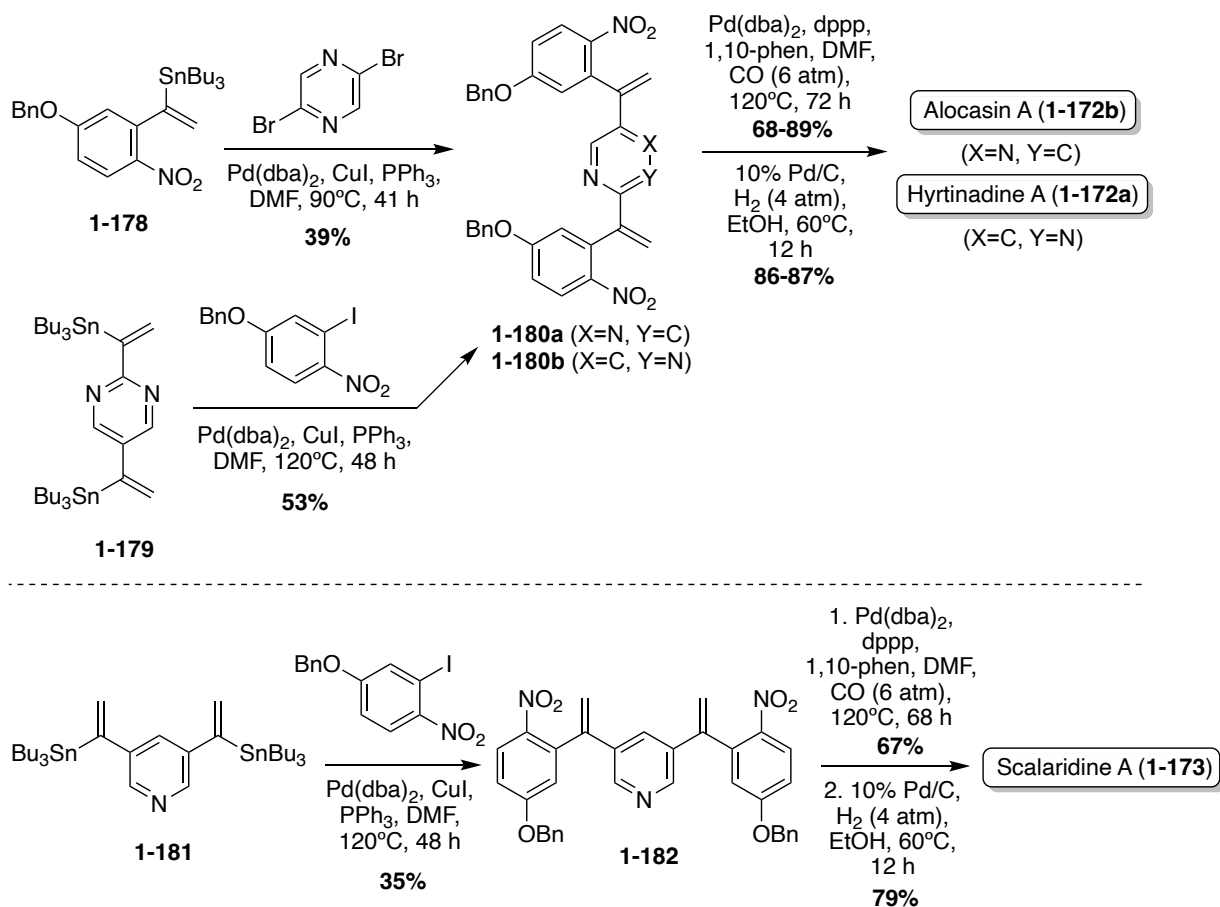


In 2015, the first total syntheses of Alocasin A (**1-172b**) and Scalaridine A (**1-173**) were completed via a similar borylation and subsequent double Suzuki coupling route as was used in the first total synthesis of Hyrtinadine A (**1-172a**), followed by de-methylation of the indolic hydroxyl groups to access Alocasin A (**1-172b**) and Scalaridine A (**1-173**) in high yields.^{103, 104}

One year later, a different approach to the total synthesis of all three natural products (**1-172a**, **1-172b**, and **1-173**), was conducted via successive palladium-catalyzed reactions; a Kosugi-Migita-Stille cross coupling reaction to install the aromatic substituents on the

heterocyclic linker, a reductive *N*-heterocyclization to form the indole moieties, and a final hydrogenolysis to access **1-172a**, **1-172b**, and **1-173** in high yields, as shown in **Scheme 1.52**.¹⁰⁵

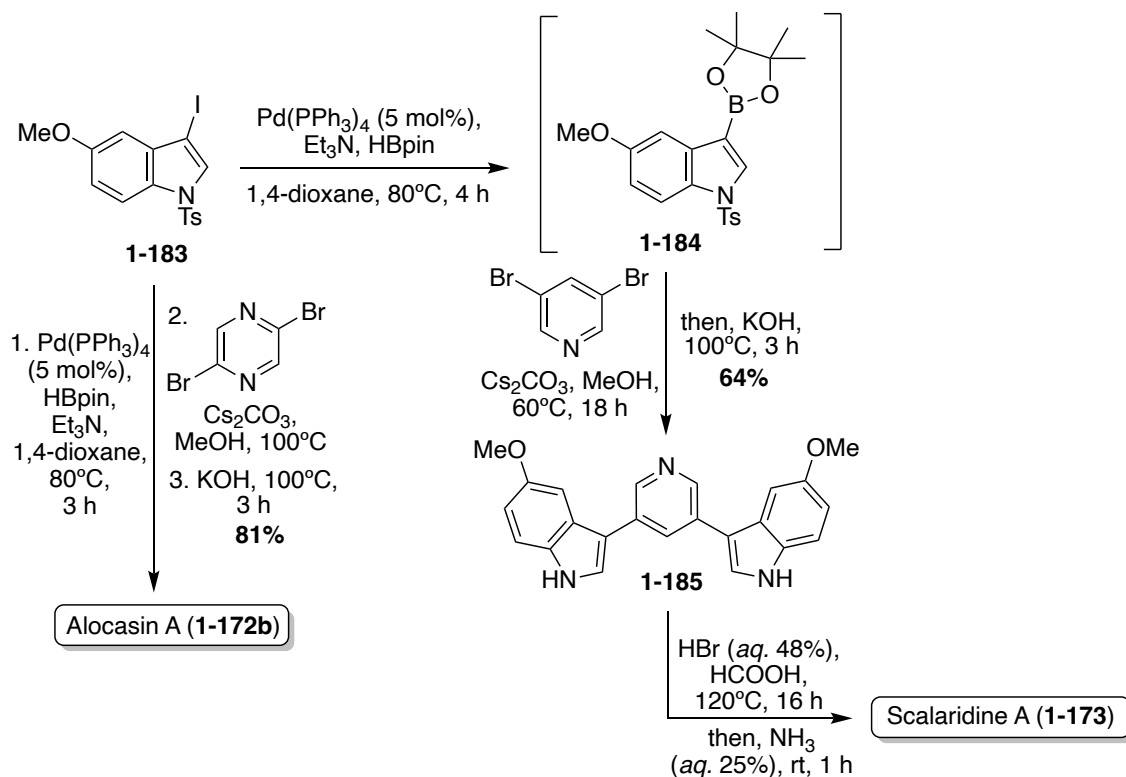
Scheme 1.52. Total synthesis of Hyrtinadine A (**1-172a**), Alocasin (**1-172b**), and Scalaridine A (**1-173**).



As can be concluded from the previously discussed syntheses of Hyrtinadine A (**1-172a**), Alocasin A (**1-172b**), and Scalaridine A (**1-173**), the common method of synthesis for these natural products is the use of palladium-catalyzed cross-coupling reactions to install the indole moieties on the aromatic *N*-heterocyclic cores. In recent years, additional total syntheses of **1-172a-b** and **1-173** have been reported using similar palladium-catalyzed cross coupling approaches.^{106, 107, 108} A couple examples of these are shown in **Scheme 1.53**, such as the 2022 total synthesis of Scalaridine A (**1-173**) and the significantly expedited one-pot approach using a

similar palladium-catalyzed methodology in the total synthesis of Alocasin A (**1-172b**). The latter achieved Alocasin A (**1-172b**) in 81% from the iodoindole intermediate (**1-183**), using a three phase, one-pot method.¹⁰⁹

Scheme 1.53. Total synthesis of Alocasin A (**1-172b**) and Scalaridine A (**1-173**).



1.3. Tris-indole Alkaloids

Compared to their previously discussed bis-indole alkaloid counterparts, tris-indole alkaloids are rarer and more elusive in nature. However, in recent years, discovery and synthesis of these natural products has become more prevalent.

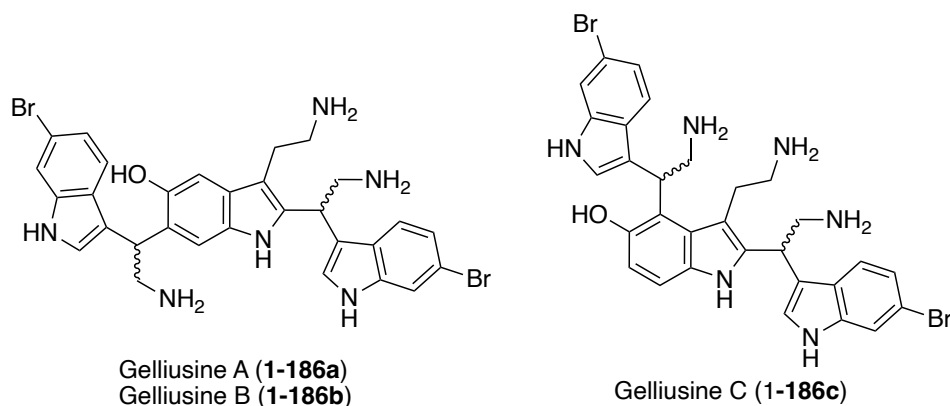
1.3.1. Aromatic *N*-heterocyclic linker moieties

1.3.1.1. Gelliusines

Gelliusines A (**1-186a**) and B (**1-186b**) were first isolated as enantiomeric pairs in 1994 by Bifulco, *et. al.* from the deep-water marine sponge *Gellius* sp. (also known as *Orina* sp.).¹¹⁰

The unique tris-indole chemical structure of these natural products, in which an indole core connects two additional indole moieties at the C-2 and C-6 positions, was elucidated via spectroscopic methods, as shown in **Scheme 1.54**. In addition, Gelliusines A (**1-186a**) and B (**1-186b**) were determined to also contain three amine substituents. These amine substituents were of particular interest as it is hypothesized that they could contribute to favorable water-solubility of these natural products, which could be beneficial in bioactive applications. The absolute stereochemistry of the chiral centers of **1-186a** and **1-186b** was inconclusive via obtained data and, because Gelliusines A (**1-186a**) and B (**1-186b**) have yet to be accessed via total synthesis, their absolute configurations remain unknown. In terms of their biological activity, Gelliusines A (**1-186a**) and B (**1-186b**) were found to display cytotoxic activity, as well as anti-serotonin activity. The latter activity is unsurprising considering the structural similarities of Gelliusines A (**1-186a**) and B (**1-186b**) and serotonin.¹¹⁰

Scheme 1.54. Chemical structures of Gelliusines A-C (**1-186a-c**).



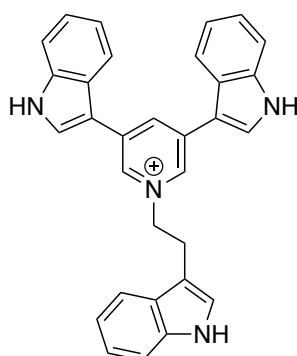
One year later, an additional structurally similar natural product of this class, Gelliusine C (**1-186c**) was isolated by the same group from the deep-water marine sponge *Gellius* sp. (also known as *Orina* sp.). As shown in **Scheme 1.54**, the chemical structure of Gelliusine C (**1-186c**) was determined to be a similar tris-indole alkaloid containing in indole core connecting two

additional indole moieties, as well as containing three amine substituents. The main difference was, instead of the 2,6-substituted indole core of **1-186a-b**, the indole core of Gelliusine C (**1-186c**) had the two additional indole moieties connected at the C2 and C4 positions. Similar to **1-186a-b**, the absolute configuration of Gelliusine C (**1-186c**) was inconclusive via obtained data and, because Gelliusines C (**1-186c**) have yet to be accessed via total synthesis, its absolute configuration also remains unknown. In terms of their biological activity, Gelliusine C (**1-186c**) exhibited cytotoxic activity, as well as anti-serotonin activity.¹¹¹

1.3.1.2. Tricepyridinium

Tricepyridinium (**1-187**) is a tris-indole alkaloid with a quaternary pyridinium core that was first isolated in 2017 by Abe *et. al.* from a culture of *Escheichia coli* clone incorporating metagenomic libraries from the marine sponge *Discodermia calyx*. The 1,3,5-tri-substituted pyridinium core connecting the three indole moieties of Tricepyridinium (**1-187**) was elucidated via spectroscopic methods, as shown in **Scheme 1.55**.¹¹²

Scheme 1.55. Chemical structure of Tricepyridinium (**1-187**).



Tricepyridinium (**1-187**)

Tricepyridinium (**1-187**) was found to display potent antibacterial activity, which is summarized in **Table 1.4**. Several bis-indole analogues of Tricepyridinium (**1-187**) were also synthesized and tested in this initial exploration of biological activity and **1-187** displayed more

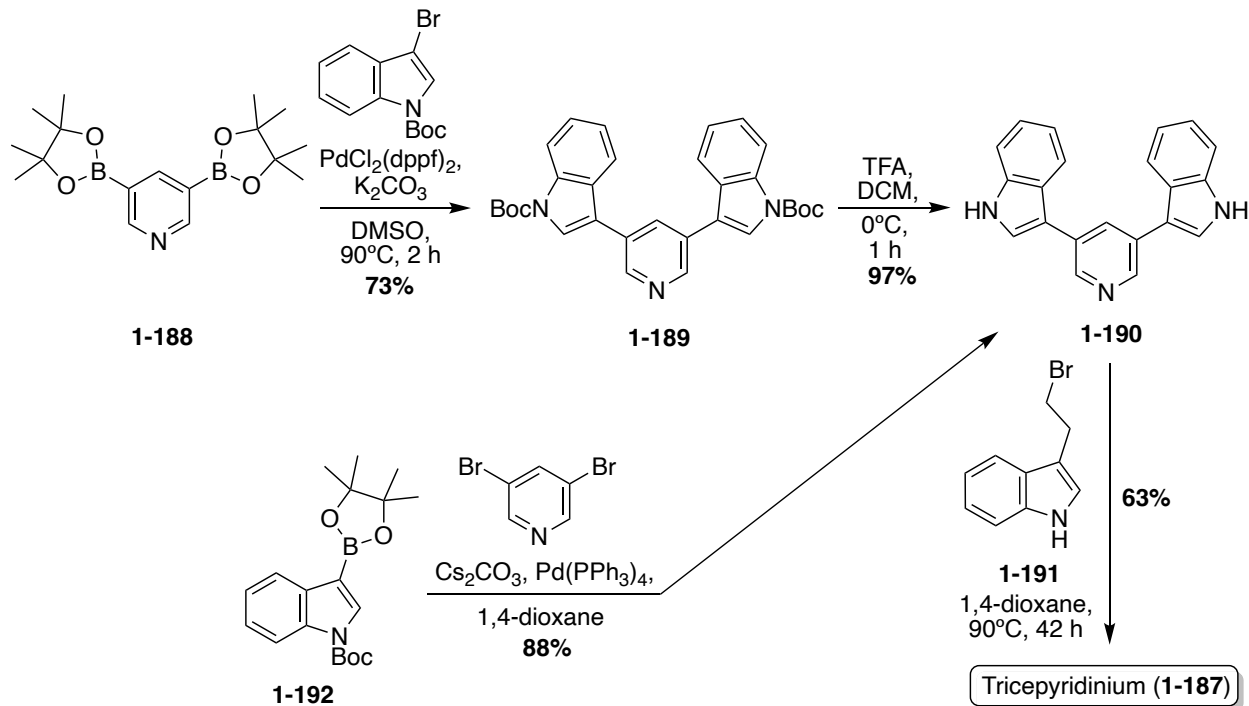
potent antibacterial activity than any of these analogues. Therefore, it was concluded that all three indole moieties of **1-187** were necessary for its potent antibacterial activity. In contrast, **1-187** did not display any cytotoxic activity against murine leukemic P388 cell line, while a bis-indole analogue of **1-187** lacking the indole moiety on the pyridinium nitrogen exhibited significant cytotoxic activity against this same cell line. This indicated that the cytotoxic activity of Tricepyridinium (**1-187**) was improved via removal of the indole in this position.¹¹²

Table 1.4. Known biological activity of Tricepyridinium (**1-187**).¹¹²

Bacteria	MIC (µg/mL)
<i>B. cerus</i>	0.78
<i>S. aureus</i> (MSSA)	1.56
<i>C. albicans</i>	12.5
<i>E. coli</i> (W3110)	>100

The first total synthesis of Tricepyridinium (**1-187**) was completed in 2017 by Abe, *et. al.* at the time of its isolation and structural elucidation to confirm its structure. As shown in **Scheme 1.56**, a bis-borylation of 3,5-dibromopyridine was completed to access intermediate **1-188**, followed by a subsequent palladium-catalyzed double Suzuki coupling to install two of the indole moieties on the pyridine ring. Boc deprotection and late-stage alkylation of the pyridine nitrogen via **1-191** to install the third indole moiety afforded Tricepyridinium (**1-187**) in high yields.¹¹²

Scheme 1.56. Total syntheses of Tricepyridinium (**1-187**).



In 2021, the total synthesis of Tricepyridinium (**1-187**) was completed via a similar approach as previously described. However, the major difference in this approach was the palladium catalyzed Suzuki coupling reaction, in which the electronics of the coupling partners were swapped. In this case, an indolic boronic ester (**1-192**) was coupled with 3,5-dibromopyridine, similar to the previously discussed approaches toward Scalaridine A (**1-173**). This approach led to a slightly higher yield of intermediate (**1-189**) of 88% compared to the previous 73% yield. Then, **1-189** was deprotected and acylated via alkyl bromide **1-191** to access Tricepyridinium (**1-187**) in 59% yield over two steps (Scheme 1.56).¹¹³

1.3.2. Non-aromatic *N*-heterocyclic linker moieties

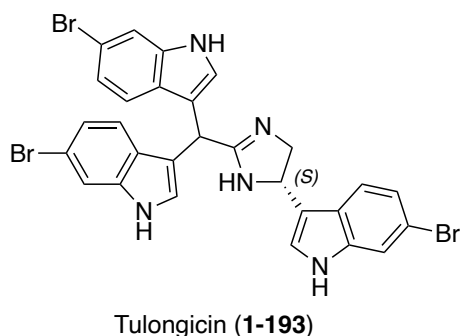
1.3.2.1. Tulongicin

Tulongicin (**1-193**) is a tri-indole alkaloid that was first isolated in 2017 by Liu *et al.* from *Topsentia* sp., along with its previously discussed bis-indole alkaloid analogues,

Dibromodeoxytopsentin (**1-1h**), Spongotine C (**1-2c**), and Dihydrospongotine C (**1-3**).

Tulongicin (**1-193**) was structurally elucidated via spectroscopic methods. As shown in **Scheme 1.57**, Tulongicin (**1-193**) is comprised of an imidazoline core that links three brominated indole moieties. It is noteworthy to mention, **1-193** was the first marine alkaloid of its kind to contain the structurally complex bis-indole methane moiety connected to an imidazoline core. The absolute configuration of (4*S*)-**1-193** was determined via comparison of experimental and calculated circular dichroism (CD) data (MPW1PW91/6-31G(d,p)). The only known biological activity of **1-193** is its strong antibacterial activity toward *S. aureus* (MIC 1.2 mg/mL), its moderate anti-HIV activity (YU2: IC₅₀ 3.9 mM, HxB2: IC₅₀ 2.7 mM), and its lack of cytotoxicity in mammalian cells. It is also noteworthy to mention that Tulongicin (**1-193**) has yet to be accessed via total synthesis.¹³

Scheme 1.57. Chemical structure of Tulongicin (**1-193**).

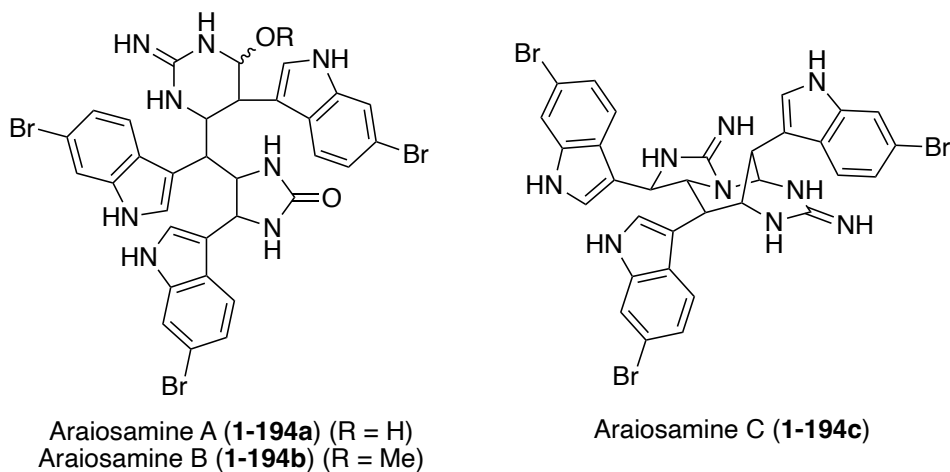


1.3.2.2. Araiosamines

The Araiosamines are arguably the most structurally complex of *N*-heterocyclic linked tris-indole alkaloid natural products that have been isolated to date. Araiosamines A-C (**1-194a-c**) were isolated in 2011 by Wei *et. al.* from the marine sponge *Clathria (Thalysias) araiosa*.¹¹⁴ As shown in **Scheme 1.58**, Araiosamines A and B (**1-194a-b**) contain three brominated indole moieties that are connected by cyclic guanidine and 2- imidazolinone linker moieties. The even

more complex Araiosamine C (**1-194c**) contain three brominated indole moieties that are connected by a very complex fused and bridged cyclic guanidine core. These complex structures were elucidated via careful spectroscopic analysis. It is noteworthy to mention that the absolute configuration of these natural products is not known. The chemical structure of Araiosamine D falls outside the scope of this review.¹¹⁴ Interestingly, at the time of their isolation, Araiosamines A-C (**1-194a-c**) were not reported to exhibit any significant biological activity. However, several years later when some of these natural products were accessed via total synthesis, the Araiosamines were reported to display significant antibacterial activity against Gram-positive and Gram-negative bacteria, such as *S. aureus* and *E. coli*.¹¹⁵

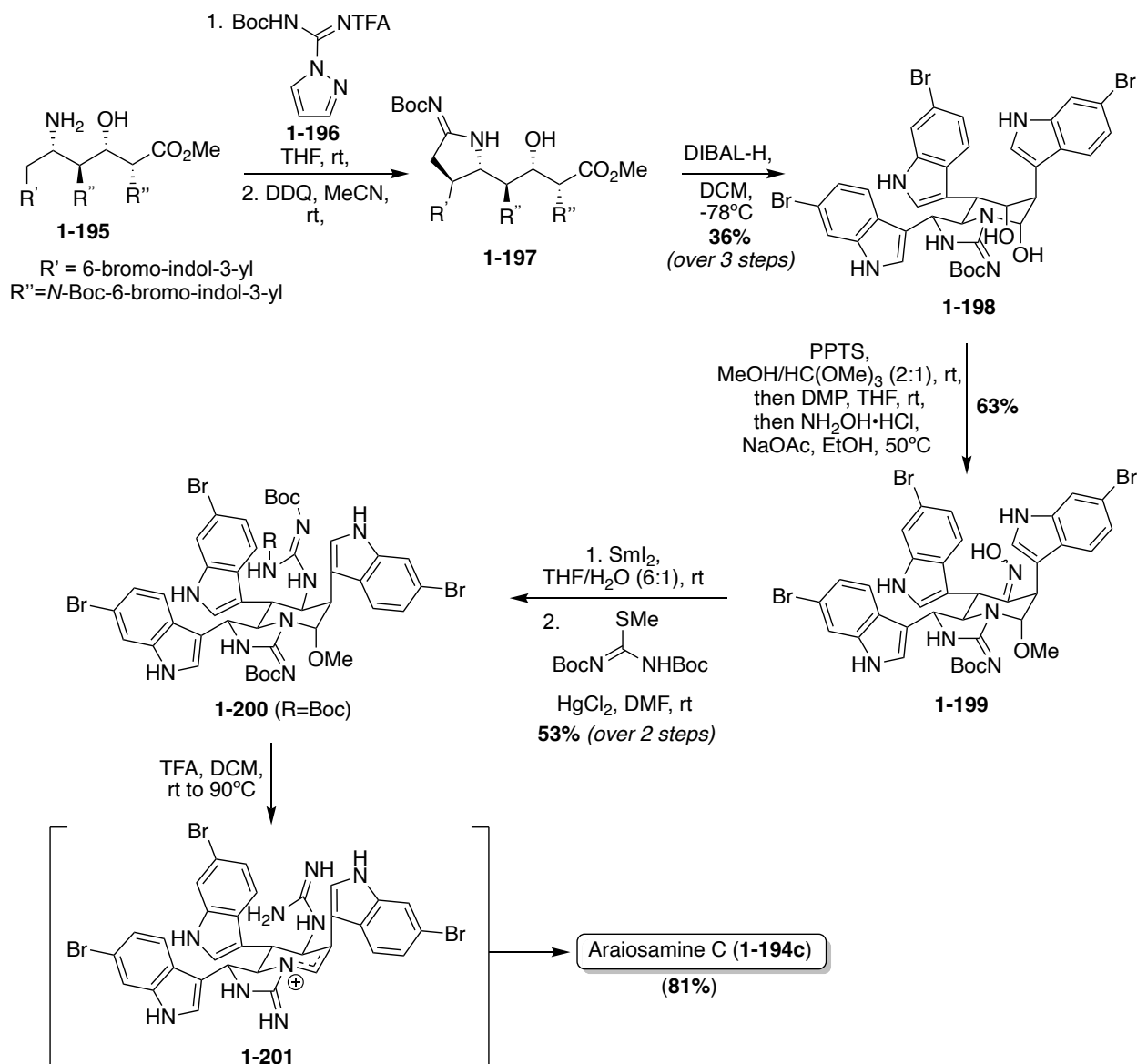
Scheme 1.58. Chemical structures of Araiosamines A-C (**1-194a-c**).



Of these Araiosamine natural products, Araiosamine C (**1-194c**) is the only one to have been accessed via total synthesis. In 2016, Baran, *et. al.* completed the first total synthesis via key guanidine installation and selective C-H functionalization steps driving toward a biomimetic final step to construct the complex core of **1-194c**. As is shown in **Scheme 1.59**, the first total synthesis of Araiosamine C (**1-194c**) began with formation of **1-195**, followed by deprotection and subsequent guanidinylation. Many guanidinylation reagents that were screened led to no reaction and it was hypothesized that the TFA group would impart adequate reactivity for the

guanidinylation reagent to react with hindered or electron deficient amines. Reduction of the ester and subsequent cyclization led to **1-198** in 36% yield over three steps. The oxime intermediate (**1-199**) was then synthesized and subsequently reduced to the primary amine intermediate via SmI₂. The reduction of the oxime (**1-199**) was very challenging because the oxime moiety is sterically encumbered by two adjacent indole groups and other functionalities such as the *N,O*-acetal or three aryl bromides are likely more prone toward reduction. After reaction of the resulting amine with *N,N*-di-Boc-*S*-methylisothiurea, the guanidine intermediate (**1-200**) was accessed in 53% over two steps.¹¹⁵ As shown in **Scheme 1.59**, after deprotection and elimination of the methoxy group via acidic conditions and high temperatures, **1-201** was setup for the pivotal cyclization of the guanidine nitrogen and the fused cyclic imine/enamine to form the characteristic bridgehead of **1-194c**. After this sequence, Araisamine C (**1-194c**) was accessed in a very high 81% yield.¹¹⁵

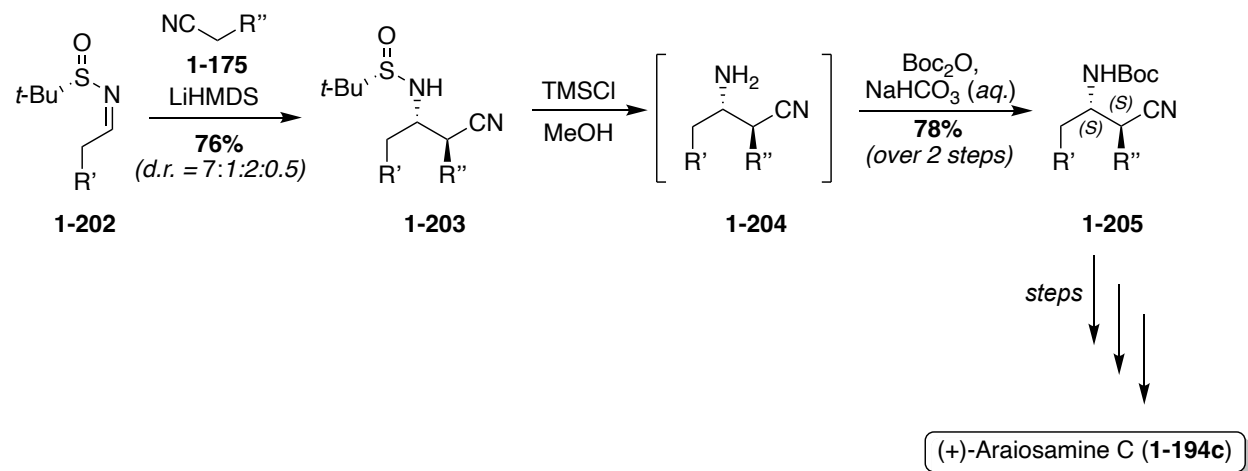
Scheme 1.59. First total synthesis of Araiosamine C (**1-194c**).



Since the absolute configuration of Araiosamine C (**1-194c**) was not known, the researchers adapted the previously discussed racemic path to **1-194c** to gain access to a stereoselective synthesis. As shown in **Scheme 1.60**, this was done by utilizing Ellman's Auxiliary to synthesize the optically active **1-203** in 76% yield as the favored diastereomer (*d.r.* = 7:1:2:0.5). This stereochemistry was then retained through to **1-205**, and using the same methodology as was previously discussed, the optically active (+)-Araiosamine C (**1-194c**) was

synthesized, which based on optical rotation data.¹¹⁵ It is noteworthy to mention that Araiosamines A and B (**1-194a-b**) have yet to be accessed via total synthesis.

Scheme 1.60. Enantioselective total synthesis of Araiosamine C (**1-194c**).



1.4. Conclusions

To conclude, the examples discussed in this review summarize the wide range of bis- and tris-indole alkaloids containing *N*-heterocyclic linker moieties that have been identified and isolated in recent years. These molecules exhibit potent biological activities, such as antibacterial, antiviral, cytotoxic, and anti-inflammatory activities. Natural products of this kind seem to share significant antibacterial activity overall. This could prove to be very advantageous in the future, as antibiotic resistance continues to be a major global issue. However, many of these previously discussed natural products have yet to be accessed via total synthesis, preventing their detailed biological evaluations. Development of synthetic methodologies to access these natural products and explore their promising biological activities will likely be of significant interest to the field in the future. It is also likely that the class of bis- and tris-indole natural products containing *N*-heterocyclic linker moieties will continue to expand as additional novel alkaloids are isolated.

REFERENCES

- (1) Kobayashi, J.; Murayama, T.; Ishibashi, M.; Kosuge, S.; Takamatsu, M.; Ohizumi, Y.; Kobayashi, H.; Ohta, T.; Nozoe, S.; Takuma, S., Hyrtiosins A and B, New Indole Alkaloids from the Okinawan Marine Sponge *Hyrtios Erecta*, *Tetrahedron*, **1990**, *46* (23), 7699–7702. [https://doi.org/10.1016/S0040-4020\(01\)90065-1](https://doi.org/10.1016/S0040-4020(01)90065-1).
- (2) Bao, B.; Sun, Q.; Yao, X.; Hong, J.; Lee, C., O.; Cho, H., Y.; Jung, J., H., Bisindole Alkaloids of the Topsentin and Hamacanthin Classes from a Marine Sponge *Spongisorites* Sp., *J. Nat. Prod.*, **2007**, *70* (1), 2–8. <https://doi.org/10.1021/np060206z>.
- (3) Golantsov, N., E.; Festa, A., A.; Karchava, A., V.; Yurovskaya, M., A., Marine Indole Alkaloids Containing an 1-(Indol-3-Yl)Ethane-1,2-Diamine Fragment (Review), *Chem. Heterocycl. Comp.*, **2013**, *49* (2), 203–225. <https://doi.org/10.1007/s10593-013-1238-9>.
- (4) Kerru, N.; Gummidi, L.; Maddila, S.; Gangu, K., K.; Jonnalagadda, S., B., A Review on Recent Advances in Nitrogen-Containing Molecules and Their Biological Applications, *Molecules*, **2020**, *25* (8), 1909. <https://doi.org/10.3390/molecules25081909>.
- (5) Bartik, K.; Braekman, J.-C.; Daloz, D.; Stoller, C.; Huysecom, J.; Vandevyver, G.; Ottinger, R., Topsentins, New Toxic Bis-Indole Alkaloids from the Marine Sponge *Topsentia Genitrix*, *Can. J. Chem.*, **1987**, *65* (9), 2118–2121. <https://doi.org/10.1139/v87-352>.
- (6) Shin, J.; Seo, Y.; Cho, K., W.; Rho, J., R.; Sim, C., J., New Bis(Indole) Alkaloids of the Topsentin Class from the Sponge *Spongisorites Genitrix*, *J. Nat. Prod.*, **1999**, *62* (4), 647–649. <https://doi.org/10.1021/np980507b>.
- (7) Bao, B.; Sun, Q.; Yao, X.; Hong, J.; Lee, C., O.; Sim, C., J.; Im, K., S.; Jung, J., H., Cytotoxic Bisindole Alkaloids from a Marine Sponge *Spongisorites* Sp., *J. Nat. Prod.*, **2005**, *68* (5), 711–715. <https://doi.org/10.1021/np049577a>.
- (8) Oh, K., B.; Mar, W.; Kim, S.; Kim, J., Y.; Oh, M., N.; Kim, J., G.; Shin, D.; Sim, C., J.; Shin, J., Bis(Indole) Alkaloids as Sortase A Inhibitors from the Sponge *Spongisorites* Sp., *Bioorganic & Medicinal Chemistry Letters*, **2005**, *15* (22), 4927–4931. <https://doi.org/10.1016/j.bmcl.2005.08.021>.
- (9) Morris, S., A.; Andersen, R., J., Nitrogenous Metabolites from the Deep Water Sponge *Hexadella* Sp., *Can. J. Chem.*, **1989**, *67* (4), 677–681. <https://doi.org/10.1139/v89-102>.
- (10) Morris, S. A.; Andersen, R. J. Brominated Bis(Indole) Alkaloids from the Marine Sponge *Hexadella* SP. *Tetrahedron* **1990**, *46* (3), 715–720. [https://doi.org/10.1016/S0040-4020\(01\)81355-7](https://doi.org/10.1016/S0040-4020(01)81355-7).
- (11) Jung, J., H.; Shinde, P., B.; Hong, J.; Liu, Y.; Sim, C., J., Secondary Metabolites from a Marine Sponge *Discodermia Calyx*, *Biochemical Systematics and Ecology*, **2007**, *35* (1), 48–51. <https://doi.org/10.1016/j.bse.2006.08.008>.

- (12) Casapullo, A.; Bifulco, G.; Bruno, I.; Riccio, R., New Bisindole Alkaloids of the Topsentin and Hamacanthin Classes from the Mediterranean Marine Sponge *Rhaphisia Lacazei*, *J. Nat. Prod.*, **2000**, *63* (4), 447–451. <https://doi.org/10.1021/np9903292>.
- (13) Liu, H., B.; Lauro, G.; O'Connor, R., D.; Lohith, K.; Kelly, M.; Colin, P.; Bifulco, G.; Bewley, C., A., Tulongicin, an Antibacterial Tri-Indole Alkaloid from a Deep-Water *Topsentia* Sp. Sponge, *J. Nat. Prod.*, **2017**, *80* (9), 2556–2560. <https://doi.org/10.1021/acs.jnatprod.7b00452>.
- (14) Sun, H.; Sun, K.; Sun, J., Recent Advances of Marine Natural Indole Products in Chemical and Biological Aspects, *Molecules*, **2023**, *28* (5), 2204. <https://doi.org/10.3390/molecules28052204>.
- (15) Braekman, J. C.; Dalozé, D.; Moussiaux, B.; Stoller, C.; Deneubourg, F., Sponge Secondary Metabolites: New Results, *Pure and Applied Chemistry*, **1989**, *61* (3), 509–512. <https://doi.org/10.1351/pac198961030509>.
- (16) Tsujii, S.; Rinehart, K., Topsentin, Bromotopsentin, and Dihydrodeoxytopsentin: Antiviral and Antitumor Bis(Indolyl)Imidazoles from Caribbean Deep-Sea Sponges of the Family Halichondriidae, Structural and Synthetic Studies, *J. Org. Chem.*, **1988**, *53* (23), 5446–5453.
- (17) Miyake, F., Y.; Yakushijin, K.; Horne, D., A., A Concise Synthesis of Topsentin A and Nortopsentins B and D, *Org. Lett.*, **2000**, *2* (14), 2121–2123. <https://doi.org/10.1021/ol000124g>.
- (18) Achab, S., A Three-Component Coupling Approach to the Marine Bis-Indole Alkaloids: Topsentin, Deoxytopsentin and Bromotopsentin, *Tetrahedron Letters*, **1996**, *37* (31), 5503–5506. [https://doi.org/10.1016/0040-4039\(96\)01148-3](https://doi.org/10.1016/0040-4039(96)01148-3).
- (19) Mal, S. K.; Bohé, L.; Achab, S., Convenient Access to Bis-Indole Alkaloids. Application to the Synthesis of Topsentins, *Tetrahedron*, **2008**, *64* (25), 5904–5914. <https://doi.org/10.1016/j.tet.2008.04.045>.
- (20) Kawasaki, I.; Katsuma, H.; Nakayama, Y.; Yamashita, M.; Ohta, S., Total Synthesis of Topsentin, Antiviral, and Antitumor Bis(Indolyl)Imidazole, *Heterocycles*, **1998**, *48* (9), 1887–1901.
- (21) Guinchard, X.; Vallée, Y.; Denis, J., N., Total Synthesis of Marine Sponge Bis(Indole) Alkaloids of the Topsentin Class, *J. Org. Chem.*, **2007**, *72* (10), 3972–3975. <https://doi.org/10.1021/jo070286r>.
- (22) Guinchard, X.; Vallée, Y.; Denis, J., N., Total Syntheses of Brominated Marine Sponge Alkaloids, *Org. Lett.*, **2007**, *9* (19), 3761–3764. <https://doi.org/10.1021/ol701626m>.

- (23) Ottoni, O.; Neder, A., D., V., F.; Dias, A., K., B.; Cruz, R., P., A.; Aquino, L., B., Acylation of Indole under Friedel–Crafts Conditions An Improved Method to Obtain 3-Acylindoles Regioselectively, *Org. Lett.*, **2001**, 3 (7), 1005–1007. <https://doi.org/10.1021/ol007056i>.
- (24) Murai, K.; Morishita, M.; Nakatani, R.; Kubo, O.; Fujioka, H.; Kita, Y., Concise Total Synthesis of (–)-Spongotone A, *J. Org. Chem.*, **2007**, 72 (23), 8947–8949. <https://doi.org/10.1021/jo701668s>.
- (25) Garg, N. K.; Sarpong, R.; Stoltz, B. M., The First Total Synthesis of Dragmacidin D, *J. Am. Chem. Soc.*, **2002**, 124 (44), 13179–13184. <https://doi.org/10.1021/ja027822b>.
- (26) Sakemi, S.; Sun, H., H., Nortopsentins A, B, and C, Cytotoxic and Antifungal Imidazolediybis[Indoles] from the Sponge Spongosorites Ruetzleri, *J. Org. Chem.*, **1991**, 56 (13), 4304–4307. <https://doi.org/10.1021/jo00013a044>.
- (27) Sun, H.; Sakemi, S.; Gunasekera, S.; Kashman, Y.; Lui, M.; Burren, N.; McCarthy, P., Bis-Indole Compounds Which Are Useful Antitumor and Antimicrobial Agents, *U.S. Pat. Appl.*, **1990**, US4970226A.
- (28) Mancini, I.; Guella, G.; Pietra, F.; Debitus, C.; Waikedre, J., From Inactive Nortopsentin D, a Novel Bis(Indole) Alkaloid Isolated from the Axinellid Sponge *Dragmacidon* Sp., from Deep Waters South of New Caledonia, to a Strongly Cytotoxic Derivative, *Helvetica Chimica Acta*, **1996**, 79 (8), 2075–2082. <https://doi.org/10.1002/hlca.19960790804>.
- (29) Tilvi, S.; Moriou, C.; Martin, M., T.; Gallard, J., F.; Sorres, J.; Patel, K.; Petek, S.; Debitus, C.; Ermolenko, L.; Al-Mourabit, A., Agelastatin E, Agelastatin F, and Benzosceptrin C from the Marine Sponge *Agelas Dendromorpha*, *J. Nat. Prod.*, **2010**, 73 (4), 720–723. <https://doi.org/10.1021/np900539j>.
- (30) Shi, M.; Kazuta, K.; Satoh, Y.; Masaki, Y., Synthesis and Investigation of C2-Symmetric Optically Active Pyrrolidinium Salts as Chiral Phase-Transfer Catalysts, *Chem. Pharm. Bull.*, **1994**, 42 (12), 2625–2628. <https://doi.org/10.1248/cpb.42.2625>.
- (31) Tan, J.; Chen, Y.; Li, H.; Yasuda, N., Suzuki-Miyaura Cross-Coupling Reactions of Unprotected Haloimidazoles, *J. Org. Chem.*, **2014**, 79 (18), 8871–8876. <https://doi.org/10.1021/jo501326r>.
- (32) Keel, K., L.; Tepe, J., J., Total Synthesis of Nortopsentin D via a Late-Stage Pinacol-like Rearrangement, *Org. Lett.*, **2021**, 23 (14), 5368–5372. <https://doi.org/10.1021/acs.orglett.1c01681>.
- (33) Sato, H.; Tsuda, M.; Watanabe, K.; Kobayashi, J., Rhopaladins A - D, New Indole Alkaloids from Marine Tunicate Rhopalaea Sp., *Tetrahedron*, **1998**, 54 (30), 8687–8690. [https://doi.org/10.1016/S0040-4020\(98\)00470-0](https://doi.org/10.1016/S0040-4020(98)00470-0).

- (34) Fresneda, P.; Molina, P.; Sanz, M., The First Synthesis of the Bis(Indole) Marine Alkaloid Rhopaladin D, *Synlett*, **2000**, *2000* (08), 1190–1192. <https://doi.org/10.1055/s-2000-6746>.
- (35) Fürstner, A.; Krause, H.; Thiel, O., R., Efficient Relay Syntheses and Assessment of the DNA-Cleaving Properties of the Pyrrole Alkaloid Derivatives Permethyl Storniamide A, Lycogalic Acid A Dimethyl Ester, and the Halitulín Core, *Tetrahedron*, **2002**, *58* (32), 6373–6380. [https://doi.org/10.1016/S0040-4020\(02\)00637-3](https://doi.org/10.1016/S0040-4020(02)00637-3).
- (36) Park, J., S.; Cho, E.; Hwang, J., Y.; Park, S., C.; Chung, B.; Kwon, O., S.; Sim, C., J.; Oh, D., C.; Oh, K., B.; Shin, J., Bioactive Bis(Indole) Alkaloids from a Spongosorites Sp. Sponge, *Marine Drugs*, **2020**, *19* (1), 3. <https://doi.org/10.3390/md19010003>.
- (37) Lecoq de Boisbaudran, P. E., *Comptes Rendus*, **1882**, *94*, 55–59.
- (38) Durán, N.; Menck, C., F., M., *Chromobacterium Violaceum* : A Review of Pharmacological and Industrial Perspectives, *Critical Reviews in Microbiology*, **2001**, *27* (3), 201–222. <https://doi.org/10.1080/20014091096747>.
- (39) Yang, L., H.; Xiong, H.; Lee, O., O.; Qi, S., H.; Qian, P., Y., Effect of Agitation on Violacein Production in *Pseudoalteromonas Luteoviolacea* Isolated from a Marine Sponge, *Lett. Appl. Microbiol.*, **2007**, *44* (6), 625–630. <https://doi.org/10.1111/j.1472-765X.2007.02125.x>.
- (40) Yada, S.; Wang, Y.; Zou, Y.; Nagasaki, K.; Hosokawa, K.; Osaka, I.; Arakawa, R.; Enomoto, K., Isolation and Characterization of Two Groups of Novel Marine Bacteria Producing Violacein, *Mar. Biotechnol.*, **2008**, *10* (2), 128–132. <https://doi.org/10.1007/s10126-007-9046-9>.
- (41) Hakvåg, S.; Fjærvik, E.; Klinkenberg, G.; Borgos, S. E.; Josefsen, K.; Ellingsen, T.; Zotchev, S., Violacein-Producing *Collimonas* Sp. from the Sea Surface Microlayer of Coastal Waters in Trøndelag, Norway, *Marine Drugs*, **2009**, *7* (4), 576–588. <https://doi.org/10.3390/md7040576>.
- (42) Jiang, P.; Wang, H.; Zhang, C.; Lou, K.; Xing, X., H., Reconstruction of the Violacein Biosynthetic Pathway from *Duganella* Sp. B2 in Different Heterologous Hosts, *Appl. Microbiol. Biotechnol.*, **2010**, *86* (4), 1077–1088. <https://doi.org/10.1007/s00253-009-2375-z>.
- (43) Hoshino, T., Violacein and Related Tryptophan Metabolites Produced by *Chromobacterium Violaceum*: Biosynthetic Mechanism and Pathway for Construction of Violacein Core, *Appl. Microbiol. Biotechnol.*, **2011**, *91* (6), 1463–1475. <https://doi.org/10.1007/s00253-011-3468-z>.
- (44) Durán, M.; Ponezi, A., N.; Faljoni-Alario, A.; Teixeira, M., F., S.; Justo, G., Z.; Durán, N., Potential Applications of Violacein: A Microbial Pigment, *Med. Chem. Res.*, **2012**, *21* (7), 1524–1532. <https://doi.org/10.1007/s00044-011-9654-9>.

- (45) Ballantine, J.; Barrett, B.; Beer, R.; Eardly, S.; Robertson, A.; Shaw, B.; Simpson, T., The Chemistry of Bacteria Part VII the Structure of Violacein, *Journal of the Chemical Society*, **1958**, 755–760.
- (46) Wille, G.; Steglich, W., A Short Synthesis of the Bacterial Pigments Violacein and Deoxyviolacein, *Synthesis*, **2001**, 2001 (05), 0759–0762. <https://doi.org/10.1055/s-2001-12776>.
- (47) Petersen, M., T.; Nielsen, T., E., Tandem Ring-Closing Metathesis/Isomerization Reactions for the Total Synthesis of Violacein, *Org. Lett.*, **2013**, 15 (8), 1986–1989. <https://doi.org/10.1021/ol400654r>.
- (48) Steglich, W.; Steffan, B.; Kopanski, L.; Eckhardt, G., Indolfarbstoffe aus Fruchtkörpern des Schleimpilzes *Arcyria denudata*, *Angew. Chem.*, **1980**, 92 (6), 463–464. <https://doi.org/10.1002/ange.19800920607>.
- (49) Nakatani, S.; Naoe, A.; Yamamoto, Y.; Yamauchi, T.; Yamaguchi, N.; Ishibashi, M., Isolation of Bisindole Alkaloids That Inhibit the Cell Cycle from Myxomycetes *Arcyria ferruginea* and *Tubifera casparyi*, *Bioorganic & Medicinal Chemistry Letters*, **2003**, 13 (17), 2879–2881. [https://doi.org/10.1016/S0960-894X\(03\)00592-4](https://doi.org/10.1016/S0960-894X(03)00592-4).
- (50) Monte, A. P.; Marona-Lewicka, D.; Cozzi, N. V.; Nichols, D. E., Synthesis and Pharmacological Examination of Benzofuran, Indan, and Tetralin Analogs of 3,4-(Methylenedioxy)Amphetamine., *J. Med. Chem.*, **1993**, 36 (23), 3700–3706. <https://doi.org/10.1021/jm00075a027>.
- (51) Mochly-Rosen, D.; Kauvar, L., M., *Advances in Pharmacology*, **1998**, 44.
- (52) Kaniwa, K.; Arai, M., A.; Li, X.; Ishibashi, M., Synthesis, Determination of Stereochemistry, and Evaluation of New Bisindole Alkaloids from the Myxomycete *Arcyria ferruginea*: An Approach for Wnt Signal Inhibitor, *Bioorganic & Medicinal Chemistry Letters*, **2007**, 17 (15), 4254–4257. <https://doi.org/10.1016/j.bmcl.2007.05.033>.
- (53) Brenner, M.; Rexhausen, H.; Steffan, B.; Steglich, W., Synthesis of *Arcyriarubin b* and Related Bisindolylmaleimides, *Tetrahedron*, **1988**, 44 (10), 2887–2892. [https://doi.org/10.1016/S0040-4020\(88\)90025-7](https://doi.org/10.1016/S0040-4020(88)90025-7).
- (54) Faul, M., M.; Sullivan, K., A.; Winneroski, L., L., A General Approach to the Synthesis of Bisindolylmaleimides: Synthesis of Staurosporine Aglycone, *Synthesis*, **1995**, 1995 (12), 1511–1516. <https://doi.org/10.1055/s-1995-4146>.
- (55) Mei, X.; Wang, J.; Zhou, Z.; Wu, S.; Huang, L.; Lin, Z.; Ling, Q., Diarylmaaleic Anhydrides: Unusual Organic Luminescence, Multi-Stimuli Response and Photochromism, *J. Mater. Chem.*, **2017**, 5 (8), 2135–2141. <https://doi.org/10.1039/C6TC05519B>.

- (56) Guo, Q.; Deng, W., F.; Xiao, J., L.; Shi, P., C.; Li, J., L.; Zhou, Z., X.; Ji, C., Synthesis, Single Crystal X-Ray Analysis and Vibrational Spectral Studies of 3,4-Di(1H-Indol-3-Yl)-1H-Pyrrole-2,5-dione, *Journal of Molecular Structure*, **2023**, *1281*, 135103. <https://doi.org/10.1016/j.molstruc.2023.135103>.
- (57) Fröde, R.; Hinze, C.; Josten, I.; Schmidt, B.; Steffan, B.; Steglich, W., Isolation and Synthesis of 3,4-Bis(Indol-3-Yl)Pyrrole-2,5-Dicarboxylic Acid Derivatives from the Slime Mould *Lycogala Epidendrum*, *Tetrahedron Letters*, **1994**, *35* (11), 1689–1690. [https://doi.org/10.1016/0040-4039\(94\)88320-3](https://doi.org/10.1016/0040-4039(94)88320-3).
- (58) Hashimoto, T.; Akiyo, Y.; Akazawa, K.; Takaoka, S.; Tori, M.; Asakawa, Y., Three Novel Dimethyl Pyrroledicarboxylate, Lycogarubins A-C, from the Myxomycetes *Lycogala Epidendrum*, *Tetrahedron Letters*, **1994**, *35* (16), 2559–2560. [https://doi.org/10.1016/S0040-4039\(00\)77170-X](https://doi.org/10.1016/S0040-4039(00)77170-X).
- (59) Nishizawa, T.; Grünschow, S.; Jayamaha, D., H., E.; Nishizawa-Harada, C.; Sherman, D., H., Enzymatic Assembly of the Bis-Indole Core of Rebeccamycin, *J. Am. Chem. Soc.*, **2006**, *128* (3), 724–725. <https://doi.org/10.1021/ja056749x>.
- (60) Chen, W.; Feng, Z.; He, X.; Zhao, Q.; Liang, Q., Design and Synthesis of 3,4-Diarylpyrrole Analogues as Potent Topoisomerase Inhibitors, *MC*, **2018**, *14* (5), 485–494. <https://doi.org/10.2174/1573406414666180226164049>.
- (61) Hinze, C.; Kreipl, A.; Terpin, A.; Steglich, W., Synthesis of Simple 3,4-Diarylpyrrole-2,5-Dicarboxylic Acids and Lukianol A by Oxidative Condensation of 3-Arylpyruvic Acids with Ammonia, *Synthesis*, **2007**, *2007* (04), 608–612. <https://doi.org/10.1055/s-2007-965876>.
- (62) Zhou, N.; Xie, T.; Liu, L.; Xie, Z., Cu/Mn Co-Oxidized Cyclization for the Synthesis of Highly Substituted Pyrrole Derivatives from Amino Acid Esters: A Strategy for the Biomimetic Syntheses of Lycogarubin C and Chromopyrrolic Acid, *J. Org. Chem.*, **2014**, *79* (13), 6061–6068. <https://doi.org/10.1021/jo500740w>.
- (63) Zheng, X.; Li, Y.; Guan, M.; Wang, L.; Wei, S.; Li, Y.; Chang, C.; Xu, Z., Biomimetic Total Synthesis of the Spiroindimicin Family of Natural Products, *Angew. Chem. Int. Ed.*, **2022**, *61* (38), e202208802. <https://doi.org/10.1002/anie.202208802>.
- (64) Fu, L.; Gribble, G., W., Total Synthesis of Lycogarubin C Utilizing the Kornfeld–Boger Ring Contraction, *Tetrahedron Letters*, **2010**, *51* (3), 537–539. <https://doi.org/10.1016/j.tetlet.2009.11.085>.
- (65) Oakdale, J., S.; Boger, D., L., Total Synthesis of Lycogarubin C and Lycogalic Acid, *Org. Lett.*, **2010**, *12* (5), 1132–1134. <https://doi.org/10.1021/ol100146b>.
- (66) McArthur, K., A.; Mitchell, S., S.; Tsueng, G.; Rheingold, A.; White, D., J.; Grodberg, J.; Lam, K., S.; Potts, B., C., M., Lynamycins A–E, Chlorinated Bisindole Pyrrole Antibiotics

- from a Novel Marine Actinomycete, *J. Nat. Prod.*, **2008**, *71* (10), 1732–1737. <https://doi.org/10.1021/np800286d>.
- (67) Sigala, I.; Ganidis, G.; Thysiadis, S.; Zografos, A. L.; Giannakouros, T.; Sarli, V.; Nikolakaki, E., Lynamycin D an Antimicrobial Natural Product Affects Splicing by Inducing the Expression of SR Protein Kinase 1, *Bioorganic & Medicinal Chemistry*, **2017**, *25* (5), 1622–1629. <https://doi.org/10.1016/j.bmc.2017.01.025>.
- (68) Zhang, W.; Ma, L.; Li, S.; Liu, Z.; Chen, Y.; Zhang, H.; Zhang, G.; Zhang, Q.; Tian, X.; Yuan, C.; Zhang, S.; Zhang, W.; Zhang, C., Indimicins A–E, Bisindole Alkaloids from the Deep-Sea-Derived *Streptomyces* Sp. SCSIO 03032, *J. Nat. Prod.*, **2014**, *77* (8), 1887–1892. <https://doi.org/10.1021/np500362p>.
- (69) Zhang, Z.; Ray, S.; Imlay, L.; Callaghan, L., T.; Niederstrasser, H.; Mallipeddi, P., L.; Posner, B., A.; Wetzel, D., M.; Phillips, M. A.; Smith, M., W., Total Synthesis of (+)-Spiroindimicin A and Congeners Unveils Their Antiparasitic Activity, *Chem. Sci.*, **2021**, *12* (30), 10388–10394. <https://doi.org/10.1039/D1SC02838C>.
- (70) Kohmoto, S.; Kashman, Y.; McConnell, O. J.; Rinehart, K. L.; Wright, A.; Koehn, F., Dragmacidin, a New Cytotoxic Bis(Indole) Alkaloid from a Deep Water Marine Sponge, Dragmacidon Sp., *J. Org. Chem.*, **1988**, *53* (13), 3116–3118. <https://doi.org/10.1021/jo00248a040>.
- (71) Fahy, E.; Potts, B., C., M.; Faulkner, D., J.; Smith, K., 6-Bromotryptamine Derivatives from the Gulf of California Tunicate *Didemnum Candidum*, *J. Nat. Prod.*, **1991**, *54* (2), 564–569. <https://doi.org/10.1021/np50074a032>.
- (72) Kawasaki, T.; Ohno, K.; Enoki, H.; Umemoto, Y.; Sakamoto, M., Syntheses of Bis(Indolyl)-Piperazine Alkaloids, Dragmacidin B and C, and Dihydrohamacanthin A, *Tetrahedron Letters*, **2002**, *43* (23), 4245–4248. [https://doi.org/10.1016/S0040-4039\(02\)00771-2](https://doi.org/10.1016/S0040-4039(02)00771-2).
- (73) Capon, R., J.; Rooney, F.; Murray, L., M.; Collins, E.; Sim, A., T., R.; Rostas, J., A., P.; Butler, M., S.; Carroll, A., R., Dragmacidins: New Protein Phosphatase Inhibitors from a Southern Australian Deep-Water Marine Sponge, *Spongosorites* Sp., *J. Nat. Prod.*, **1998**, *61* (5), 660–662. <https://doi.org/10.1021/np970483t>.
- (74) Cutignano, A.; Bifulco, G.; Bruno, I.; Casapullo, A.; Gomez-Paloma, L.; Riccio, R., Dragmacidin F: A New Antiviral Bromoindole Alkaloid from the Mediterranean Sponge *Halicortex* Sp., *Tetrahedron*, **2000**, *56* (23), 3743–3748. [https://doi.org/10.1016/S0040-4020\(00\)00281-7](https://doi.org/10.1016/S0040-4020(00)00281-7).
- (75) Garg, N., K.; Caspi, D., D.; Stoltz, B., M., The Total Synthesis of (+)-Dragmacidin F, *J. Am. Chem. Soc.*, **2004**, *126* (31), 9552–9553. <https://doi.org/10.1021/ja046695b>.

- (76) Feldman, K., S.; Ngermeesri, P., Total Synthesis of (±)-Dragmacidin E, *Org. Lett.*, **2011**, *13* (20), 5704–5707. <https://doi.org/10.1021/ol202535f>.
- (77) Wright, A.; Killday, K.; Chakrabarti, D.; Guzmán, E.; Harmody, D.; McCarthy, P.; Pitts, T.; Pomponi, S.; Reed, J.; Roberts, B.; Rodrigues Felix, C.; Rohde, K., Dragmacidin G, a Bioactive Bis-Indole Alkaloid from a Deep-Water Sponge of the Genus Spongosorites, *Marine Drugs*, **2017**, *15* (1), 16. <https://doi.org/10.3390/md15010016>.
- (78) Jiang, B.; Smallheer, J., M.; Amaral-Ly, C.; Wuonola, M., A., Total Synthesis of (+-)-Dragmacidin: A Cytotoxic Bis(Indole)Alkaloid of Marine Origin, *J. Org. Chem.*, **1994**, *59* (22), 6823–6827. <https://doi.org/10.1021/jo00101a051>.
- (79) Whitlock, C., R.; Cava, M., P., A Total Synthesis of Dragmacidin B, *Tetrahedron Letters*, **1994**, *35* (3), 371–374. [https://doi.org/10.1016/0040-4039\(94\)85056-9](https://doi.org/10.1016/0040-4039(94)85056-9).
- (80) Kawasaki, T.; Enoki, H.; Matsumura, K.; Ohyama, M.; Inagawa, M.; Sakamoto, M., First Total Synthesis of Dragmacidin A via Indolyglycines, *Org. Lett.*, **2000**, *2* (19), 3027–3029. <https://doi.org/10.1021/ol006394g>.
- (81) Yang, C., G.; Wang, J.; Tang, X., X.; Jiang, B., Asymmetric Aminohydroxylation of Vinyl Indoles: A Short Enantioselective Synthesis of the Bisindole Alkaloids Dihydrohamacanthin A and Dragmacidin A, *Tetrahedron: Asymmetry*, **2002**, *13* (4), 383–394. [https://doi.org/10.1016/S0957-4166\(02\)00111-8](https://doi.org/10.1016/S0957-4166(02)00111-8).
- (82) Yang, C., G.; Wang, J.; Tang, X., X.; Jiang, B., Asymmetric Aminohydroxylation of Vinyl Indoles: A Short Enantioselective Synthesis of the Bisindole Alkaloids Dihydrohamacanthin A and Dragmacidin A, *Tetrahedron: Asymmetry*, **2002**, *13* (4), 383–394. [https://doi.org/10.1016/S0957-4166\(02\)00111-8](https://doi.org/10.1016/S0957-4166(02)00111-8).
- (83) Miyake, F., Y.; Yakushijin, K.; Horne, D., A., A Facile Synthesis of Dragmacidin B and 2,5-Bis(6'-Bromo-3'-Indolyl)Piperazine, *Org. Lett.*, **2000**, *2* (20), 3185–3187. <https://doi.org/10.1021/ol0001970>.
- (84) Tonsiengson, F.; Yakushijin, K.; Horne, D. A., *Synthesis*, **2006**, *49*.
- (85) Zhang, F.; Wang, B.; Prasad, P.; Capon, R., J.; Jia, Y., Asymmetric Total Synthesis of (+)-Dragmacidin D Reveals Unexpected Stereocomplexity, *Org. Lett.*, **2015**, *17* (6), 1529–1532. <https://doi.org/10.1021/acs.orglett.5b00327>.
- (86) Gunasekera, S., P.; McCarthy, P., J.; Kelly-Borges, M., Hamacanthins A and B, New Antifungal Bis Indole Alkaloids from the Deep-Water Marine Sponge, Hamacantha Sp., *J. Nat. Prod.*, **1994**, *57* (10), 1437–1441. <https://doi.org/10.1021/np50112a014>.
- (87) Jiang, B.; Yang, C., G.; Wang, J., Enantioselective Synthesis for the (–)-Antipode of the Pyrazinone Marine Alkaloid, Hamacanthin A, *J. Org. Chem.*, **2001**, *66* (14), 4865–4869. <https://doi.org/10.1021/jo010265b>.

- (88) Jiang, B.; Yang, C., G.; Wang, J., Enantioselective Synthesis of Marine Indole Alkaloid Hamacanthin B, *J. Org. Chem.*, **2002**, *67* (4), 1396–1398. <https://doi.org/10.1021/jo0108109>.
- (89) Kawasaki, T.; Kouko, T.; Totsuka, H.; Hiramatsu, K., Synthesis of Marine Bisindole Alkaloids, Hamacanthins A and B through Intramolecular Transamidation–Cyclization, *Tetrahedron Letters*, **2003**, *44* (49), 8849–8852. <https://doi.org/10.1016/j.tetlet.2003.09.184>.
- (90) Higuchi, K.; Takei, R.; Kouko, T.; Kawasaki, T., Total Synthesis of Marine Bisindole Alkaloid (+)- *Cis* -Dihydrohamacanthin B, *Synthesis*, **2007**, *2007* (5), 669–674. <https://doi.org/10.1055/s-2007-965907>.
- (91) Kozlovsky, A., G.; Vinokurova, N., G.; Adanin, V., M.; Burkhardt, G.; Dahse, H., M.; Gräfe, U., New Diketopiperazine Alkaloids from *Penicillium Fellutanum*, *J. Nat. Prod.*, **2000**, *63* (5), 698–700. <https://doi.org/10.1021/np9903853>.
- (92) Hayashi, H., Bioactive Alkaloids of Fungal Origin, *Studies in Natural Products Chemistry; Elsevier*, **2005**, *32*, 549–609. [https://doi.org/10.1016/S1572-5995\(05\)80064-X](https://doi.org/10.1016/S1572-5995(05)80064-X).
- (93) Schkeryantz, J., M.; Woo, J., C., G.; Danishefsky, S., J., Total Synthesis of Gypsetin, *J. Am. Chem. Soc.*, **1995**, *117* (26), 7025–7026. <https://doi.org/10.1021/ja00131a035>.
- (94) Schkeryantz, J., M.; Woo, J., C., G.; Siliphaivanh, P.; Depew, K., M.; Danishefsky, S., J., Total Synthesis of Gypsetin, Deoxybrevianamide E, Brevianamide E, and Tryprostatin B: Novel Constructions of 2,3-Disubstituted Indoles, *J. Am. Chem. Soc.*, **1999**, *121* (51), 11964–11975. <https://doi.org/10.1021/ja9925249>.
- (95) Joshi, K., B.; Verma, S., Participation of Aromatic Side Chains in Diketopiperazine Ensembles, *Tetrahedron Letters*, **2008**, *49* (27), 4231–4234. <https://doi.org/10.1016/j.tetlet.2008.04.156>.
- (96) Cheng, X.; Ma, L., Enzymatic Synthesis of Fluorinated Compounds, *Appl. Microbiol. Biotechnol.*, **2021**, *105* (21), 8033–8058.
- (97) Usuki, H.; Yamamoto, Y.; Arima, J.; Iwabuchi, M.; Miyoshi, S.; Nitoda, T.; Hatanaka, T., Peptide Bond Formation by Aminolysin-A Catalysis: A Simple Approach to Enzymatic Synthesis of Diverse Short Oligopeptides and Biologically Active Puromycins, *Org. Biomol. Chem.*, **2011**, *9* (7), 2327. <https://doi.org/10.1039/c0ob00403k>.
- (98) Kelly, S., P.; Shende, V., V.; Flynn, A., R.; Dan, Q.; Ye, Y.; Smith, J., L.; Tsukamoto, S.; Sigman, M., S.; Sherman, D., H., Data Science-Driven Analysis of Substrate-Permissive Diketopiperazine Reverse Prenyltransferase NotF: Applications in Protein Engineering and Cascade Biocatalytic Synthesis of (–)-Eurotiumin A, *J. Am. Chem. Soc.*, **2022**, *144* (42), 19326–19336. <https://doi.org/10.1021/jacs.2c06631>.

- (99) Endo, T.; Tsuda, M.; Fromont, J.; Kobayashi, J., Hyrtinadine A, a Bis-Indole Alkaloid from a Marine Sponge, *J. Nat. Prod.*, **2007**, *70* (3), 423–424. <https://doi.org/10.1021/np060420n>.
- (100) Zhu, L.; Chen, C.; Wang, H.; Ye, W.; Zhou, G., Indole Alkaloids from *Alocasia Macrorrhiza*, *Chem. Pharm. Bull.*, **2012**, *60* (5), 670–673. <https://doi.org/10.1248/cpb.60.670>.
- (101) Lee, Y., J.; Lee, D., G.; Rho, H., S.; Krasokhin, V., B.; Shin, H., J.; Lee, J., S.; Lee, H., S., Cytotoxic 5-Hydroxyindole Alkaloids from the Marine Sponge *Scalarispongia* Sp., *J. Heterocyclic Chem.*, **2013**, *50* (6), 1400–1404. <https://doi.org/10.1002/jhet.1599>.
- (102) Tasch, B., O., A.; Merkul, E.; Müller, T., J., J., One-Pot Synthesis of Diazine-Bridged Bisindoles and Concise Synthesis of the Marine Alkaloid Hyrtinadine A., *Eur. J. Org. Chem.*, **2011**, *2011* (24), 4532–4535. <https://doi.org/10.1002/ejoc.201100680>.
- (103) Kim, S., H.; Sperry, J., Synthesis of Alocasin A, *J. Nat. Prod.*, **2015**, *78* (12), 3080–3082. <https://doi.org/10.1021/acs.jnatprod.5b00853>.
- (104) Kim, S., H.; Sperry, J. Synthesis of Scalaridine A, *Tetrahedron Letters*, **2015**, *56* (43), 5914–5915. <https://doi.org/10.1016/j.tetlet.2015.09.033>.
- (105) Ansari, N., H.; Söderberg, B., C., G., Short Syntheses of the Indole Alkaloids Alocasin A, Scalaridine A, and Hyrtinadine A-B, *Tetrahedron*, **2016**, *72* (29), 4214–4221. <https://doi.org/10.1016/j.tet.2016.05.057>.
- (106) Ranjani, G.; Nagarajan, R., Insight into Copper Catalysis: In Situ Formed Nano Cu₂O in Suzuki–Miyaura Cross-Coupling of Aryl/Indolyl Boronates., *Org. Lett.*, **2017**, *19* (15), 3974–3977. <https://doi.org/10.1021/acs.orglett.7b01669>.
- (107) Kruppa, M.; Sommer, G. A.; Müller, T., J., J., Concise Syntheses of Marine (Bis)Indole Alkaloids Meridianin C, D, F, and G and Scalaridine A via One-Pot Masuda Borylation-Suzuki Coupling Sequence, *Molecules*, **2022**, *27* (7), 2233. <https://doi.org/10.3390/molecules27072233>.
- (108) Dong, J.; Ma, H.; Wang, B.; Yang, S.; Wang, Z.; Li, Y.; Liu, Y.; Wang, Q., Discovery of Hyrtinadine A and Its Derivatives as Novel Antiviral and Anti-Phytopathogenic-Fungus Agents, *Molecules*, **2022**, *27* (23), 8439. <https://doi.org/10.3390/molecules27238439>.
- (109) Rehberg, N.; Sommer, G., A.; Drießen, D.; Kruppa, M.; Adeniyi, E., T.; Chen, S.; Wang, L.; Wolf, K.; Tasch, B., O., A.; Ioerger, T., R.; Zhu, K.; Müller, T., J., J.; Kalscheuer, R., Nature-Inspired (Di)Azine-Bridged Bisindole Alkaloids with Potent Antibacterial *In Vitro* and *In Vivo* Efficacy against Methicillin-Resistant *Staphylococcus Aureus*, *J. Med. Chem.*, **2020**, *63* (21), 12623–12641. <https://doi.org/10.1021/acs.jmedchem.0c00826>.

- (110) Bifulco, G.; Bruno, I.; Minale, L.; Riccio, R.; Calignano, A.; Debitus, C., (\pm)-Gelliusines A and B, Two Diastereomeric Brominated Tris-Indole Alkaloids from a Deep Water New Caledonian Marine Sponge (Gellius or Orina Sp.), *J. Nat. Prod.*, **1994**, *57* (9), 1294–1299. <https://doi.org/10.1021/np50111a020>.
- (111) Bifulco, G.; Bruno, I.; Riccio, R.; Lavayre, J.; Bourdy, G., Further Brominated Bis- and Tris-Indole Alkaloids from the Deep-Water New Caledonian Marine Sponge Orina Sp., *J. Nat. Prod.*, **1995**, *58* (8), 1254–1260. <https://doi.org/10.1021/np50122a017>.
- (112) Okada, M.; Sugita, T.; Wong, C. P.; Wakimoto, T.; Abe, I., Identification of Pyridinium with Three Indole Moieties as an Antimicrobial Agent, *J. Nat. Prod.*, **2017**, *80* (4), 1205–1209. <https://doi.org/10.1021/acs.jnatprod.6b01152>.
- (113) Garrison, M., A.; Mahoney, A., R.; Wuest, W., M., Tricepyridinium-inspired QACs Yield Potent Antimicrobials and Provide Insight into QAC Resistance, *Chem. Med. Chem.*, **2021**, *16* (3), 463–466. <https://doi.org/10.1002/cmdc.202000604>.
- (114) Wei, X.; Henriksen, N., M.; Skalicky, J., J.; Harper, M., K.; Cheatham, T., E.; Ireland, C., M.; Van Wagoner, R., M., Araisamines A–D: Tris-Bromoindole Cyclic Guanidine Alkaloids from the Marine Sponge *Clathria (Thalysias) Araisosa*, *J. Org. Chem.*, **2011**, *76* (14), 5515–5523. <https://doi.org/10.1021/jo200327d>.
- (115) Tian, M.; Yan, M.; Baran, P., S., 11-Step Total Synthesis of Araisamines, *J. Am. Chem. Soc.*, **2016**, *138* (43), 14234–14237. <https://doi.org/10.1021/jacs.6b09701>.

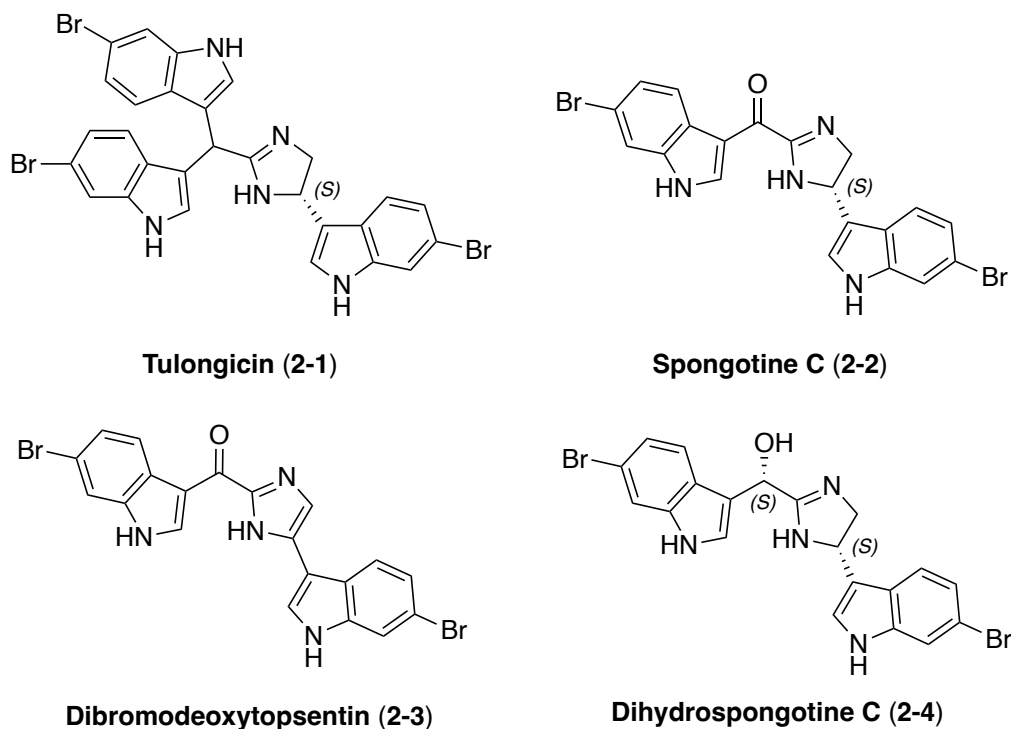
Chapter 2: Efforts Toward the Total Synthesis of Tulongicin and Its Related Natural Product Analogues

2.1 Introduction

Indole alkaloids are commonly found in a variety of marine sources, including sponges, tunicates, red alga, acorn worms, and symbiotic bacteria, and they represent the largest, and among the most complicated, class of the marine alkaloids.¹ Indole alkaloids have been shown to display diverse biological activities, including cytotoxic, antitumor, antiviral, antibacterial, and anti-inflammatory activities.²

Tulongicin **2-1** is a tri-indole alkaloid that was first isolated from *Topsentia* sp. by Hong-Bing Liu in 2017 near the Ulong Channel in Koror, Palau, along with its bis-indole alkaloids Spongotine C **2-2**, Dibromodeoxytopsentin **2-3**, and Dihydrospingotine C (**2-4**).³ This constituted the first isolation of **2-1** and **2-4**, however, **2-2** and **2-3** have both been previously isolated. Dibromodeoxytopsentin (**2-3**) was first isolated in 2005 from *Spongosorites* sp. and Spongotine C (**2-2**) was first isolated in 2007 from the same *Spongosorites* sp.^{2,4} In the isolation process of these natural products, a 1g sample of *Topsentia* sp. was extracted with MeOH/DCM (1:1) and compounds were separated via column chromatography to afford Tulongicin (1.6 mg), Spongotine C (7.3 mg), Dibromodeoxytopsentin (1.9 mg), and Dihydrospingotine (134.9 mg). The chemical structures of these natural products are shown in **Scheme 2.1**. As shown, the chemical structure of Tulongicin (**2-1**) is comprised of three indole moieties connected by an imidazoline linker. In addition, Tulongicin (**2-1**) was the first example of a natural product containing a bis-indolemethane moiety linked to an imidazoline ring, making **2-1** an attractive target for total synthesis.³

Scheme 2.1. Chemical structures, and absolute stereochemistry of Tulongicin, Spongotine C, Dibromodeoxytropsentin, and Dihydrospogotine C.



Tulongicin (**2-1**) was characterized and structurally elucidated via mass spectrometry (HRESIMS) and various nuclear magnetic resonance (NMR) experiments, including ^1H , ^{13}C , ^1H - ^1H COSY, HSQC, and HMBC.³ The absolute configuration of (*4S*)-**2-1** was determined via comparison of experimental and calculated circular dichroism (CD) data (MPW1PW91/6-31G(d,p)). Using similar methods, the absolute stereochemistry of **2-4** was also determined to be (*4S,6S*)-**2-4b**.³

The biological properties of Tulongicin (**2-1**) have not been fully explored. As shown in Table 2.1, the only known biological activity of **2-1** is its strong antibacterial activity toward *S. aureus*, its moderate anti-HIV activity, and its lack of cytotoxicity in mammalian cells. Compounds **2-2** and **2-4** have been shown to display similar strong antibacterial and moderate

anti-HIV activity. Compound **2-2** exhibited the strongest antibacterial activity, while **2-3** displayed significantly decreased activity (**Table 2.1**).³

Table 2.1. Biological activity of Tulongicin (**2-1**) and its related natural product analogues.

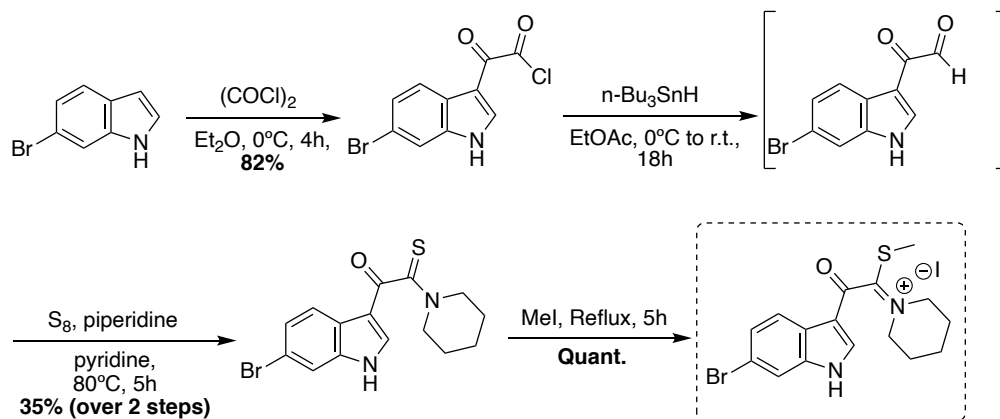
Natural Product	Antibacterial activity		Anti-HIV activity	
	<i>S. aureus</i> (MIC)	YU2 (IC ₅₀)	HxB2 (IC ₅₀)	
2-1	1.2 mg/mL	3.9 mM	2.7 mM	
2-2	1.1 mg/mL	9.5 mM	12.0 mM	
2-3	11.0 mg/mL	57.0 mM	N/A	
2-4	3.7mg/mL	3.5 mM	4.5 mM	

It is notable to mention that both **2-2** and **2-3** have been previously accessed via total synthesis. The first total syntheses of both **2-2** and **2-3** were completed by Guinchard, *et. al.*, in 2007.⁵ This first total synthesis of **2-2** and **2-3** is shown in in **Scheme 2.2**. As shown, **2-2** was accessed via cyclization of a diamine fragment and a keto-thioimide fragment to form the imidazoline core. Then, compound **2-3** was accessed via oxidation of **2-2**. The keto-thioimide fragment was synthesized in four steps from the commercially available 6-bromo-1*H*-indole. However, the diamine fragment was synthesized in 5 steps from the non-commercially available brominated indolic N-hydroxylamine (**Scheme 2.2**). Therefore, it is important to note that two additional steps, nitrene formation and subsequent indolic hydroxylamine synthesis, were necessary to access this hydroxylamine starting material from commercially available *tert*-butyl (2-oxoethyl) carbamate, *N*-benzylhydroxylamine, and 6-bromo-1*H*-indole.⁶ Thus, **2-2** and **2-3** were accessed in seven and eight linear steps, respectively, from commercially available starting materials.

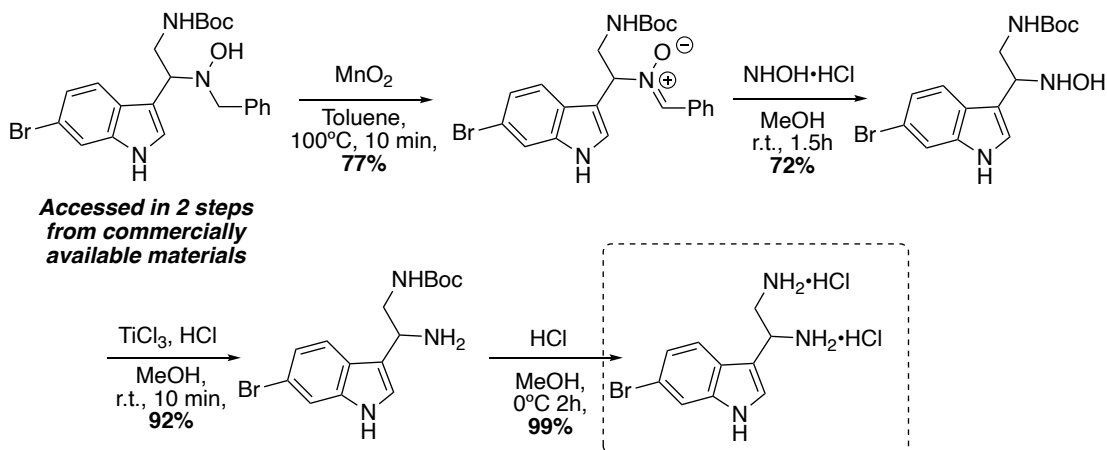
Scheme 2.2. First total syntheses of Spongotine C (**2-2**) and Dibromodeoxytospentin (**2-3**).

2.2a. Synthesis of 1-(2-(6-bromo-1H-indol-3-yl)-1-(methylthio)-2-oxoethylidene)piperidin-1-ium

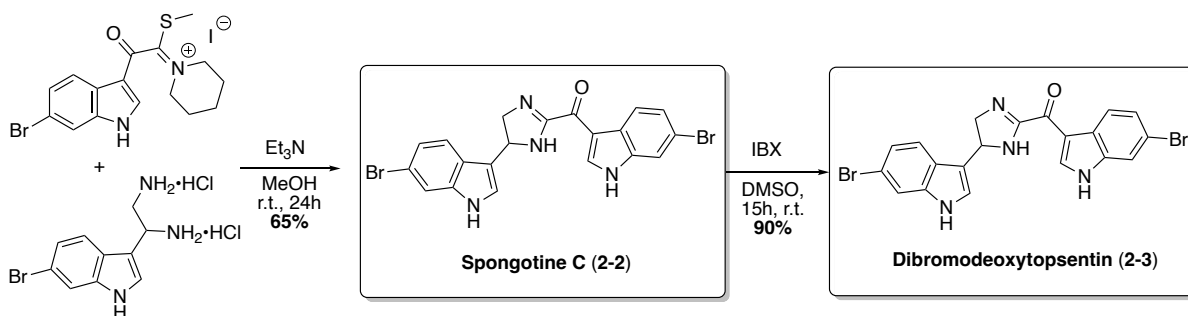
fragment:



2.2b. Synthesis of 1-(6-bromo-1H-indol-3-yl)ethane-1,2-diamine dihydrochloride fragment:



2.2c. Synthesis of Spongotine C (**2-2**) and Dibromodeoxytospentin (**2-3**):



Tulongicin (**2-1**) and Dihydrospogotine C (**2-4**) are some of the known tris- and bis-indole alkaloids that have yet to be accessed via total synthesis, as highlighted in chapter 1 of this thesis. Chapter 2 of this thesis will discuss efforts in the first total syntheses of Tulongicin (**2-1**) and Dihydrospogotine C (**2-4**), as well as expedited total syntheses of Spogotine C (**2-2**) and Dibromodeoxytopsentin (**2-3**).

2.2 Results & Discussion

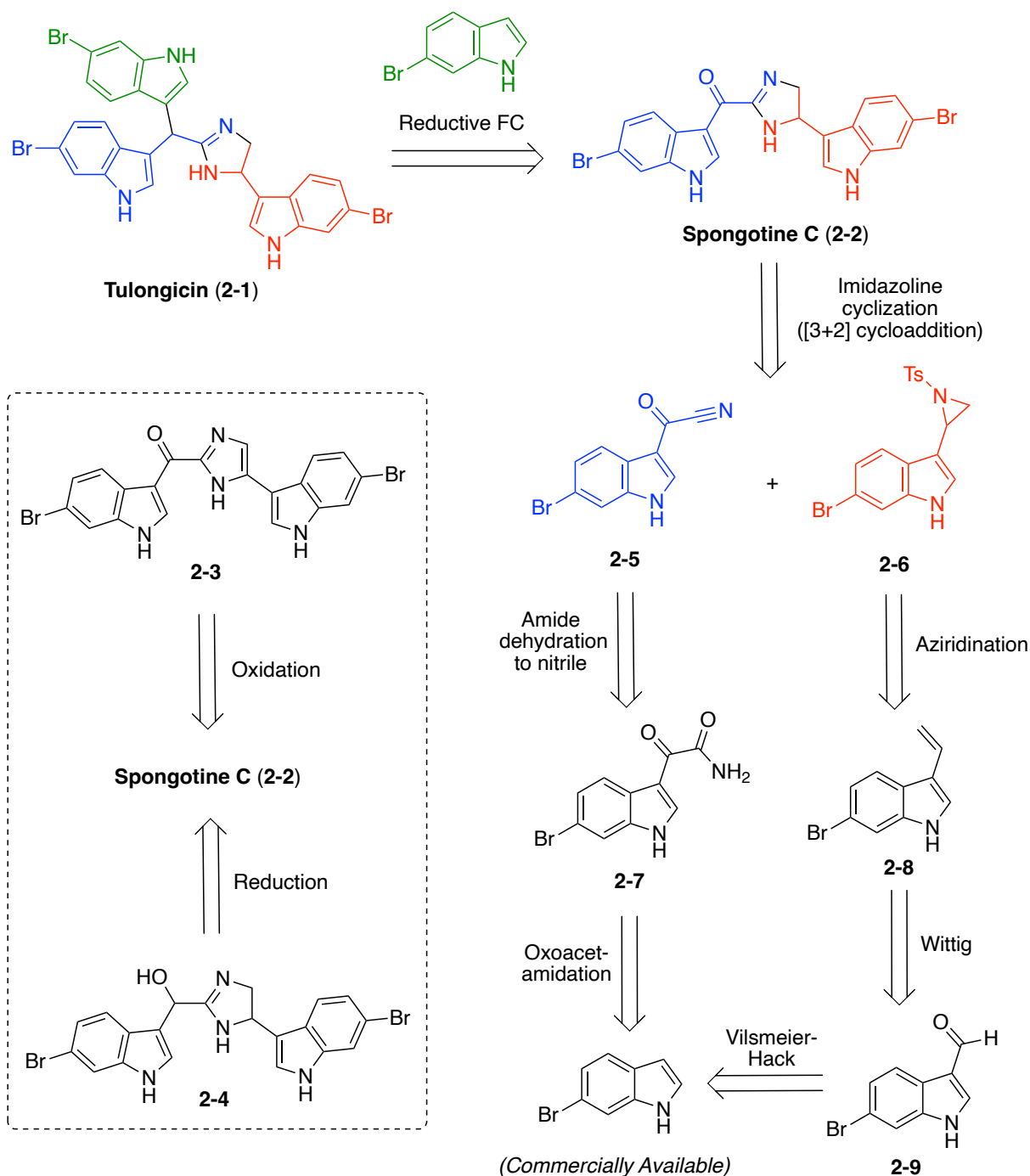
Although a considerable amount is known about the biosynthesis of indole alkaloids^{7,8}, studies of the specific chemotypes in Tulongicin (**2-1**) and Dihydrospogotine C (**2-4**) have yet to be published.³ However, the fact that **2-1**, **2-2**, **2-3**, and **2-4** were all isolated from *Topsentia* sp. can give some insight into potential transformations that could lead to these compounds from one another. For instance, it is conceivable that **2-1** could be accessed via a Friedel Craft's alkylation of **2-2** or **2-4** and that **2-3** and **2-4** could be accessed via oxidation and reduction of **2-2**, respectively. This potential interconversion of these related natural products was taken into consideration when planning the first total synthesis of Tulongicin **2-1** and its analogues (**2-2**, **2-3**, and **2-4**). In addition, particular consideration was given to the Friedel Craft's alkylation step in planning the first total synthesis of **2-1**, as, to the best of my knowledge, a reaction such as this has never been utilized to access a similar complex bis-indole methane moiety attached to an imidazoline ring.

2.2.1. Initial retrosynthetic analysis for the total synthesis of Tulongicin (**2-1**) via Spogotine C (**2-2**) as an intermediate (Route A)

My initial retrosynthesis for the first total synthesis of Tulongicin (**2-1**) (Route A) is shown in **Scheme 2.3**. It was hypothesized that **2-1** could be accessed via a reductive Friedel Craft's alkylation of **2-2**. In turn, **2-2** could be accessed through a [3+2] cyclization of 6-bromo-

1*H*-indole-3-carbonyl cyanide (**2-5**) and 6-bromo-3-(1-tosylaziridin-2-yl)-1*H*-indole (**2-6**). The cyclization of cyanide and aziridine moieties to form imidazoline rings is preceded in literature, however the use of a carbonyl cyanide moiety would be an expansion upon previous work and has yet to be attempted to the best of my knowledge.⁹ As shown below, **2-5** and **2-6** could be accessed in 2 and 3 steps, respectively from the same, commercially available 6-bromo-1*H*-indole starting material.^{10,11,12} This approach would also be an expedited total synthesis of **2-2** compared to its aforementioned previous first total synthesis (**Scheme 2.2**). In addition, as is shown in **Scheme 2.3**, it is hypothesized that Dibromodeoxytospentin (**2-3**) and Dihydrospogotine C (**2-4**) could also be accessed via Spogotine C (**2-2**) as an intermediate via a single oxidative or reductive step, respectively.

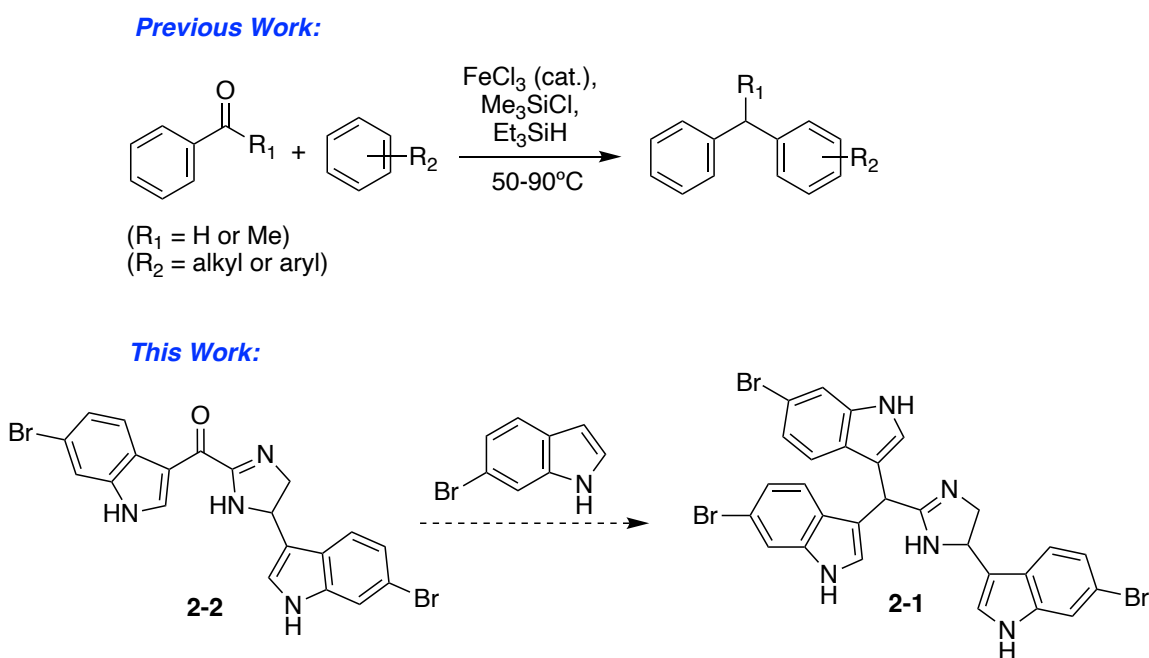
Scheme 2.3. Initial retrosynthesis of Tulongicin (**2-1**), Spongotine C (**2-2**), Dibromodeoxytospentin (**2-3**), Dihydrospogotine C (**2-4**) – Route A.



The transformation of **2-2** to **2-1** via a reductive Friedel Craft's alkylation is based off previous work by Savela *et. al.* As shown in **Scheme 2.4**, Savela and co-workers showed that

triaryl products could be accessed via a one-pot FeCl₃-catalyzed, silane-mediated reductive Friedel Craft's alkylation.¹³ However, Savela's methodology had only been applied to substituted benzaldehydes or benzyl ketones with substituted benzene nucleophiles. Therefore, applying a similar approach for the transformation of **2-2** to **2-1** to form the synthetically challenging bis indole methane moiety linked to the imidazoline ring would be a significant expansion of this methodology.

Figure 2.4. Literature precedence for reductive Friedel Craft's alkylation, as well as the proposed expansion of this methodology in the first total synthesis of (**2-1**).

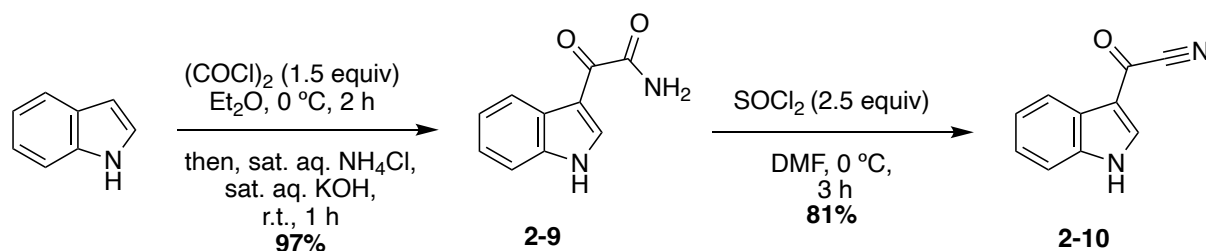


2.2.1.1. Indole carbonyl cyanide fragment synthesis

The indole carbonyl cyanide (**2-10**) was synthesized from *1H*-indole in two steps, as shown in **Scheme 2.5**.¹⁰ It is important to note that, for cost purposes, *1H*-indole was used as a model starting material in this synthesis rather than 6-bromo-*1H*-indole in progress toward **2-5** to allow for preliminary optimization. The first step involved oxoacetamidation of *1H*-indole to

afford the 2-(1*H*-indol-3-yl)-2-oxoacetamide intermediate (**2-9**) (97%). Subsequent amide dehydration to the nitrile afforded **2-10** in high yield (79%).

Scheme 2.5. Synthesis of the indole carbonyl cyanide fragment (**2-10**).



2.2.1.2. Indolic aziridine fragment synthesis

The synthesis of **2-6** was identified as a key step for optimization. This was because previous reports have highlighted aziridination of electron dense systems, such as this indole system, to be significantly more difficult than that of more electron poor systems.^{14,15,16,17}

Therefore, model systems were used for initial optimization of this aziridination toward the synthesis of **2-6**. First, a styrene model system was used. As shown in **Scheme 2.6**, the 2-phenyl-1-tosylaziridine product (**2-11a**) was accessed in high yield (70%) using Chloramine-T $\cdot\text{H}_2\text{O}$ as the nitrogen source (**Table 2.1**). Next, in order to more closely represent the electron rich indole ring system of **2-6**, a para-methoxy styrene model system was used to further optimize reaction conditions. As shown by the data in **Table 2.1**, the yields were significantly lower for the 2-(4-methoxyphenyl)-1-tosylaziridine product (**2-11b**) (8-16%) compared to that of the (**2-11a**) (70%) utilizing a variety of reaction conditions.

Scheme 2.6. Aziridination of styrene model systems to afford (**2-11a**) and (**2-11b**).

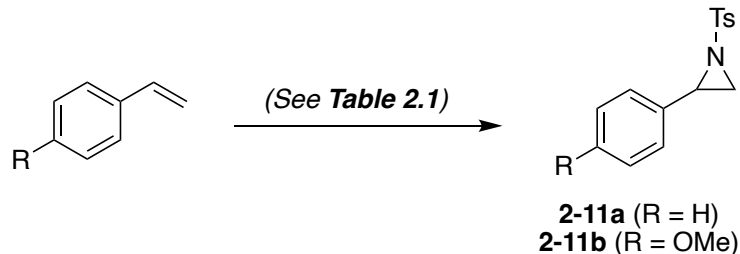


Table 2.1. Reaction condition screening for aziridination of styrene model systems.

R	Nitrogen Source	Catalysts/Additives*	Solvent	Temp	Rxn Time	Yield
H	Chloramine-T• H ₂ O (1 equiv)	I ₂ / TBAB	DCM/H ₂ O (2:1)	rt	24 h	70%
OMe	Chloramine-T• H ₂ O (1 equiv)	I ₂ / TBAB	DCM/H ₂ O (2:1)	rt	24 h	8%
OMe	Chloramine-T• H ₂ O (1 equiv.)	CuI/ TBAB	DCM/H ₂ O (2:1)	rt	24 h	15%
OMe	PhINTs (1 equiv)	I ₂ / TBAI	CH ₃ CN	rt	3 h	15%
OMe	PhINTs (1 equiv)	I ₂ / TBAI	CH ₃ CN	rt	18 h	10%

*Catalytic amount = 10. mol%

As shown in **Table 2.1**, this decreased yield can likely be attributed to the increased electron density of the para-methoxy styrene model system. It is also evident from the data that copper aids in activating this alkene toward aziridination, as shown by the slightly higher yields of the CuI catalyzed reactions (**Table 2.1**). Also, as shown by the data, it appears that Chloramine-T•H₂O and *N*-tosyliminobenzylidiodane (PhINTs) were similar in their effectiveness as a nitrogen source. However, it is not clear if PhINTs was allowed to reach its full potential as it suffered significant degradation issues, evidenced by isolation of significant amounts of *p*-toluenesulfonamide and iodobenzene degradation products after purification. This degradation can also explain why the yields of the PhINTs-mediated aziridinations decreased as time increased (**Table 2.1**). If this degradation issue were to be solved or mitigated, PhINTs may be a superior nitrogen source for aziridinations of electron dense alkene systems, as has been reported in literature.^{14,15}

Though the yields of (**2-11b**) were relatively low, the focus was shifted to the target compound, **2-6** in the interest of time. It is noteworthy to mention that, for cost purposes, *1H*-indole was used as a model starting material for initial optimization. In the synthesis of **2-15**, first, the 1-tosyl-3-vinyl-*1H*-indole intermediate (**2-14**) was synthesized in three steps from *1H*-indole (**Scheme 2.7**).^{11,12,18} The first step toward (**2-14**) was the Vilsmeier-Haack formylation of *1H*-indole at the C-3 position to afford **2-12** in good yield (53%).¹² Next, an *N*-tosylation of **2-12** was completed to access **2-13** in quantitative yield, followed by a subsequent Wittig reaction to afford the vinyl indole intermediate **2-14** in good yield (70%).^{11,18} Once **2-14** was accessed, the aziridination of this compound was explored (**Scheme 2.8**). **Table 2.2** details the various conditions that were explored in the synthesis of **2-15** via aziridination of **2-14**.

Scheme 2.7. Synthesis of the 1-tosyl-3-vinyl-*1H*-indole intermediate (**2-14**).

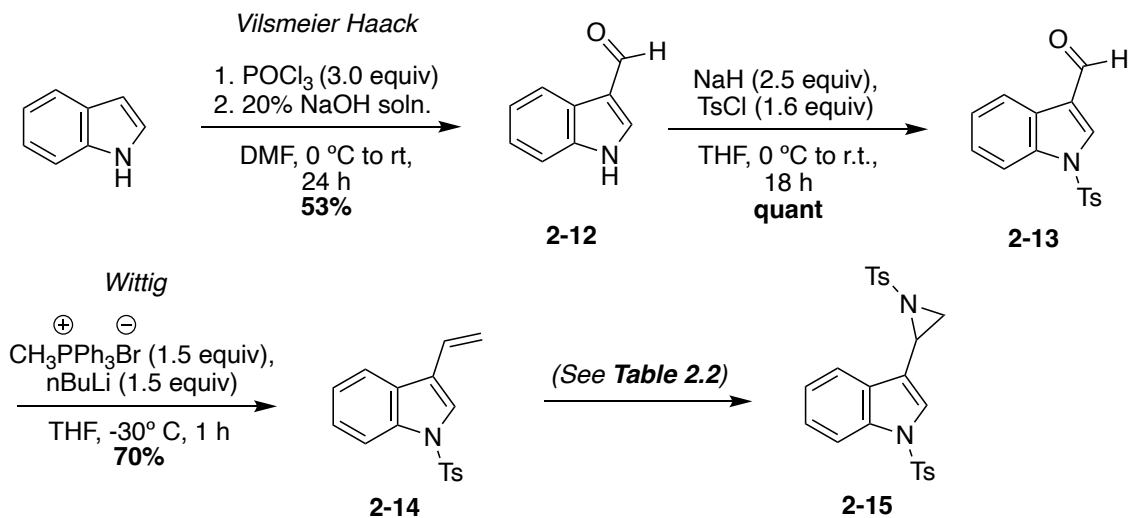


Table 2.2. Aziridination of 3-vinyl indole reaction conditions.

Nitrogen Source	Catalysts/Additives	Solvent	Temp	Rxn Time	Yield
Chloramine-T• H ₂ O (1 equiv)	CuI (0.1 equiv)/ TBAB (0.1 equiv)	DCM/H ₂ O (2:1)	rt	24 h	No pure product isolated*
PhINTs (1 equiv)	CuI (0.1 equiv)/ TBAI (0.05 equiv)	MeCN	rt	24 h	No pure product isolated*
TsNH ₂ (2.0 equiv)	PhI(OAc) ₂ (1 equiv)/ Cu(CH ₃ CN) ₄ PF ₆ (0.05 equiv)	DCM	rt	24 h	No pure product isolated*

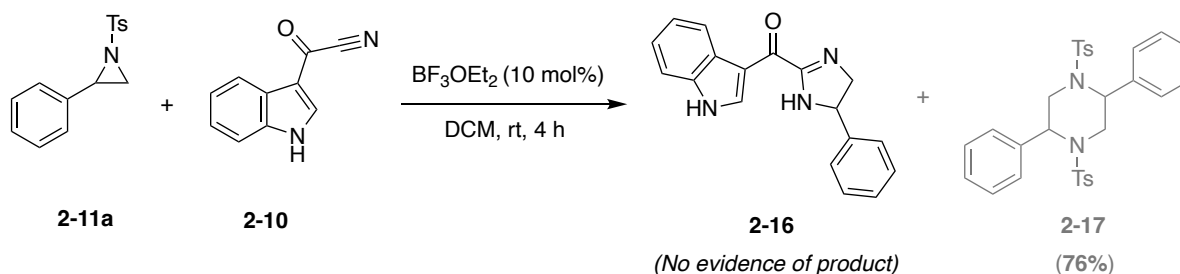
***2-15** identified via crude NMR and mass spectrometry (HRMS-ESI (*m/z*): Calculated for C₂₄H₂₂N₂O₄S₂ (*M+H*)⁺: 467.1099, Found: 467.1110).

As shown by the results outlined in **Table 2.2**, the aziridination of **2-14** proved to be very difficult. Though a variety of reaction conditions were explored, no desired product **2-15** was ever isolated (**Table 2.2**). As shown in **Table 2.2**, conditions to form PhINTs in situ were also explored utilizing *p*-toluenesulfonamide and PhI(OAc)₂ in efforts to avoid the aforementioned problematic degradation of PhINTs.¹⁹ However, **2-15** was detected via crude NMR and mass spectrometry in all trials detailed in **Table 2.2**. Therefore, it is believed that the problem with this aziridination was not the efficiency of the reaction, but the stability of the product, leading to difficulty isolating **2-15**. This instability is likely because the indole ring system of **2-14** is more electron dense than that of the previous para-methoxy styrene model system. In fact, the presence of its heteroatomic nitrogen atom allows for potential intramolecular nucleophilic ring opening of the strained aziridine ring of **2-15**, especially in the presence of any mild acid upon workup. Specifically, cascade of the indole nitrogen lone pair of electrons through the ring could result in formation of an exocyclic alkene, opening the aziridine. The *N*-tosyl moiety was strategically present in (**2-14**) to mitigate this issue. However, it is evident that, while this *N*-tosylation may have allowed for the aziridination to occur, it did not allow for product stability. This was the first problem that indicated this initial synthetic route to access **2-2** may needed to be adapted.

2.2.1.3. Exploration of the [3+2] imidazoline cyclization

Another unforeseen problem with this initial synthetic approach (Route A) was identified in the initial explorations of the [3+2] imidazoline cyclization step. Preliminary exploration was conducted via a model system in which **2-11a** was cyclized with **2-10**, as shown in **Scheme 2.8**. Notably, there was no desired product formation, rather, an unexpected major side product was isolated instead.

Scheme 2.8. Initial exploration of the [3+2] imidazoline cyclization – side product formation.



As shown in **Scheme 2.8**, the desired [3+2] cycloaddition reaction to form the imidazoline core did not occur in this model system. Instead, the unexpected 2,5-diphenyl-1,4-ditosylpiperazine side product **2-17** was isolated in significant yield (76%) as the only product formed. It was hypothesized that **2-17** was afforded by the cyclization of **2-11a** with another molecule of itself. This was confirmed by subsequent control reactions in which **2-11a** was reacted with and without Lewis acid (10 mol% BF_3OEt_2), as shown in **Scheme 2.9**. The results and specific reaction conditions of these control reactions are outlined in **Table 2.3**.

Scheme 2.9. Side product formation – control experiments.

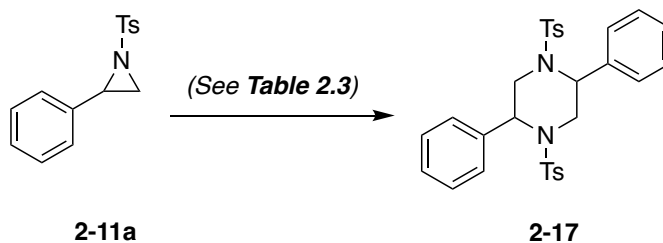
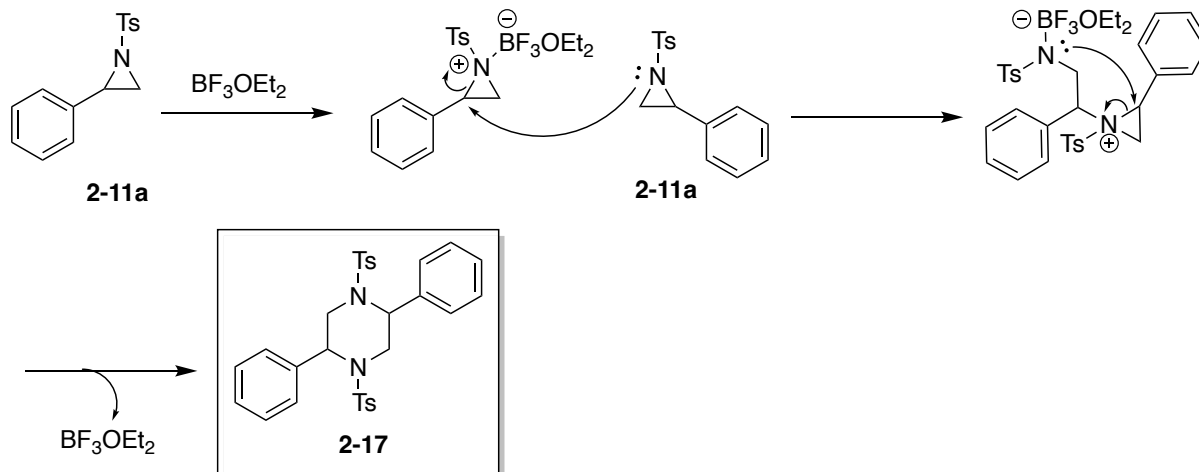


Table 2.3. Exploration of side product (**2-17**) formation – reaction conditions.

Trial	Lewis Acid	Solvent	Temp. (°C)	Time	Yield of (2-17)
1	BF ₃ OEt ₂ (10 mol%)	DCM	20 °C	4 h	Major product in crude NMR
2	None	DCM	20 °C	4 h	No product formation identified

As shown, the data indicated not only that **2-11a** can cyclize with itself, but also that the Lewis acid is necessary in the cyclization of the piperazine ring, which supported the hypothesized mechanism. Therefore, a potential mechanism for this cyclization was determined, as shown in **Scheme 2.10**, in which the BF₃OEt₂ coordinates to, and activates, the nitrogen atom of **2-11a**. This facilitates nucleophilic attack by the nitrogen atom of another **2-11a** molecule. Once this intermediate is formed, the now activated remaining aziridine can then open via nucleophilic attack of the other N atom and undergo subsequent cyclization. This likely arises from the combination of the very reactive activated aziridine and the weakly nucleophilic cyanide (**2-10**), leading to a faster reaction between **2-11a** and itself than the desired reaction between **2-11a** and **2-10**. Similar Lewis acid-catalyzed cyclizations of aziridines to form piperazine rings have been reported in literature.²⁰ Considering these problems that arose with Route A, adaptations were made in order to mitigate these issues.

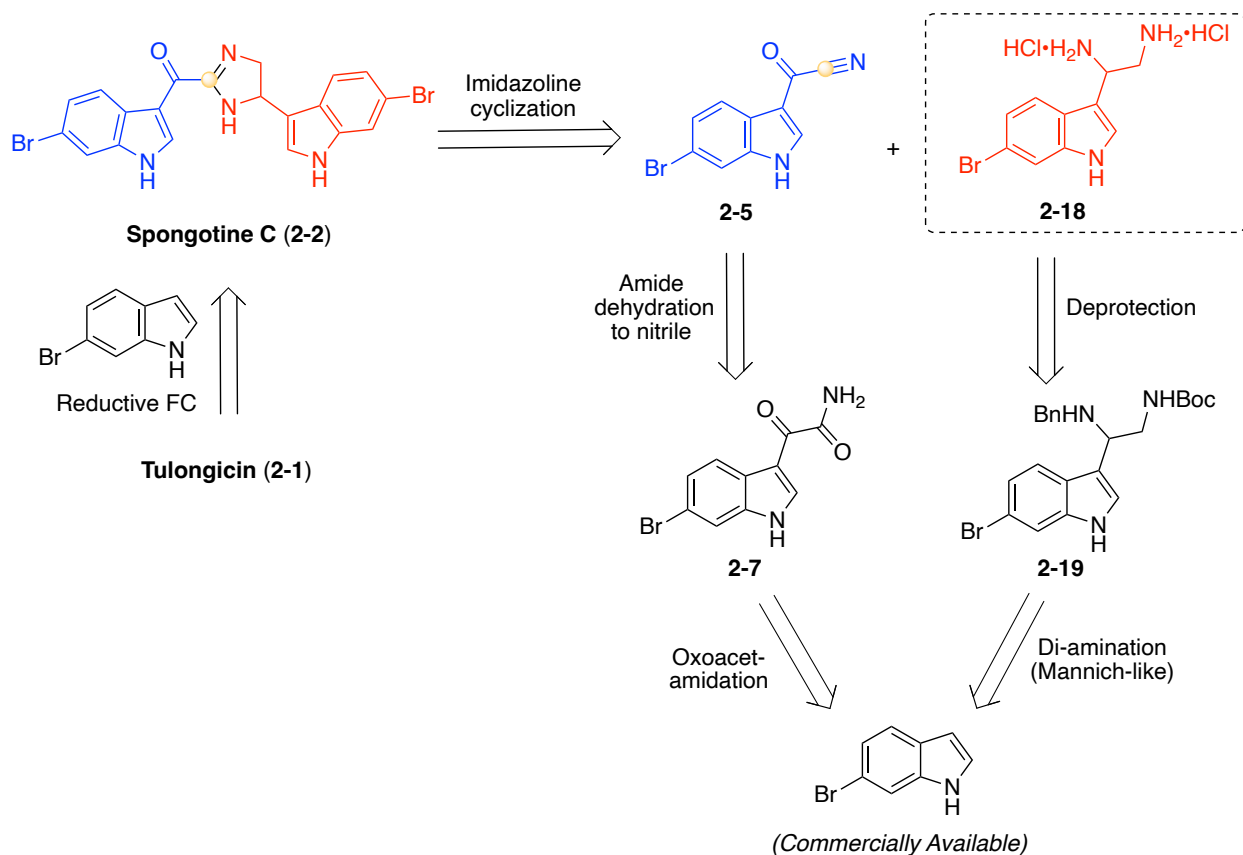
Scheme 2.10. Proposed mechanism of piperazine side product (**2-17**) formation.



2.2.2. Adapted retrosynthetic analysis for the total synthesis of tulongicin (**2-1**) via Spongotine C (**2-2**) as an intermediate (Route B)

To address both major problems associated with Route A, a newly adapted route Route B was developed, as shown in **Scheme 2.11**. This route was hypothesized to solve the problems of aziridine instability (**2-6**) and its problematic dimerization by utilizing a more stable diamine fragment (**2-18**) to cyclize with **2-5** to form the imidazoline core of Spongotine C (**2-2**) (**Scheme 2.11**). Despite the use of the same cyanide fragment (**2-5**), the mechanism of this imidazoline cyclization would likely be more favorable than Route A because **2-5** would now act as the electrophile rather than the nucleophile. Similar cyclizations have been previously reported via indolic carbonyl cyanides and cysteine methyl esters to form thiazolines.²¹ Therefore, this approach would be an expansion upon this previous work to utilize a diamine fragment instead (**2-18**). As shown in **Scheme 2.11**, it was hypothesized that **2-18** could be synthesized in two steps from the commercially available 6-bromo-1*H*-indole via di-amination and subsequent bis-deprotection. This adapted route would also be a more expeditious way to access (**2-2**) with a longest linear sequence (LLS) of three steps as opposed to the five steps in Route A.

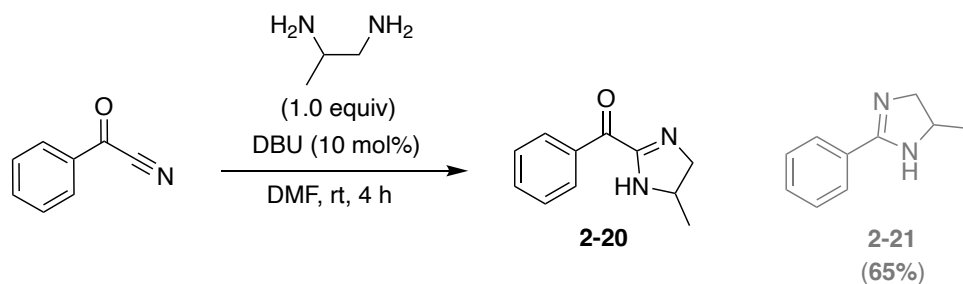
Scheme 2.11. Adapted retrosynthesis of Tulongicin (**2-1**) via Spongotine C (**2-2**) as an intermediate – Route B.



2.2.2.1. Initial exploration of imidazoline cyclization using a model system

To explore the feasibility of this approach, a model system was first investigated using commercially available starting materials. As in **Scheme 2.12**, propane-1,2-diamine and benzoyl cyanide underwent cyclization catalyzed by 1,8-diazabicyclo[5.4.0]undec-7-ene (DBU). However, rather than the desired cyclized product (**2-20**), the unexpected imidazoline side product (**2-21**) was isolated in good yield (**65%**). This likely occurred due to initial attack of the more electrophilic carbonyl moiety, rather than the cyanide, leading to loss of cyanide as a leaving group and subsequent cyclization to the imidazoline (**2-21**).

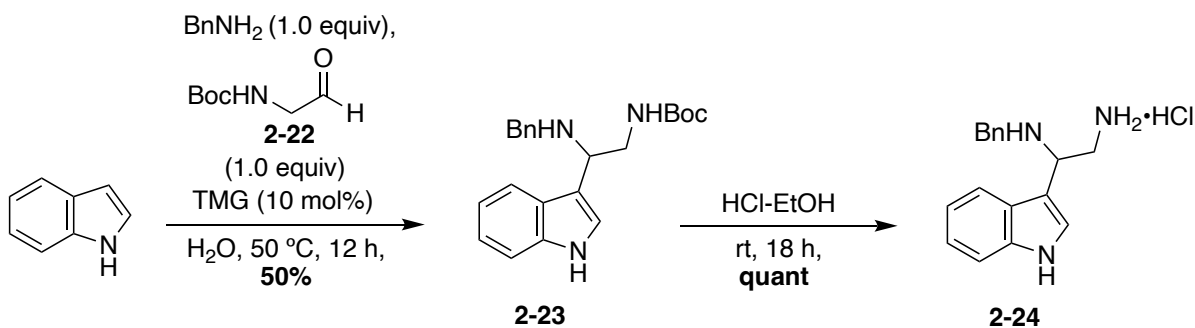
Scheme 2.12. Exploration of model imidazoline cyclization via a model system to access **2-21**.



2.2.2.2. Indolic diamine fragment synthesis

Despite the identification of this side product, the focus was moved to the target compound since this carbonyl cyanide was electronically different than the model benzoyl cyanide, containing a less electrophilic ketone. First, the synthesis of a model diamine was carried out, as shown in **Scheme 2.13**, in 2 steps from *1H*-indole.²² Again, for initial optimization *1H*-indole was used as a model starting material for cost purposes. First, the di-protected diamine (**2-23**) was accessed via a Mannich-like di-amination of *1H*-indole in good yields (50%). Subsequently, **2-23** underwent Boc-deprotection via ethanolic hydrochloric acid to remove the Boc protecting group, as shown in **Scheme 2.13**, to access **2-24**. It is noteworthy to mention the debenylation was postponed to a later stage to prevent rotamers, allowing for more facile analysis of the cyclization step. The debenylation remains a point of future optimization.

Scheme 2.13. Synthesis of diamine fragment (**2-24**).



2.2.2.3. Exploration of imidazoline cyclization via indolic diamine and carbonyl cyanide fragments

Next, the imidazoline cyclization of the diamine fragment (**2-24**) and the carbonyl cyanide fragment (**2-10**) was investigated (**Scheme 2.14**). However, as shown in **Table 2.4**, no evidence of the desired product (**2-25**) was identified among several different reaction conditions. Due to the fact that this cyclization of **2-24** and **2-10** was not leading to any desired product formation, the synthetic route toward Spongotine C (**2-2**) was again adapted.

Scheme 2.14. Imidazoline cyclization of the indolic diamine fragment (**2-24**) and the carbonyl cyanide fragment (**2-10**).

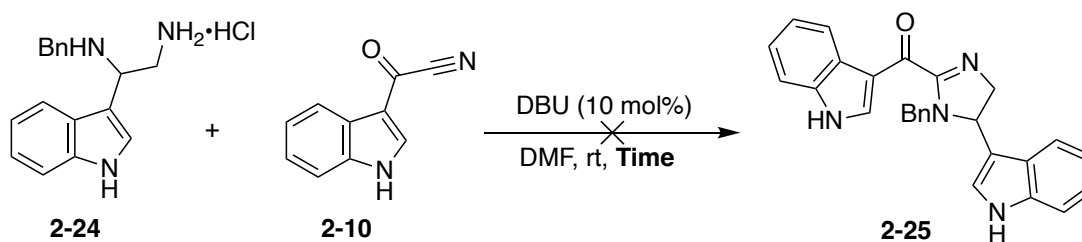


Table 2.4. Reaction condition screening for the imidazoline cyclization of **2-24** and **2-10**.

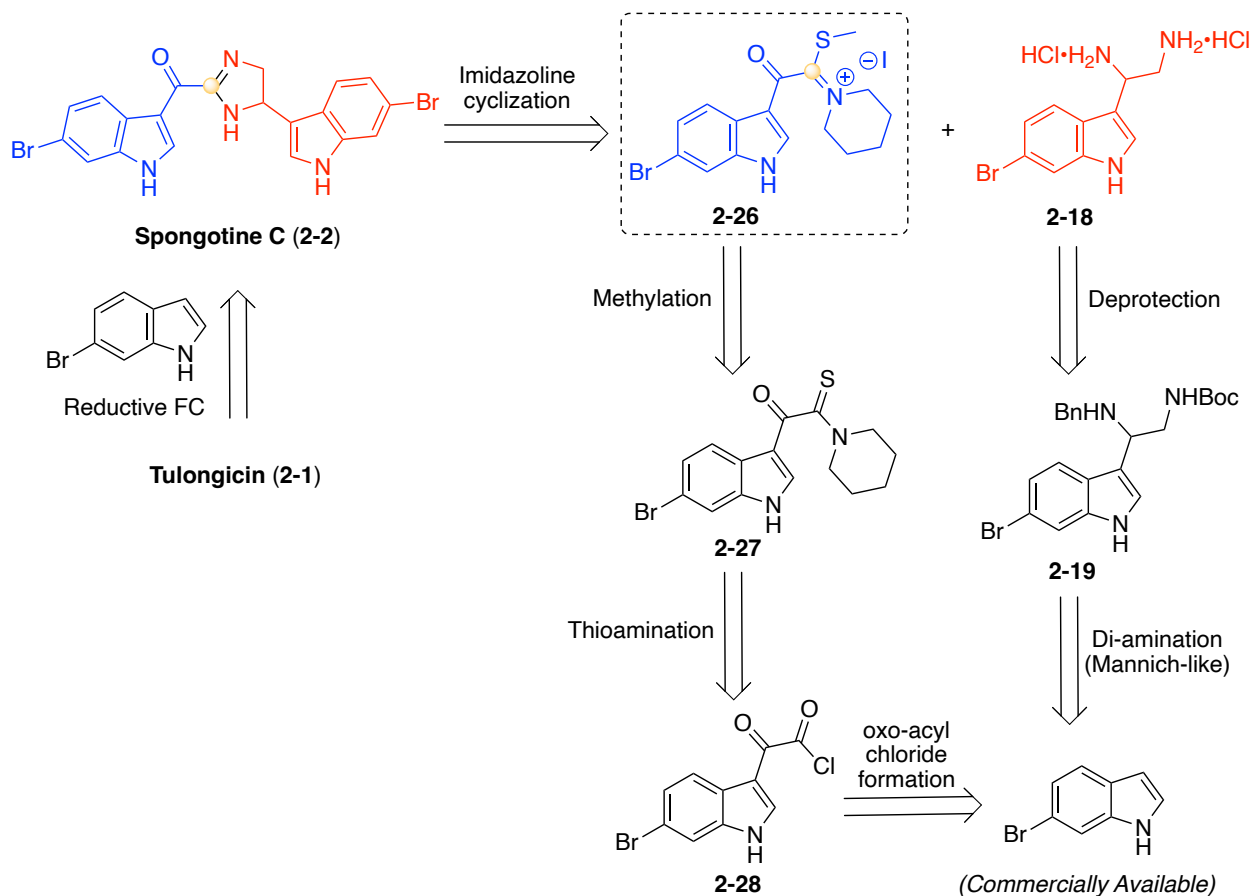
Trial	Time	Yield
1	4 h	No desired product isolated
2	24 h	No desired product isolated
3	48 h	No desired product isolated

2.2.3. Adapted retrosynthetic analysis for the total synthesis of Tulongicin (**2-1**) via Spongotine C (**2-2**) as an intermediate (Route C)

Due to this lack of reactivity in (**Scheme 2.14**), an adapted synthetic route (Route C) was developed. In Route C, the same diamine fragment (**2-24**) was used in the key cyclization to form the imidazoline core of Spongotine C (**2-2**), as well as a new keto-thioimidate fragment (**2-**

26) (Scheme 2.15). This approach is similar to that of the first total synthesis of Spongotone C **(2-2)** (Scheme 2.2). However, this approach is more expedited (LLS: 5), particularly in the synthesis of the diamine fragment **(2-18)**. As is shown in **Scheme 2.15**, this keto-thioimideate fragment **(2-26)** could be synthesized in three steps from the commercially available 6-bromo-1*H*-indole, following the same reaction sequence as the first total synthesis of Spongotone C **(2-2)** (Scheme 2.2).⁵ It was hypothesized that the keto-thioimideate fragment **(2-26)** is essentially a more activated version of that of the previously explored carbonyl cyanide fragment **(2-5)**. The more electrophilic imideate moiety and a good sulfur leaving group will, ideally, drive the reaction to occur.

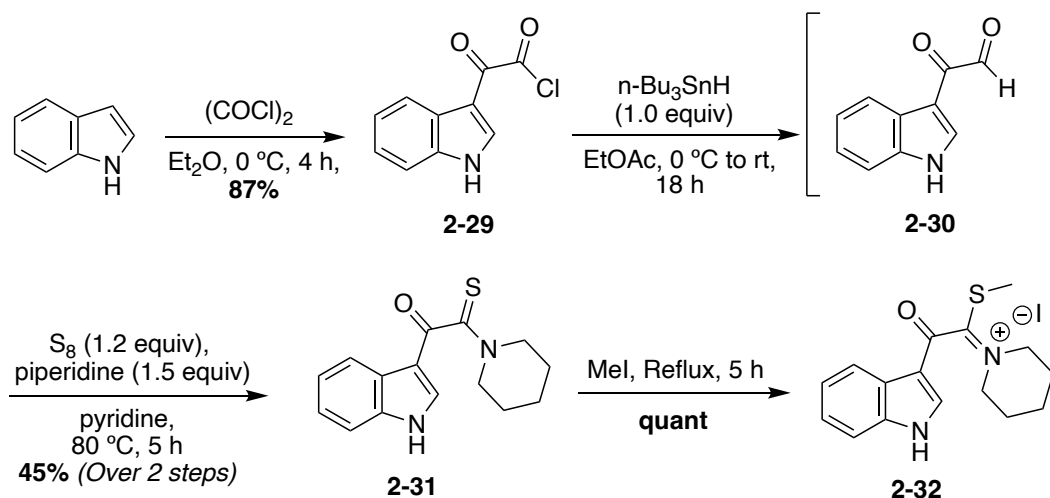
Scheme 2.15. Adapted retrosynthesis of Tulongicin **(2-1)** via Spongotone C **(2-2)** as an intermediate – Route C.



2.2.3.1. Indolic keto-thioimide fragment synthesis

In exploration of Route C, the keto-thioimide fragment (**2-32**) was synthesized in three isolated steps from the commercially available 1*H*-indole (used as a model starting material) (**Scheme 2.16**). First, 1*H*-indole was treated with oxalyl chloride to afford **2-29** in excellent yield (87%). Next, **2-29** was reduced using *n*-Bu₃SnH to the ketoaldehyde intermediate (**2-30**), which immediately underwent a reaction with S₈ and piperidine to afford **2-31** in good yield (45% over two steps). Lastly, **2-31** was *S*-methylated to access **2-32** in quantitatively.

Scheme 2.16. Synthesis of the keto-thioimide fragment (**2-26**).



2.2.3.2. Exploration of the base mediated imidazoline cyclization via the keto-thioimide and diamine fragments

Next, the base-mediated imidazoline cyclization of the keto-thioimide fragment (**2-32**) and the diamine fragment (**2-24**) was explored, as shown in **Scheme 2.17**. As is detailed in **Table 2.5**, of the reaction conditions screened, the highest yield of the desired imidazoline product (**2-25**) was achieved using triethylamine (Et₃N) as a base and a 48-hour reaction time (53%). This marked exciting progress toward the first total synthesis of Tulongicin and its related analogues, as this was the first successful imidazoline cyclization. As shown in **Table 2.5**, overall, yields of

this cyclization were lower when Amberlyst-A21 was used as the base. It is notable to mention that this is likely due to the difficult workup, rather than efficiency of the reaction. Upon workup, the resin proved difficult to sufficiently wash and extract the product.

Scheme 2.17. Base-mediated imidazoline cyclization of the keto-thioimide fragment (**2-32**) and the diamine fragment (**2-24**).

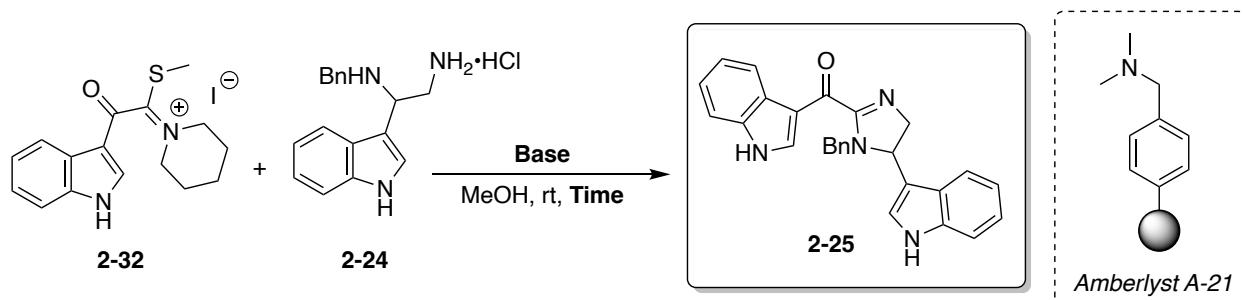


Table 2.5. Reaction time optimization for the base-mediated imidazoline cyclization of the keto-thioimide fragment (**2-32**) and the diamine fragment (**2-24**).

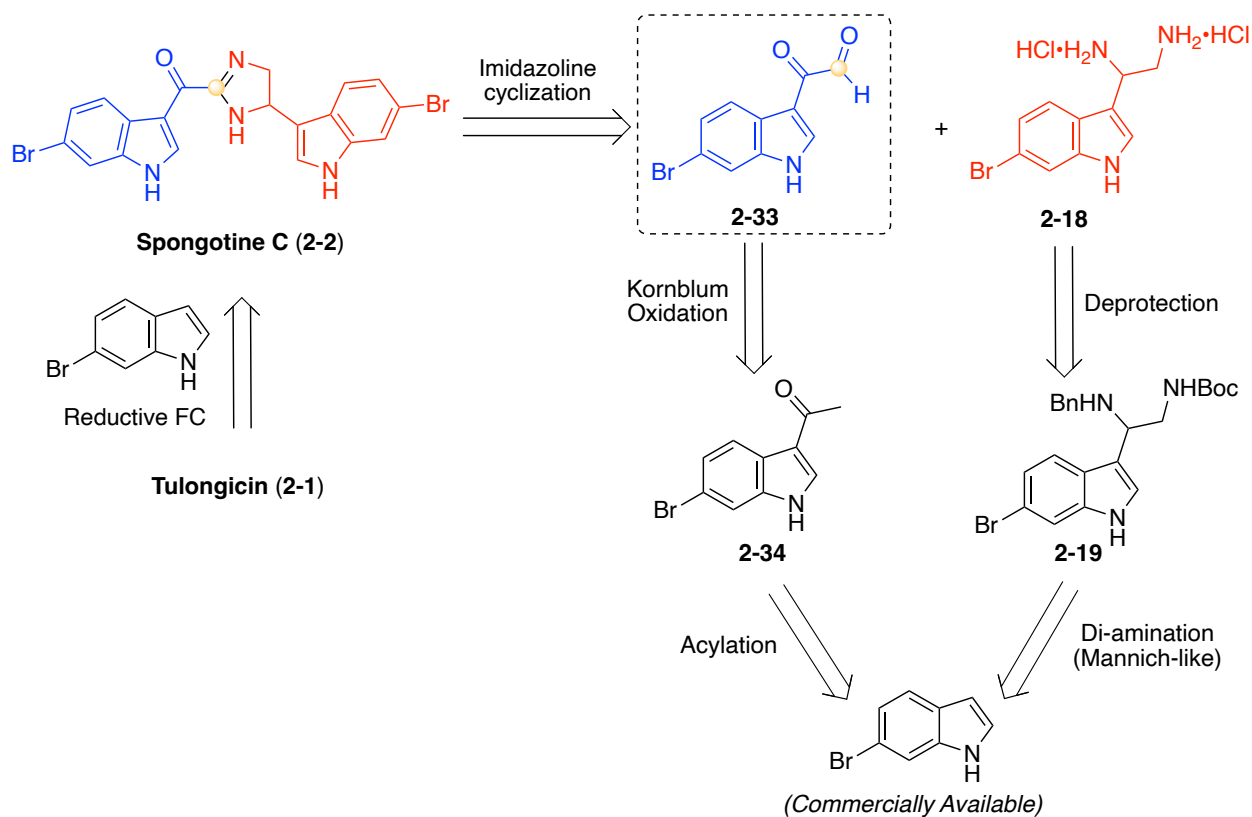
Base	Time	Yield
Amberlyst A-21	24h	26%
Amberlyst A-21	36h	32%
Amberlyst A-21	48h	32%
Et ₃ N	24h	49%
Et ₃ N	48h	53%
Et ₃ N	60h	52%

2.2.4. Adapted retrosynthetic analysis for the total synthesis of Tulongicin (**2-1**) via Spongotine C (**2-2**) as an intermediate (Route D)

In the search of a more optimized and novel synthetic route toward Tulongicin (**2-1**) and its related analogues, a more expedited synthetic route was developed (Route D). As shown by the retrosynthetic detailed in **Scheme 2.18**, it was hypothesized that the imidazoline core could be formed via a cyclization of a diamine fragment (**2-18**) and a keto aldehyde fragment (**2-33**).

Such cyclizations have been preceded in literature.^{23, 24} It was hypothesized that **2-33** could be accessed in two steps from commercially available 1-(6-bromo-1*H*-indol-3-yl)ethan-1-one (**Scheme 2.18**). This route to access Spongotine C (**2-2**) would be significantly more expeditious (LLS = 3), compared to Route C (LLS = 5) and the first total synthesis of Spongotine C (**2-2**) (LLS = 7) (**Scheme 2.2**). This approach would also allow for the first total synthesis of Tulongicin (**2-1**) in four linear steps.

Scheme 2.18. Adapted retrosynthesis of Tulongicin (**2-1**) via Spongotine C (**2-2**) as an intermediate – Route D.

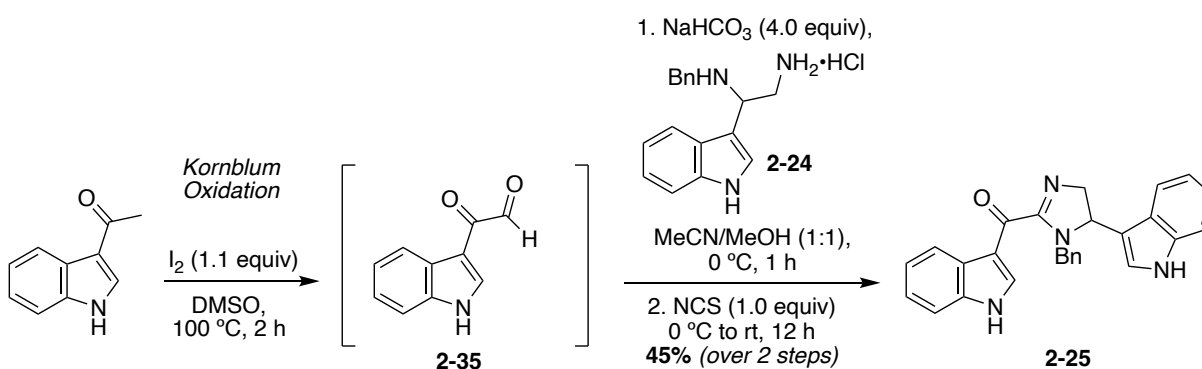


2.2.4.1. Indolic keto-aldehyde fragment synthesis via Kornblum oxidation and subsequent imidazoline cyclization – non-brominated model system

The indolic keto-aldehyde intermediate (**2-35**) was accessed in one step from 1*H*-indol-3-yl)ethan-1-one as a model starting material for initial optimization. As shown in **Scheme 2.19**,

1*H*-indol-3-yl)ethan-1-one underwent iodination and subsequent Kornblum Oxidation²⁵ to access **2-35**. This was then directly carried forward to the imidazoline cyclization with the diamine fragment (**2-24**) in a one-pot method, followed by subsequent oxidation via NCS to afford the imidazoline product (**2-25**) in good yield over two steps (45%) (**Scheme 2.19**). This was a very significant result toward the first total synthesis of Tulongicin (**2-1**) and its related analogues in that it constituted the most expeditious route to access **2-25** thus far. In addition, intermediate **2-25** is only one debenzoylation step away from a non-brominated Spongotone C analogue. Considering the previously reported problematic de-halogenation of heterocycles when subjected to hydrogenative debenzoylation conditions,²² it was hypothesized that the final debenzoylation reaction would be better optimized using the target brominated scaffold, rather than the non-brominated model system (**2-25**). This would allow for monitoring of any potential de-halogenation when screening debenzoylation conditions. Therefore, the final debenzoylation step remains a point of exploration and optimization for the future.

Scheme 2.19. Synthesis of imidazoline intermediate (**2-25**) via Kornblum oxidation and subsequent oxidative imidazoline cyclization.

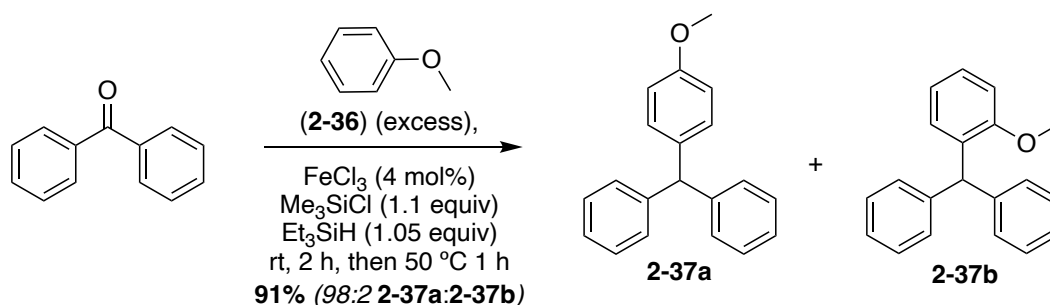


2.2.5. Optimization of a one-pot reductive Friedel Craft's methodology

2.2.5.1. Reductive Friedel Craft's alkylation of benzophenone with anisole – model system.

In the exploration and optimization of the one-pot reductive Friedel Craft's alkylation, model systems were first explored. The first model system explored was the FeCl₃-catalyzed reductive alkylation of benzophenone with anisole (**2-36**) as the nucleophile, as in **Scheme 2.20**. This model system afforded the desired product (**2-37**) in high yields and regioselectivity (91% (98:2 para:ortho)).

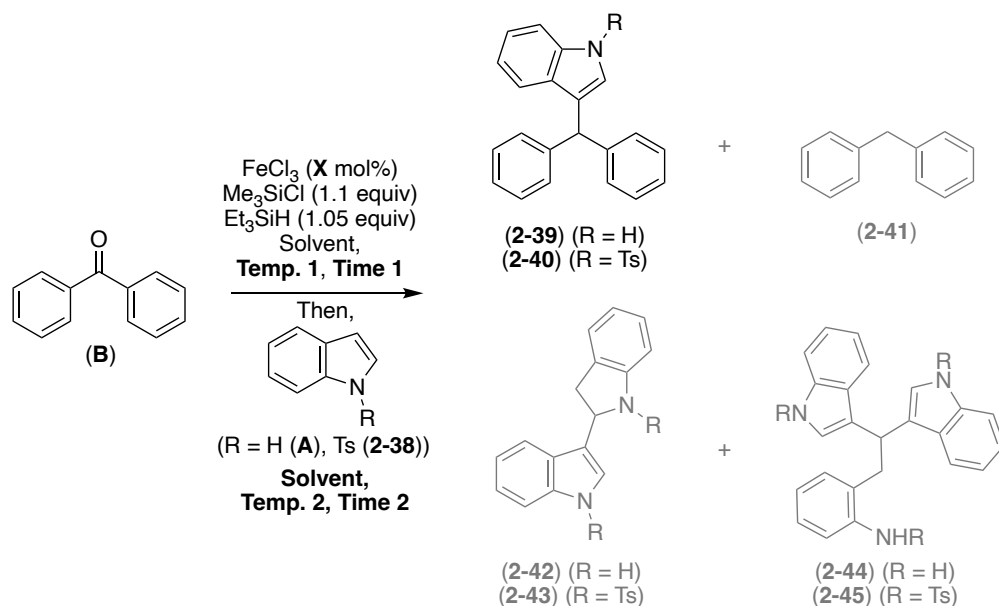
Scheme 2.20. Reductive Friedel Craft's alkylation of benzophenone with anisole – model system.



2.2.5.2. Reductive Friedel Craft's alkylation of benzophenone with indole nucleophiles – model system.

Another reductive Friedel Craft's model system was then explored. The FeCl₃-catalyzed reductive alkylation of benzophenone (**B**) with indole nucleophiles was explored, as it was more representative of the target methodology for the total synthesis of Tulongicin (**2-1**). Both 1*H*-indole (**A**) and *N*-tosyl-1*H*-indole (**2-38**) were investigated as shown in **Scheme 2.21**.

Scheme 2.21. Reductive Friedel Craft's alkylation of benzophenone with indole nucleophiles – model system.



This second model system of the reductive Friedel Craft's alkylation (**Scheme 2.21**) proved to be more difficult than the first model system. This was due to competitive side reactions. One side product that was isolated was diphenylmethane (**2-41**). This was likely a result of competitive over-reduction of benzophenone via the triethyl silane reducing agent due to the slower alkylation reaction times for this model system. However, this over-reduction occurred before complete consumption of the benzophenone starting material (**B**), as significant amounts of (**B**) were recovered in all trials.

This increased reaction time correlated to the tendency of these indole nucleophiles, *1H*-indole (**A**) or *N*-tosyl-*1H*-indole (**2-38**), to polymerization in Lewis acidic conditions.^{26,27,28} From these model reactions, indole dimer (**2-42** or **2-43**) and trimer side products (**2-44** or **2-45**) were identified and/or isolated, as shown in **Table 2.6**. In several of these trials, varying amounts of a brown/black insoluble precipitate was produced. This was likely correlated to further, more complex indole polymerization.^{26,27} In order to mitigate this problem of indole polymerization,

several different parameters were investigated including temperature, time, solvent, etc. as shown in **Table 2.6**.

Table 2.6. Reductive Friedel Craft's Alkylation Optimization.

Trial	R	Solvent	Mol% FeCl ₃ (X)	Equiv (B)	Equiv (A) or (2-38)	Temp 1	Temp 2	Time 1	Time 2	Yield
1*	H	DCE	4	1.0	5.0	rt à 50 °C	50 °C	1 h	3 h	2-39 (0%) 2-41 (19%) 2-42 (23%) 2-44 (10%)
2*	H	DCE	4	1.0	1.0	rt à 50 °C	50 °C	1 h	3 h	2-39 (0%) 2-41 (18%) 2-42 (22%) 2-44 (10%)
3*	H	DCE	4	1.0	2.0	rt à 50 °C	0 °C à rt	1 h	2 h (0 °C), 10 h (rt)	2-39 (0%) 2-41 (15%) 2-42 (20%) 2-44 (7%)
4	Ts	DCE	4	1.0	2.0	rt à 50 °C	rt à 60 °C	1 h	12 h	2-40 (0%) 2-41 (19%) 2-43 (9%) 2-45 (Trace)**
5	Ts	DCE	10	1.0	2.0	rt à 50 °C	rt à 60 °C	1 h	12 h	2-40 (0%) 2-41 (18%) 2-43 (8%) 2-45 (Trace)**
6	H	NO ₂ Me	4	1.0	2.0	rt	rt	1 h	12 h	2-39 (11%) 2-41 (15%) 2-42 (15%) 2-44 (5%)
7	H	NO ₂ Me	10	1.0	2.0	rt	0 °C à rt	1 h	2 h (0 °C), 12 h (rt)	2-39 (14%) 2-41 (11%)* 2-42 (12%) 2-44 (6%)
8	Ts	NO ₂ Me	10	1.0	2.0	rt	rt à 60 °C	1 h	2 h (rt), 12 h (60 °C)	2-40 (0%) 2-41 (17%) 2-43 (4%) 2-45 (0%)
9	H	NO ₂ Me	10	1.0	2.0	rt	-15 °C à rt	1 h	2 h (-15 °C), 12 h (rt)	2-39 (17%) 2-41 (14%) 2-42 (10%) 2-44 (5%)
10	H	NO ₂ Me	10	1.0	2.0	rt	-15 °C à rt	0 h	2 h (-15 °C), 12 h (rt)	2-39 (16%) 2-41 (12%) 2-42 (14%) 2-44 (6%)

*black insoluble precipitate formed (likely indole polymer)

****(2-45)** identified via crude mass spec (HRMS-ESI (m/z): Calculated for C₄₅H₃₈N₃O₆S₃ (M+H)⁺: 814.2079, Found: 814.2099.)

***Data Outlier due to minor spill

It was found that, as temperature was lowered during addition of the indole nucleophile, (**A**) or (**2-38**), the dimerization slightly decreased. In addition, *N*-tosylation of the indole also significantly lowered dimerization. However, *N*-tosylation also decreased the reactivity of the indole nucleophile, resulting in no alkylation. As shown in **Table 2.6**, it was found that solvent and slow addition of (**A**) or (**2-38**) had the most significant impact on the reaction. The only trials in which the desired alkylated product (**2-39**) was isolated in moderate yield (11-17%) were trials 6, 7, 9 and 10 (**Table 2.6**). The highest yielding was trial 9 in which the solvent was nitromethane (NO₂Me) and (**A**) was added dropwise at cold temperatures (-15°C). Nitromethane has been reported to selectively solubilize the activated Lewis acid coordinated indole intermediate, facilitating alkylation to form the desired product. NO₂Me does not solubilize the indole species which are not coordinated to the Lewis acid, preventing excessive indole polymerization in solution.²⁹ The cold temperatures also seem help in slowing this fast polymerization to some extent.

Trial 10 (**Table 2.6**) was an attempt to additionally mitigate the over-reduction of benzophenone by decreasing Time 1. Though this led to a slight decrease in the yield of the over-reduction side product (**2-41**), this earlier addition of indole also contributed to a slight increase in polymerization. Overall, it was found that the slower indole alkylation reaction was unable to compete with the faster polymerization and over-reduction side reactions, leading to relatively low yields of the desired product (**2-39**) using the most optimized conditions.

To further study this indole polymerization, a few control reactions were run, as shown in **Scheme 2.22**, in which 1*H*-indole was allowed to react with only the Lewis acid (FeCl₃). As shown in **Table 2.7**, in the presence of the Lewis acid, the indole polymerization was fast. In fact, this polymerization was observed after only one hour of reacting with the Lewis acid (**Table**

2.7). However, in the case where no Lewis acid was present, no reaction was observed, confirming that the Lewis acid catalyzes this polymerization reaction.

Scheme 2.22. Indole polymerization control reactions.

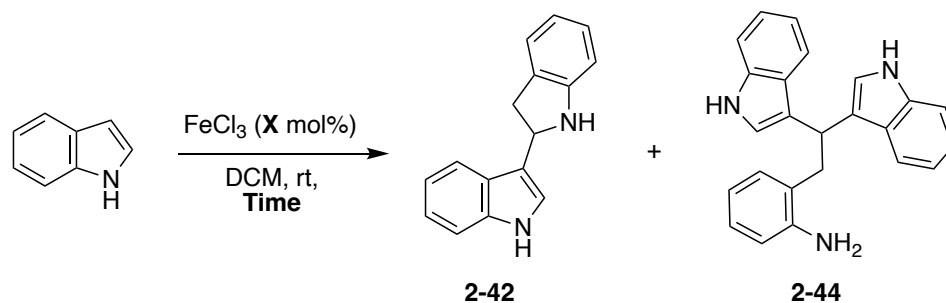


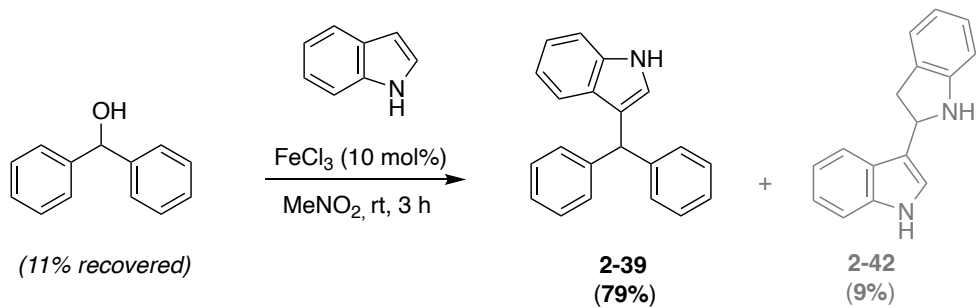
Table 2.7. Indole polymerization control reactions – reaction condition screening.

R	X (mol%)	Time	Observations
H	0	24 h	No reaction
H	10	1 h	(2-42) and (2-44) identified via NMR
H	10	14 h	(2-42) and (2-44) identified via NMR

2.2.5.3. Exploration of Friedel Craft's alkylation step

Due to the previously discussed low-yielding indole model systems, the one-pot reductive Friedel Craft's alkylation was then broken up into separate steps to analyze each individually. To analyze the Friedel Craft's alkylation step alone, similar conditions were run to those previously discussed, yet the reduction conditions were omitted. The Friedel Craft's alkylation conditions were run with diphenyl methanol as the substrate and 1*H*-indole as the nucleophile (**Scheme 2.23**). The desired alkylated product (**2-39**) was accessed in high yields (78%) with minor amounts of the indole dimer side product (**2-42**) isolated.

Scheme 2.23. Friedel Craft's alkylation of diphenylmethanol with 1*H*-indole as the nucleophile.



2.2.5.4. Exploration of ketone reduction step

Since the Friedel Craft's alkylation of diphenylmethanol was high yielding, the focus was transitioned from these simpler model systems to the target imidazoline intermediate (2-25) for exploration of the reduction step (Scheme 2.24). As outlined in Table 2.8, several reducing agents, from moderate to strong, were screened in the reduction of (2-25). However, none of these reducing agents afforded the desired product (2-46).

Scheme 2.24. Ketone reduction of the imidazoline intermediate (2-25).

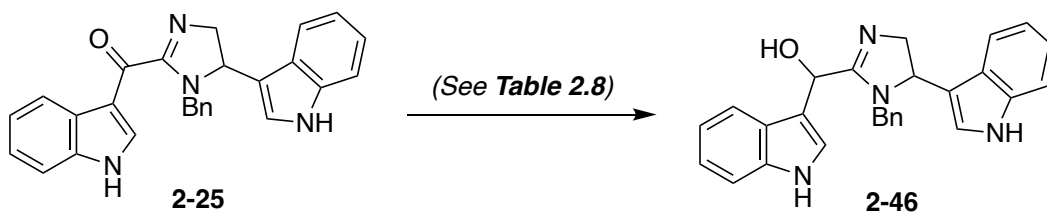


Table 2.8. Ketone reduction of the imidazoline intermediate (**2-25**) – reaction condition screening.

Reducing Agent	Solvent	Temp	Time	Yield
Et ₃ SiH (1.1 equiv)	MeOH	rt à 60 °C	24 h	No evidence of desired product*
NaBH ₄ (1.5 equiv)	MeOH	0 °C à rt	24 h	No evidence of desired product*
NaBH ₄ (1.5 equiv)	EtOH	0 °C à reflux	24 h	No evidence of desired product*
LiBH ₄ (1.1 equiv)	EtOH	0 °C à rt	24 h	No evidence of desired product*
LiBH ₄ (1.1 equiv)	EtOH	0 °C à reflux	24 h	No evidence of desired product*
DIBAL-H (1.1 equiv)	MeOH	0 °C à rt	24 h	No evidence of desired product*
DIBAL-H (1.1 equiv)	EtOH	rt à 60 °C	24 h	No evidence of desired product**
LiAlH ₄ (1.1 equiv)	MeOH	0 °C à rt	24 h	No evidence of desired product**

* Only starting material recovered

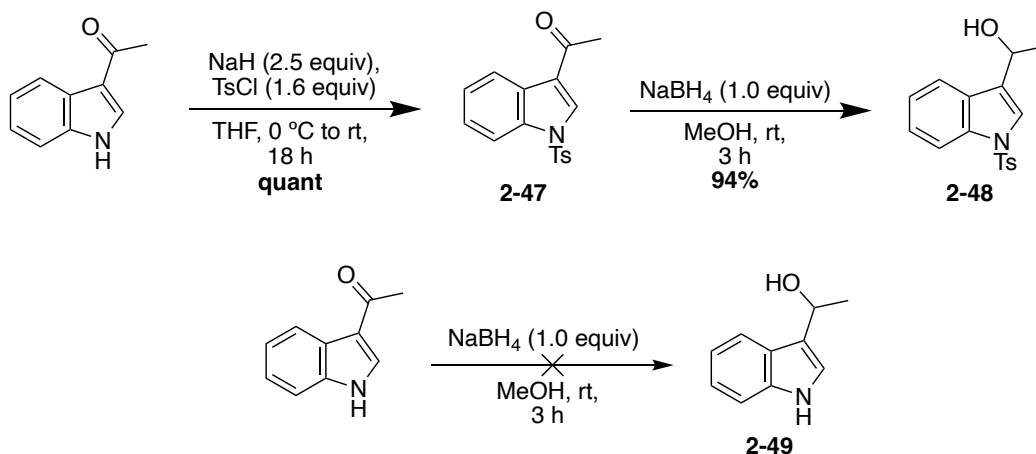
** Evidence of reductive imidazoline ring opening identified

The non-brominated, benzylated Spongotine C intermediate (**2-25**) was difficult to reduce, even with relatively strong reducing agents, such as DIBAL-H and LiAlH₄. This is likely due to the significant electron donation from the indole, contributing to the decreased electrophilicity of the carbonyl. It is also noteworthy to mention that evidence of reductive imidazoline ring opening was identified when using stronger reducing agents, such as DIBAL-H and LiAlH₄. Similar reductive imidazoline ring openings have been reported in literature.³⁰ In order to mitigate this issue, it was hypothesized that protecting the indole nitrogen, thus significantly decreasing its electron donation, could help to push this reaction forward and potentially allow for the use of milder reducing agents.

To test this hypothesis, a model system was explored in which tosylated (**2-47**) and un-tosylated 3-acyl-1*H*-indoles underwent reduction with relatively mild NaBH₄ as a reducing agent, following literature procedures (**Scheme 2.25**).³¹ As shown, in the case of (**2-47**) this reduction proceeded in excellent yields to access the reduced product (**2-48**) (94%). However, in the case of 3-acyl-1*H*-indole, no reaction was observed. These results supported the hypothesis

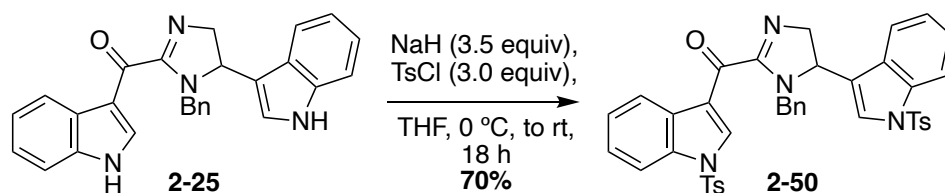
that *N*-protection of the indole could allow for more facile reduction of this ketone. Therefore, this approach was identified as a promising path forward for the reduction of **2-25**.

Scheme 2.25. Ketone reduction of 3-acetyl-1*H*-indole model system – effect of *N*-tosylation.



Considering these findings, the imidazoline intermediate (**2-25**) was tosylated to access the bis-protected intermediate (**2-50**) in 70% yield, as shown in **Scheme 2.26**.

Scheme 2.26. Bis-tosylation of the imidazoline intermediate (**2-25**).



Once the bis-tosylated imidazoline intermediate (**2-50**) was accessed, it subsequently was subjected to various reductive conditions in attempts to access intermediate **2-51** (**Scheme 2.27**). NaBH_4 was initially used as the reducing agent, similar to the reduction in **Scheme 2.25** (**Table 2.9**). Unfortunately, no desired product was identified among several different NaBH_4 -mediated reduction reactions. As is shown in **Table 2.9**, parameters such as temperature and equivalents of reducing agent were screened. In addition, CeCl_3 (Luche conditions)³² was explored as a catalyst to coordinate to the ketone and facilitate hydride attack. However, despite screening various equivalents of reducing agent and catalyst loadings, no desired product was isolated (**Table 2.9**).

Notably, with increased equivalents of the reducing agent, evidence of reductive imidazoline ring opening was identified. This evidence indicates that the imidazoline is sensitive to reductive conditions. Moreover, the reduction of the ketone and the reductive ring opening of the imidazoline are likely competitive reactions. Due to this issue, the synthetic approach toward the first total synthesis of Tulongicin (**2-1**) was adapted.

Scheme 2.27. Ketone reduction of the bis-tosylated imidazoline intermediate (**2-50**).

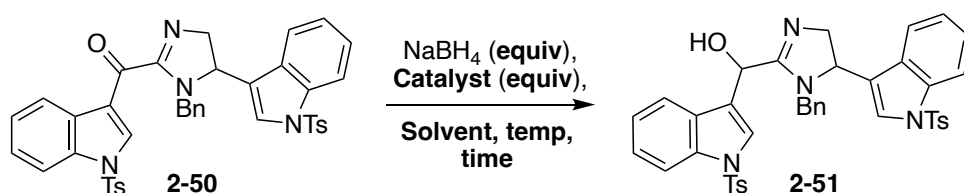


Table 2.9. Ketone reduction of the bis-tosylated imidazoline intermediate (**2-50**) – reaction condition screening.

Reducing Agent	Catalyst	Solvent	Temp	Time	Yield
NaBH ₄ (1.0 equiv)	None	MeOH	rt	24 h	Trace ^a
NaBH ₄ (1.5 equiv)	None	MeOH	rt	24 h	Trace ^a
NaBH ₄ (1.5 equiv)	CeCl ₃ (10 mol%)	MeOH	rt	24 h	Trace ^a
NaBH ₄ (1.5 equiv)	CeCl ₃ (10 mol%)	MeOH	reflux	24 h	Trace ^a
NaBH ₄ (5.0 equiv)	CeCl ₃ (10 mol%)	MeOH	rt	24 h	Trace ^{a, b}
NaBH ₄ (5.0 equiv)	CeCl ₃ (10 mol%)	MeOH	reflux	24 h	Trace ^{a, b}
NaBH ₄ (10.0 equiv)	CeCl ₃ (10 mol%)	MeOH	reflux	24 h	Trace ^{a, b}

^a Evidence of desired product identified in mass spectrometry (HRMS-ESI (*m/z*): Calculated for C₄₁H₃₆N₄O₅S₂ (*M+H*)⁺: 729.2205, Found: 729.2230)

^b Evidence of reductive imidazoline ring opening identified

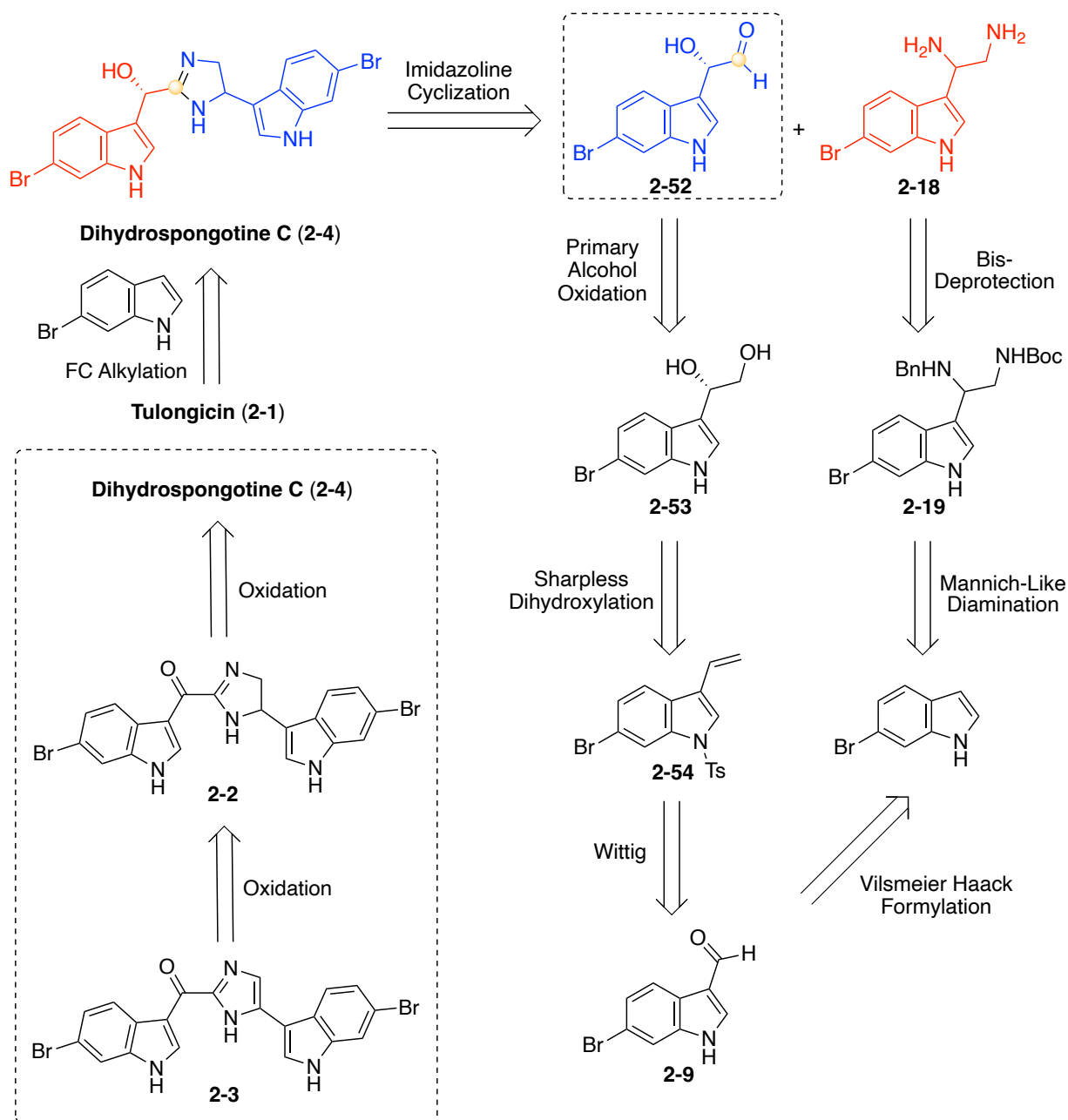
2.2.6. Adapted retrosynthetic analysis for the total synthesis of Tulongicin (**2-1**) via

Dihydrospogotine C (**2-4**) as an intermediate (Route E)

Considering these previously discussed issues, an updated retrosynthetic approach for the first total synthesis of Tulongicin (**2-1**) was completed, as shown in **Scheme 2.28**. It was

hypothesized that **2-1** could be accessed via a key Friedel Craft's alkylation of Dihydrospogotone C (**2-4**) and that this could circumvent the problems associated with the previous reductive conditions. It was also hypothesized that Dihydrospogotone (**2-4**) could be accessed via an imidazoline cyclization of (*S*)-2-(6-bromo-1*H*-indol-3-yl)-2-hydroxyacetaldehyde (**2-52**) and 1-(6-bromo-1*H*-indol-3-yl)ethane-1,2-diamine (**2-18**). Similar transformations have been reported in literature.³³ However, though various aldehyde fragments have been explored in literature, to the best of my knowledge, this would be the first use of an alpha hydroxyaldehyde fragment in such cyclizations. The diamine fragment (**2-18**) was proposed to be synthesized via the same aforementioned Mannich-like di-amination and subsequent bis-deprotection of commercially available 6-bromo-1*H*-indole.²² In addition, it was hypothesized that the hydroxyacetaldehyde intermediate (**2-52**) could be accessed via a selective primary alcohol oxidation of the diol intermediate (**2-53**), as similar transformations have been reported in literature.³⁴ Synthesis of the diol intermediate (**2-53**) was proposed to follow subsequent Vilsmeier Haack Formylation, Wittig, and Sharpless dihydroxylation steps of the commercially available 6-bromo-1*H*-indole. This adapted route would not only allow for the synthesis of Tulongicin (**2-1**) and Dihydrospogotone C (**2-4**) in a longest linear sequence (LLS) of 6 steps and 5 steps, respectively, but it would also allow for the potential of an enantioselective synthesis.

Scheme 2.28. Adapted retrosynthetic analysis for the total synthesis of Tulongicin (**2-1**) via Dihydrospogotine C (**2-4**) as an intermediate – Route E.

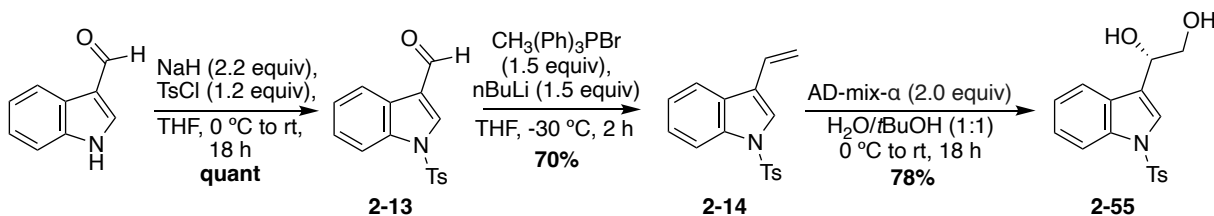


2.2.6.1. Synthesis of diol intermediate

It is worth noting that, for cost purposes, 1*H*-indole was used as a model system instead of 6-bromo-1*H*-indole for preliminary optimization. As shown in **Scheme 2.29**, in the synthesis

of the model diol intermediate), commercially available 1*H*-indole-3-carboxaldehyde was quantitatively *N*-protected with a tosyl group to access **2-13**. Then, **2-13** was subjected to a Wittig reaction to afford the 3-vinyl indole intermediate (**2-14**) in 70% yield, which subsequently underwent a Sharpless dihydroxylation to access (*S*)-**2-55** in high yield.

Scheme 2.29. Synthesis of diol intermediate (*S*)-(**2-55**).



2.2.6.2. Exploration of the selective primary alcohol oxidation and subsequent imidazoline cyclization

As is shown in **Scheme 2.30**, the alcohol intermediate (*S*)-**2-55** was then subjected to a selective primary alcohol oxidation via 2,2,6,6-tetramethyl-1-piperidinyloxy (TEMPO) as the catalytic oxidant and phenyliodine (III) diacetate (PIDA) as the co-oxidant. Similar selective primary alcohol oxidation such as this have been carried out in literature.³⁵ As shown in **Table 2.10**, despite screening various reaction times and equivalents of PIDA, no evidence of the desired product was found in this reaction. Instead of isolation of the desired product, across multiple trials, four different side products were isolated: (**2-58**), (**2-59**), (**2-13**), and (**2-60**). As is shown in **Table 2.10**, in the first trial with 1.75 equivalents of PIDA and an 18-hour reaction time, 48% yield of **2-58**, 33% yield of **2-59**, 21% yield of **2-13**, and 76% yield of **2-60** were isolated. When this reaction was closely monitored via thin layer chromatography (TLC), it was discovered that this reaction was very fast. In fact, the starting material was consumed in one hour. Therefore, a 1-hour reaction time was used in subsequent trials. As shown in **Table 2.10**, with 1.75 equivalents of PIDA and a 1-hour reaction time, 46% yield of **2-58**, 30% yield of **2-59**,

32% yield of **2-13**, and 71% yield of **2-60** were isolated. In attempts to slow this reaction, less equivalents of PIDA (1.2 equiv) were used, along with the same 1-hour reaction time. However, comparable yields of the aforementioned side products were isolated, as shown in **Table 2.10**.

Overall, despite screening different reaction times and equivalents of PIDA, similar results were obtained across trials.

Scheme 2.30. Exploration of the selective primary alcohol oxidation and subsequent imidazoline cyclization.

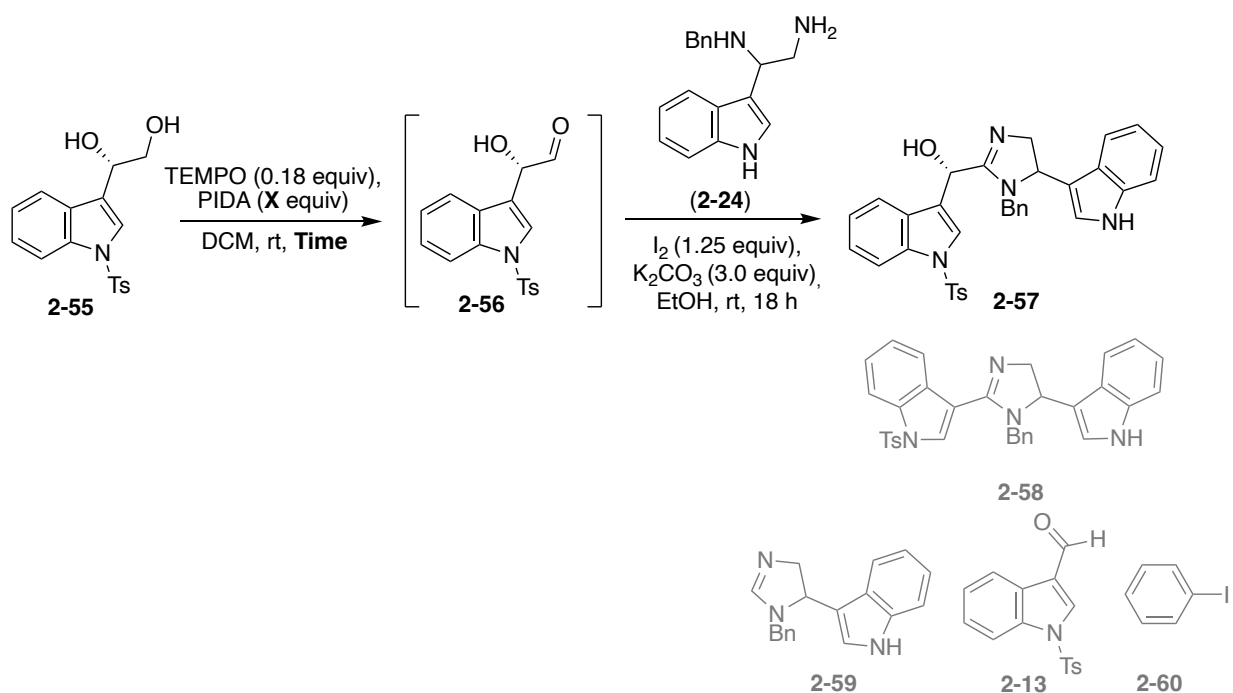


Table 2.10. Exploration of the selective primary alcohol oxidation and subsequent imidazoline cyclization – conditions screened.

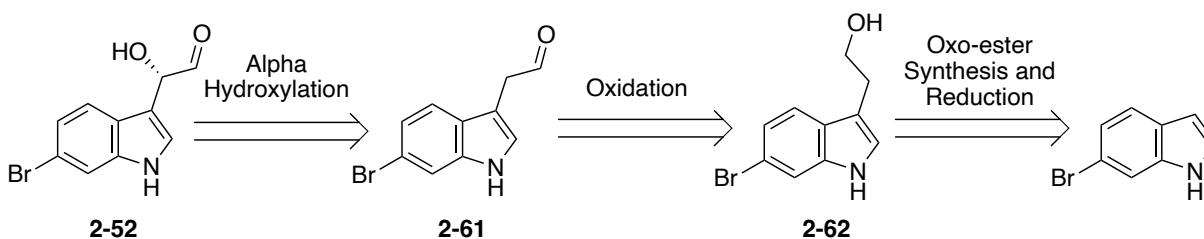
PIDA (equiv)	Time	Yield (2-57)	Yield (2-58)	Yield (2-59)	Yield (2-13)	Yield (2-60)
1.75	18 h	No evidence of desired product	48%	33%	21%	76%
1.75	1 h	No evidence of desired product	46%	30%	32%	71%
1.2	1 h	No evidence of desired product	45%	28%	34%	70%

Considering the significant formation of these side products, it was important to determine a potential mechanism by which they could be formed. Though not as common as other oxidants, it has been reported in literature that when PIDA is used in the oxidation of 1,2-diols it leads to oxidative cleavage, following a similar mechanism to that of sodium periodate (**Scheme 2.31**).³⁶ As shown, the first step of the mechanism likely involves sequential nucleophilic displacements of the acetate groups of PIDA and proton transfer steps to afford the 5-membered ring intermediate (**II**) and two equivalents of acetic acid. This 5-membered ring intermediate would then readily undergo oxidative cleavage to form the aldehyde intermediate (**2-13**), formaldehyde, and iodobenzene (**2-60**). As shown, this oxidative cleavage mechanism can explain the formation of the aldehyde (**2-13**) and the iodobenzene (**2-60**) side products. However, when considering the presence of the diamine intermediate (**2-24**) in the reaction, the remaining imidazoline side products can be explained by cyclization of the diamine fragment (**2-24**) with the aldehyde side product (**2-13**) or formaldehyde to access side products **2-58** or **2-59**, respectively.

2.2.6.3. Adapted synthesis of (*S*)-2-(6-bromo-1*H*-indol-3-yl)-2-hydroxyacetaldehyde (**2-52**)

Along with the continuing optimization of the aforementioned reduction of the alcohol intermediate (**2-55**), an expedited synthetic route toward the hydroxyacetaldehyde intermediate (**2-52**) was explored. As shown in **Scheme 2.33**, this expedited approach would allow **2-52** to be accessed in three steps opposed to the previous four steps necessary in the previous approach. As shown in **Scheme 2.33**, it was proposed that **2-52** could be accessed via an alpha hydroxylation of the aldehyde intermediate (**2-61**). Similar alpha hydroxylation reactions have been reported for various alkyl and aryl aldehydes, however, aldehydes with complex indole substituents, such as (**2-61**) have yet to be explored.^{37,38} It was hypothesized that this aldehyde (**2-61**) could be accessed by oxidation of the alcohol intermediate (**2-62**). It is notable to mention that there is significantly more literature precedence for alpha hydroxylation of ketones, yet aldehyde substrates tend to be more elusive. The proposed synthesis of the alcohol intermediate (**2-62**) includes oxo-ester synthesis and subsequent oxidation of the commercially available 1*H*-indole starting material.³⁹

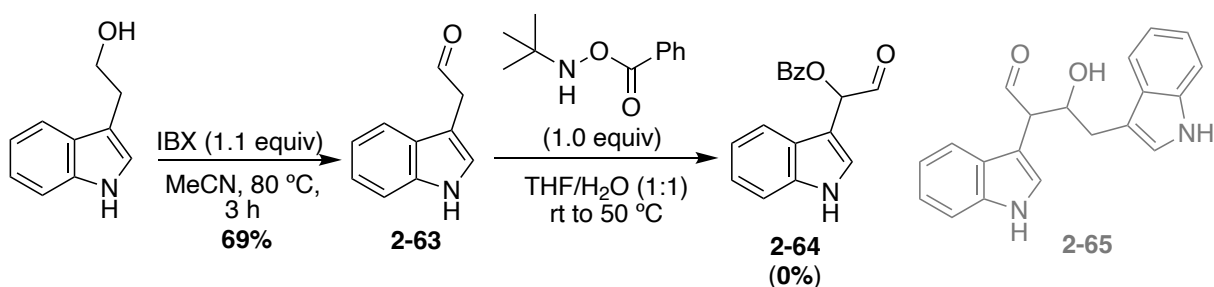
Scheme 2.33. Expedited retrosynthetic analysis of hydroxyacetaldehyde intermediate (**2-52**).



Progress in the forward direction has been made toward this expedited synthesis of **2-52** using commercially available 2-(1*H*-indol-3-yl)ethan-1-ol as a model starting material for initial optimization. As shown in **Scheme 2.34**, the aldehyde intermediate (**2-63**) was synthesized via an IBX oxidation of 2-(1*H*-indol-3-yl)ethan-1-ol in high yields (69%). Then, the aldehyde intermediate (**2-63**) was subjected to the mild hydroxylamine alpha oxidation reagent, *O*-

benzoyl-*N*-(*tert*-butyl)hydroxylamine in efforts to access the alpha-oxidized intermediate (**2-64**) (**Scheme 2.34**). This reaction proceeds via an imine intermediate that subsequently tautomerizes to the enamine, which undergoes a heat-induced sigmatropic rearrangement to access the alpha-oxidized product (**2-64**).³⁷ However, this reaction did not afford the desired product (**2-64**). Instead, an unexpected dimer side product (**2-65**) was identified via crude mass spectrometry (HRMS-ESI (*m/z*): Calculated for C₂₀H₁₈N₂O₂ (M+H)⁺: 319.1447, Found: 319.1461) (**Scheme 2.34**). The only other compound that was recovered was the hydroxylamine starting material (57%). This dimer side product (**2-65**) was likely the result of an aldol condensation of **2-63** with another molecule of itself. Considering this hypothesis, along with the recovery of the hydroxylamine starting material, it is likely that this aldol reaction is faster than the desired alpha hydroxylation reaction, especially at elevated temperatures. Therefore, the prevention of the aldol condensation remains the focus of future optimization. One proposed solution includes the protection of the indole moiety with an electron withdrawing group, such as a tosyl group, to decrease the reactivity of **2-63**.

Scheme 2.34. Synthesis of intermediate (**2-64**).

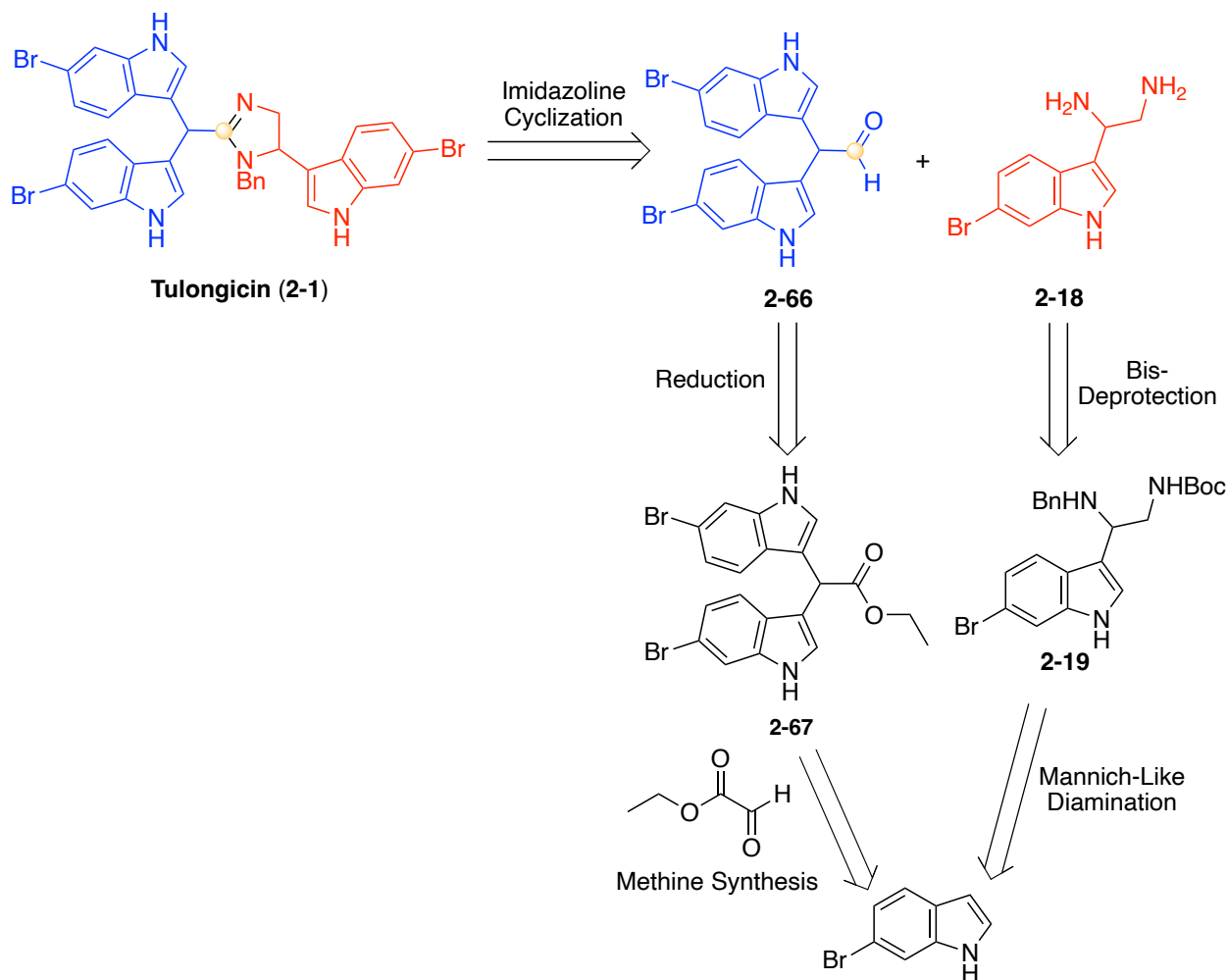


2.2.7. Adapted retrosynthetic analysis for the total synthesis of Tulongicin (**2-1**) via a bis-indole intermediate (Route F)

Though additional exploration and optimization remains a priority for Route E, simultaneously, an additional bis-indole approach (Route F), was developed. While this approach

would not allow for the first total synthesis of Dihydrospogotine C (**2-4**) as an intermediate, it would have the benefit of being the most expedited route yet (LLS: 3steps) (**Scheme 2.35**). As shown in **Scheme 2.35**, it is hypothesized that Tulongicin (**2-1**) could be accessed via an imidazoline cyclization of a bis-indole aldehyde fragment (**2-66**) and a diamine fragment (**2-18**). Similar imidazoline cyclizations have been reported in literature, however, to the best of my knowledge, there has been no reported imidazoline cyclization resulting in the synthesis of an imidazoline bearing a complex 2-bis-indole methane moiety. The diamine fragment (**2-18**) was proposed to follow the same Mannich-like di-amination and deprotection procedure, as was previously discussed.²² It was hypothesized that the bis-indole aldehyde fragment (**2-66**) could be accessed via reduction of the bis-indole ester intermediate (**2-67**). The proposed synthesis of **2-67** included a methine synthesis using the commercially available ethyl-2-oxoacetate and 6-bromo-1*H*-indole, as has been reported in literature.⁴⁰

Scheme 2.35. Adapted retrosynthetic analysis for the total synthesis of Tulongicin (**2-1**) via a bis-indole intermediate – Route F.



2.2.7.1. Synthesis of brominated bis indole aldehyde fragment

First, 6-bromo-1*H*-indole was subjected to a methine synthesis with ethyl 2-oxoacetate, using scandium triflate ($\text{Sc}(\text{OTf})_2$) as a catalyst, to afford the desired bis-indole ester intermediate (**2-67**) in quantitative yield (**Scheme 2.36**). Then, **2-67** underwent a DIBAL-H reduction at -78°C to afford the desired bis-indole aldehyde product (**2-66**). As is shown in **Table 2.11**, various equivalents of DIBAL-H reducing agent were explored with the optimal conditions being 1.8 equivalents of DIBAL-H to access **2-66** in 72% yield. The quench temperature of this

reaction was also found to have a great impact on yield. For instance, a 20°C quench temperature suffered from a low yield of **2-66** and an increased formation of an over-reduced alcohol product (Table 2.11).

Scheme 2.36. Synthesis of bis-indole aldehyde intermediate (**2-66**).

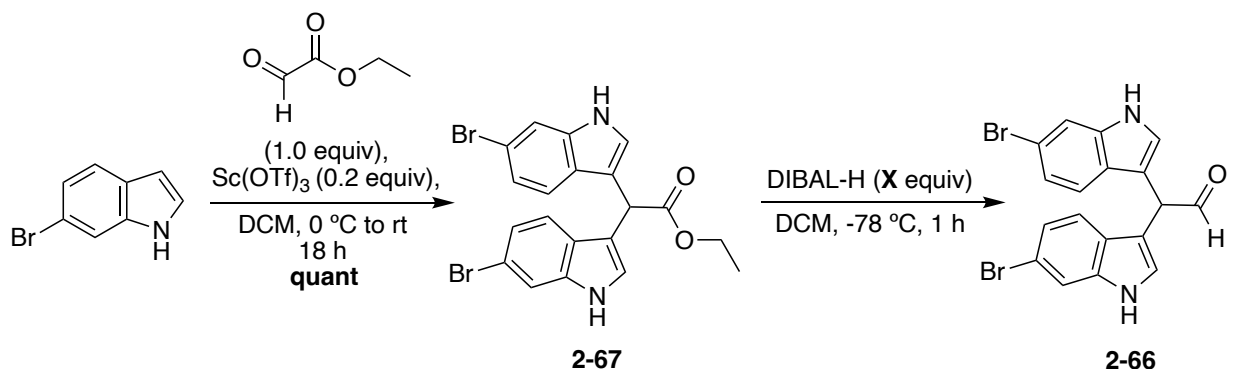


Table 2.11. Ester reduction of **2-67** to access the aldehyde fragment (**2-66**) – Reaction conditions screened.

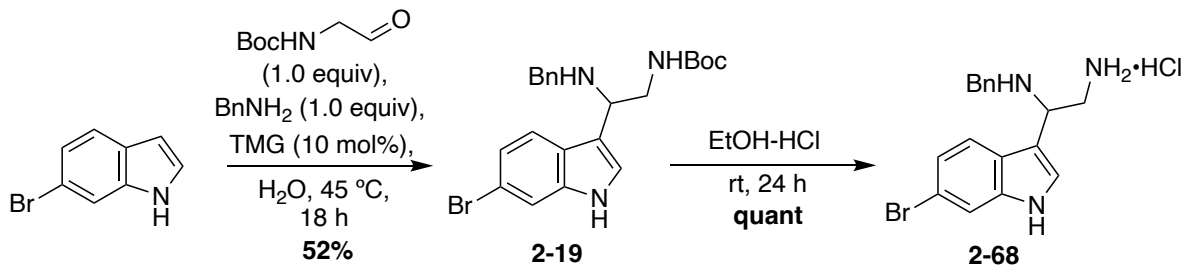
DIBAL-H (equiv)	Quench Temperature	Yield (2-66)
1.0	20 °C (rt)	15%*
1.0	-78 °C	48%
1.8	-78 °C	81%
2.0	-78 °C	67%*

*over-reduced alcohol product was present

2.2.7.2. Synthesis of brominated indolic diamine fragment

As shown in **Scheme 2.37**, the brominated indolic diamine fragment was synthesized in the same manner as the aforementioned indolic diamine model system (**Scheme 2.13**). First, commercially available 6-bromo-1*H*-indole underwent di-amination to access the di-protected diamine (**2-19**) in 52% yield. Then, as shown in **Scheme 2.37**, the di-protected diamine (**2-19**) was quantitatively Boc-protected to access the mono-protected diamine (**2-68**).

Scheme 2.37. Synthesis of brominated indolic diamine fragment (**2-68**).



2.2.7.3. Exploration of imidazoline cyclization via bis-indole aldehyde and diamine fragments

As shown in **Scheme 2.38**, the base-mediated imidazoline cyclization between the bis-indole aldehyde fragment (**2-66**) and the indolic diamine fragment (**2-68**) was explored using potassium carbonate as the base and iodine to oxidize the cyclized intermediate to the imidazoline product (**2-69**). As shown in **Table 2.12**, despite screening a variety of reaction times and temperatures, the desired product was only found in trace amounts at best, as determined by crude mass spectrometry. At elevated temperatures, messy NMRs and large masses in mass spectrometry were found (**Table 2.12**). This data could likely correspond to some sort of dimer or polymer of the aldehyde fragment, as one could envision the alpha proton of this intermediate to be very sensitive to basic conditions and elevated temperatures. For instance, if **2-66** were to form an enolate, a myriad of problematic side reactions could occur, such as aldol condensations, etc. Therefore, since elevated temperatures and base are necessary for this imidazoline formation, the bis-indole aldehyde (**2-66**) may not be a viable fragment for this reaction.

Scheme 2.38. Imidazoline cyclization via bis-indole aldehyde (**2-66**) and diamine fragments (**2-68**).

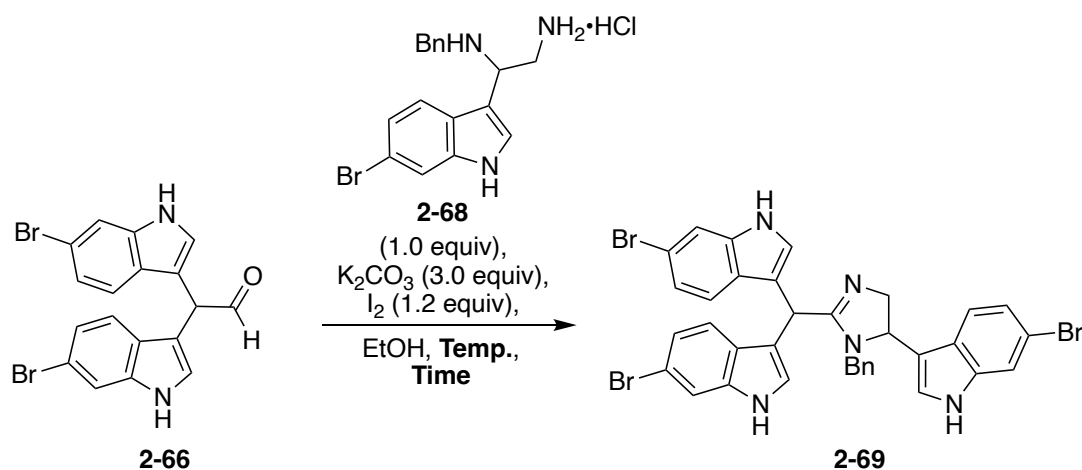


Table 2.12. Imidazoline cyclization – reaction condition screening.

Temperature	Time	Yield (2-69)
rt	5 h	No evidence of product
rt	18 h	No evidence of product
rt to 50°C	18 h	Trace ^{a, b}
rt to 50°C	3 h	Trace ^{a, b}

a. Mass of desired product (**2-69**) identified in crude mass spectrometry (HRMS-ESI (m/z): Calculated for $C_{33}H_{26}Br_3N_5$ ($M+H$)⁺, ($Br^{79}, Br^{79}, Br^{79}$); ($Br^{81}, Br^{79}, Br^{79}$); ($Br^{81}, Br^{81}, Br^{79}$); ($Br^{81}, Br^{81}, Br^{81}$): 753.9817; 755.9796; 757.9776; 759.9755, Found: 753.9833; 755.9807; 757.9791; 759.9774).

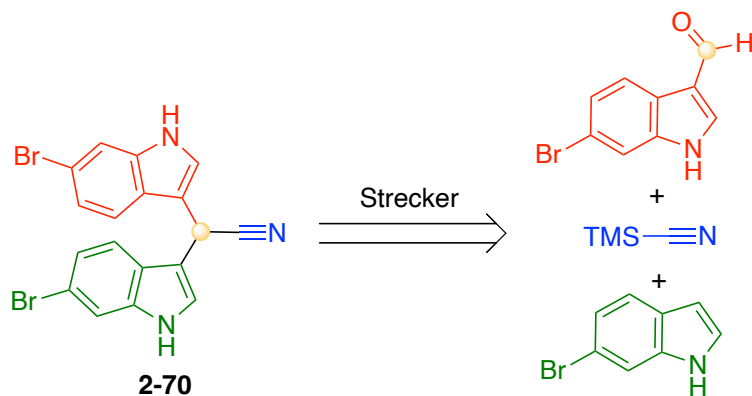
b. Messy crude NMRs and large masses in crude MS (potential polymerization).

2.2.7.4. Synthesis of bis-indole cyanide

To address the previously discussed problems with the aldehyde intermediate, it was hypothesized that bis-indole cyanide intermediate (**2-70**) could be cyclized with the diamine fragment (**2-18**) to form the imidazoline core of Tulongicin (**2-1**) (**Scheme 2.39**). Similar cyclizations have been reported for less complex substrates in literature.⁴¹ This bis-indole cyanide intermediate would be less reactive and, therefore, less susceptible to polymerization or other side reactions. It was proposed that the bis-indole cyanide (**2-70**) could be accessed in one step via an adapted Strecker reaction from the commercially available 6-bromo-1*H*-indole-3-

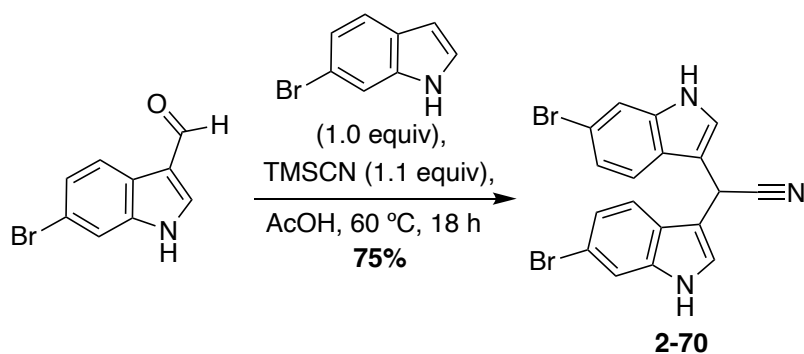
carbaldehyde, trimethylsilanecarbonitrile (TMSCN), and 6-bromo-1*H*-indole, as shown in **Scheme 2.39**.⁴²

Scheme 2.39. Retrosynthesis of the bis indole cyanide intermediate (**2-70**).



As shown in **Scheme 2.40**, the bis-indole cyanide intermediate (**2-70**) was synthesized via an acid-mediated Strecker reaction with the commercially available 6-bromo-1*H*-indole-3-carbaldehyde, trimethylsilanecarbonitrile (TMSCN) in 75% yield. This reaction was reproducible at multi-gram scale.

Scheme 2.40. Synthesis of the bis indole cyanide intermediate (**2-70**).

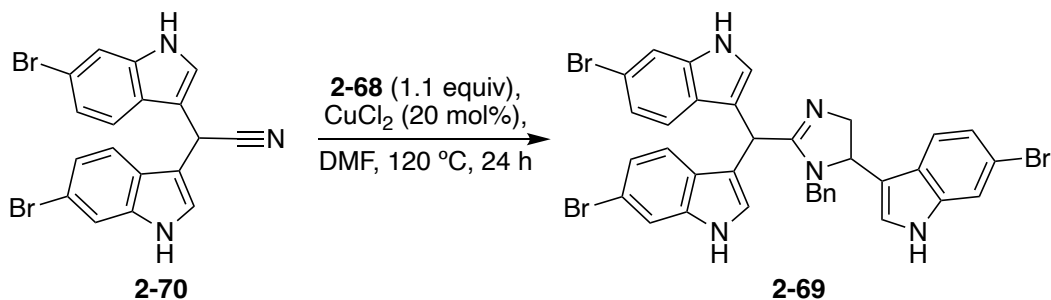


2.2.7.5. Exploration of imidazoline cyclization via bis-indole cyanide and diamine fragments

Once **2-70** was accessed, the imidazoline cyclization between the bis-indole cyanide fragment (**2-70**) and the indolic diamine fragment (**2-68**) was explored. As was previously

mentioned, the bis-indole cyanide (**2-70**) is less reactive than the previously used aldehyde intermediate (**2-66**). Therefore, a copper catalyst was used in this cyclization reaction, as well as heat. As shown in **Scheme 2.41**, **2-70** was reacted with the diamine (**2-68**) and CuCl_2 as a catalyst at 120°C for 24 hours. Notably, no side reactions were identified during this cyclization. The only compounds identified after this reaction was run were the starting materials (**2-70** and **2-68**) and the product (**2-69**). Unfortunately, the diamine starting material (**2-68**) and the desired imidazoline product co-eluted, contributing to difficult purification. Due to this difficult purification, the desired cyclized product has yet to be isolated. However, **2-69** has been identified via mass spectrometry (HRMS-ESI (m/z): Calculated for $\text{C}_{35}\text{H}_{26}\text{Br}_3\text{N}_5$ ($\text{M}+\text{H}$)⁺, (Br^{79} , Br^{79} , Br^{79}); (Br^{81} , Br^{79} , Br^{79}); (Br^{81} , Br^{81} , Br^{79}); (Br^{81} , Br^{81} , Br^{81}): 753.9817; 755.9796; 757.9776; 759.9755, Found: 753.9833; 755.9807; 757.9791; 759.9774). This was very exciting progress toward the first total synthesis of Tulongicin, as intermediate **2-69** is only one deprotection step away from Tulongicin (**2-1**). Additional optimization of this reaction, as well as its final deprotection, remain the focus for the future of this project, as Route F has shown the most promise toward the first total synthesis of Tulongicin (**2-1**).

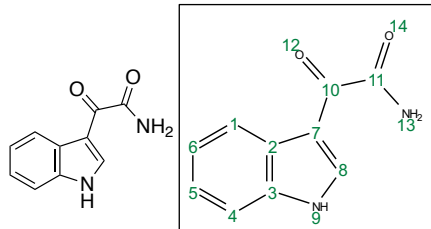
Scheme 2.41. Imidazoline cyclization via bis-indole cyanide (**2-70**) and diamine fragments (**2-68**).



2.3. Conclusions

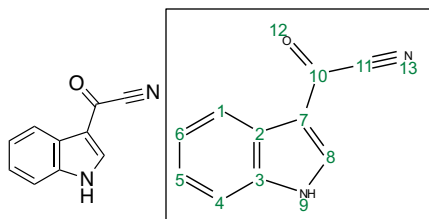
In conclusion, this chapter summarizes the synthetic efforts toward the total synthesis of Tulongicin (**2-1**) and its related natural product analogues Spongotine C (**2-2**), Dibromodeoxytopsentin (**2-3**), and Dihydrospogotine C (**2-4**). As has been discussed in this chapter, key challenges in these syntheses were identified which hindered their completion at the present time. However, despite the fact that these total syntheses of Tulongicin (**2-1**) and its related natural product analogues have not yet been achieved, these studies have provided valuable insights to, hopefully, allow for future achievement in their syntheses. Currently, further research building upon these findings toward the total synthesis of Tulongicin (**2-1**) is underway in the Tepe lab.

2.4. Experimental



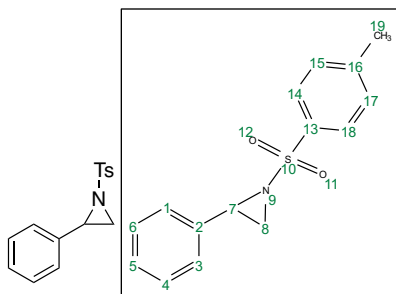
2-(1*H*-indol-3-yl)-2-oxoacetamide (2-9)

Oxalyl chloride (0.5 mL, 6.4 mmol, 1.5 equiv.) was added dropwise to a stirred solution of indole (0.5 g, 4.3 mmol, 1.0 equiv.) in anhydrous Et₂O (10 mL) at 0°C under an atmosphere of argon gas. The mixture was then stirred for 2 hours at 0°C under argon gas. A fresh NH₃ solution was then prepared by mixing equal parts saturated aqueous NH₄Cl solution and saturated aqueous KOH solution. After consumption of starting material by TLC, the freshly prepped saturated ammonia solution was added to the mixture (5 mL). This was allowed to stir for 1 hour at room temperature. The resulting yellow precipitate was then vacuum filtered, using a Buchner funnel, and washed with large amounts of chloroform to yield the 2-(1*H*-indol-3-yl)-2-oxoacetamide product as a yellow solid. This crude product was used in the next step without any additional purification (97% by NMR). **Mp**: 220°C (decomp.). **¹H NMR** (500 MHz, DMSO) δ 12.27 (s, 1H, (**H9**)), 8.68 (d, *J* = 3.2 Hz, 1H, (**H8**)), 8.22 (d, *J* = 6.3 Hz, 1H, (**H1**)), 8.08 (s, 1H, (**H13**)), 7.72 (s, 1H, (**H13**)), 7.53 (d, *J* = 5.8 Hz, 1H, (**H4**)), 7.28 – 7.22 (m, 2H, (**H5**, **H6**)). **¹³C NMR** (126 MHz, DMSO) δ 183.42 (**C10**), 166.47 (**C11**), 138.70 (**C8**), 136.73 (**C3**), 126.58 (**C2**), 123.81 (**C5**), 122.91 (**C6**), 121.67 (**C1**), 112.99 (**C4**), 112.50 (**C7**). **FTIR (cm⁻¹)**: 3419, 3381, 3301, 3066, 1741, 1661, 1554. **HRMS-ESI (m/z)**, calculated for C₁₀H₈N₂O₂ (M+H)⁺: 189.0664, Found: 189.0681.



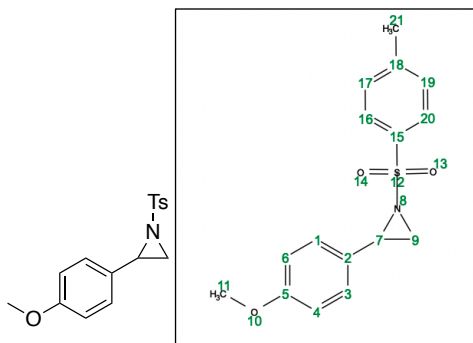
1*H*-Indole Carbonyl Cyanide (2-10)

SOCl₂ (0.57 mL, 7.8 mmol, 2.5 equiv) was added dropwise to a stirred solution of 2-(1*H*-indol-3-yl)-2-oxoacetamide (0.45 g, 3.9 mmol, 1.0 equiv.) in anhydrous DMF at 0°C under an atmosphere of argon gas. This solution was allowed to stir at 0°C for 2 hours. The reaction mixture was then quenched with a few drops of water and the organic layer was extracted with EtOAc (3x30mL). The combined organic layers were then washed with saturated aqueous LiCl solution (3x30mL) to ensure the removal of DMF from the organic layer. The combined organic layers were then dried with MgSO₄, filtered, and the solvent was removed in vacuo to afford the 1*H*-indole-3-carbonyl cyanide product as a yellow-tan solid (0.54 g, 81%). **Mp:** 167°C (decomp.). **¹H NMR** (500 MHz, DMSO) δ 12.92 (s, 1H, (**H9**)), 8.65 (d, *J* = 3.5 Hz, 1H, (**H8**)), 8.04 (d, *J* = 7.5 Hz, 1H, (**H1**)), 7.59 (d, *J* = 7.6 Hz, 1H, (**H4**)), 7.37 (td, *J* = 7.5, 7.3, 1.4 Hz, 1H, (**H5**)), 7.33 (td, *J* = 7.4, 7.3, 1.3 Hz, 2H, (**H6**)). **¹³C NMR** (126 MHz, DMSO) δ 158.60 (**C10**), 141.49 (**C8**), 137.58 (**C3**), 124.98 (**C5**), 124.23 (**C2**), 123.87 (**C6**), 121.00 (**C1**), 116.21 (**C7**), 114.39 (**C11**), 113.35 (**C4**). **FTIR (cm⁻¹):** 3401, 3072, 2900, 2249, 1724, 1512. **HRMS-ESI (m/z)**, calculated for C₁₀H₆N₂O (M+H)⁺: 171.0558, Found: 171.0573.



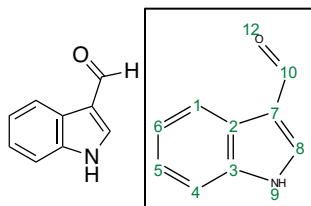
2-phenyl-1-tosylaziridine (2-11a)

To a mixture of I₂ (0.13 g, 0.5 mmol, 0.1 equiv.), TBAB (0.16 g, 0.5 mmol, 0.1 equiv.), and chloramine-T monohydrate (1.2 g, 5.0 mmol, 1.0 equiv.) in DCM/H₂O (2:1, 50:25 mL) was added styrene (0.58 mL, 5.0 mmol, 1.0 equiv.) at 20°C, under ambient conditions. This mixture was stirred vigorously overnight under ambient conditions. The reaction mixture was then treated with saturated aqueous Na₂S₂O₃ (5 mL) and extracted with DCM (3x30 mL). The combined organic extracts were then dried over Na₂SO₄, filtered, and concentrated in vacuo. The crude product was purified via silica gel flash column chromatography (EtOAc/Hexanes) to afford the desired product as a white crystalline solid (0.95 g, 70%). **Mp:** 87-89°C. **¹H NMR** (500 MHz, CDCl₃) δ 7.87 (d, *J* = 8.3 Hz, 2H, (**H14**, **H18**)), 7.33 (d, *J* = 8.2 Hz, 2H, (**H15**, **H17**)), 7.30 – 7.26 (m, 3H, (**H4**, **H5**, **H6**)), 7.24 – 7.19 (m, 2H, (**H1**, **H3**)), 3.78 (dd, *J* = 7.2, 4.5 Hz, 1H, (**H7**)), 2.99 (d, *J* = 7.2 Hz, 1H, (**H8**)), 2.43 (s, 3H, (**H19**)), 2.39 (d, *J* = 4.5 Hz, 1H, (**H8**)). **¹³C NMR** (126 MHz, CDCl₃) δ 144.77 (**C16**), 135.14 (**C2**), 135.06 (**C13**), 129.87 (**C15**, **C17**), 128.66 (**C4**, **C6**), 128.41 (**C5**), 128.07 (**C14**, **C18**), 126.66 (**C1**, **C3**), 41.13 (**C7**), 36.05 (**C8**), 21.76 (**C19**). **FTIR (cm⁻¹):** 3041, 2878, 1551, 1356, 1155. **HRMS-ESI (m/z)**, calculated for C₁₅H₁₅NO₂S (M+H)⁺: 274.0902, Found: 274.0904.



2-(4-methoxyphenyl)-1-tosylaziridine (2-11b)

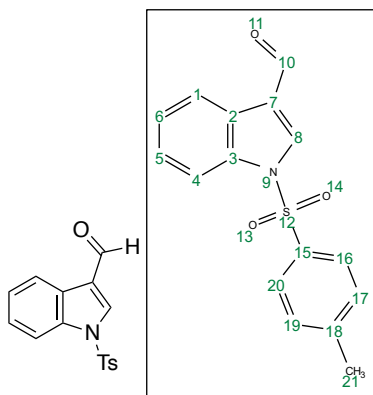
To a mixture of TBAB (64 mg, 0.2 mmol, 0.1 equiv.), CuI (38 mg, 0.2 mmol, 0.1 equiv.), chloramine-T•H₂O (0.5 mg, 2.0 mmol, 1.0 equiv.), in DCM/H₂O (2:1), was added 1-methoxy-4-vinylbenzene (0.54 mL, 4.0 mmol, 2.0 equiv.) dropwise at 20°C under ambient conditions. The reaction mixture was stirred vigorously overnight under ambient conditions. The reaction mixture was then treated with saturated aqueous Na₂S₂O₃ (3 mL) and extracted with DCM (3x30 mL). The combined organic extracts were then dried over Na₂SO₄, filtered, and concentrated in vacuo. The crude product was purified via silica gel flash column chromatography (EtOAc/Hexanes) to afford the desired product as a white crystalline solid (95 mg, 15%). **Mp:** 89-91°C. ¹H NMR (500 MHz, CDCl₃) δ 7.85 (d, *J* = 8.3 Hz, 2H, (**H16**, **H20**)), 7.31 (d, *J* = 8.4 Hz, 2H, (**H17**, **H19**)), 7.12 (d, *J* = 8.7 Hz, 2H, (**H1**, **H3**)), 6.81 (d, *J* = 8.7 Hz, 2H, (**H4**, **H6**)), 3.75 (s, 3H, (**H11**)), 3.73 (dd, *J* = 7.2, 4.6 Hz, 1H, (**H7**)), 2.95 (d, *J* = 7.2 Hz, 1H, (**H9**)), 2.42 (s, 3H, (**H21**)), 2.37 (d, *J* = 4.6 Hz, 1H, (**H9**)). ¹³C NMR (126 MHz, CDCl₃) δ 159.74 (**C5**), 144.65 (**C18**), 135.14 (**C15**), 129.80 (**C17**, **C19**), 127.97 (**C16**, **C20**), 127.88 (**C4**, **C6**), 127.01 (**C2**), 114.06 (**C1**, **C3**), 55.32 (**C11**), 40.97 (**C7**), 35.81 (**C9**), 21.68 (**C21**). **FTIR (cm⁻¹):** 3013, 2875, 1514, 1351, 1252, 1153, 1039. **HRMS-ESI (m/z)**, calculated for C₁₆H₁₇NO₃S (M+H)⁺: 304.1007, Found: 304.1070, calculated for C₁₆H₁₈NO₃SNa (M+H)⁺: 327.0905, Found: 327.0925.



***1H*-indole-3-carbaldehyde (2-12)**

Anhydrous DMF (3 mL) was added to an oven-dried flask. This was then cooled to 0°C under an atmosphere of nitrogen gas. Then, POCl₃ (1.2 mL, 12.4 mmol, 3.0 equiv) was added dropwise and the reaction was stirred for 10 minutes at 0°C to allow formation of the Vilsmeier reagent. After 10 minutes, *1H*-indole (0.57 g, 4.9 mmol, 1.0 equiv) was added in a minimal amount of anhydrous DMF. The reaction mixture was then placed in a pre-heated oil bath at 80°C. The reaction was then allowed to stir overnight at 80°C under nitrogen gas. The reaction was then slowly cooled to 0°C, quenched with deionized H₂O (2 mL), and treated with 20% Aqueous NaOH solution until the reaction mixture reaches a pH of ~9-11. The resulting solution was then extracted with EtOAc (3x40 mL) and the combined organic layers were washed with LiCl (3x40mL) to ensure removal of DMF from the organic layers. The combined organic fractions were then dried over Na₂SO₄, filtered, and concentrated in vacuo. The crude residue was then purified via silica gel flash column chromatography (EtOAc/Hexanes) to yield the desired product as a yellow solid. This yellow solid was then recrystallized (Et₂O) to yield yellow crystals (0.37 g, 53%). **Mp:** 198-199°C. **¹H NMR** (500 MHz, DMSO) δ 12.12 (s, 1H, (**H9**)), 9.92 (s, 1H, (**H10**)), 8.27 (s, 1H, (**H8**)), 8.07 (d, *J* = 7.6 Hz, 1H, (**H1**)), 7.49 (d, *J* = 8.0 Hz, 1H, (**H4**)), 7.24 (td, *J* = 8.0, 7.1, 1.3 Hz, 1H, (**H5**)), 7.20 (td, *J* = 7.7, 7.2, 1.2 Hz, 1H, (**H6**)). **¹³C NMR** (126 MHz, DMSO) δ 185.41 (**C10**), 138.94 (**C3**), 137.49 (**C8**), 124.55 (**C2**), 123.91 (**C5**), 122.57 (**C6**), 121.27 (**C1**), 118.60 (**C7**), 112.87 (**C4**). **FTIR (cm⁻¹**

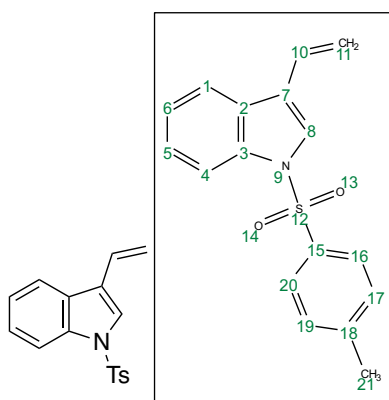
1): 3401, 3036, 2908, 1712, 1520. **HRMS-ESI (m/z)**, calculated for C_9H_7NO (M+H) $^+$: 146.0606, Found: 146.0621.



1-tosyl-1*H*-indole-3-carbaldehyde (2-13)

To an oven-dried flask, charged with N_2 gas, was added anhydrous THF (20mL). Then, 60% NaH solution in mineral oil (0.30 g, 7.5 mmol, 2.5 equiv) was added and this mixture was cooled to $0^\circ C$. Next, a solution of 1*H*-indole-3-carbaldehyde (0.44 g, 3.0 mmol, 1.0 equiv) in anhydrous THF (10mL) was added dropwise at $0^\circ C$ under an atmosphere of N_2 gas. This pink reaction mixture was allowed to stir for 20 minutes at $0^\circ C$ under N_2 . After 20 minutes, Tosyl Chloride (0.92 g, 4.8 mmol, 1.6 equiv) was added at $0^\circ C$, resulting in an immediate yellow color change. The reaction mixture was allowed to warm to $20^\circ C$ and was stirred for 12 hours. When TLC showed complete consumption of starting material, the reaction was quenched slowly with deionized water (3mL) dropwise. The reaction mixture was then extracted with EtOAc (3x40mL). The combined organic layers were then dried over Na_2SO_4 , filtered, and concentrated in vacuo. The crude product was purified via silica gel flash column chromatography (EtOAc/Hexanes) to yield the desired product as an off-white solid (0.90 g, Quantitative). **Mp:** 147-149°C. 1H NMR (500 MHz, $CDCl_3$) δ 10.10 (s, 1H, (**H10**)), 8.26 (d, $J = 7.8$ Hz, 1H, (**H1**)),

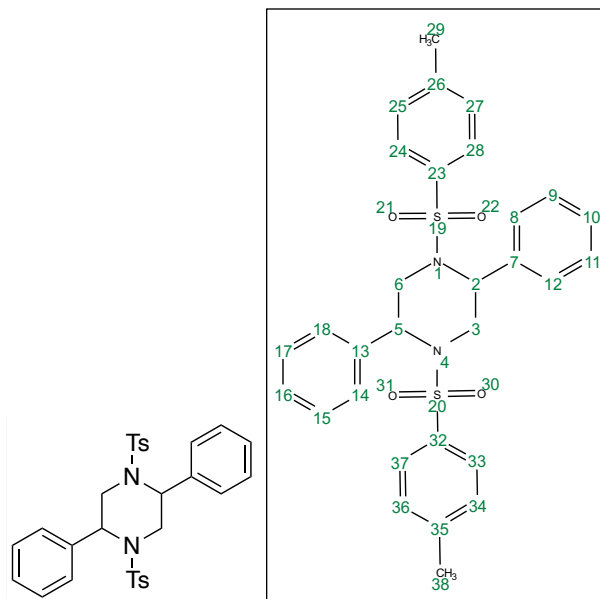
8.23 (s, 1H, **(H8)**), 7.95 (d, $J = 8.3$ Hz, 1H, **(H4)**), 7.85 (d, $J = 8.4$ Hz, 2H, **(H16, H20)**), 7.41 (td, $J = 8.4, 7.2, 1.3$ Hz, 1H, **(H5)**), 7.36 (td, $J = 7.8, 7.3, 1.3$ Hz, 1H, **(H6)**), 7.30 (d, $J = 8.2$ Hz, 2H, **(H17, H19)**), 2.38 (s, 3H, **(H21)**). ^{13}C NMR (126 MHz, CDCl_3) δ 185.23 (**(C10)**), 146.05 (**(C18)**), 136.11 (**(C8)**), 135.45 (**(C3)**), 134.42 (**(C15)**), 130.22 (**(C17, C19)**), 127.13 (**(C16, C20)**), 126.20 (**(C5)**), 126.17 (**(C2)**), 124.94 (**(C6)**), 122.50 (**(C1)**), 122.25 (**(C7)**), 113.13 (**(C4)**), 21.57 (**(C21)**). FTIR (cm^{-1}): 3118, 3069, 1701, 1537, 1245, 1037. HRMS-ESI (m/z), calculated for $\text{C}_{16}\text{H}_{13}\text{NO}_3\text{S}$ ($\text{M}+\text{H}$) $^+$: 300.0694, Found: 300.0709.



1-tosyl-3-vinyl-1H-indole (2-14)

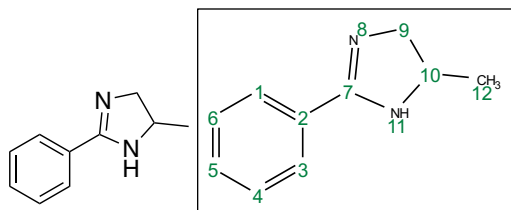
To an oven-dried flask was added methyltriphenylphosphonium bromide (1.3 g, 3.6 mmol, 1.5 equiv) and anhydrous THF (20mL). This was cooled to -30°C and stirred under an atmosphere of N_2 gas. After the mixture reached -30°C , $n\text{BuLi}$ (2.5M in Hexanes) (1.44 mL, 3.6 mmol, 1.5 equiv) was added dropwise. This was stirred for 1 hour at -30°C under N_2 . After 1 hour, 1-tosyl-1H-indole-3-carbaldehyde (720 mg, 2.4 mmol, 1 equiv) was added in a solution of anhydrous THF (10 mL) dropwise. The reaction mixture was then stirred for an additional 1 hour at -30°C under N_2 . Once TLC showed consumption of starting material, the reaction was quenched with DI H_2O (0.5 mL), poured into Et_2O (150 mL), dried with Na_2SO_4 , filtered, and concentrated in

vacuo. The crude residue was then purified via silica gel flash column chromatography (EtOAc/Hexanes) to yield the desired product as a white solid. (0.51 g, 70%). **Mp:** 99-101°C. **¹H NMR** (500 MHz, CDCl₃) δ 7.99 (d, *J* = 8.3 Hz, 1H, **(H1)**), 7.77 (d, *J* = 8.4 Hz, 2H, **(H16, H20)**), 7.74 (d, *J* = 7.9 Hz, 1H, **(H4)**), 7.60 (s, 1H, **(H8)**), 7.33 (td, *J* = 8.3, 7.3, 1.1 Hz, 1H, **(H6)**), 7.27 (td, *J* = 7.9, 7.3, 1.1 Hz, 1H, **(H5)**), 7.22 (d, *J* = 8.2 Hz, 2H, **(H17, H19)**), 6.77 (dd, *J* = 17.8, 11.3 Hz, 1H, **(H10)**), 5.79 (d, *J* = 17.9 Hz, 1H, **(H11)**), 5.35 (d, *J* = 11.3 Hz, 1H, **(H11)**), 2.34 (s, 3H, **(H21)**). **¹³C NMR** (126 MHz, CDCl₃) δ 145.18 (**(C18)**), 135.61 (**(C3)**), 135.23 (**(C15)**), 130.06 (**(C17, C19)**), 129.13 (**(C2)**), 127.69 (**(C10)**), 127.00 (**(C16, C20)**), 125.04 (**(C8)**), 124.21 (**(C1)**), 123.64 (**(C6)**), 121.06 (**(C7)**), 120.55 (**(C5)**), 115.47 (**(C11)**), 113.86 (**(C4)**), 21.72 (**(C21)**). **FTIR (cm⁻¹):** 3082, 3007, 2895, 1636, 1596, 1251, 1043. **HRMS-ESI (m/z)**, calculated for C₁₇H₁₅NO₂S (M+H)⁺: 298.0902, Found: 298.0923.



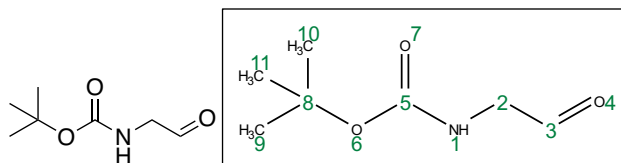
2,5-diphenyl-1,4-ditosylpiperazine (2-17)

This side product was isolated as a clear, colorless oil. $^1\text{H NMR}$ (500 MHz, CDCl_3) δ 7.47 (d, J = 8.3 Hz, 4H, (**H24**, **H28**, **H33**, **H37**)), 7.31 – 7.22 (m, 6H, (**H8**, **H12**, **H10**, **H18**, **H14**, **H16**)), 7.20 (d, J = 8.2 Hz, 4H, (**H25**, **H27**, **H34**, **H36**)), 7.18 – 7.14 (m, 4H, (**H9**, **H11**, **H14**, **H18**)), 4.83 (dd, J = 10.3, 5.8 Hz, 2H, (**H2**, **H5**)), 3.93 (dd, J = 14.9, 5.8 Hz, 2H, (**H3**, **H6**)), 3.54 (dd, J = 14.9, 10.4 Hz, 2H, (**H3**, **H6**)), 2.41 (s, 6H, (**H29**, **H38**)). $^{13}\text{C NMR}$ (126 MHz, CDCl_3) δ 143.75 (**C23**, **C32**), 138.52 (**C7**, **C13**), 136.83 (**C26**, **C35**), 129.75 (**C25**, **C27**, **C34**, **C36**), 128.78 (**C8**, **C12**, **C18**, **C14**), 128.25 (**C10**, **C16**), 127.29 (**C24**, **C28**, **C33**, **C37**), 126.71 (**C9**, **C11**, **C15**, **C17**), 58.33 (**C2**, **C5**), 47.72 (**C3**, **C6**), 21.68 (**C29**, **C38**). FTIR (cm^{-1}): 3032, 2890, 1522, 1349, 1159. HRMS-ESI (m/z): calculated for $\text{C}_{30}\text{H}_{30}\text{N}_2\text{O}_4\text{S}_2$ ($\text{M}+\text{H}$) $^+$: 547.1725, Found: 547.1742.



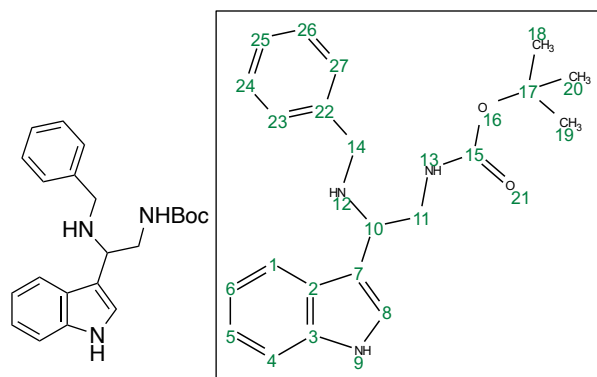
5-methyl-2-phenyl-4,5-dihydro-1*H*-imidazole (2-21)

Benzoyl cyanide (0.12 g, 1.0 mmol, 1.0 equiv), was dissolved in minimal DMF. Methyl diamine (0.9 mL, 1.0 mmol, 1.0 equiv) was then added, followed by DBU (0.015 mL, 0.1 mmol, 0.1 equiv). This was then placed in a pre-heated oil bath and was stirred at 40°C under N₂ for 4 hours. After 4 hours, the reaction was allowed to cool to 20°C, was extracted with ethyl acetate (3x20 mL), and concentrated in vacuo. The crude residue was then purified via silica gel flash column chromatography (EtOAc/Hexanes) to yield this side product as white solid. (0.10 g, 65%). **Mp:** 102-103°C. **¹H NMR** (500 MHz, CDCl₃) Mixture of tautomers δ 7.83 – 7.77 (m, 2H, (**H1**, **H3**)), 7.52 – 7.44 (m, 1H, (**H5**)), 7.44 – 7.37 (m, 2H, (**H4**, **H6**)), 7.36 – 7.28 (m, 1H, (**H11** or **H8**)), 7.10 – 7.05 (m, 1H, (**H11** or **H8**)), 4.46 – 4.34 (m, 1H, (**H10**)), 3.76 – 3.66 (m, 1H, (**H9**)), 3.53 – 3.44 (m, 1H, (**H9**)), 1.32 (d, *J* = 6.7 Hz, 3H, (**H12**)). **¹³C NMR** (126 MHz, CDCl₃) Mixture of tautomers δ 168.94 (**C7**) and 168.35 (**C7**), 134.16 (**C2**) and 134.02 (**C2**), 131.76 (**C5**) and 131.72 (**C5**), 128.73 (**C4**, **C6**) and 128.71 (**C4**, **C6**), 127.16 (**C1**, **C3**) and 127.15 (**C1**, **C3**), 47.41 (**C10**), 46.75 (**C9**), 18.58 (**C12**). **FTIR (cm⁻¹):** 3385, 3071, 2983, 1637, 1542. **HRMS-ESI (m/z):** calculated for C₁₀H₁₂N₂ (M+H)⁺: 161.1073, Found: 161.1082.



tert-butyl (2-oxoethyl)carbamate (2-22)

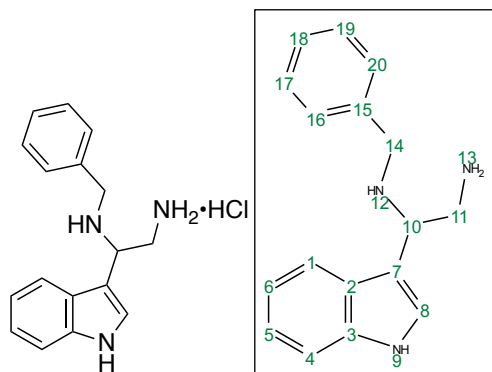
In a round-bottom flask *tert*-butyl (2,3-dihydroxypropyl)carbamate (1.0 g, 5.2 mmol, 1.0 equiv) was dissolved in DI water at room temperature under an atmosphere of N₂ gas. The flask was then covered in aluminum foil to protect the reaction mixture from light. Then, NaIO₄ (1.3 g, 6.2 mmol, 1.2 equiv) was added at room temperature under an atmosphere of N₂ gas. This mixture was allowed to stir for 1 hour under N₂ gas, covered in aluminum foil. After 1 hour, a white precipitate had formed. This white precipitate was then filtered out by filtration via a buchner funnel. The filtrate was then extracted with DCM (3x30 mL), dried over Na₂SO₄, and concentrated in vacuo to afford the desired product as a yellow oil, which afforded a white crystalline solid upon recrystallization in the freezer. (0.66 g, 80%). **Mp:** 37-38°C. **¹H NMR** (500 MHz, CDCl₃) δ 9.65 (s, 1H, (**H3**)), 5.20 (s, 1H, (**H1**)), 4.07 (d, *J* = 4.8 Hz, 2H, (**H2**)), 1.45 (s, 9H, (**H9, H10, H11**)). **¹³C NMR** (126 MHz, CDCl₃) δ 197.81 (**C3**), 155.90 (**C5**), 80.17 (**C8**), 51.28 (**C2**), 28.27 (**C9, C10, C11**). **FTIR (cm⁻¹):** 3321, 2981, 2878, 1738, 1685, 1523, 1252. **HRMS-ESI (m/z):** calculated for C₇H₁₃NO₃ (M+H)⁺: 160.0974, Found: 160.0998.



tert-butyl (2-(benzylamino)-2-(1H-indol-3-yl)ethyl)carbamate (2-23)

Indole (0.70g, 6.0 mmol, 2.0 equiv), benzyl amine (0.33 mL, 3.0 mmol, 1.0 equiv), N-Boc Glycinal (0.48 g, 3.0 mmol, 1.0 equiv), and 1,1,3,3-tetramethyl guanidine (0.033 mL, 0.3 mmol, 0.1 equiv) were added sequentially to DI H₂O (8 mL) at 20°C. The reaction mixture was then added to a pre-heated oil bath (45°C). The reaction was then stirred for 12 hours at 45°C under an atmosphere of N₂ gas. After completion of the reaction, the reaction mixture was diluted with EtOAc (50 mL) and water (20 mL). The organic layer was then extracted with EtOAc (3x30 mL), dried over Na₂SO₄, filtered, and concentrated in vacuo. The crude residue was then purified via silica gel flash column chromatography (EtOAc/Hexanes) to yield the desired product as an orange-brown oil. (0.42 g, 50%). ¹H NMR (500 MHz, CDCl₃) δ 7.67 (d, *J* = 7.8 Hz, 1H, (**H1**)), 7.40 (d, *J* = 8.1 Hz, 1H, (**H4**)), 7.36 – 7.17 (m, 7H, (**H5**, **H8**, **H22**, **H23**, **H24**, **H25**, **H26**)), 7.14 (t, *J* = 7.3 Hz, 1H, (**H6**)), 5.31 – 5.25 (m, 1H, (**H10**)), 4.63 (s, 1H, (**H13**)), 3.73 – 3.66 (m, 1H, (**H11**)), 3.64 (d, *J* = 13.1 Hz, 1H, (**H14**)), 3.54 (d, *J* = 13.3 Hz, 1H, (**H14**)), 3.49 – 3.38 (m, 1H, (**H11**)), 2.24 (s, 1H, (**H12**)), 1.41 (s, 9H, (**H18**, **H19**, **H20**)). ¹³C NMR (126 MHz, CDCl₃) δ 156.22 (**C15**), 139.34 (**C22**), 136.16 (**C3**), 129.16 (**C2**), 128.57 (**C23**, **C27**), 128.32 (**C24**, **C26**), 127.34 (**C25**), 124.27 (**C8**), 121.83 (**C5**), 121.17 (**C1**), 119.91 (**C6**), 109.97 (**C4**), 102.64, (**C7**), 79.90, (**C17**), 69.71 (**C10**), 49.83 (**C14**), 45.36 (**C11**), 28.42 (**C18**, **C19**, **C20**). FTIR (cm⁻¹):

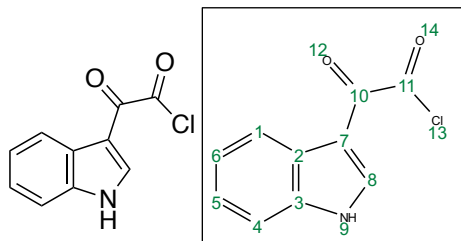
3413, 3341, 3313, 3054, 2886, 1690, 1508, 1245. **HRMS-ESI (m/z)**, calculated for C₂₂H₂₇N₃O₂ (M+H)⁺: 366.2181, Found: 366.2199.



1-(1*H*-indol-3-yl)ethane- N-Benzyl-1,2-diamine hydrochloride (2-24)

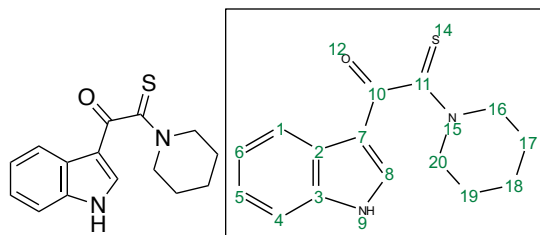
To an oven-dried flask was added tert-butyl (2-(benzylamino)-2-(1*H*-indol-3-yl)ethyl)carbamate (0.26 g, 1.0 mmol, 1.0 equiv) and ethanolic HCl (3.3M in EtOH, 5.0 mL). This was stirred at 20°C under an atmosphere of N₂ gas for 18 hours. After completion, as indicated by TLC, the reaction mixture was concentrated in vacuo to obtain a semi-solid. This semi-solid was triturated with Et₂O (5.0 mL) and concentrated in vacuo to afford the crude product as a reddish-brown crystalline foam. This was used in subsequent steps without any further purification (>99% determined by NMR, quantitative). ¹H NMR (500 MHz, CD₃OD) δ 7.80 (s, 1H, (**H8**)), 7.78 (d, *J* = 7.9 Hz, 1H, (**H1**)), 7.53 (d, *J* = 8.2 Hz, 1H, (**H4**)), 7.51 – 7.36 (m, 5H, (**H16**, **H17**, **H18**, **H19**, **H20**)), 7.27 (t, *J* = 7.7 Hz, 1H, (**H5**)), 7.20 (t, *J* = 7.6 Hz, 1H, (**H6**)), 5.12 (dd, *J* = 10.1, 5.1 Hz, 1H, (**H10**)), 4.27 (d, *J* = 12.9 Hz, 1H, (**H14**)), 3.96 (d, *J* = 12.9 Hz, 1H, (**H14**)), 3.90 – 3.78 (m, 2H, (**H11**)). ¹³C NMR (126 MHz, CD₃OD) δ 138.24 (**C3**), 132.02 (**C15**), 131.12 (**C16**, **C20**), 130.57 (**C18**), 130.11 (**C17**, **C19**), 128.10 (**C8**), 127.54 (**C2**), 123.94 (**C5**), 121.66 (**C6**), 118.95 (**C1**), 113.30 (**C4**), 104.22 (**C7**), 53.63 (**C10**), 50.59 (**C11**), 41.54 (**C14**). FTIR (cm⁻¹): 3412,

3345, 3299, 3012, 2892, 1552. **HRMS-ESI (m/z)**, calculated for C₁₇H₁₉N₃ (M+H)⁺: 266.1657, Found: 266.1681.



2-(1*H*-indol-3-yl)-2-oxoacetyl chloride (2-29)

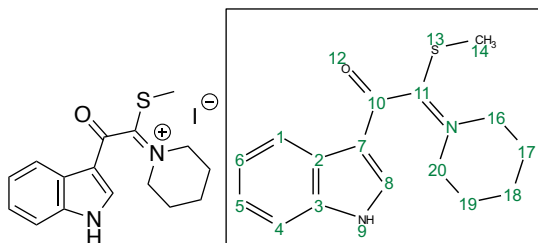
To an oven-dried flask, charged with N₂ gas, was added 1*H*-indole (0.5 g, 4.3 mmol, 1.0 equiv). This was dissolved in anhydrous Et₂O (10 mL). This solution was cooled to 0°C and switched to an atmosphere of Argon gas. After 3 hours, the reaction was warmed to 20°C and stirred an additional 1 hour. The resulting yellow precipitate was isolated by vacuum filtration, via a Buchner funnel, and was washed with minimal Et₂O. The resulting yellow solid was dried on vacuum overnight to afford the desired product as a yellow crystalline solid (0.77 g, 87%). **Mp:** 128-130°C. **¹H NMR** (500 MHz, DMSO) δ 12.39 (s, 1H, (**H9**)), 8.42 (d, *J* = 3.3 Hz, 1H, (**H8**)), 8.17 (d, *J* = 7.0 Hz, 1H, (**H1**)), 7.54 (d, *J* = 7.1 Hz, 1H, (**H4**)), 7.29 (ddd, *J* = 7.2, 5.7, 1.6 Hz, 1H, (**H5**)), 7.26 (ddd, *J* = 7.1, 5.4, 1.5 Hz, 1H, (**H6**)). **¹³C NMR** (126 MHz, DMSO) δ 180.89 (**C10**), 165.37 (**C11**), 138.19 (**C8**), 136.87 (**C3**), 125.75 (**C2**), 123.87 (**C5**), 122.89 (**C6**), 121.30 (**C1**), 112.89 (**C4**), 112.47 (**C7**). **FTIR (cm⁻¹):** 3405, 3015, 2869, 1771, 1702, 1511. **HRMS-ESI (m/z)**, calculated for C₁₀H₆ClNO₂ (M+H)⁺: 208.0165, 210.0138, Found: 208.0180, 210.0153.



1-(1*H*-indol-3-yl)-2-(piperidin-1-yl)-2-thioxoethan-1-one (2-31)

2-(1*H*-indol-3-yl)-2-oxoacetyl chloride (0.21 g, 1.0 mmol, 1.0 equiv), was dissolved in anhydrous EtOAc (2.0 mL). To this was added a solution of *n*-Bu₃SnH (0.30 mL, 1.0 mmol, 1.0 equiv) in anhydrous EtOAc (1.0 mL) at 0°C under an atmosphere of N₂ gas. The reaction mixture was then stirred for 30 minutes at 0°C. The reaction was then allowed to warm to 20°C and was stirred for 16 hours at 20°C under N₂. After 16 hours, hexanes was added and the resulting yellow precipitate was washed with large amounts of hexanes and collected by vacuum filtration. This crude product was then dissolved in a minimal amount of piperidine. To this was added S₈ (0.33 g, 1.2 mmol, 1.2 equiv), followed by piperidine (0.15 mL, 1.5 mmol, 1.5 equiv) at 20°C under N₂. The reaction mixture was then warmed to 80°C and was stirred for 5 hours under N₂. After 5 hours, the reaction was allowed to cool to 20°C, then DI H₂O was added (15 mL). The organic layer was extracted with EtOAc (3x30 mL), the combined organic layers were then washed with brine (30 mL), dried over Na₂SO₄, filtered, and concentrated in vacuo. The crude residue was then purified via silica gel flash column chromatography (EtOAc/Hexanes) to yield the desired product as a brown oil. (0.14 g, 45% over 2 steps). ¹H NMR (500 MHz, CD₃OD) δ 8.17 (d, *J* = 7.1 Hz, 1H, **(H1)**), 8.01 (s, 1H, **(H8)**), 7.48 (d, *J* = 7.1, 2.0 Hz, 1H, **(H4)**), 7.27 (td, *J* = 7.3, 5.5, 1.4 Hz, 1H, **(H5)**), 7.24 (td, *J* = 7.2, 5.6, 1.3 Hz, 1H, **(H6)**), 4.27 – 4.21 (m, 2H, **(H16, H20)**), 3.62 – 3.55 (m, 2H, **(H16, H20)**), 1.81 – 1.68 (m, 4H, **(H17, H19)**), 1.58 – 1.54 (m, 2H, **(H18)**). ¹³C NMR (126 MHz, CD₃OD) δ 196.45 (**(C11)**), 187.66 (**(C10)**), 138.60 (**(C3)**), 137.44 (**(C8)**),

126.82 (C2), 124.83 (C5), 123.78 (C6), 122.49 (C1), 114.35 (C7), 113.30 (C4), 53.97 (C16, C20), 49.21 (C16, C20), 27.67 (C18), 26.39 (C17, C19), 25.04 (C17, C19). FTIR (cm⁻¹): 3437, 3065, 2873 1695, 1542, 1132. HRMS-ESI (m/z), calculated for C₁₅H₁₇N₂OS (M+H)⁺: 273.1062, Found: 273.1100, C₁₅H₁₇N₂OSNa (M+H)⁺: 296.0959, Found: 296.0972.

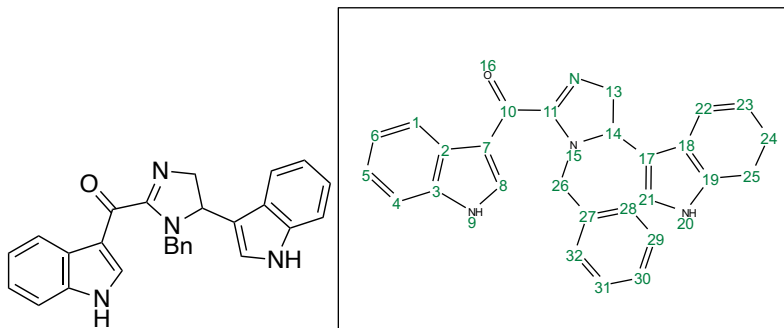


1-(2-(1*H*-indol-3-yl)-1-(methylthio)-2-oxoethylidene)piperidin-1-ium iodide (2-32)

1-(1*H*-indol-3-yl)-2-(piperidin-1-yl)-2-thioethan-1-one (0.13 g, 0.46 mmol, 1.0 equiv) was dissolved in iodomethane (1.3 mL, 9.2 mmol, 20.0 equiv) in an oven-dried flask under N₂ gas. This solution was refluxed for 5 hours under N₂. After completion of the reaction (indicated by TLC), the reaction mixture was allowed to cool to 20°C. Then, any excess iodomethane was evaporated in vacuo to afford the desired product as an off-white semi-solid (0.19 g, Quantitative). This was used in subsequent steps without any further purification. ¹H NMR (500 MHz, CD₃OD) δ 8.53 (s, 1H, (H8)), 8.27 (d, *J* = 7.0 Hz, 1H, (H1)), 7.60 (d, *J* = 7.1 Hz, 1H, (H4)), 7.41 (pd, *J* = 7.3, 7.2, 7.2, 7.1, 1.4 Hz, 2H, (H5, H6)), 4.26 – 4.18 (m, 1H, (H16, H20)), 4.16 – 4.09 (m, 1H, (H16 or H20)), 4.09 – 4.01 (m, 1H, (H16 or H20)), 3.94 – 3.85 (m, 1H, (H16 or H20)), 2.66 (s, 3H, (H14)), 2.15 – 2.09 (m, 1H, (H18)), 2.05 – 1.94 (m, 1H, (H18)), 1.92 – 1.77 (m, 4H, (H17, H19)). ¹³C NMR (126 MHz, CD₃OD) δ 186.03 (C10), 176.79 (C11), 140.23 (C8), 139.28 (C3), 126.52 (C5), 125.79 (C2), 125.35 (C6), 122.66 (C1), 114.32 (C7), 114.08 (C4), 58.68 (C20, C16), 55.78 (C20, C16), 28.15 (C17, C19), 26.77 (C18), 23.49 (C17,

C19), 16.77 (**C14**). **FTIR** (cm^{-1}): 3403, 3068, 2885, 1699, 1628, 1520. **HRMS-ESI** (m/z):

Calculated for $\text{C}_{16}\text{H}_{19}\text{NOS}^+$: 287.1218, Found: 287.1232.



(1-benzyl-5-(1H-indol-3-yl)-4,5-dihydro-1H-imidazol-2-yl)(1H-indol-3-yl)methanone (2-25)

Procedure A:

To a stirred solution of N^1 -benzyl-1-(1H-indol-3-yl)ethane-1,2-diamine hydrochloride (**2-24**) (150.7 mg, 0.5 mmol, 1 equiv) and the thioimidate fragment **2-32** (0.21 g, 0.5 mmol, 1.0 equiv) in anhydrous MeOH (3 mL) was added Amberlyst A-21 (0.35 g). This was allowed to stir at 20°C under N_2 for 36 hours. Then the MeOH was concentrated in vacuo and ethyl acetate (25 mL) and water (10 mL) were added. The organic layer was then extracted with EtOAc (3x25 mL), dried over Na_2SO_4 , filtered, and concentrated in vacuo. The crude residue was then purified via silica gel flash column chromatography (EtOAc/Hexanes) to yield the desired product as a tan-brown semi-solid. (0.067 g, 32%).

Procedure B:

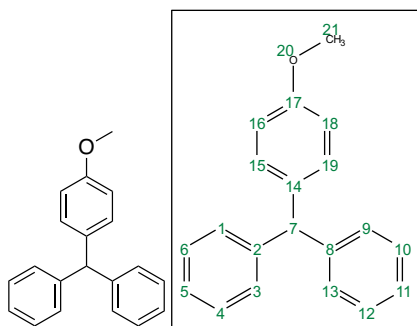
To a stirred solution of N^1 -benzyl-1-(1H-indol-3-yl)ethane-1,2-diamine hydrochloride (**2-24**) (0.15 g, 0.5 mmol, 1.0 equiv) and the thioimidate fragment **2-32** (0.21 g, 0.5 mmol, 1.0 equiv) in anhydrous MeOH (5.0 mL) was added triethylamine (0.18 mL, 2.5 equiv). This was allowed to stir at 20°C under N_2 for 48 hours. Then the MeOH was concentrated in vacuo and ethyl acetate

(25 mL) and water (10 mL) were added. The organic layer was then extracted with EtOAc (3x25 mL), dried over Na₂SO₄, filtered, and concentrated in vacuo. The crude residue was then purified via silica gel flash column chromatography (EtOAc/Hexanes) to yield the desired product as a tan-brown semi-solid. (0.11 g, 53%).

Procedure C:

To an oven-dried flask purged with N₂ gas was added I₂ (0.28 g, 1.1 mmol, 1.1 equiv). To this was added 1-(1*H*-indol-3-yl)ethan-1-one (0.16 g, 1.0 mmol, 1.0 equiv) dissolved in DMSO (2.5 mL) at 20°C under an atmosphere of N₂ gas. This reaction mixture was then heated to 100°C and was stirred for 2h. The resulting solution was then slowly cooled to 0°C and the reaction mixture was treated with NaHCO₃ (0.34 g, 4.0 mmol, 4.0 equiv). *N*¹-benzyl-1-(1*H*-indol-3-yl)ethane-1,2-diamine hydrochloride (**2-24**) (0.30 g, 1.0 mmol, 1.0 equiv) in MeCN/MeOH (1:1) (5.0 mL/5.0 mL) was also added and the reaction was allowed to stir for 1 hour at 0°C under N₂. After 1h, NCS (0.13 g, 1.0 mmol, 1.0 equiv) was added at 0°C and the reaction was allowed to stir for 20 minutes at 0°C. Then, the reaction mixture was allowed to warm to room temperature and was stirred for an additional 12 hours at 20°C under N₂ gas. The solvent was then removed in vacuo and the crude residue was dissolved in chloroform (30 mL). This solution was then washed with saturated aqueous, NaHCO₃ (50 mL), saturated aqueous Na₂S₂O₃ (50 mL) and ice cold saturated aqueous NaCl (3x50mL). The organic layer was then dried over Na₂SO₄, filtered, and concentrated in vacuo. The crude residue was then purified via silica gel flash column chromatography (EtOAc/Hexanes) to yield the desired product as a tan-brown semi-solid. (0.19 g, 45%). ¹H NMR (500 MHz, CD₃OD) δ 8.33 (d, *J* = 6.6 Hz, 1H, (**H1**)), 8.31 (s, 1H, (**H8**)), 7.65 (d, *J* = 6.9 Hz, 1H, (**H22**)), 7.50 (d, *J* = 6.5, Hz, 1H, (**H4**)), 7.42 (d, *J* = 8.2 Hz, 1H, (**H25**)), 7.32 – 7.26 (m, 2H, (**H5**, **H6**)), 7.21 – 7.13 (m, 5H, (**H21**, **H24**, **H28**, **H30**, **H32**)), 7.15 – 7.00 (m, 3H,

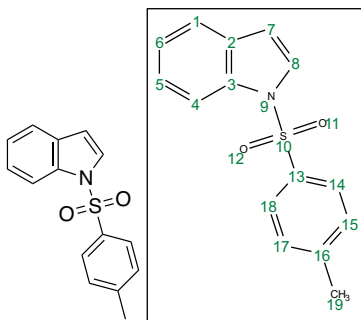
(**H23, H29, H31**)), 5.04 (dd, $J = 11.8, 9.5$ Hz, 1H, (**H14**)), 4.66 (d, $J = 15.6$ Hz, 1H, (**H26**)), 4.29 (dd, $J = 14.7, 11.9$ Hz, 1H, (**H13**)), 4.03 (dd, $J = 14.7, 9.5$ Hz, 1H, (**H13**)), 3.90 (d, $J = 15.6$ Hz, 1H, (**H26**)). ^{13}C NMR (126 MHz, CD_3OD) δ 184.12 (**C10**), 164.16 (**C11**), 139.42 (**C8**), 138.99 (**C19**), 138.67 (**C3**), 138.30 (**C27**), 129.42 (**C29, C31**), 129.28 (**C28, C32**), 128.40 (**C30**), 127.01 (**C2**), 126.63 (**C18**), 125.52 (**C21**), 125.13 (**C5**), 124.07 (**C6**), 122.98 (**C1**), 122.93 (**C24**), 120.32 (**C23**), 120.11 (**C22**), 117.17 (**C7**), 114.38 (**C17**), 113.28 (**C4**), 112.88 (**C25**), 60.77 (**C13**), 58.78 (**C14**), 48.23 (**C26**). FTIR (cm^{-1}): 3405, 3399, 3052, 2877, 1709, 1637, 1536. HRMS-ESI (m/z): Calculated for $\text{C}_{27}\text{H}_{22}\text{N}_4\text{O}$ ($\text{M}+\text{H}$) $^+$: 419.1872, Found: 419.1891.



((4-methoxyphenyl)methylene)dibenzene (2-37)

To a flame-dried r.b. flask was added anisole (1 mL, 18.4 mmol, 10 equiv). To this was added FeCl_3 (11.0 mg, 0.07 mmol, 0.04 equiv), followed by benzophenone (0.32 g, 1.8 mmol, 1.0 equiv) at room temperature, under an atmosphere of N_2 gas. Next Me_3SiCl (0.25 mL, 1.9 mmol, 1.1 equiv) was added to the mixture, which dissolved the FeCl_3 . Then, Et_3SiH (0.30 mL, 1.9 mmol, 1.05 equiv) was diluted to a total volume of 1 mL with anisole. This was then added dropwise (0.1 mL/ 5 min). The resulting solution was then stirred for 2 hours at room temperature under an atmosphere of N_2 gas. Then, the reaction mixture was heated to 50°C until full conversion was observed via TLC (~1 hour). After completion, the solution was allowed to

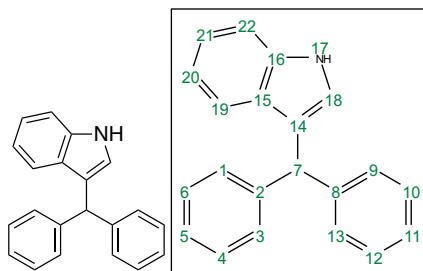
cool to room temperature and the solution was then diluted with EtOAc (30 mL) and washed with aqueous sodium bicarbonate solution (2x 3 mL), extracted with EtOAc (3 x 30 mL), dried over Na₂SO₄, filtered, and concentrated in vacuo the crude residue was then purified via silica gel flash column chromatography (EtOAc/Hexanes) to yield the desired product as a clear, colorless oil. (0.44 g, 91% [98:2 para:ortho]). ¹H NMR (500 MHz, CDCl₃) δ 7.29 (t, *J* = 7.5 Hz, 4H, (**H4**, **H6**, **H8**, **H12**)), 7.21 (t, *J* = 7.2 Hz, 2H, (**H5**, **H13**)), 7.12 (d, *J* = 7.7 Hz, 4H, (**H1**, **H3**, **H9**, **H13**)), 7.04 (d, *J* = 8.5 Hz, 2H, (**H15**, **H19**)), 6.84 (d, *J* = 8.8 Hz, 2H, (**H16**, **H18**)), 5.52 (s, 1H, (**H7**)), 3.79 (s, 3H, (**H21**)). ¹³C NMR (126 MHz, CDCl₃) δ 158.13, (**C17**), 144.37, (**C2**, **C8**), 136.21, (**C14**), 130.49, (**C15**, **C19**), 129.50, (**C1**, **C3**, **C9**, **C13**), 128.40, (**C4**, **C6**, **C10**, **C12**), 126.35, (**C5**, **C11**), 113.77, (**C16**, **C18**), 56.12, (**C7**), 55.35, (**C21**). FTIR (cm⁻¹): 3083, 3061, 2954, 1564, 1250, 1041. HRMS-ESI (*m/z*): Calculated for C₂₀H₁₈O (M+H)⁺: 275.1436, Found: 275.1447.



1-tosyl-1*H*-indole (2-38)

To an oven-dried flask, charged with N₂ gas, was added anhydrous THF (20mL). Then, 60% NaH solution in mineral oil (0.3 g, 7.5 mmol, 2.5 equiv) was added and this mixture was cooled to 0°C. Next, a solution of 1*H*-indole (0.35 g, 3.0 mmol, 1.0 equiv) in anhydrous THF (10 mL) was added dropwise at 0°C under an atmosphere of N₂ gas. This gray reaction mixture was

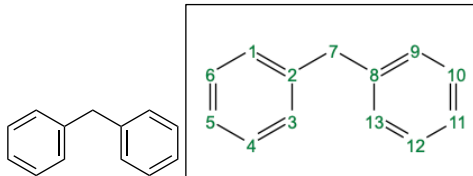
allowed to stir for 20 minutes at 0°C under N₂. After 20 minutes, tosyl-chloride (0.92 g, 4.8 mmol, 1.6 equiv) was added at 0°C, resulting in an immediate gray-blue color change. The reaction mixture was allowed to warm to 20°C and was stirred for 12 hours. When TLC showed complete consumption of starting material, the reaction was quenched slowly with deionized water (3mL) dropwise. The reaction mixture was then extracted with EtOAc (3x40mL). The combined organic layers were then dried over Na₂SO₄, filtered, and concentrated in vacuo. The crude product was purified via silica gel flash column chromatography (EtOAc/Hexanes) to yield the desired product as a clear, colorless oil (0.82 g, Quantitative). ¹H NMR (500 MHz, CDCl₃) δ 7.84 (s, 1H, **(H17)**), 7.40 – 7.26 (m, 12H, **(H1, H3, H4, H5, H6, H9, H10, H11, H12, H13, H19, H22)**), 7.23 (t, *J* = 7.4 Hz, 1H, **(H21)**), 7.06 (t, *J* = 7.5 Hz, 1H, **(H20)**), 6.56 (d, *J* = 1.4 Hz, 1H, **(H18)**), 5.75 (s, 1H, **(H7)**). ¹³C NMR (126 MHz, CDCl₃) δ 145.02, **(C16)**, 135.34, **(C13)**, 134.89, **(C3)**, 130.83, **(C2)**, 129.95, **(C15, C17)**, 126.88, **(C14, C18)**, 126.42, **(C8)**, 124.63, **(C5)**, 123.36, **(C6)**, 121.46, **(C4)**, 113.61, **(C1)**, 109.12, **(C7)**, 21.62, **(C19)**. FTIR (cm⁻¹): 3100, 3067, 3047, 2917, 1582, 1355, 1156. HRMS-ESI (*m/z*): Calculated for C₁₅H₁₃NO₂S (M+H)⁺: 272.0745, Found: 272.0766.



3-benzhydryl-1H-indole (2-39)

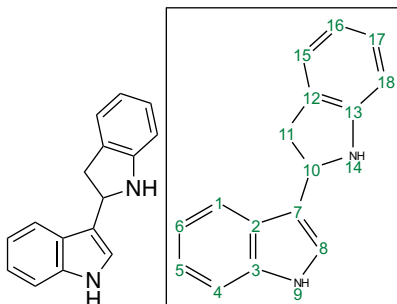
To an oven-dried round-bottom flask was added FeCl₃ (16 mg, 0.10 mmol, 0.1 equiv) at room temperature under an atmosphere of nitrogen gas. Next, benzophenone (0.18 g, 1.0 mmol, 1.0 equiv) was added in 0.5 mL NO₂Me, followed by Me₃SiCl (0.14 mL, 1.1 mmol, 1.1 equiv). Then, Et₃SiH (0.17 mL, 1.05 mmol, 1.05 equiv) (diluted to 1.0 mL with NO₂Me) dropwise and in increments of 0.1 mL every 5 minutes. Lastly, indole (0.23 g, 2.0 mmol, 2.0 equiv) was added dropwise in minimal NO₂Me at -15°C. The resulting solution was allowed to stir at -15°C for 2 hours and then was allowed to warm to room temperature and was stirred for another 12 hours at rt under an atmosphere of nitrogen gas. The reaction mixture was then concentrated in vacuo and the resulting crude residue was purified via silica gel flash column chromatography (EtOAc/Hexanes) to afford the desired product as an off-white crystalline solid (54 mg, 17%).

Mp: 118-120°C. **¹H NMR** (500 MHz, CDCl₃) δ 7.84 (s, 1H, (**H17**)), 7.40 – 7.26 (m, 12H, (**H1**, **H3**, **H4**, **H5**, **H6**, **H9**, **H10**, **H11**, **H12**, **H13**, **H19**, **H22**)), 7.23 (t, *J* = 7.4 Hz, 1H, (**H21**)), 7.06 (t, *J* = 7.5 Hz, 1H, (**H20**)), 6.56 (d, *J* = 1.4 Hz, 1H, (**H18**)), 5.75 (s, 1H, (**H7**)). **¹³C NMR** (126 MHz, CDCl₃) δ 144.04 (**C2**, **C8**), 136.75 (**C16**), 129.11 (**C1**, **C3**, **C9**, **C13**), 128.39 (**C4**, **C6**, **C10**, **C12**), 127.05 (**C15**), 126.34 (**C5**, **C11**), 124.19 (**C18**), 122.18 (**C21**), 120.00 (**C19**), 119.90 (**C14**), 119.48 (**C20**), 111.18 (**C22**), 48.90 (**C7**). **FTIR (cm⁻¹):** 3456, 3083, 2926, 1592. **HRMS-ESI (m/z):** Calculated for C₂₁H₁₇N (M+H)⁺: 284.1403, Found: 284.1425.



Diphenyl methane (2-41)

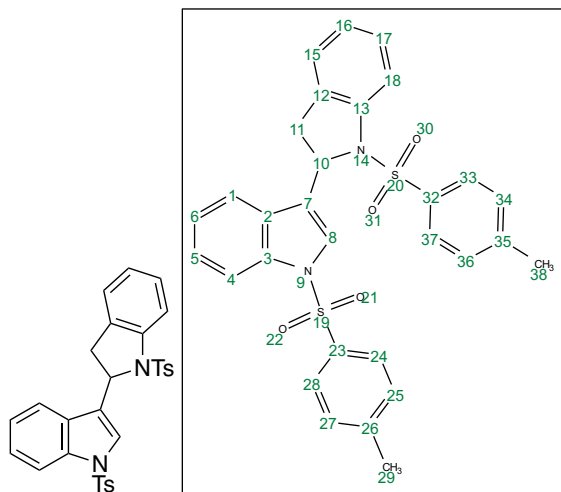
This side product was isolated as a clear, colorless oil. $^1\text{H NMR}$ (500 MHz, CDCl_3) δ 7.46 – 7.37 (m, 1H, (**H4**, **H6**, **H10**, **H12**)), 7.35 – 7.29 (m, 1H, (**H1**, **H3**, **H5**, **H9**, **H11**)), 4.11 (s, 1H, (**H7**)). $^{13}\text{C NMR}$ (126 MHz, CDCl_3) δ 141.24 (**C2**, **C8**), 129.06 (**C4**, **C6**, **C10**, **C12**), 128.57 (**C1**, **C3**, **C9**, **C13**), 126.18 (**C5**, **C11**), 42.08 (**C7**). **FTIR** (cm^{-1}): 3059, 2836, 1512. **GC-MS**: Product mass identified via GC-MS (See Appendix (2-41)).



3-(indolin-2-yl)-1H-indole (2-42)

This side Product was isolated as a light purple-brown colored semi-solid. $^1\text{H NMR}$ (500 MHz, CDCl_3) δ 7.99 (s, 1H, (**H14**)), 7.62 (d, $J = 7.9$ Hz, 1H, (**H1**)), 7.34 (d, $J = 8.0$ Hz, 1H, (**H4**)), 7.24 (t, $J = 7.6$ Hz, 1H, (**H5**)), 7.20 (d, $J = 7.4$ Hz, 1H, (**H15**)), 7.15 – 7.09 (m, 3H, (**H6**, **H8**, **H17**)), 6.81 (t, $J = 7.4$ Hz, 1H, (**H16**)), 6.70 (d, $J = 7.7$ Hz, 1H, (**H18**)), 5.26 (t, $J = 8.7$ Hz, 1H, (**H10**)), 3.50 (dd, $J = 15.6, 9.1$ Hz, 1H, (**H11**)), 3.24 (dd, $J = 15.6, 8.3$ Hz, 1H, (**H11**)). $^{13}\text{C NMR}$

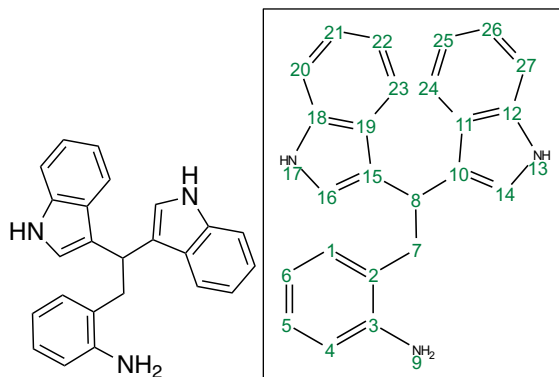
(126 MHz, CDCl₃) δ 150.99, (C13), 136.81, (C3), 129.05, (C12), 127.56, (C17), 125.84, (C2), 124.80, (C15), 122.36, (C5), 121.32, (C8), 119.66, (C6), 119.55, (C1), 119.33, (C7), 118.90, (C16), 111.45, (C4), 109.39, (C18), 56.42, (C10), 37.70, (C11). FTIR (cm⁻¹): 3452, 3383, 3082, 2869, 1540. HRMS-ESI (m/z): Calculated for C₁₆H₁₄N₂ (M+H)⁺: 235.1235, Found: 235.1253.



1-tosyl-3-(1-tosylindolin-2-yl)-1H-indole (2-43)

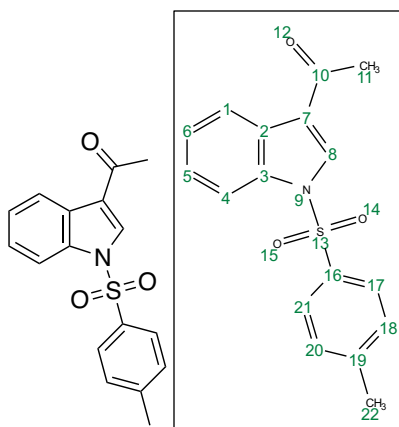
This side Product was isolated as a pinkish off-white semi-solid. ¹H NMR (500 MHz, CDCl₃) δ 7.88 (d, *J* = 8.4 Hz, 1H, (H1)), 7.76 – 7.71 (m, 3H, (H4, H24, H28)), 7.58 (s, 1H, (H8)), 7.45 (d, *J* = 8.3 Hz, 2H, (H33, H37)), 7.32 – 7.22 (m, 3H, (H5, H17, H18)), 7.20 (d, *J* = 8.1 Hz, 2H, (H25, H27)), 7.15 (d, *J* = 7.8 Hz, 1H, (H15)), 7.09 – 7.05 (m, 2H, (H6, H16)), 7.02 (d, *J* = 8.2 Hz, 2H, (H34, H36)), 5.53 (dd, *J* = 10.1, 3.1 Hz, 1H, (H10)), 3.23 (dd, *J* = 16.1, 10.1 Hz, 1H, (H11)), 2.95 (dd, *J* = 16.2, 3.2 Hz, 1H, (H11)), 2.32 (s, 3H, (H29)), 2.30 (s, 3H, (H38)). ¹³C NMR (126 MHz, CDCl₃) δ 144.97, (C26), 143.86, (C35), 141.56, (C13), 135.60, (C3), 135.07, (C32), 135.01, (C23), 131.24, (C2), 129.91, (C25, C27), 129.42, (C34, C36), 128.80, (C12), 128.14, (C5), 126.93, (C33, C37), 126.91, (C24, C28), 125.07, (C17), 124.75, (C6), 124.69,

(C18), 124.40, (C8), 123.34, (C7), 123.20, (C16), 119.95, (C15), 116.85, (C4), 113.77, (C1), 58.57, (C10), 35.68, (C11), 21.58, (C29), 21.49, (C38). FTIR (cm⁻¹): 3072, 2926, 1526, 1362, 1345, 1174, 1157. HRMS-ESI (m/z): Calculated for C₃₀H₃₆N₂O₄S₂ (M+H)⁺: 543.1412, Found: 543.1435.



2-(2,2-di(1H-indol-3-yl)ethyl)aniline (2-44)

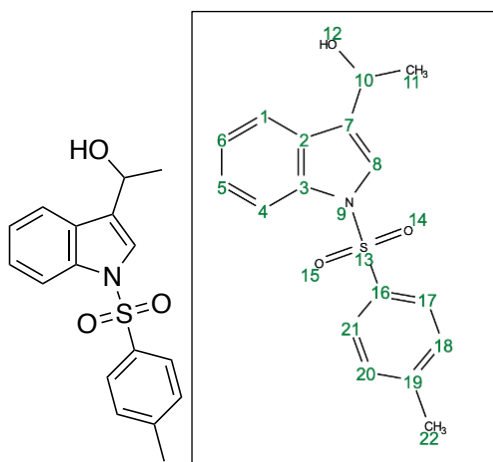
This side product was isolated as a brown semi-solid. ¹H NMR (500 MHz, CDCl₃) δ 7.89 (s, 2H, (H9)), 7.48 (d, *J* = 7.9 Hz, 2H, (H23, H24)), 7.28 (d, *J* = 8.0 Hz, 2H, (H20, H27)), 7.14 (td, *J* = 7.8, 7.5, 1.0 Hz, 2H, (H21, H26)), 7.03 – 6.94 (m, 4H, (H1, H5, H22, H25)), 6.92 (d, *J* = 1.5 Hz, 2H, (H14, H16)), 6.63 (td, *J* = 7.5, 7.4, 1.2 Hz, 1H, (H6)), 6.55 (d, *J* = 7.3 Hz, 1H, (H4)), 4.85 (t, *J* = 7.3 Hz, 1H, (H8)), 3.41 (d, *J* = 7.3 Hz, 1H, (H7)). ¹³C NMR (126 MHz, CDCl₃) δ 144.78, (C3), 136.64, (C12, C18), 130.42, (C1), 126.96, (C5), 126.10, (C2), 122.01, (C14, C16), 121.90, (C21, C26), 119.71, (C23, C24), 119.59, (C11, C19) 119.19, (C22, C25), 118.87, (C4), 115.81, (C6), 111.20, (C20, C27), 111.15, (C10, C15), 37.18, (C7), 34.48, (C8). FTIR (cm⁻¹): 3438, 3315, 3056, 2884, 1512. HRMS-ESI (m/z): Calculated for C₂₄H₂₁N₃ (M+H)⁺: 352.1814, Found: 352.1835.



1-(1-tosyl-1*H*-indol-3-yl)ethan-1-one (2-47)

To an oven-dried flask, charged with N₂ gas, was added anhydrous THF (20mL). Then, 60% NaH solution in mineral oil (0.10 g, 2.5 mmol, 2.5 equiv) was added and this mixture was cooled to 0°C. Next, a solution of 1-(1*H*-indol-3-yl)ethan-1-one (0.16 g, 1.0 mmol, 1.0 equiv) in anhydrous THF (10mL) was added dropwise at 0°C under an atmosphere of N₂ gas. This gray reaction mixture was allowed to stir for 20 minutes at 0°C under N₂. After 20 minutes, Tosyl Chloride (0.31 g, 1.6 mmol, 1.6 equiv) was added at 0°C. The reaction mixture was allowed to warm to 20°C and was stirred for 12 hours. When TLC showed complete consumption of starting material, the reaction was quenched dropwise with deionized water (3mL) dropwise until bubbles subsided and the reaction mixture became clear. This reaction mixture was then extracted with EtOAc (3x30mL). The combined organic layers were then dried over Na₂SO₄, filtered, and concentrated in vacuo. The crude product was purified via silica gel flash column chromatography (EtOAc/Hexanes) to yield the desired product as a white solid (0.31 g, Quantitative). **M.p.:** 150-151°C. ¹H NMR (500 MHz, CDCl₃) δ 8.33 (d, *J* = 7.5 Hz, 1H, (**H1**)), 8.21 (s, 1H, (**H8**)), 7.92 (d, *J* = 8.1 Hz, 1H, (**H4**)), 7.84 (d, *J* = 8.5 Hz, 2H, (**H17**, **H21**)), 7.37 (td, *J* = 8.0, 7.3, 1.4 Hz, 1H, (**H5**)), 7.33 (td, *J* = 7.7, 1.2 Hz, 1H, (**H6**)), 7.28 (d, *J* = 8.1 Hz, 2H,

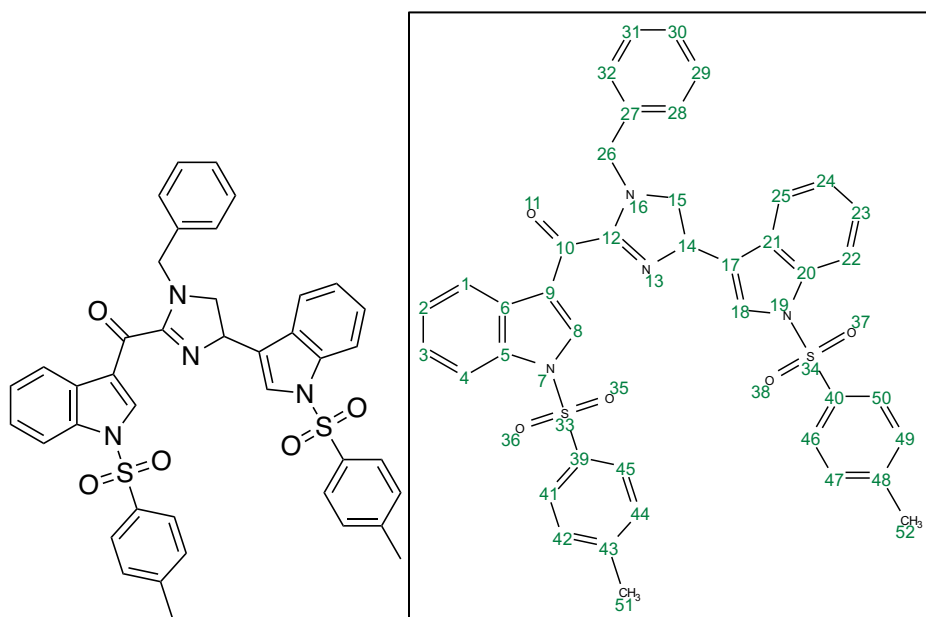
(**H18**, **H20**)), 2.57 (s, 3H, (**H11**)), 2.36 (s, 3H, (**H22**)). ^{13}C NMR (126 MHz, CDCl_3) δ 193.61, (**C10**), 146.07, (**C19**), 135.00, (**C3**), 134.61, (**C16**), 132.33, (**C8**), 130.37, (**C18**, **C20**), 127.63, (**C2**), 127.27, (**C17**, **C21**), 125.86, (**C5**), 124.95, (**C6**), 123.24, (**C1**), 121.70, (**C7**), 113.16, (**C4**), 27.93, (**C22**), 21.78, (**C11**). FTIR (cm^{-1}): 3060, 2853, 1692, 1564, 1346, 1157. HRMS-ESI (m/z): Calculated for $\text{C}_{17}\text{H}_{15}\text{NO}_3\text{S}$ ($\text{M}+\text{H}$) $^+$: 314.0851, Found: 314.0881.



1-(1-(1-tosyl-1*H*-indol-3-yl)ethan-1-yl)ethan-1-ol (2-48)

To an oven-dried flask charged with N_2 gas was added 1-(1-(1-tosyl-1*H*-indol-3-yl)ethan-1-yl)ethan-1-ol (0.16 g, 0.5 mmol, 1.0 equiv) in MeOH (5.0 mL). At 20°C, under an atmosphere of N_2 gas, was then added NaBH_4 (18.9 mg, 0.5 mmol, 1.0 equiv). This reaction mixture was then allowed to stir for 3 hours at 20°C under an atmosphere of N_2 gas. Once the reaction had reached complete conversion as indicated by TLC, the solvent was removed in vacuo. The crude residue was then dissolved in EtOAc (25 mL) and water (20 mL), extracted with EtOAc (3x25 mL), dried over Na_2SO_4 , filtered, and concentrated in vacuo. The resulting crude residue was then purified via silica gel flash column chromatography (EtOAc/Hexanes) to yield the desired product as a white solid (0.15 g, 94%). **M.p.:** 113-115°C. ^1H NMR (500 MHz, CDCl_3) δ 7.97 (d, $J = 8.3$ Hz, 1H,

(**H1**)), 7.76 (d, $J = 8.4$ Hz, 2H, (**H17**, **H21**)), 7.65 (d, $J = 7.8$ Hz, 1H, (**H4**)), 7.50 (s, 1H, (**H8**)), 7.32 (t, $J = 7.8$ Hz, 1H, (**H5**)), 7.27 – 7.19 (m, 3H, (**H6**, **H18**, **H20**)), 5.12 (q, $J = 12.9, 6.4$ Hz, 1H, (**H10**)), 2.33 (s, 3H, (**H22**)), 1.61 (d, $J = 6.5$ Hz, 3H, (**H11**)). ^{13}C NMR (126 MHz, CDCl_3) δ 145.10, (**C19**), 135.63, (**C3**), 135.33, (**C16**), 130.02, (**C18**, **C20**), 129.04, (**C2**), 127.14, (**C7**), 126.96, (**C17**, **C21**), 124.95, (**C5**), 123.27, (**C6**), 122.20, (**C8**), 120.50, (**C4**), 113.83, (**C1**), 63.97, (**C10**), 23.56, (**C22**), 21.69, (**C11**). FTIR (cm^{-1}): 3321, 3191, 2905, 1574, 1348, 1201, 1166. HRMS-ESI (m/z): Calculated for $\text{C}_{17}\text{H}_{17}\text{NO}_3\text{S}$ ($\text{M}+\text{H}$) $^+$: 316.1007, Found: 316.1027.



(1-benzyl-4-(1-tosyl-1H-indol-3-yl)-4,5-dihydro-1H-imidazol-2-yl)(1-tosyl-1H-indol-3-yl)methanone (2-50)

To an oven-dried flask was added anhydrous THF (5 mL). This was then cooled to 0°C and NaH (42 mg (60% in mineral oil), 3.5 equiv) was added. Then, the imidazoline intermediate (0.13 g, 1.0 equiv) was added dropwise in THF (5 mL) at 0°C under an atmosphere of N_2 gas. This mixture was then allowed to stir for 1 hour at 0°C . After 1 hr, TsCl (0.17 g, 3.0 equiv.) was

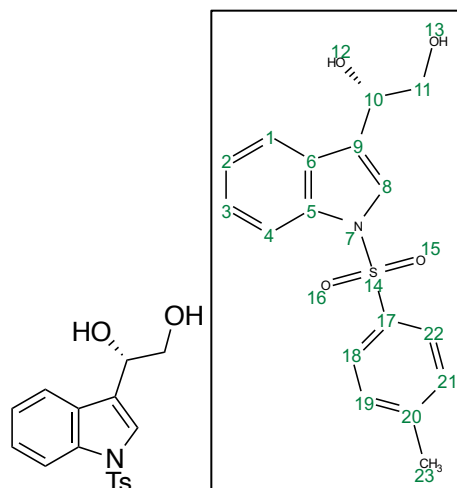
added and the reaction was allowed to warm to room temperature and was stirred overnight under an atmosphere of N₂ gas. After the reaction had reached complete conversion, as indicated by TLC, it was slowly (dropwise) quenched with DI water. The reaction was then extracted with ethyl acetate (3 X 25mL), the organic layer was dried over Na₂SO₄, filtered, and concentrated in vacuo. The resulting crude residue was then purified via silica gel flash column chromatography (EtOAc/Hexanes) to yield the desired product as an off-white/ yellow semi-solid (155 mg, 70%).

¹H NMR (500 MHz, CDCl₃) δ 8.93 (s, 1H, **(H8)**), 8.42 (d, *J* = 7.0 Hz, 1H, **(H1)**), 8.04 (d, *J* = 8.4 Hz, 1H, **(H25)**), 7.94 (d, *J* = 7.6 Hz, 1H, **(H4)**), 7.89 (d, *J* = 8.4 Hz, 2H, **(H41, H45)**), 7.79 (d, *J* = 8.4 Hz, 2H, **(H46, H50)**), 7.59 (d, *J* = 7.8 Hz, 1H, **(H22)**), 7.48 (s, 1H, **(H18)**), 7.42 – 7.33 (m, 4H, **(H2, H3, H23, H24)**), 7.32 – 7.17 (m, 7H, **(H28, H30, H32, H42, H44, H47, H49)**), 7.07 – 7.01 (m, 2H, **(H29, H31)**), 4.96 (d, *J* = 15.8 Hz, 1H, **(H26)**), 4.85 (dd, *J* = 11.9, 9.9 Hz, 1H, **(H14)**), 4.38 (dd, *J* = 16.0, 11.9 Hz, 1H, **(H15)**), 4.01 (dd, *J* = 16.0, 9.9 Hz, 1H, **(H15)**), 3.82 (d, *J* = 15.8 Hz, 1H, **(H26)**), 2.36 (s, 3H, **(H51)**), 2.34 (s, 3H, **(H52)**).

¹³C NMR (126 MHz, CDCl₃) δ 182.55 (**(C10)**), 160.86 (**(C12)**), 146.14 (**(C43)**), 145.29 (**(C48)**), 137.28 (**(C27)**), 136.75 (**(C5)**), 135.97 (**(C39)**), 135.11 (**(C40)**), 134.70 (**(C20)**), 130.37 (**(C42, C44)**), 130.04 (**(C47, C49)**), 128.67 (**(C29, C31)**), 128.42 (**(C6)**), 128.09 (**(C41, C45)**), 127.91 (**(C21)**), 127.62 (**(C30)**), 127.47 (**(C46, C50)**), 126.92 (**(C28, C32)**), 125.97 (**(C8)**), 125.28 (**(C3)**), 125.14 (**(C23)**), 124.67 (**(C2)**), 123.64 (**(C24)**), 123.10 (**(C22)**), 121.27 (**(C17)**), 120.42 (**(C18)**), 119.23 (**(C9)**), 114.05 (**(C25)**), 113.19 (**(C4)**), 60.45 (**(C14)**), 55.91 (**(C15)**), 47.86 (**(C26)**), 21.72 (**(C51)**), 21.65 (**(C52)**).

FTIR (cm⁻¹): 3001, 2946, 1709, 1521, 1442, 1373, 1179.

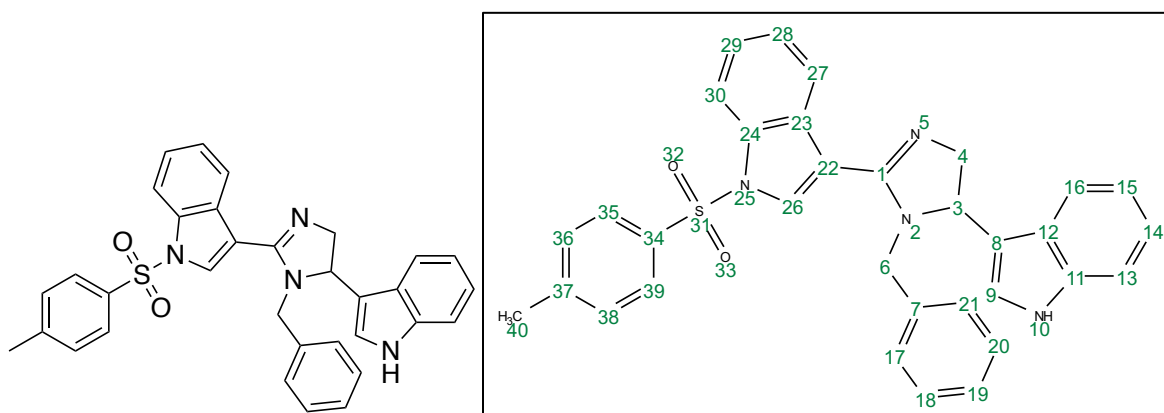
HRMS-ESI (m/z): Calculated for C₄₁H₃₄N₄O₅S₂ (M+H)⁺: 727.2049, Found: 727.2061.



(S)-1-(1-tosyl-1H-indol-3-yl)ethane-1,2-diol (2-55)

To an oven-dried round bottom flask was added a solution of AD-mix- α (1.25 g, 1.6 mmol, 2.0 equiv) in *t*-BuOH/H₂O (1:1, 10 mL:10 mL). This solution was then stirred vigorously at 20°C under an atmosphere of N₂ gas for 1 hour. After 1 hour, the reaction mixture was then cooled to 0°C and then 3-vinyl indole (0.24 g, 0.80 mmol, 1.0 equiv) was then added under an atmosphere of N₂ gas. The resulting reaction mixture was then allowed to stir for 3 hours at 0°C. After 3 hours, the reaction was allowed to warm to 20°C and was then stirred overnight at 20°C, under an atmosphere of N₂. After 18 hours, the reaction was quenched at 20°C with Na₂SO₃ (1.50 g). This was then allowed to stir at 20°C for an additional 2 hours. After 2 hours, the aqueous layer was then extracted with EtOAc (3x20 mL), dried over Na₂SO₄, filtered, and concentrated in vacuo. The crude residue was then purified via silica gel column chromatography (EtOAc/Hexanes) to yield the desired product as a clear, pale yellow oil (0.20 g, 78%). **Mp:** 118-120°C. **¹H NMR** (500 MHz, CDCl₃) δ 7.94 (d, J = 8.4 Hz, 1H, (**H1**)), 7.70 (d, J = 8.4 Hz, 2H, (**H18**, **H22**)), 7.59 (s, 1H, (**H8**)), 7.47 (d, J = 7.8 Hz, 1H, (**H4**)), 7.27 (t, J = 7.9 Hz, 1H, (**H3**)), 7.12 (t, J = 7.6 Hz, 1H, (**H2**)), 7.05 (d, J = 8.2 Hz, 2H, (**H19**, **H21**)), 4.99 (dd, J = 7.4, 2.4 Hz, 1H, (**H10**)), 3.80 (dd, J = 11.4, 2.2 Hz,

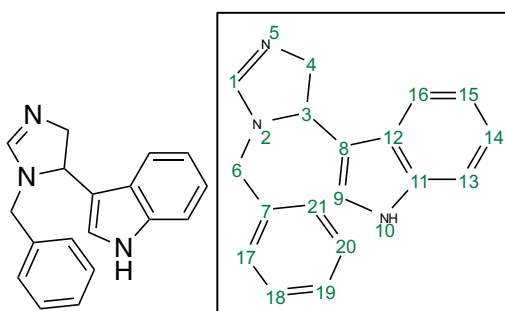
1H, (**H11**)), 3.73 (dd, $J = 11.3, 7.9$ Hz, 1H, (**H11**)), 3.67 (s, 1H, (**H12 or H13**)), 2.19 (s, 3H, (**H23**)). **¹³C NMR** (126 MHz, CDCl₃) δ 145.06 (**C20**), 135.18 (**C5**), 134.91 (**C17**), 129.87 (**C19, C21**), 128.89 (**C6**), 126.81 (**C18, C22**), 124.86 (**C3**), 123.48 (**C8**), 123.29 (**C2**), 122.19 (**C9**), 120.12 (**C4**), 113.65 (**C1**), 68.56 (**C10**), 66.48 (**C11**), 21.44 (**C23**). **FTIR** (cm⁻¹): 3321, 3043, 2897, 1596, 1356, 1167, 1098, 1056. **HRMS-ESI** (m/z): calculated for C₁₇H₁₇NO₄S (M+H)⁺: 332.0957, Found: 332.0971.



3-(1-benzyl-5-(1H-indol-3-yl)-4,5-dihydro-1H-imidazol-2-yl)-1-tosyl-1H-indole (2-58)

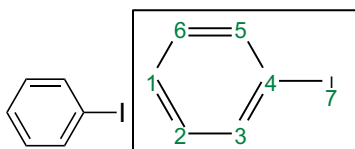
This side product was isolated as a light brown semi-solid. **¹H NMR** (500 MHz, CD₃OD) δ 8.31 (s, 1H, (**H26**)), 8.08 (d, $J = 8.4$ Hz, 1H, (**H27**)), 7.84 (d, $J = 8.6$ Hz, 2H, (**H35, H39**)), 7.64 (d, $J = 8.1$ Hz, 1H, (**H30**)), 7.55 (d, $J = 8.1$ Hz, 1H, (**H16**)), 7.49 – 7.44 (m, 2H, (**H13, H29**)), 7.37 – 7.31 (m, 2H, (**H9, H28**)), 7.29 – 7.23 (m, 5H, (**H18, H19, H20, H36, H38**)), 7.21 (t, $J = 8.2$ Hz, 1H, (**H14**)), 7.08 (t, $J = 7.5$ Hz, 1H, (**H15**)), 6.99 – 6.93 (m, 2H, (**H17, H21**)), 5.38 (dd, $J = 12.7, 8.7$ Hz, 1H, (**H3**)), 4.52 (d, $J = 16.2$ Hz, 1H, (**H6**)), 4.41 (t, $J = 12.7$ Hz, 1H, (**H4**)), 4.16 (dd, $J = 13.1, 8.7$ Hz, 1H, (**H4**)), 4.08 (d, $J = 16.2$ Hz, 1H, (**H6**)), 2.28 (s, 3H, (**H40**)). **¹³C NMR** (126 MHz, CD₃OD) δ 161.51 (**C1**), 147.73 (**C37**), 139.11 (**C11**), 136.45 (**C34**), 136.03 (**C24**), 135.53

(C7), 131.36 (C36, C38), 131.06 (C23), 130.77 (C26), 129.96 (C18, C20), 129.12 (C19), 128.61 (C17, C21), 128.32 (C35, C39), 127.31 (C29), 126.60 (C9), 126.15 (C12), 125.87 (C28), 123.41 (C14), 121.58 (C30), 120.88 (C15), 119.34 (C16), 115.25 (C27), 113.36 (C13), 112.54 (C8), 109.67 (C22), 59.66 (C3), 54.81 (C4), 49.85 (C6), 21.50 (C40). FTIR (cm⁻¹): 3404, 3091, 2905, 1640, 1344, 1166. HRMS-ESI (m/z): Calculated for C₃₃H₂₈N₄O₂S (M+H)⁺: 545.2011, Found: 545.2029.



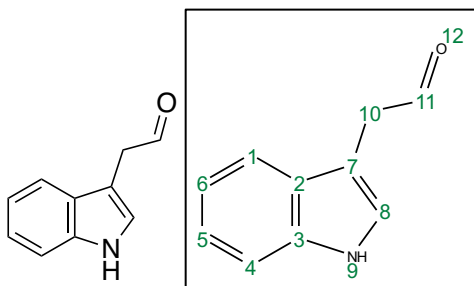
3-(1-benzyl-4,5-dihydro-1H-imidazol-5-yl)-1H-indole (2-59)

This side product was isolated as a reddish-brown semi-solid. ¹H NMR (500 MHz, CD₃OD) δ 7.46 (d, *J* = 8.2 Hz, 1H, (H16)), 7.44 (d, *J* = 8.5 Hz, 1H, (H13)), 7.38 (s, 1H, (H1)), 7.34 – 7.28 (m, 3H, (H17, H21, H19)), 7.24 (s, 1H, (H9)), 7.21 – 7.17 (m, 1H, (H14)), 7.18 – 7.13 (m, 2H, (H18, H20)), 7.06 (t, *J* = 7.5 Hz, 1H, (H15)), 5.12 (dd, *J* = 12.1, 9.3 Hz, 1H, (H3)), 4.55 (d, *J* = 15.0 Hz, 1H, (H6)), 4.25 (t, *J* = 12.6 Hz, 1H, (H4)), 4.04 – 3.96 (m, 2H, (H4, H6)). ¹³C NMR (126 MHz, CD₃OD) δ 156.91 (C1), 135.00 (C7), 128.49 (C17, C21), 128.06 (C18, C20), 127.83 (C11), 127.74 (C19), 127.59 (C12), 124.77 (C8), 121.87 (C9), 119.29 (C14), 118.07 (C15), 116.84 (C16), 111.78 (C13), 57.73 (C3), 56.97 (C4), 44.28 (C6). FTIR (cm⁻¹): 3427, 3048, 2899, 1639, 1556. HRMS-ESI (m/z): Calculated for C₁₈H₁₇N₃ (M+H)⁺: 276.1501, Found: 276.1523.



Iodobenzene (2-60)

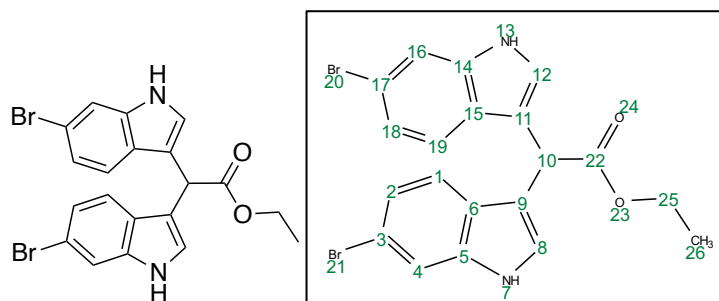
This side product was isolated as a clear, colorless oil. $^1\text{H NMR}$ (500 MHz, CDCl_3) δ 7.72 (d, $J = 7.9$ Hz, 1H, (**H3**, **H5**)), 7.34 (t, $J = 7.5$ Hz, 1H, (**H1**)), 7.12 (t, $J = 7.8$ Hz, 1H, (**H2**, **H6**)). $^{13}\text{C NMR}$ (126 MHz, CDCl_3) δ 137.62 (**C3**, **C5**), 130.38 (**C2**, **C6**), 127.60 (**C1**), 94.52 (**C4**). FTIR (cm^{-1}): 3081, 2898, 1541.



2-(1*H*-indol-3-yl)acetaldehyde (2-63)

To an oven-dried round bottom flask purged with N_2 gas was added 2-(1*H*-indol-3-yl)ethan-1-ol (0.24 g, 1.5 mmol, 1.0 equiv) dissolved in anhydrous DMSO (3.0 mL) at 20°C . Then IBX (0.46 g, 1.7 mmol, 1.1 equiv) was added at 20°C , under an atmosphere of N_2 gas. The resulting solution was then heated to 80°C and allowed to stir for 3 hours under N_2 gas. After 2 hours, the reaction was allowed to cool to room temperature and was diluted with ice cold H_2O (20 mL), extracted with EtOAc (3x30 mL), dried over Na_2SO_4 , filtered, and concentrated in vacuo to afford the desired product as a orange-red oil (0.16 g, 69%). $^1\text{H NMR}$ (500 MHz, CDCl_3) δ 9.77 (t, $J = 2.5$ Hz, 1H, (**H11**)), 8.19 (s, 1H, (**H9**)), 7.55 (d, $J = 8.0$ Hz, 1H, (**H1**)), 7.41 (d, $J = 8.1$ Hz,

1H, (**H4**)), 7.26 – 7.21 (m, 1H, (**H5**)), 7.20 – 7.13 (m, 2H, (**H6**, **H8**)), 3.82 (d, $J = 2.5$ Hz, 2H, (**H10**)). ^{13}C NMR (126 MHz, CDCl_3) δ 199.76 (**C11**), 136.00 (**C3**), 127.51 (**C2**), 123.52 (**C8**), 122.73 (**C5**), 120.13 (**C6**), 118.66 (**C1**), 111.47 (**C4**), 106.30 (**C7**), 40.50 (**C10**). FTIR (cm^{-1}): 3399, 3051, 2890, 1725, 1596. HRMS-ESI (m/z), calculated for $\text{C}_{10}\text{H}_9\text{NO}$ ($\text{M}+\text{H}$) $^+$: 160.0762, Found: 160.0769.



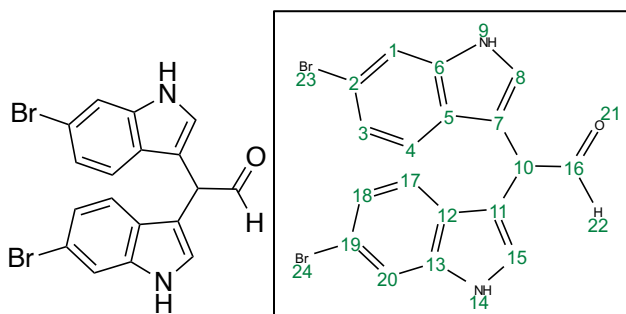
ethyl 2,2-bis(6-bromo-1*H*-indol-3-yl)acetate (**2-67**)

To an oven-dried round bottom flask was added 6-bromo-1-*H*-indole (1.18 g, 6.0 mmol, 1.0 equiv) dissolved in anhydrous DCM (10 mL) at 20°C under an atmosphere of N_2 gas. The resulting solution was then cooled to 0°C. To this was then added ScOTf_3 (0.30 g, 0.6 mmol, 0.2 equiv) and ethyl glyoxylate solution (50 wt% in Toluene) (0.61 g, 3.0 mmol, 1.0 equiv) at 0°C under an atmosphere of N_2 . The resulting solution was then allowed to warm to 20°C and was stirred for 18 hours under N_2 . After 18 hours, the reaction was quenched with DI H_2O (20 mL), extracted with DCM (3x30mL), dried over Na_2SO_4 , filtered, and concentrated in vacuo to yield the desired product as a red-orange foaming solid (>98% purity by NMR).

^1H NMR (500 MHz, CDCl_3) δ 8.11 (s, 2H, (**H7**, **H13**)), 7.46 – 7.42 (m, 4H, (**H1**, **H4**, **H16**, **H19**)), 7.17 (dd, $J = 8.5, 1.8$ Hz, 2H, (**H2**, **H18**)), 6.98 (d, $J = 1.9$ Hz, 2H, (**H8**, **H12**)), 5.40 (s, 1H, (**H10**)), 4.22 (q, $J = 7.1$ Hz, 2H, (**H25**)), 1.26 (t, $J = 7.1$ Hz, 3H, (**H26**)). ^{13}C NMR (126

MHz, CDCl₃) δ 173.38 (C22), 137.21(C5, C14), 129.17 (C6, C15), 125.51 (C3, C17), 124.01 (C2, C18), 123.08 (C1, C19), 120.63 (C8, C12), 115.90 (C9, C11), 114.37 (C4, C16), 61.58 (C25), 40.63 (C10), 14.35 (C26). FTIR (cm⁻¹): 3398, 3061, 2902, 1698, 1596, 1197, 1102.

HRMS-ESI (m/z): Calculated for C₂₀H₁₆Br₂N₂O₂ (M+H)⁺, (Br⁷⁹, Br⁷⁹); (Br⁷⁹, Br⁸¹); (Br⁸¹, Br⁸¹): 474.9657; 476.9636; 478.9616, Found: 474.9675; 476.9657; 478.9631.

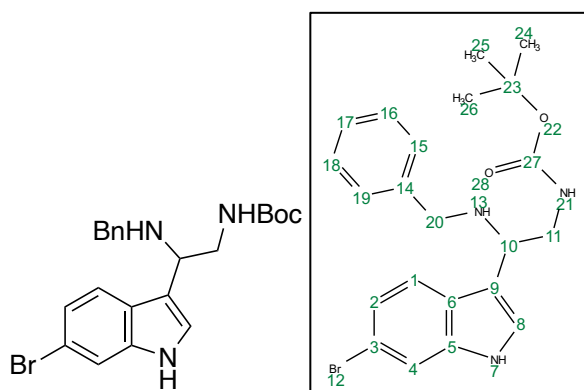


2,2-bis(6-bromo-1H-indol-3-yl)acetaldehyde (2-66)

To an oven-dried flask was added ethyl 2,2-di(6-bromo-1H-indol-3-yl)acetate (1.4 g, 3.0 mmol, 1.0 equiv), dissolved in anhydrous DCM (10 mL). The resulting solution was then cooled to -78°C, under an atmosphere of N₂ gas. At -78°C, under N₂, DIBAL-H solution (1.0M in hexane, 5.4 mL, 5.4 mmol, 1.8 equiv) was added dropwise, slowly. The resulting solution was then allowed to stir for 1 hour at -78°C, under N₂. After 1h, the reaction was allowed to warm to room temperature and was quenched with 2M HCl solution (20mL) and was allowed to stir at rt for 30 minutes. After 30 minutes, the reaction was then extracted with DCM (3x30mL), dried over Na₂SO₄, filtered, and concentrated in vacuo. The resulting crude residue was then purified via silica gel column chromatography (hexanes/ethyl acetate) to yield the desired product as a red/brown oil. (1.05 g, 81%). ¹H NMR (500 MHz, CDCl₃) δ 9.90 (d, *J* = 2.6 Hz, 1H, (H22)), 8.21 (s, 2H, (H9, H14)), 7.55 (d, *J* = 1.5 Hz, 2H, (H1, H20)), 7.36 (d, *J* = 8.5 Hz, 2H, (H4,

H17)), 7.19 (dd, $J = 8.4, 1.5$ Hz, 2H, (**H3, H18**)), 7.10 (d, $J = 2.3$ Hz, 2H, (**H8, H15**)), 5.30 (d, $J = 2.6$ Hz, 2H, (**H10**)). ^{13}C NMR (126 MHz, CDCl_3) δ 197.02 (**C16**), 137.35 (**C6, C13**), 125.67 (**C5, C12**), 124.12 (**C8, C15**), 123.43 (**C3, C18**), 120.67 (**C4, C17**), 116.31 (**C2, C19**), 114.48 (**C1, C20**), 110.93 (**C7, C11**), 47.94 (**C10**). FTIR (cm^{-1}): 3413, 3085, 2887, 1730, 1533.

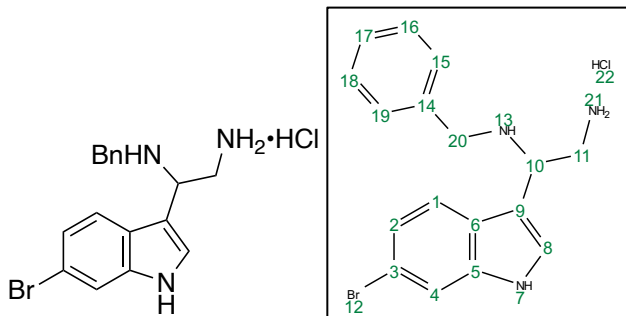
HRMS-ESI (m/z): Calculated for $\text{C}_{18}\text{H}_{12}\text{Br}_2\text{N}_2\text{O}$ ($\text{M}+\text{H}$) $^+$, ($\text{Br}^{79}, \text{Br}^{79}$); ($\text{Br}^{79}, \text{Br}^{81}$); ($\text{Br}^{81}, \text{Br}^{81}$): 430.9395; 432.9374; 434.9354, Found: 430.948; 432.9389; 434.9368.



***tert*-butyl (2-(benzylamino)-2-(6-bromo-1H-indol-3-yl)ethyl)carbamate (2-19)**

6-bromo-1H-indole (1.18 g, 6.0 mmol, 2.0 equiv), benzyl amine (0.33 mL, 3.0 mmol, 1.0 equiv), N-Boc Glycinal (0.48 g, 3.0 mmol, 1.0 equiv), and 1,1,3,3-tetramethyl guanidine (0.033 mL, 0.3 mmol, 0.1 equiv) were added sequentially to DI H_2O (8 mL) at 20°C . The reaction mixture was then added to a pre-heated oil bath (45°C). The reaction was then stirred for 12 hours at 45°C under an atmosphere of N_2 gas. After completion of the reaction, the reaction mixture was diluted with EtOAc (50 mL) and water (20 mL). The organic layer was then extracted with EtOAc (3x30 mL), dried over Na_2SO_4 , filtered, and concentrated in vacuo. The crude residue was then purified via silica gel flash column chromatography (EtOAc/Hexanes) to yield the desired product as a yellow-brown oil. (1.39 g, 52%). ^1H NMR (500 MHz, CDCl_3) δ 7.53 (s,

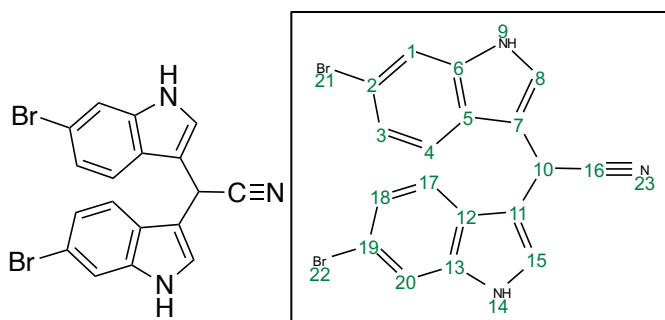
1H, (**H4**)), 7.48 (d, $J = 8.5$ Hz, 1H, (**H1**)), 7.36 – 7.26 (m, 4H, (**H2**, **H16**, **H17**, **H18**)), 7.25 – 7.17 (m, 3H, (**H8**, **H15**, **H19**)), 5.18 (t, $J = 5.8$ Hz, 1H, (**H10**)), 4.58 (s, 1H, (**H13**)), 3.71 – 3.60 (m, 2H, (**H11**, **H20**)), 3.51 (d, $J = 13.3$ Hz, 1H, (**H20**)), 3.42 – 3.31 (m, 1H, (**H11**)), 2.24 (s, 1H, (**H21**)), 1.41 (s, 9H, (**H24**, **H25**, **H26**)). ^{13}C NMR (126 MHz, CDCl_3) δ 156.20 (**C27**), 139.08 (**C14**), 137.14 (**C5**), 128.65 (**C16**, **C18**), 128.34 (**C15**, **C19**), 127.94 (**C6**), 127.66 (**C9**), 127.47 (**C17**), 124.93 (**C2**), 123.20 (**C8**), 122.32 (**C1**), 115.49 (**C3**), 113.07 (**C4**), 79.90 (**C23**), 69.99 (**C10**), 49.91 (**C20**), 45.48 (**C11**), 28.43 (**C24**, **C25**, **C26**). FTIR (cm^{-1}): 3405, 3355, 3052, 2925, 1689, 1525, 1221. HRMS-ESI (m/z): Calculated for $\text{C}_{22}\text{H}_{26}\text{BrN}_3\text{O}_2$ ($\text{M}+\text{H}$) $^+$, (Br^{79}); (Br^{81}): 444.1287; 446.1266, Found: 444.1305; 446.1290.



***N*¹-benzyl-1-(6-bromo-1*H*-indol-3-yl)ethane-1,2-diamine hydrochloride (2-68)**

To an oven-dried flask was added tert-butyl (2-(benzylamino)-2-(6-bromo-1*H*-indol-3-yl)ethyl)carbamate (0.44 g, 1.0 mmol, 1.0 equiv) and ethanolic HCl (3.3M in EtOH, 5.0 mL). This was stirred at 20°C under an atmosphere of N_2 gas for 18 hours. After completion, as indicated by TLC, the reaction mixture was concentrated in vacuo to obtain a semi-solid. This semi-solid was triturated with Et_2O (5.0 mL) and concentrated in vacuo to afford the crude product as a reddish-purple foaming solid. This was used in subsequent steps without any further purification (>99% determined by NMR, quantitative). ^1H NMR (500 MHz, CD_3OD) δ 7.81 (s,

1H, (**H4**)), 7.71 (d, $J = 1.4$ Hz, 1H, (**H8**)), 7.68 (d, $J = 8.5$ Hz, 1H, (**H1**)), 7.51 – 7.41 (m, 5H, (**H15**, **H16**, **H17**, **H18**, **H19**)), 7.31 (d, $J = 8.6$ Hz, 1H, (**H2**)), 5.09 (dd, $J = 10.3, 4.6$ Hz, 1H, (**H10**)), 4.27 (d, $J = 12.9$ Hz, 1H, (**H20**)), 3.97 (d, $J = 12.9$ Hz, 1H, (**H20**)), 3.88 – 3.71 (m, 2H, (**H11**)). ^{13}C NMR (126 MHz, CD_3OD) δ 141.26 (**C14**), 139.15 (**C5**), 131.15 (**C16**, **C18**), 130.73 (**C2**), 130.25 (**C15**, **C19**), 130.22 (**C17**), 129.97 (**C8**), 126.67 (**C6**), 124.91 (**C1**), 122.54 (**C9**), 120.61 (**C4**), 116.09 (**C3**), 53.35 (**C10**), 50.37 (**C20**), 41.41 (**C11**). FTIR (cm^{-1}): 3407, 3350, 3318, 3055, 2919, 1515. HRMS-ESI (m/z): Calculated for $\text{C}_{17}\text{H}_{18}\text{BrN}_3$ ($\text{M}+\text{H}$) $^+$, (Br^{79}); (Br^{81}): 344.0762; 346.0742, Found: 344.0781; 346.0760.



2,2-bis(6-bromo-1H-indol-3-yl)acetonitrile (2-70)

To an oven-dried rb flask was added 6-bromo-1H-indole (0.19 g, 1.0 mmol, 1.0 equiv) and 6-bromo-1H-indole-3-aldehyde (0.22 g, 1.0 mmol, 1.0 equiv) in glacial acetic acid (2.5 mL) at room temperature, under an atmosphere of N_2 gas. To this was then added TMS-CN (0.15 mL, 1.2 mmol, 1.2 equiv) at room temperature, under N_2 gas. The resulting mixture was then heated to 60°C and was stirred for 18 hours at 60°C under N_2 gas. After 18 hours, the reaction mixture was diluted with ethyl acetate (30 mL), then quenched with saturated aqueous NaHCO_3 and extracted with ethyl acetate (3x30mL). The organic extracts were then dried over Na_2SO_4 , filtered, and concentrated in vacuo. The resulting crude residue was then purified via silica gel

column chromatography (hexanes/ ethyl acetate) to afford the desired product as an orange-brown semi-solid (0.18 g, 68%). **¹H NMR** (500 MHz, CDCl₃) δ 8.19 (s, 2H, (**H9**, **H14**)), 7.56 (d, *J* = 1.6 Hz, 2H, (**H1**, **H20**)), 7.40 (d, *J* = 8.4 Hz, 2H, (**H4**, **H17**)), 7.21 (dd, *J* = 8.5, 1.6 Hz, 2H, (**H3**, **H18**)), 7.17 (dd, *J* = 2.6, 0.9 Hz, 2H, (**H8**, **H15**)), 5.59 (s, 1H, (**H10**)). **¹³C NMR** (126 MHz, CDCl₃) δ 137.46 (**C6**, **C13**), 124.42 (**C5**, **C12**), 123.90 (**C8**, **C15**), 123.83 (**C3**, **C18**), 120.25 (**C4**, **C17**), 119.36 (**C16**), 116.71 (**C2**, **C19**), 114.67 (**C1**, **C20**), 110.54 (**C7**, **C11**), 26.29 (**C10**). **FTIR (cm⁻¹):** 3422, 3077, 2876, 2250, 1526. **HRMS-ESI (m/z):** Calculated for C₁₈H₁₁Br₂N₃ (M+H)⁺, (Br⁷⁹, Br⁷⁹); (Br⁷⁹, Br⁸¹); (Br⁸¹, Br⁸¹): 427.9398; 429.9378; 431.9357, Found: 427.9398; 429.9378; 431.9357.

REFERENCES

- (1) Kobayashi, J.; Murayama, T.; Ishibashi, M.; Kosuge, S.; Takamatsu, M.; Ohizumi, Y.; Kobayashi, H.; Ohta, T.; Nozoe, S.; Takuma, S., Hyrtiosins A and B, New Indole Alkaloids from the Okinawan Marine Sponge *Hyrtios Erecta*, *Tetrahedron*, **1990**, *46* (23), 7699–7702. [https://doi.org/10.1016/S0040-4020\(01\)90065-1](https://doi.org/10.1016/S0040-4020(01)90065-1).
- (2) Bao, B.; Sun, Q.; Yao, X.; Hong, J.; Lee, C.-O.; Cho, H. Y.; Jung, J. H., Bisindole Alkaloids of the Topsentin and Hamacanthin Classes from a Marine Sponge, *Spongosorites*, *Sp. J. Nat. Prod.* **2007**, *70* (1), 2–8. <https://doi.org/10.1021/np060206z>.
- (3) Liu, H.-B.; Lauro, G.; O'Connor, R. D.; Lohith, K.; Kelly, M.; Colin, P.; Bifulco, G.; Bewley, C. A., Tulongicin, an Antibacterial Tri-Indole Alkaloid from a Deep-Water *Topsentia* Sp. Sponge, *J. Nat. Prod.*, **2017**, *80* (9), 2556–2560. <https://doi.org/10.1021/acs.jnatprod.7b00452>.
- (4) Bao, B.; Sun, Q.; Yao, X.; Hong, J.; Lee, C.-O.; Sim, C. J.; Im, K. S.; Jung, J. H., Cytotoxic Bisindole Alkaloids from a Marine Sponge *Spongosorites* Sp., *J. Nat. Prod.*, **2005**, *68* (5), 711–715. <https://doi.org/10.1021/np049577a>.
- (5) Guinchard, X.; Vallée, Y.; Denis, J., N., Total Syntheses of Brominated Marine Sponge Alkaloids, *Org. Lett.*, **2007**, *9* (19), 3761–3764. <https://doi.org/10.1021/ol701626m>.
- (6) Burchak, O. N.; Pihive, E. L.; Maigre, L.; Guinchard, X.; Bouhours, P.; Jolival, C.; Schneider, D.; Maurin, M.; Giglione, C.; Meinel, T.; Paris, J.-M.; Denis, J., N., Synthesis and Evaluation of 1-(1H-Indol-3-Yl)Ethanamine Derivatives as New Antibacterial Agents, *Bioorganic & Medicinal Chemistry*, **2011**, *19* (10), 3204–3215. <https://doi.org/10.1016/j.bmc.2011.03.060>.
- (7) Alkhalaf, L. M.; Ryan, K. S., Biosynthetic Manipulation of Tryptophan in Bacteria: Pathways and Mechanisms, *Chemistry & Biology*, **2015**, *22* (3), 317–328. <https://doi.org/10.1016/j.chembiol.2015.02.005>.
- (8) Ryan, K., S.; Drennan, C. L., Divergent Pathways in the Biosynthesis of Bisindole Natural Products, *Chemistry & Biology*, **2009**, *16* (4), 351–364. <https://doi.org/10.1016/j.chembiol.2009.01.017>.
- (9) Mehedi, M., S., A.; Tepe, J. J., Recent Advances in the Synthesis of Imidazolines (2009–2020), *Adv Synth Catal*, **2020**, *362* (20), 4189–4225. <https://doi.org/10.1002/adsc.202000709>.
- (10) Veale, C., G., L., A New Synthesis of Versatile Indolyl-3-Carbonylnitriles, *Tetrahedron Letters*, **2015**, *56* (38), 5287–5290. <https://doi.org/10.1016/j.tetlet.2015.07.075>.
- (11) Yang, C., G.; Wang, J.; Tang, X., X.; Jiang, B., Asymmetric Aminohydroxylation of Vinyl Indoles: A Short Enantioselective Synthesis of the Bisindole Alkaloids Dihydrohamacanthin

- A and Dragmacidin A, *Tetrahedron: Asymmetry*, **2002**, *13* (4), 383–394.
[https://doi.org/10.1016/S0957-4166\(02\)00111-8](https://doi.org/10.1016/S0957-4166(02)00111-8).
- (12) Zhang, M., Z.; Mulholland, N.; Seville, A.; Hough, G.; Smith, N.; Dong, H., Q.; Zhang, W., H.; Gu, Y., C., First Discovery of Pimprinine Derivatives and Analogs as Novel Potential Herbicidal, Insecticidal and Nematicidal Agents, *Tetrahedron*, **2021**, *79*, 131835.
<https://doi.org/10.1016/j.tet.2020.131835>.
- (13) Savela, R.; Majewski, M.; Leino, R., Iron-Catalyzed Arylation of Aromatic Ketones and Aldehydes Mediated by Organosilanes, *Eur J Org Chem* **2014**, *2014* (19), 4137–4147.
<https://doi.org/10.1002/ejoc.201402023>.
- (14) Wu, H.; Xu, L.; Xia, C.; Ge, J.; Yang, L., Convenient Metal-Free Aziridination of Alkenes with Chloramine-T Using Tetrabutylammonium Iodide in Water, *Synthetic Communications*, **2005**, *35* (10), 1413–1417. <https://doi.org/10.1081/SCC-200057302>.
- (15) Wu, H.; Xu, L., W.; Xia, C., G.; Ge, J.; Zhou, W.; Yang, L., Efficient Aziridination of Olefins with Chloramine-T Using Copper Iodide in Water, *Catalysis Communications*, **2005**, *6* (3), 221–223. <https://doi.org/10.1016/j.catcom.2004.12.013>.
- (16) Ye, H.; Liu, R.; Li, D.; Liu, Y.; Yuan, H.; Guo, W.; Zhou, L.; Cao, X.; Tian, H.; Shen, J.; Wang, P., G., A Safe and Facile Route to Imidazole-1-Sulfonyl Azide as a Diazotransfer Reagent, *Org. Lett.*, **2013**, *15* (1), 18–21. <https://doi.org/10.1021/ol3028708>.
- (17) Gopalan, G.; Dhanya, B. P.; Saranya, J.; Reshmitha, T. R.; Baiju, T. V.; Meenu, M. T.; Nair, M. S.; Nisha, P.; Radhakrishnan, K. V., Metal-Free *Trans*-Aziridination of Zerumbone: Synthesis and Biological Evaluation of Aziridine Derivatives of Zerumbone, *Eur. J. Org. Chem.*, **2017**, *2017* (21), 3072–3077. <https://doi.org/10.1002/ejoc.201700410>.
- (18) Ji, X.; Guo, J.; Liu, Y.; Lu, A.; Wang, Z.; Li, Y.; Yang, S.; Wang, Q., Marine-Natural-Product Development: First Discovery of Nortopsentin Alkaloids as Novel Antiviral, Anti-Phytopathogenic-Fungus, and Insecticidal Agents, *J. Agric. Food Chem.*, **2018**, *66* (16), 4062–4072. <https://doi.org/10.1021/acs.jafc.8b00507>.
- (19) Kwong, H.-L.; Liu, D.; Chan, K., Y.; Lee, C., S.; Huang, K., H.; Che, C., M., Copper(I)-Catalyzed Asymmetric Alkene Aziridination Mediated by PhI(OAc)₂: A Facile One-Pot Procedure, *Tetrahedron Letters*, **2004**, *45* (20), 3965–3968.
<https://doi.org/10.1016/j.tetlet.2004.03.107>.
- (20) Trinchera, P.; Musio, B.; Degennaro, L.; Moliterni, A.; Falcicchio, A.; Luisi, R., One-Pot Preparation of Piperazines by Regioselective Ring-Opening of Non-Activated Arylaziridines, *Org. Biomol. Chem.*, **2012**, *10* (10), 1962. <https://doi.org/10.1039/c2ob07099e>.
- (21) J. Song; S. Zhang; G. Li; L. Yang., *US Patent Pub. No. 2019/0284149*, **2019**, 1-63.

- (22) Srinivasan, A.; Banerjee, S.; Pachore, S.; Syam-Kumar, U., Three-Component Coupling–Oxidative Amidation–Heterocycloannulation: Synthesis of the Indole Alkaloids Hamacanthin A and Trans-2,5-Bis(3'-Indolyl)Piperazine, *Synlett*, **2017**, 28 (09), 1057–1064. <https://doi.org/10.1055/s-0036-1588961>.
- (23) Golantsov, N.; Festa, A.; Varlamov, A.; Voskressensky, L., Revision of the Structure and Total Synthesis of Topsentin C, *Synthesis*, **2017**, 49 (11), 2562–2574. <https://doi.org/10.1055/s-0036-1588731>.
- (24) Fujioka, H.; Murai, K.; Ohba, Y.; Hiramatsu, A.; Kita, Y., A Mild and Efficient One-Pot Synthesis of 2-Dihydroimidazoles from Aldehydes, *Tetrahedron Letters*, **2005**, 46 (13), 2197–2199. <https://doi.org/10.1016/j.tetlet.2005.02.025>.
- (25) Kornblum, N.; Jones, W. J.; Anderson, G. J., A New and Selective Method of Oxidation. The Conversion of Alkyl Halides and Alkyl Tosylates to Aldehydes, *J. Am. Chem. Soc.*, **1959**, 81 (15), 4113–4114. <https://doi.org/10.1021/ja01524a080>.
- (26) Ishii, H.; Murakami, K.; Sakurada (Née Kawanabe), E.; Hosoya, K.; Murakami, Y., Polymerisation of Indole. Part 2. A New Indole Trimer, *J. Chem. Soc., Perkin Trans. 1*, **1988**, No. 8, 2377–2385. <https://doi.org/10.1039/P19880002377>.
- (27) Fujino, K.; Yanase, E.; Shinoda, Y.; Nakatsuka, S., Oligomerization of *N*-Tosylindole with Aluminum Chloride, *Bioscience, Biotechnology, and Biochemistry*, **2004**, 68 (3), 764–766. <https://doi.org/10.1271/bbb.68.764>.
- (28) Chatterjee, R.; Santra, S.; Zyryanov, G. V.; Majee, A., Brønsted Acidic Ionic Liquid–Catalyzed Tandem Trimerization of Indoles: An Efficient Approach towards the Synthesis of Indole 3,3'-trimers under Solvent-free Conditions, *Journal of Heterocyclic Chem*, **2020**, 57 (4), 1863–1874. <https://doi.org/10.1002/jhet.3914>.
- (29) Ottoni, O.; Neder, A., V., F; Dias, A., K., B.; Cruz, R., P., A.; Aquino, L., B., Acylation of Indole under Friedel–Crafts Conditions An Improved Method to Obtain 3-Acylindoles Regioselectively, *Org. Lett.*, **2001**, 3 (7), 1005–1007. <https://doi.org/10.1021/ol007056i>.
- (30) Sapegin, A.; Krasavin, M. Ring-Opening Reactions of 2-Imidazolines and Their Applications. In *Advances in Heterocyclic Chemistry*; Elsevier, 2020, 130, 195–250. <https://doi.org/10.1016/bs.aihch.2019.10.004>.
- (31) Xu, M., M.; Kou, L., Y.; Bao, X., G.; Xu, X., P.; Ji, S., J., A Radical Addition and Cyclization Relay Promoted by Mn(OAc)₃·2H₂O: Synthesis of 1,2-Oxaphospholindoles and Mechanistic Study, *Chinese Chemical Letters*, **2021**, 32 (6), 1915–1919. <https://doi.org/10.1016/j.ccllet.2021.02.001>.
- (32) Luche, J. L., Lanthanides in Organic Chemistry, Selective 1,2 Reductions of Conjugated Ketones, *J. Am. Chem. Soc.*, **1978**, 100 (7), 2226–2227. <https://doi.org/10.1021/ja00475a040>.

- (33) Ishihara, M.; Togo, H., Direct Oxidative Conversion of Aldehydes and Alcohols to 2-Imidazolines and 2-Oxazolines Using Molecular Iodine, *Tetrahedron*, **2007**, *63* (6), 1474–1480. <https://doi.org/10.1016/j.tet.2006.11.077>.
- (34) Guérin, C.; Bellosta, V.; Guillamot, G.; Cossy, J., Mild Nonpimerizing *N*-Alkylation of Amines by Alcohols without Transition Metals, *Org. Lett.*, **2011**, *13* (13), 3534–3537. <https://doi.org/10.1021/ol201351a>.
- (35) Khan, I. A.; Saxena, A. K., Metal-Free, Mild, Nonpimerizing, Chemo- and Enantio- or Diastereoselective *N*-Alkylation of Amines by Alcohols via Oxidation/Imine–Iminium Formation/Reductive Amination: A Pragmatic Synthesis of Octahydropyrazinopyridoindoles and Higher Ring Analogues, *J. Org. Chem.*, **2013**, *78* (23), 11656–11669. <https://doi.org/10.1021/jo4012249>.
- (36) Nicolaou, K. C.; Adsool, V. A.; Hale, C. R. H., An Expedient Procedure for the Oxidative Cleavage of Olefinic Bonds with $\text{PhI}(\text{OAc})_2$, NMO, and Catalytic OsO_4 , *Org. Lett.*, **2010**, *12* (7), 1552–1555. <https://doi.org/10.1021/ol100290a>.
- (37) Beshara, C. S.; Hall, A.; Jenkins, R. L.; Jones, T. C.; Parry, R. T.; Thomas, S. P.; Tomkinson, N. C. O., A Simple Method for the α -Oxygenation of Aldehydes, *Chem. Commun.*, **2005**, No. 11, 1478–1480. <https://doi.org/10.1039/B418101H>.
- (38) Hayashi, Y.; Yamaguchi, J.; Sumiya, T.; Hibino, K.; Shoji, M., Direct Proline-Catalyzed Asymmetric α -Aminoxylation of Aldehydes and Ketones, *J. Org. Chem.*, **2004**, *69* (18), 5966–5973. <https://doi.org/10.1021/jo049338s>.
- (39) Fuchs, J. R.; Funk, R. L., Total Synthesis of (\pm)-Perophoramidine, *J. Am. Chem. Soc.*, **2004**, *126* (16), 5068–5069. <https://doi.org/10.1021/ja049569g>.
- (40) Kang, J.; Gao, Y.; Zhang, M.; Ding, X.; Wang, Z.; Ma, D.; Wang, Q., Streptindole and Its Derivatives as Novel Antiviral and Anti-Phytopathogenic Fungus Agents, *J. Agric. Food Chem.*, **2020**, *68* (30), 7839–7849. <https://doi.org/10.1021/acs.jafc.0c03994>.
- (41) Zhang, J.; Wang, X.; Yang, M.; Wan, K.; Yin, B.; Wang, Y.; Li, J.; Shi, Z., Copper-Catalyzed Synthesis of 2-Imidazolines and Their *N*-Hydroxyethyl Derivatives under Various Conditions, *Tetrahedron Letters*, **2011**, *52* (14), 1578–1582. <https://doi.org/10.1016/j.tetlet.2011.01.082>.
- (42) Yazawa, T.; Nakajima, M.; Nemoto, T., Abnormal Strecker Reaction of 3-Formylindole and Aniline, *Heterocycles*, **2022**, *105* (1), 532–543.

APPENDIX

Figure 2.1. ^1H NMR and ^{13}C NMR spectra of compound 2-9.

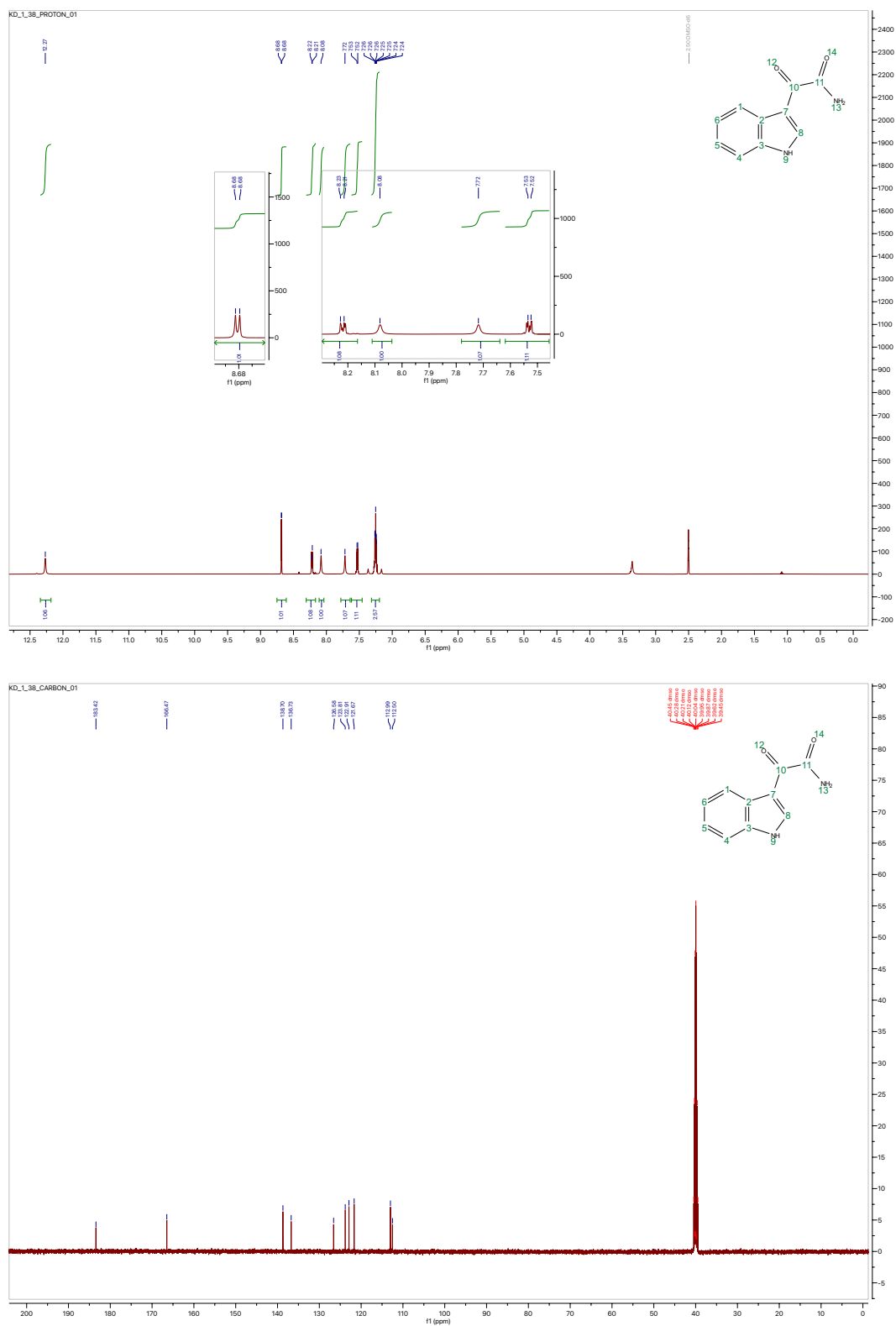


Figure 2.3. ^1H NMR and ^{13}C NMR spectra of compound **2-11a**.

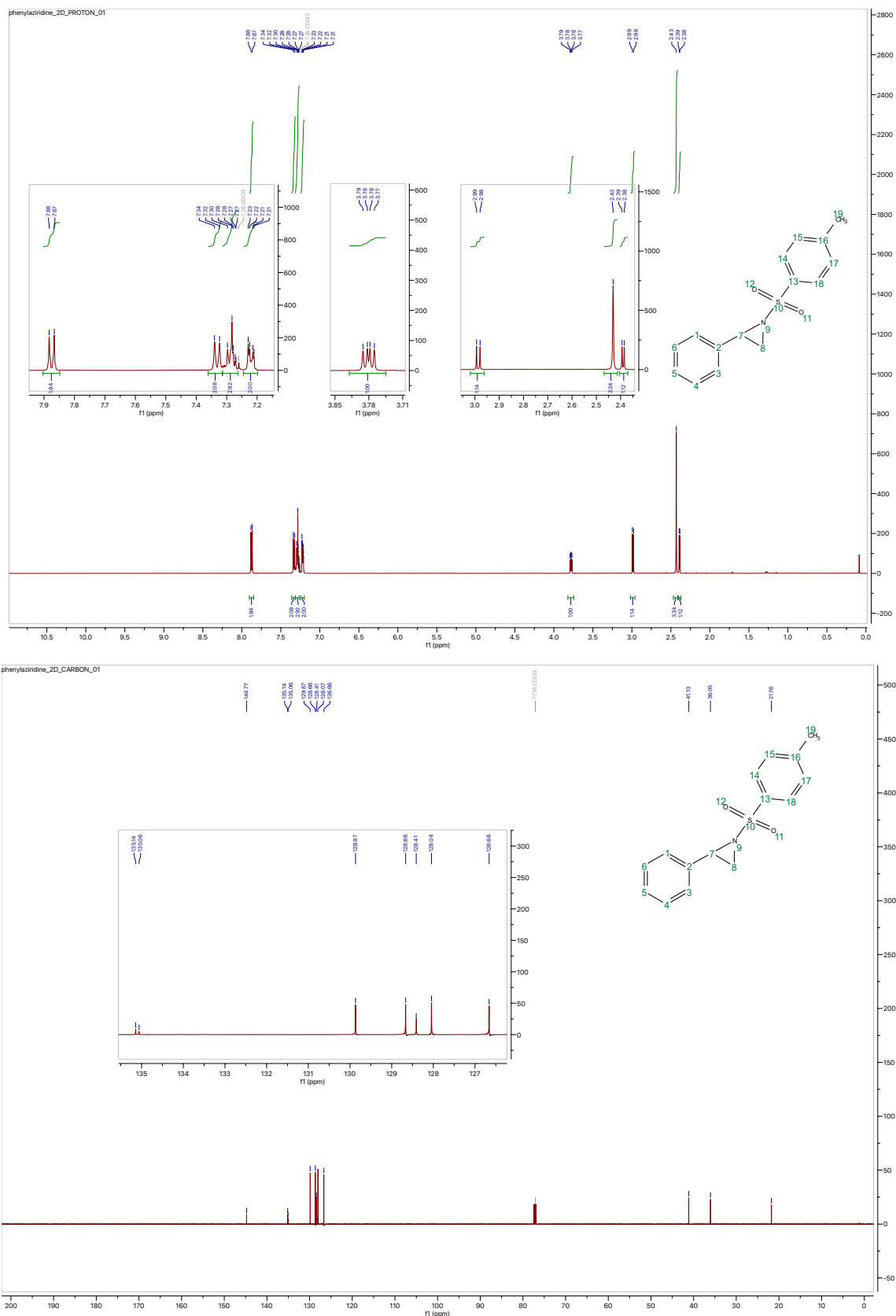


Figure 2.4. ^1H NMR and ^{13}C NMR spectra of compound **2-11b**.

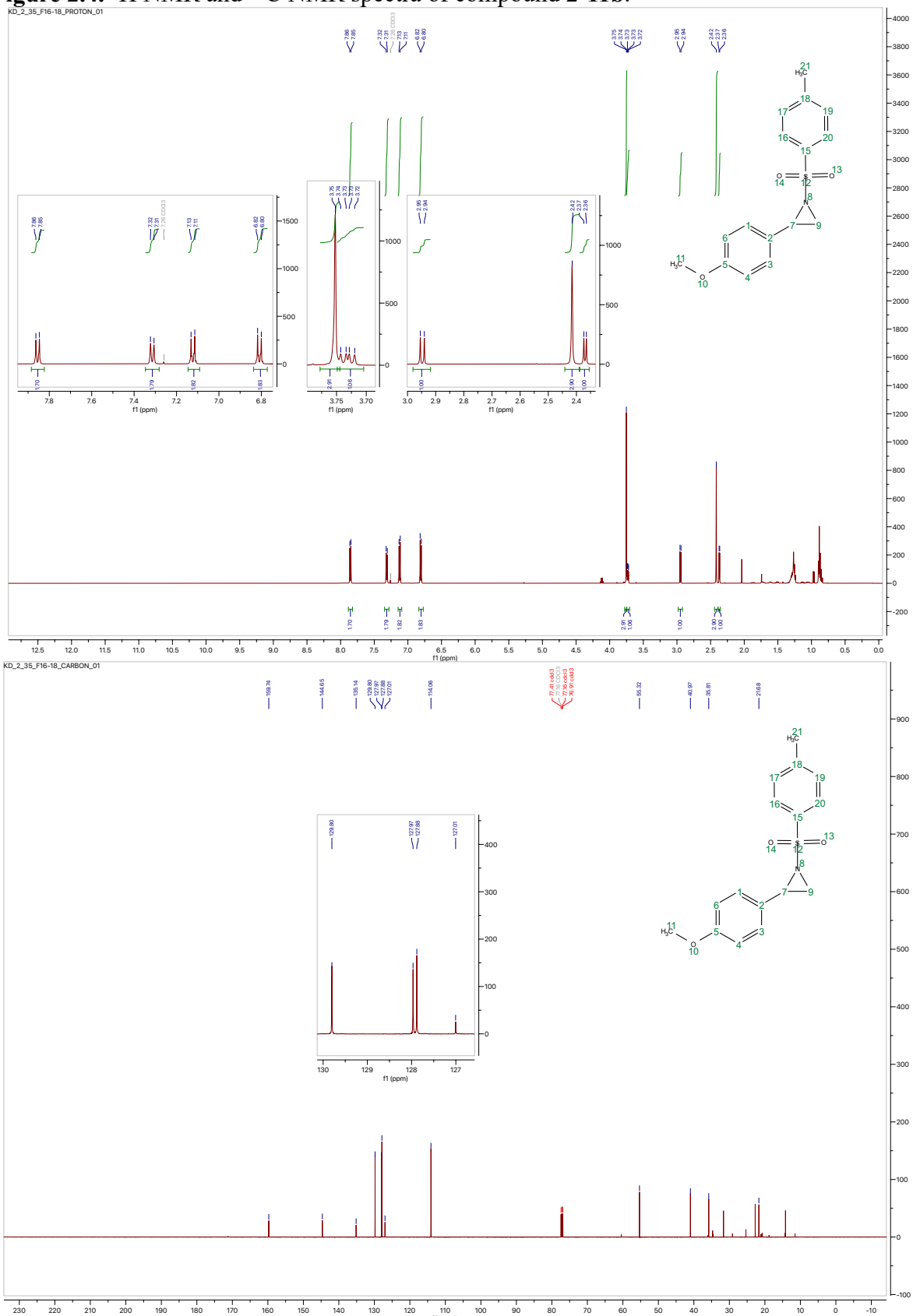


Figure 2.5. ^1H NMR and ^{13}C NMR spectra of compound **2-12**.

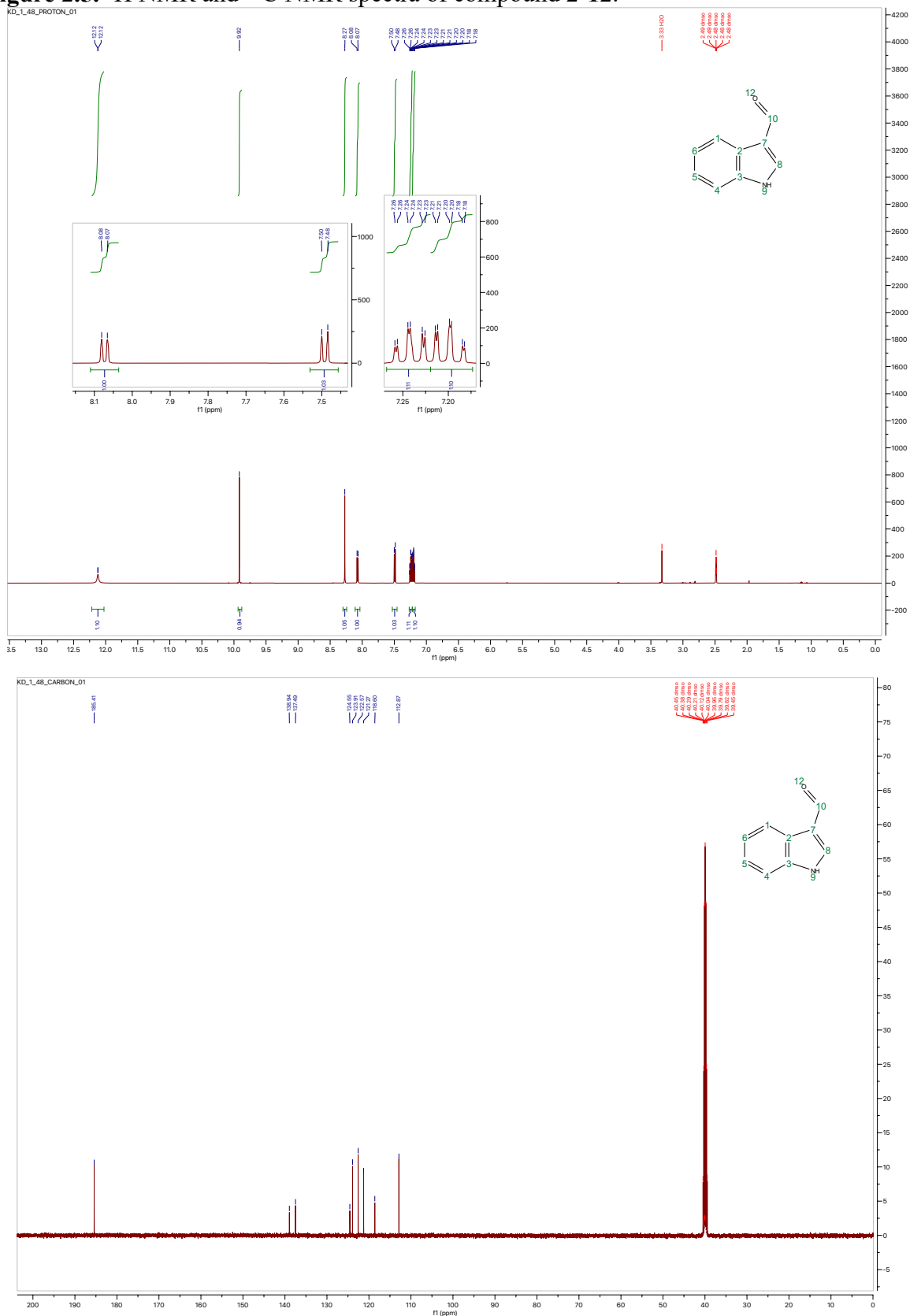


Figure 2.6. ^1H NMR and ^{13}C NMR spectra of compound 2-13.

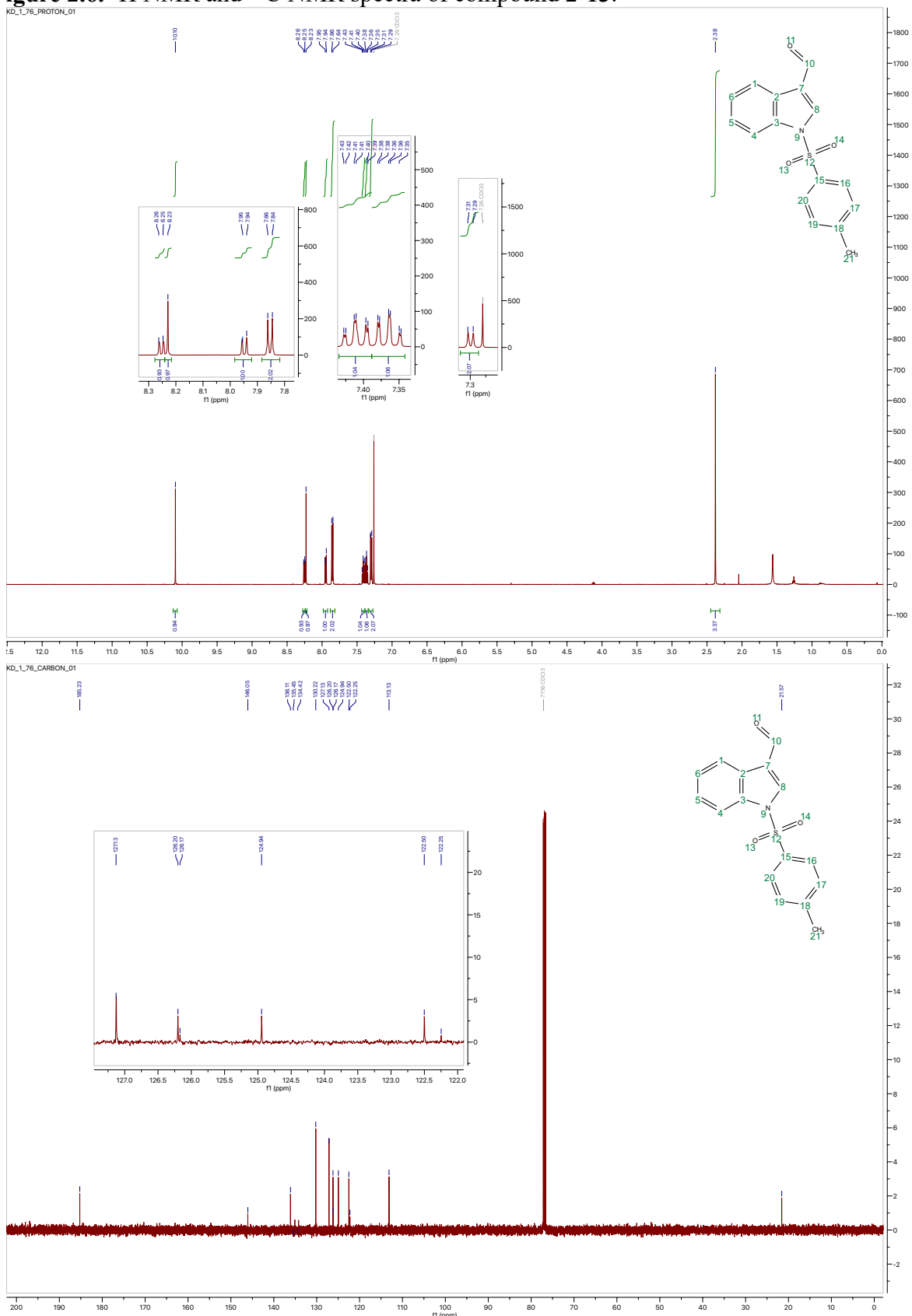


Figure 2.7. ^1H NMR and ^{13}C NMR spectra of compound 2-14.

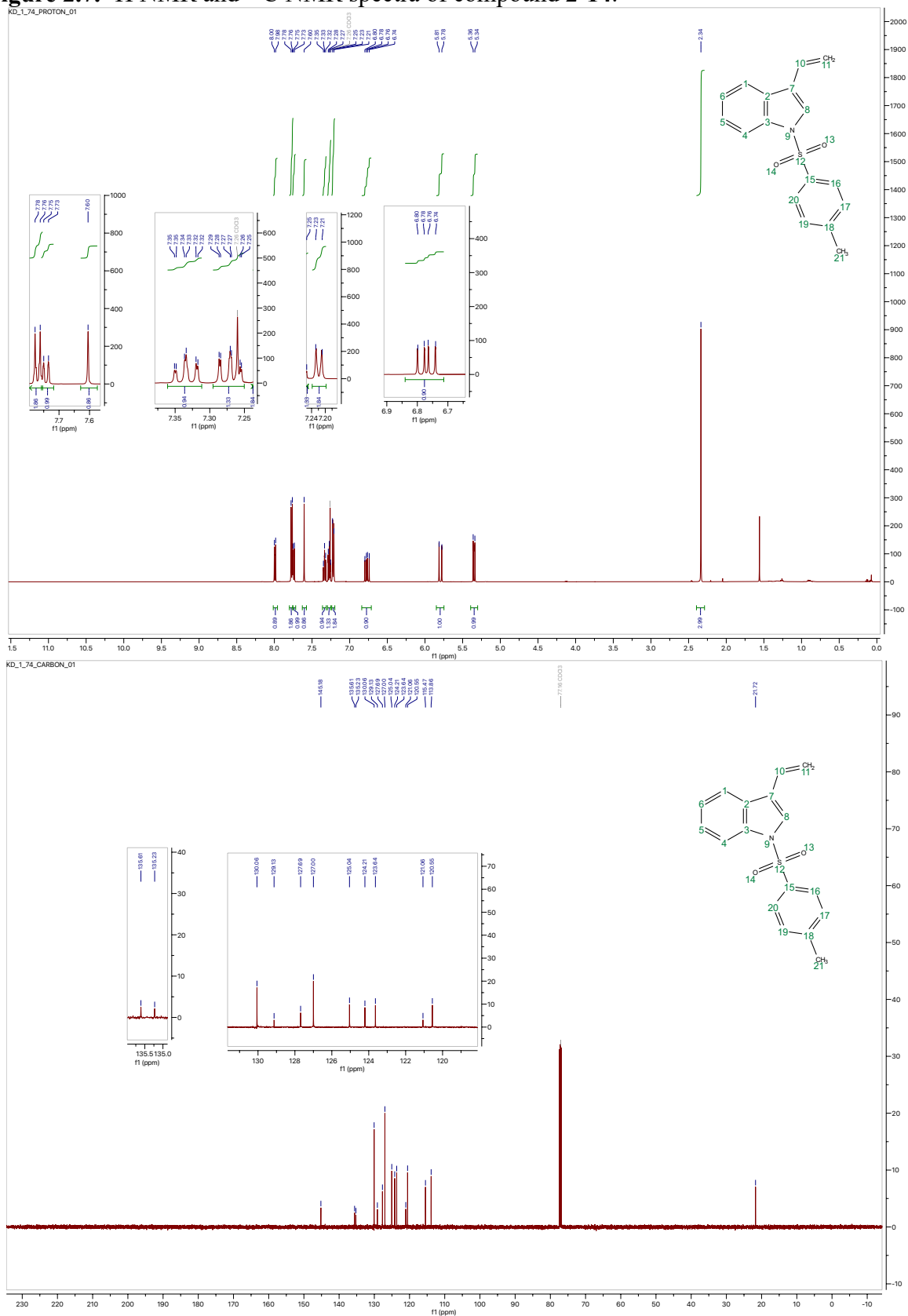


Figure 2.8. ^1H NMR and ^{13}C NMR spectra of compound **2-17**.

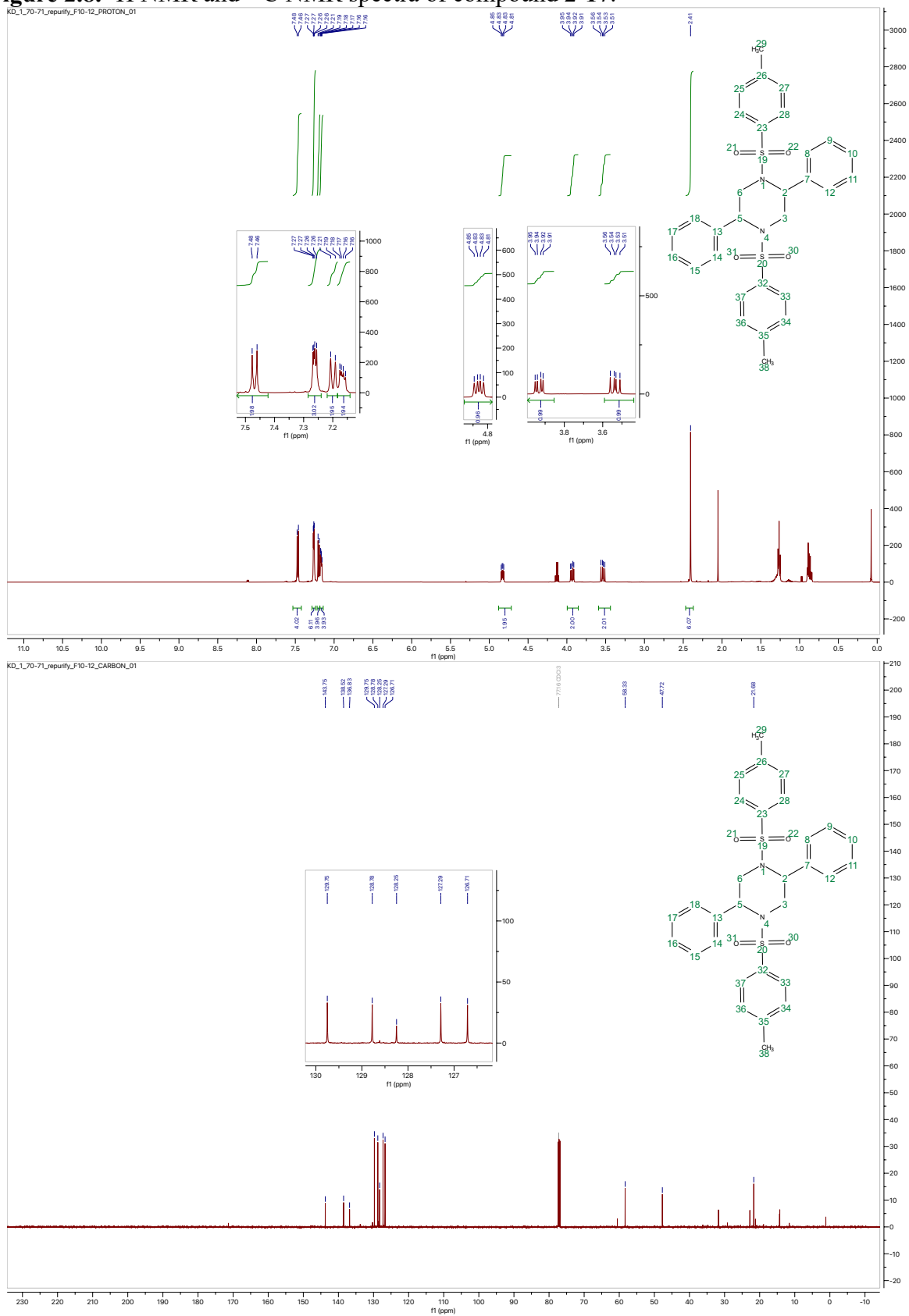


Figure 2.9. ^1H NMR and ^{13}C NMR spectra of compound 2-21.

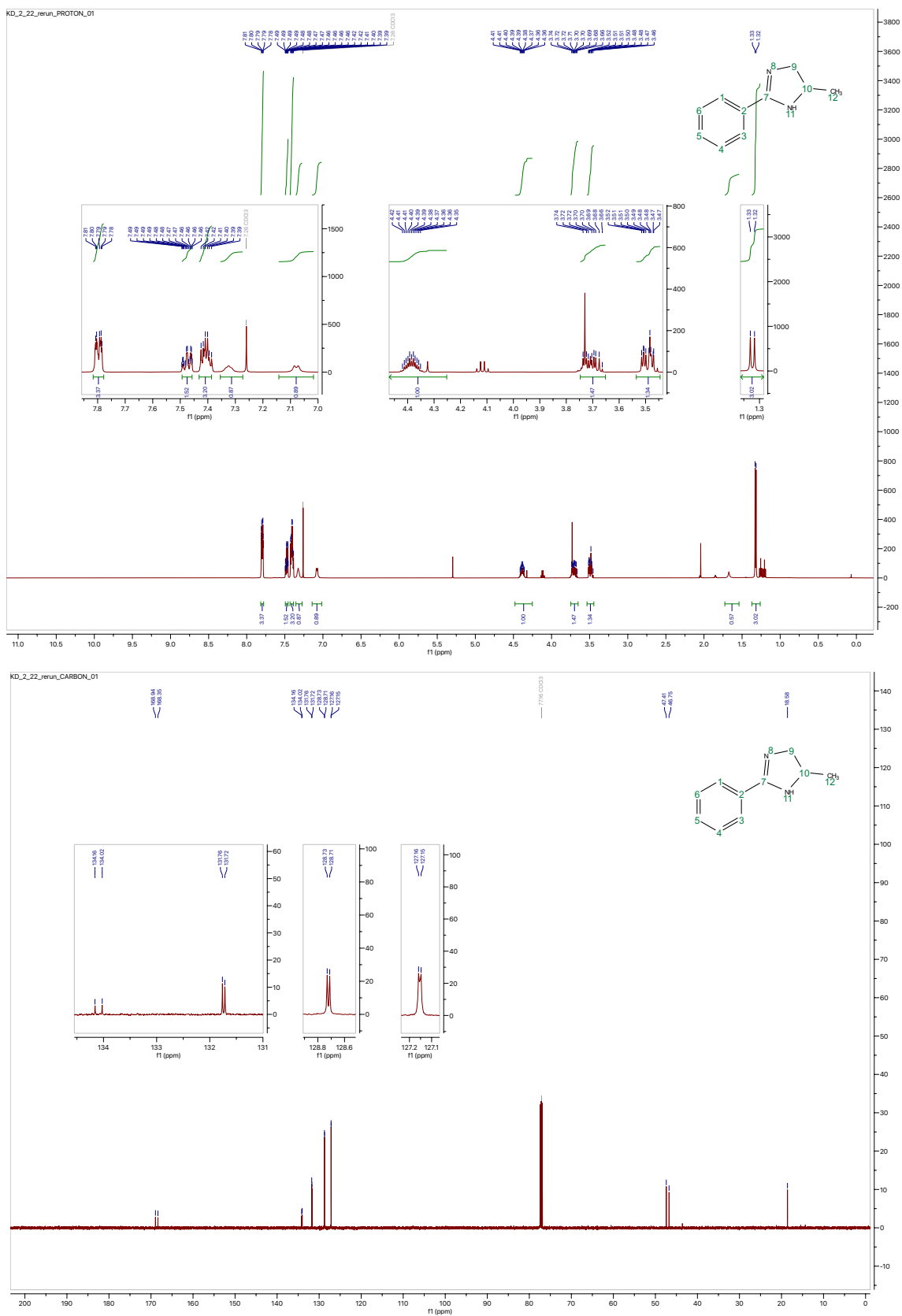


Figure 2.10. ^1H NMR and ^{13}C NMR spectra of compound **2-22**.

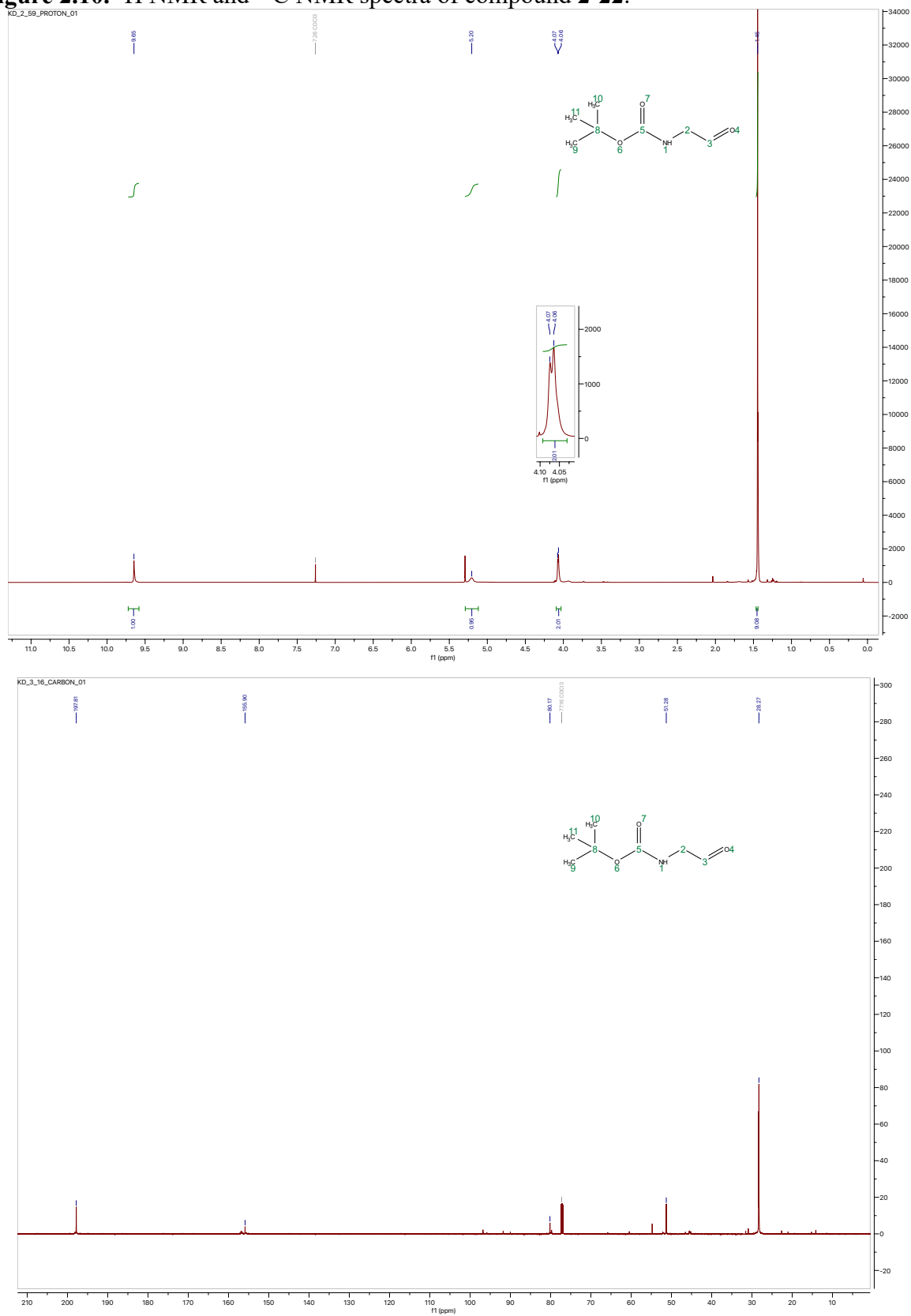


Figure 2.11. ^1H NMR and ^{13}C NMR spectra of compound 2-23.

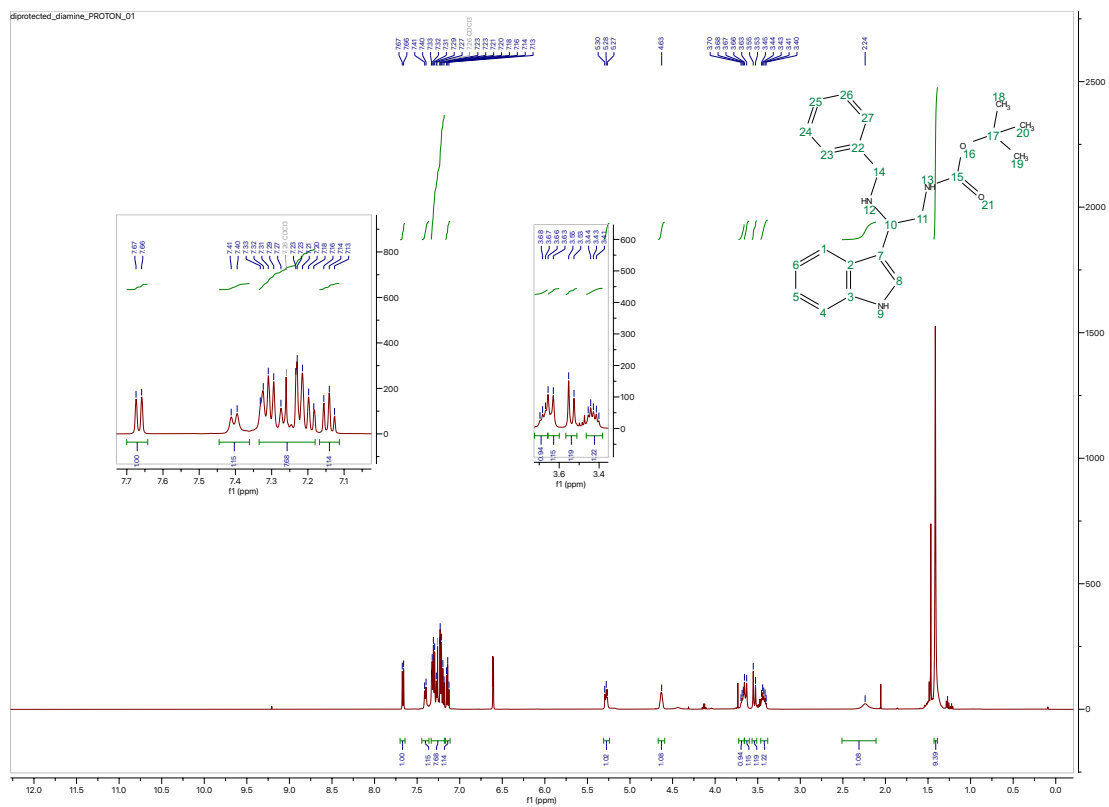
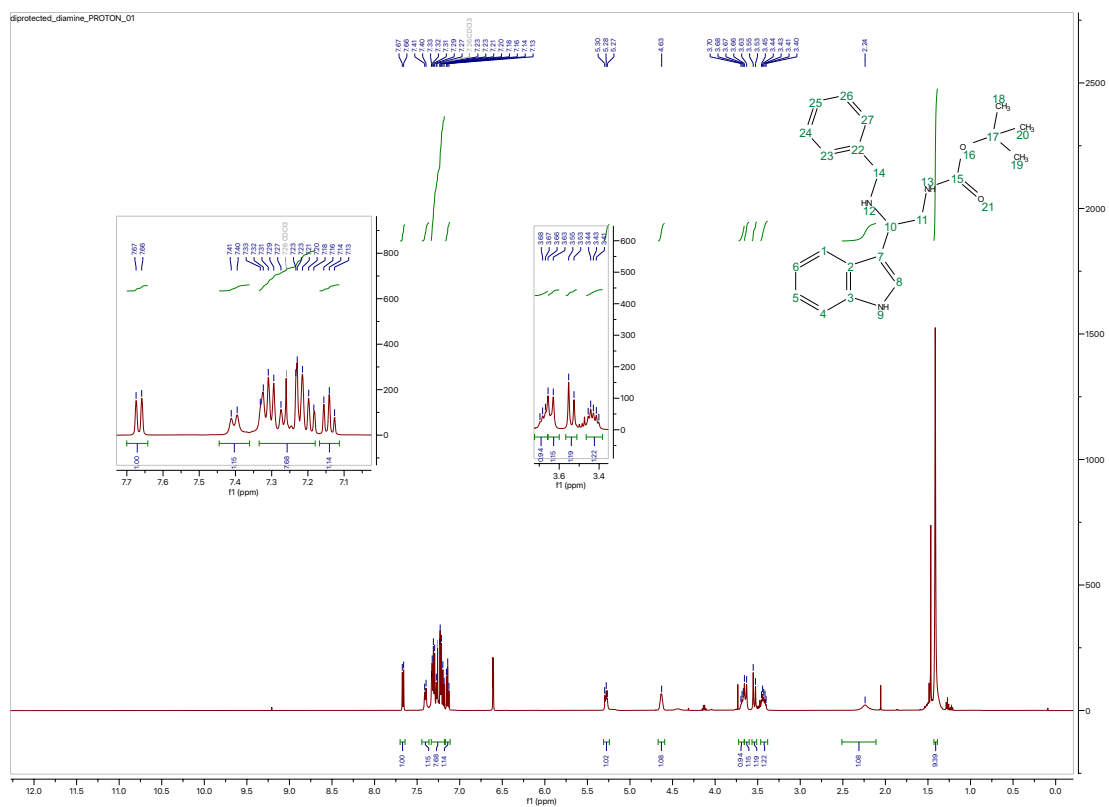


Figure 2.12. ^1H NMR and ^{13}C NMR spectra of compound 2-24.

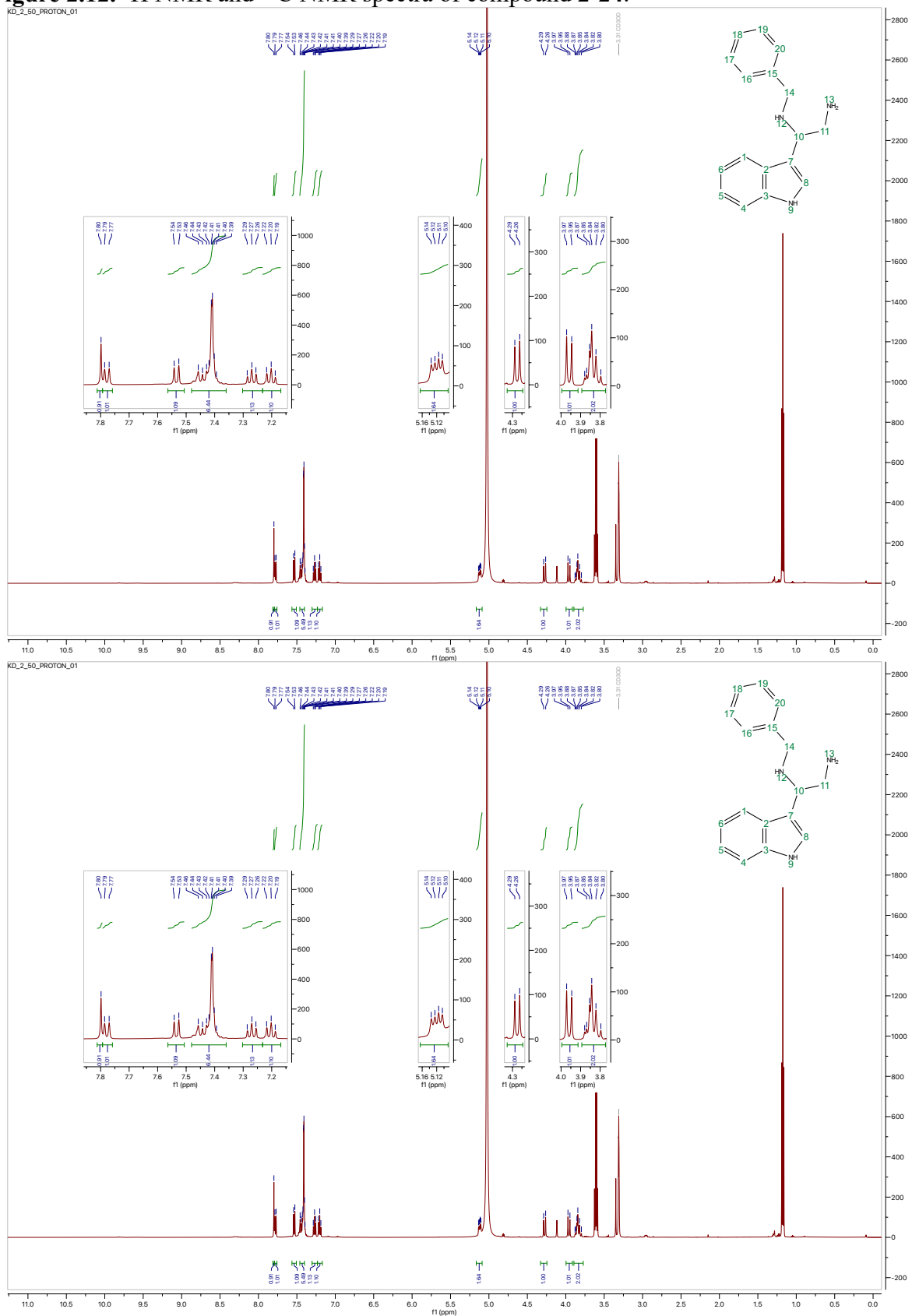


Figure 2.13. ^1H NMR and ^{13}C NMR spectra of compound 2-29.

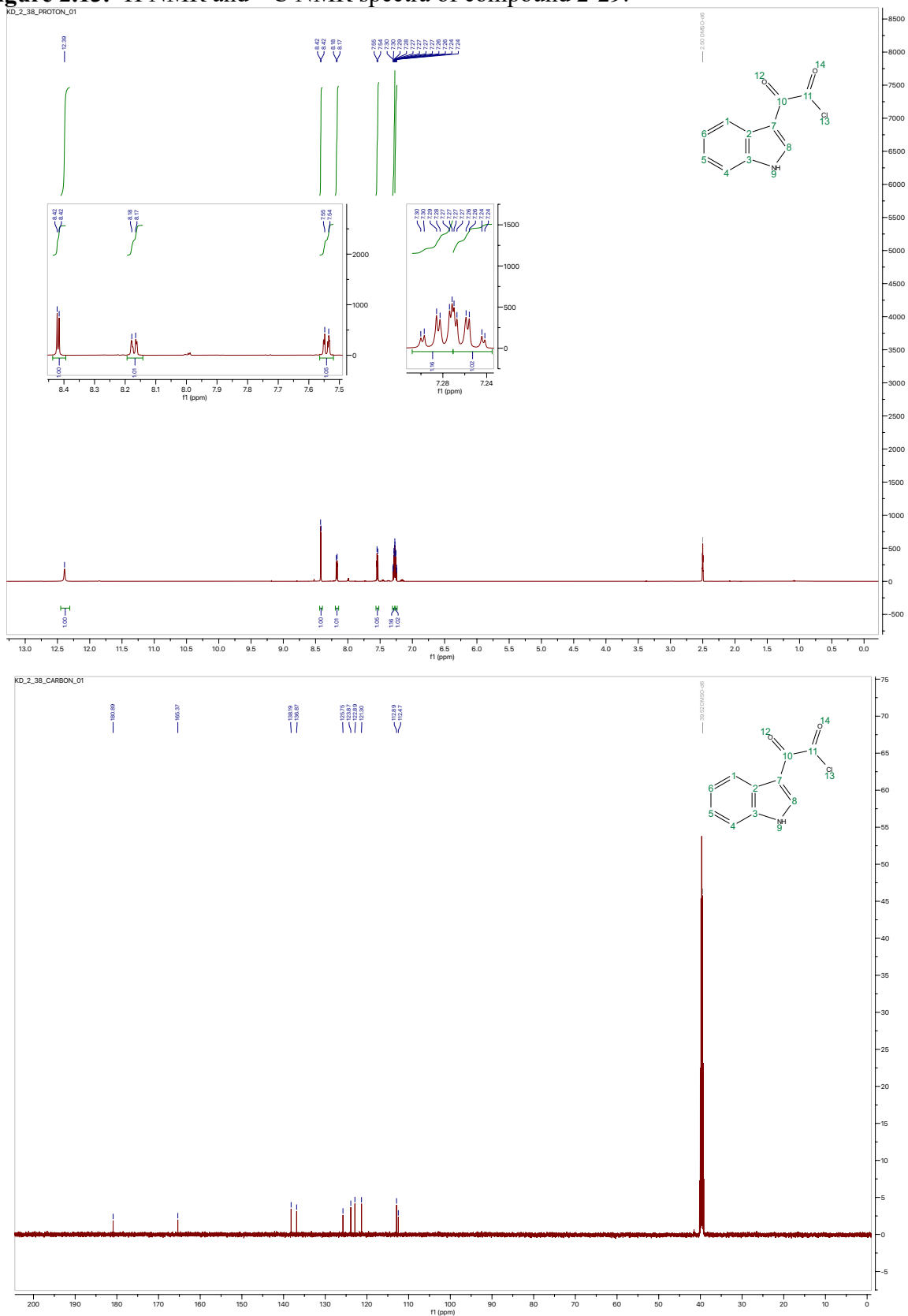


Figure 2.14. ^1H NMR and ^{13}C NMR spectra of compound **2-31**.

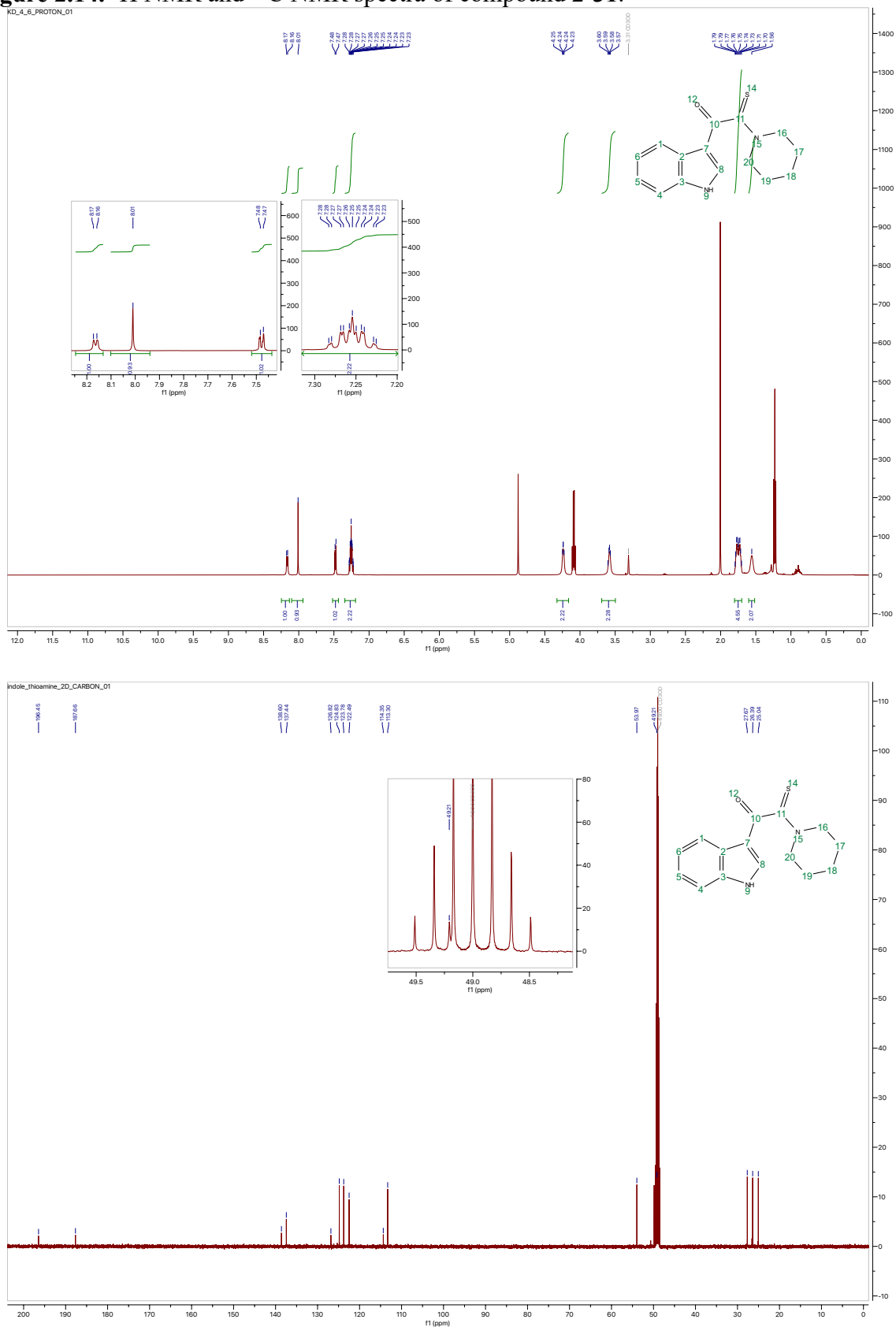


Figure 2.17. ^1H NMR and ^{13}C NMR spectra of compound 2-37.

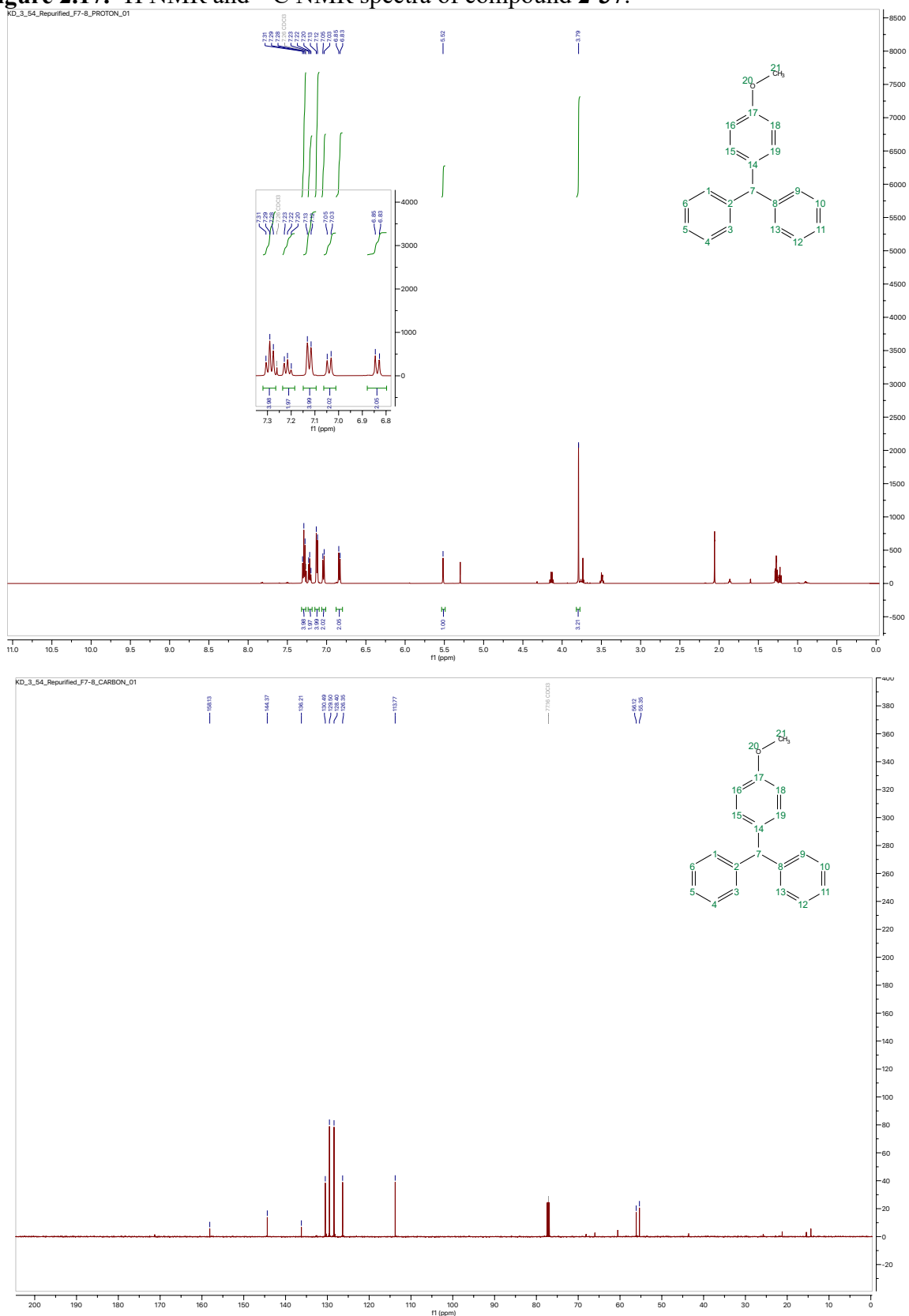


Figure 2.18. ^1H NMR and ^{13}C NMR spectra of compound 2-38.

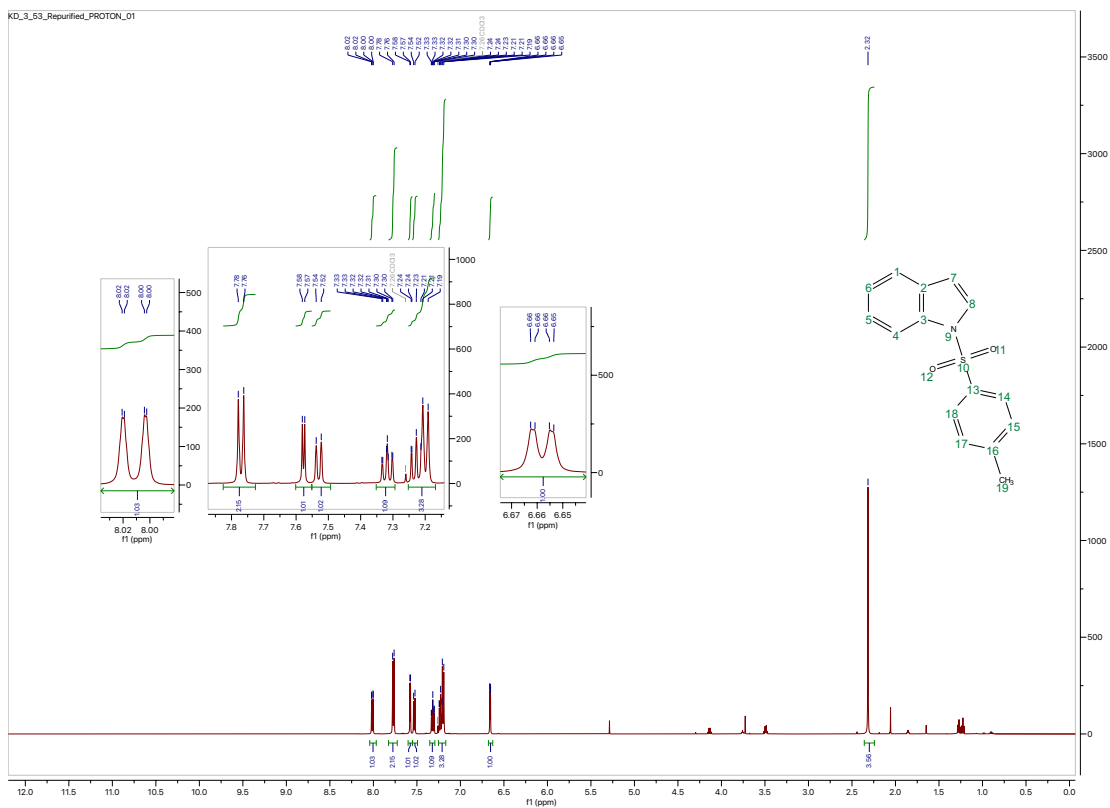
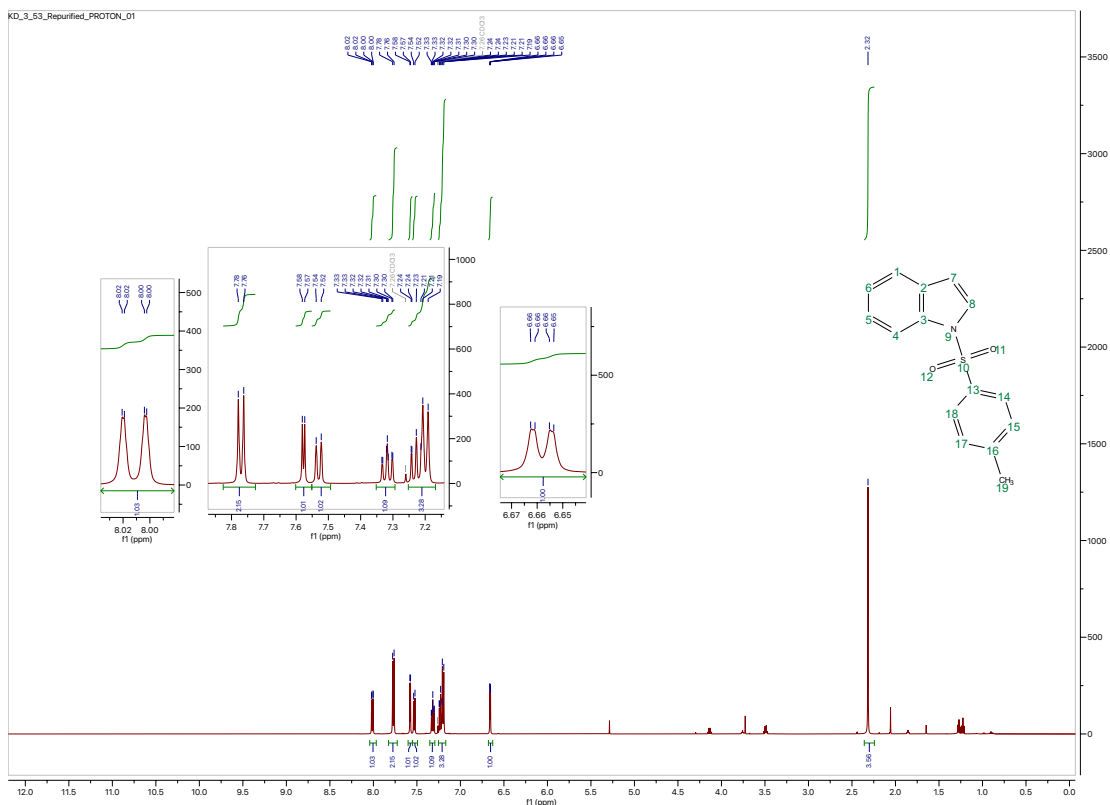


Figure 2.20. ^1H NMR and ^{13}C NMR spectra of compound **2-41**.

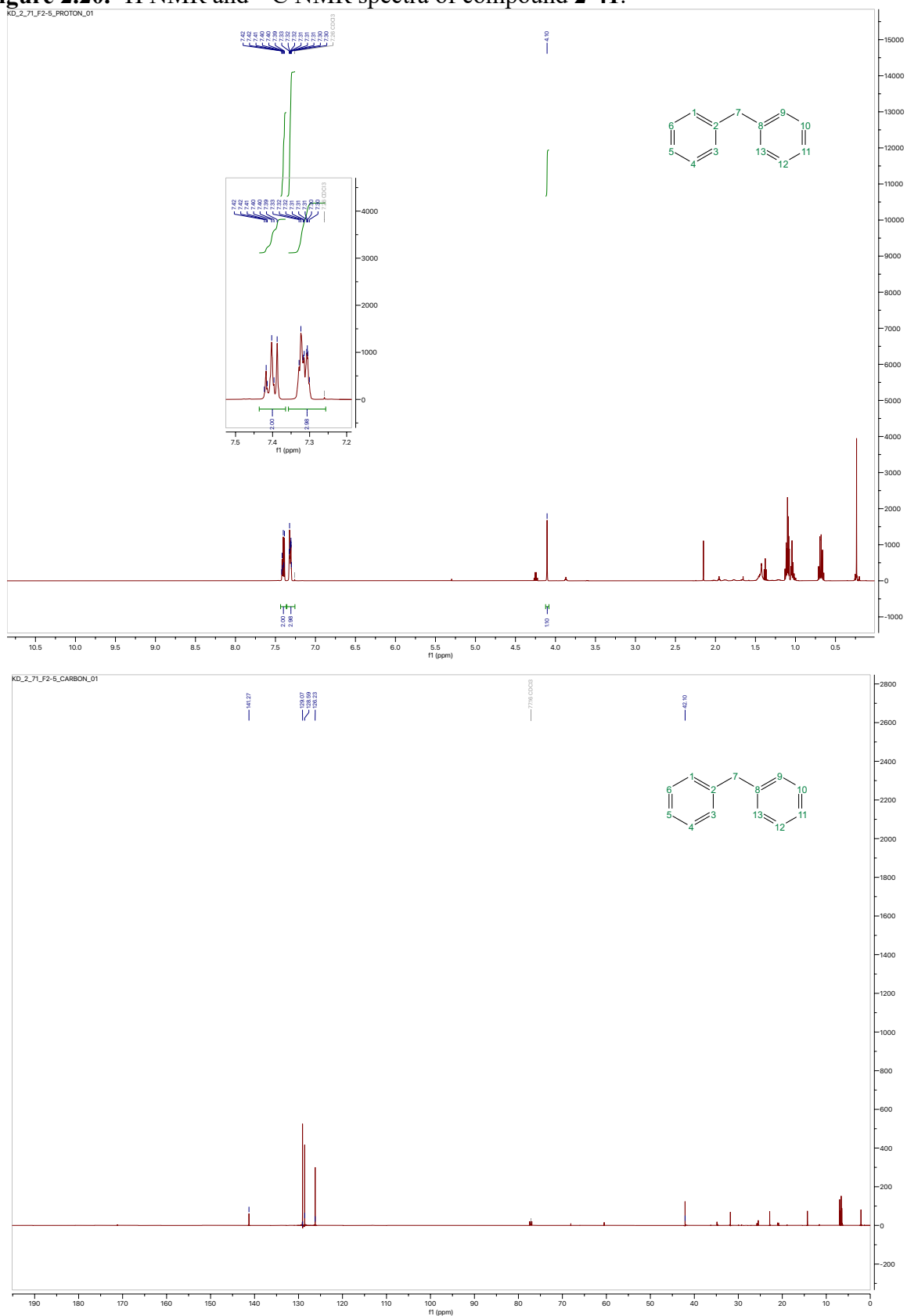


Figure 2.21. Gas-Chromatography Mass Spectrometry (GC-MS) spectrum of compound **2-41** (top) vs reported GC-MS spectrum (bottom, NIST database).

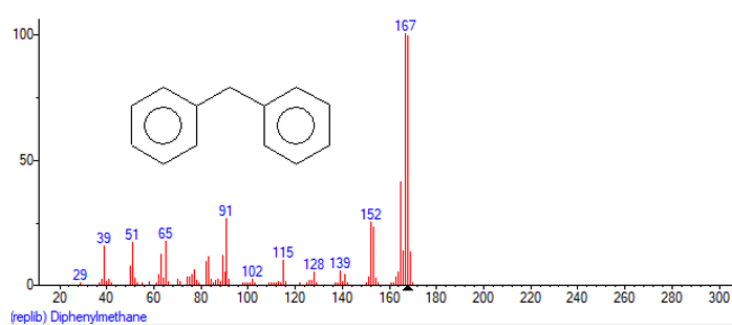
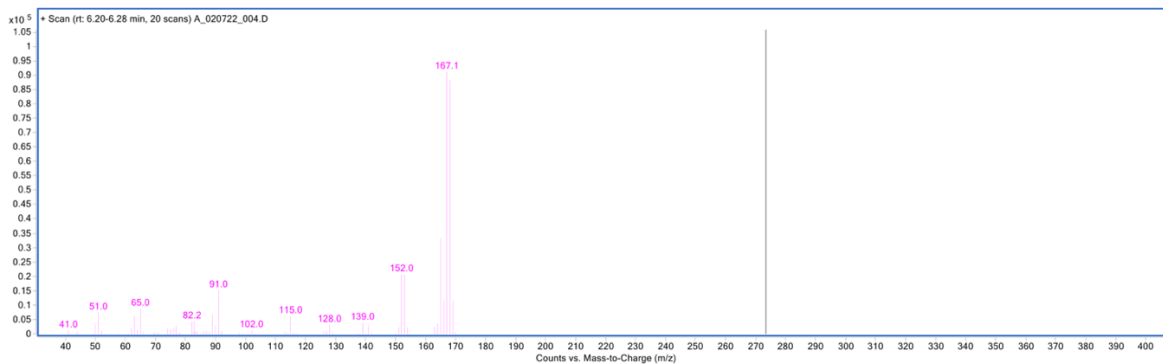


Figure 2.22. ^1H NMR and ^{13}C NMR spectra of compound 2-42.

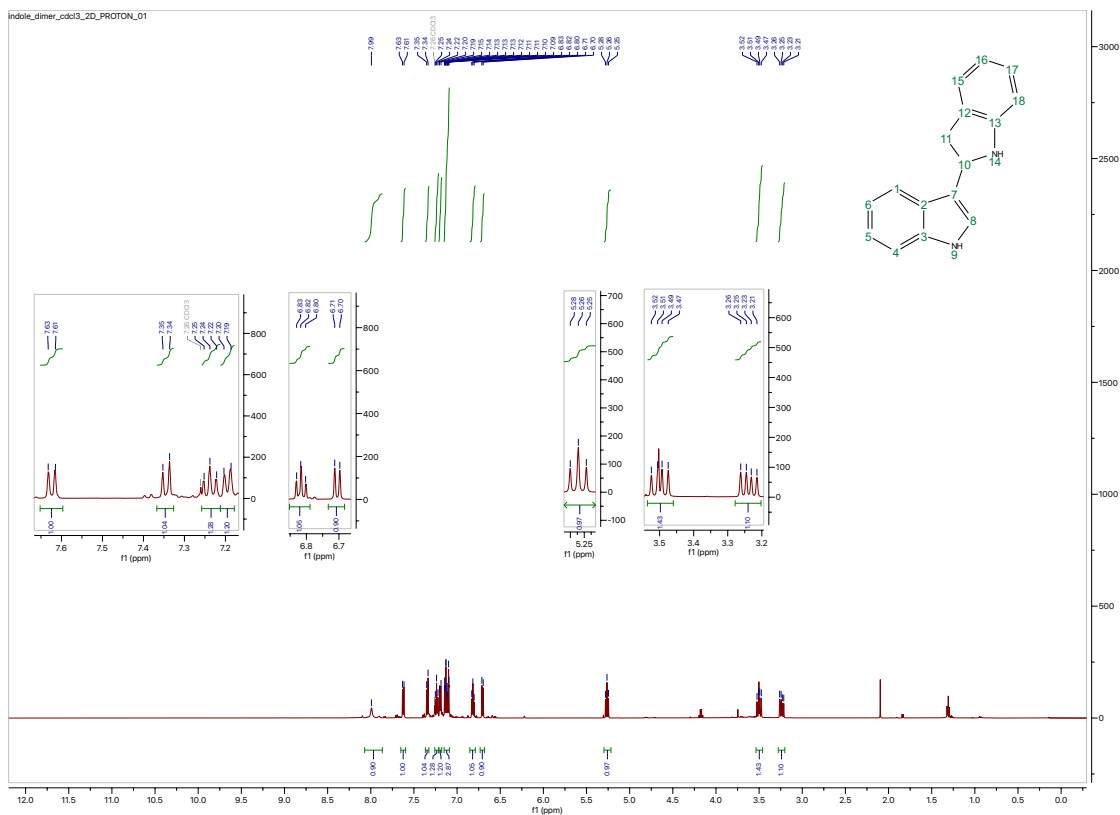
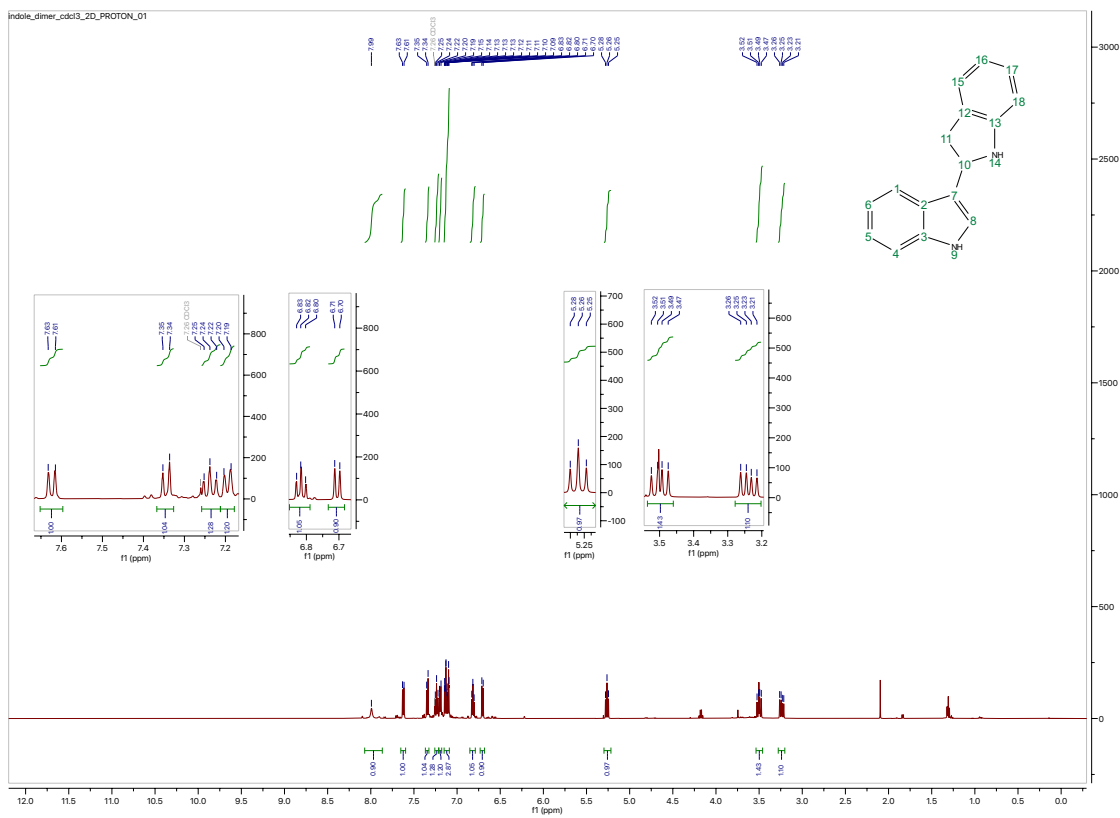


Figure 2.26. ^1H NMR and ^{13}C NMR spectra of compound **2-48**.

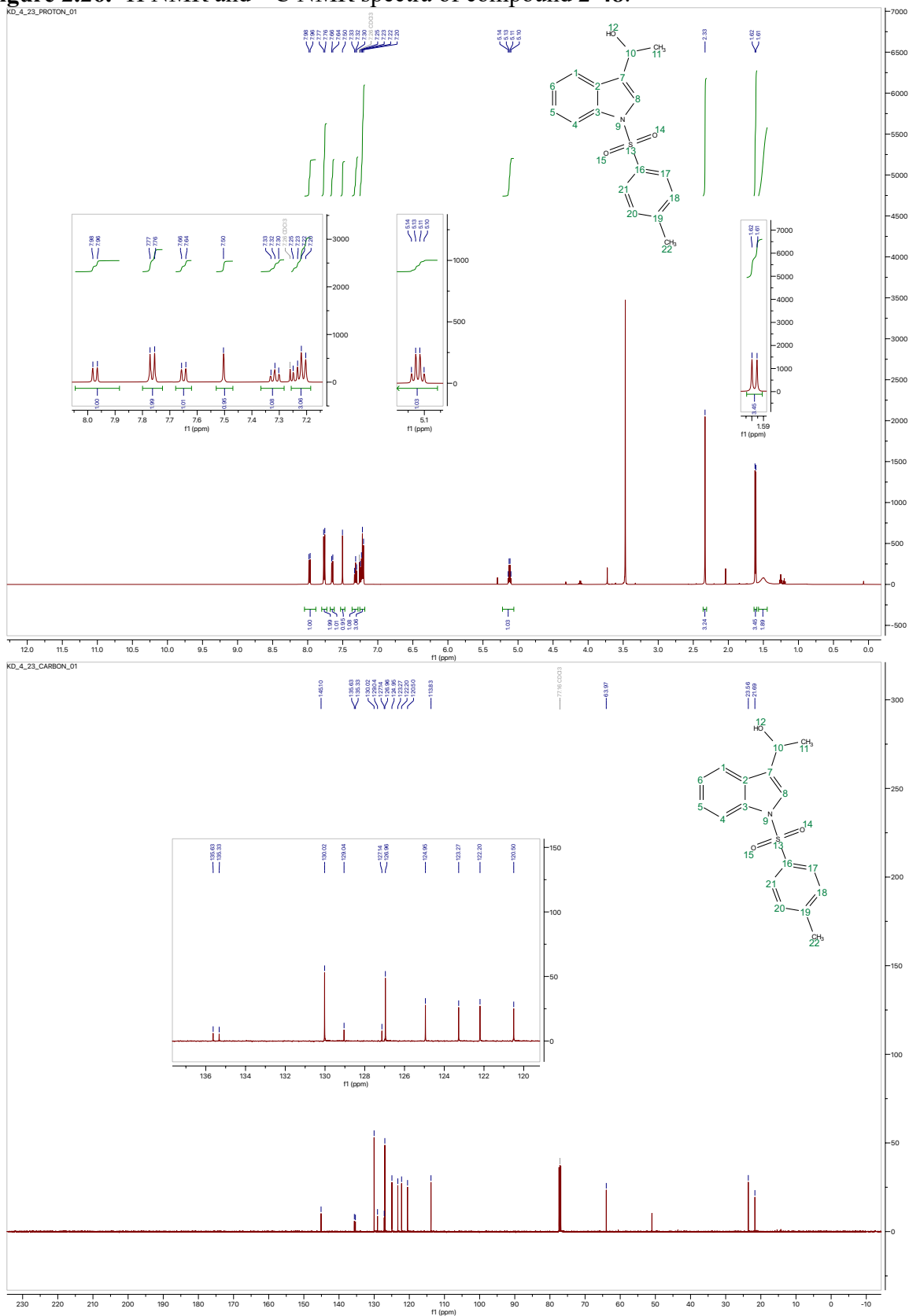


Figure 2.27. ^1H NMR and ^{13}C NMR spectra of compound 2-50.

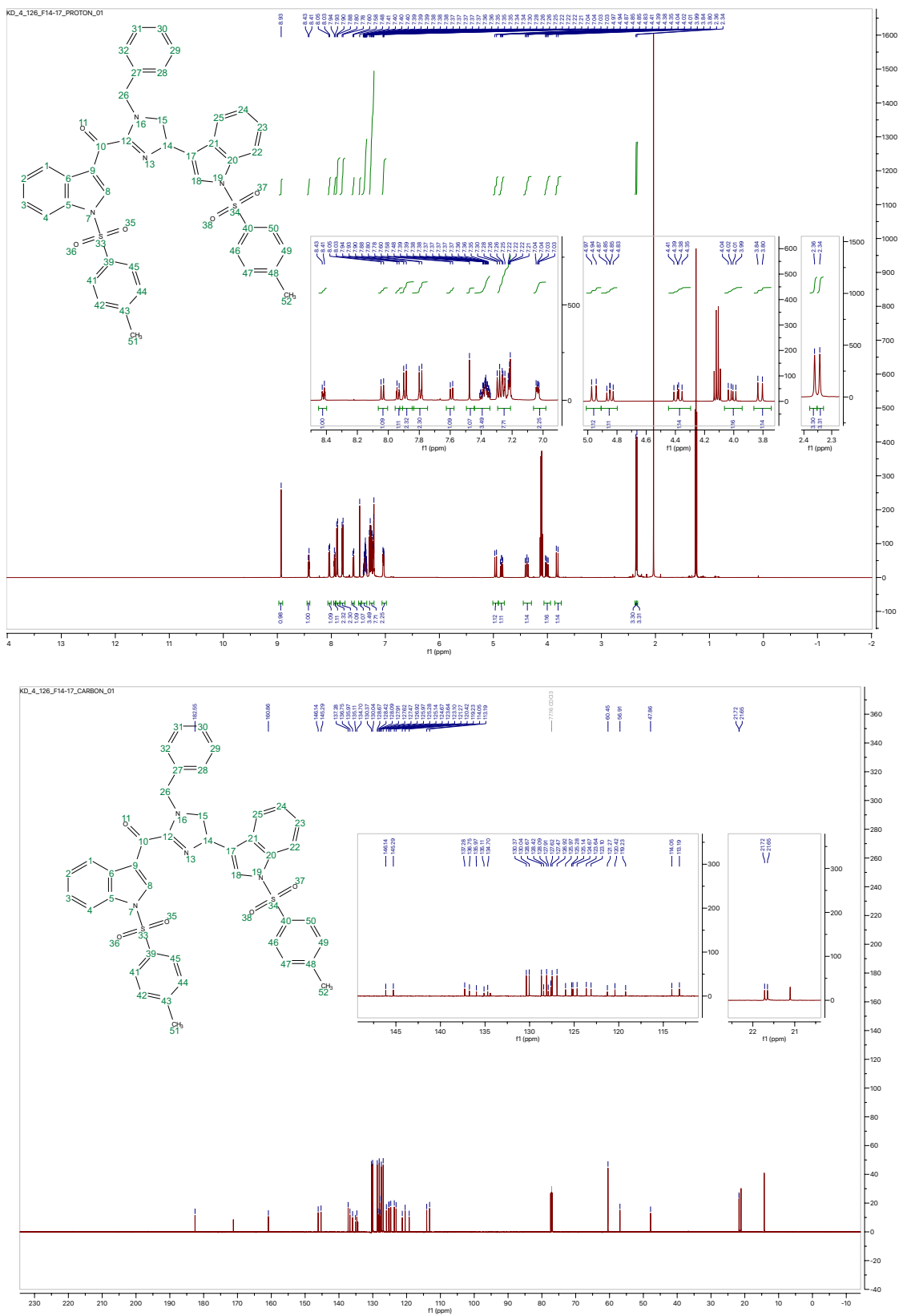


Figure 2.28. ^1H NMR and ^{13}C NMR spectra of compound 2-55.

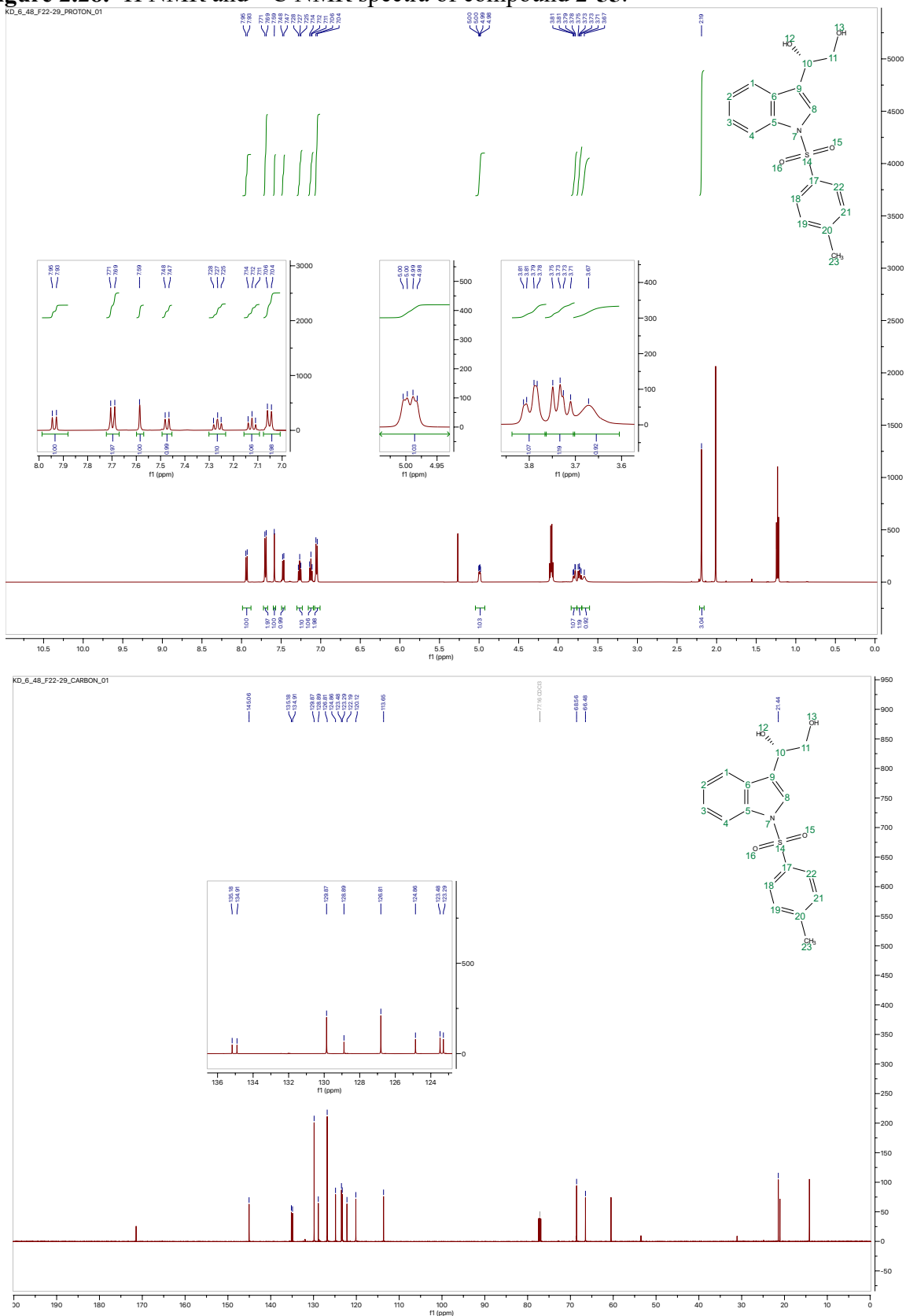


Figure 2.29. ^1H NMR and ^{13}C NMR spectra of compound **2-58**

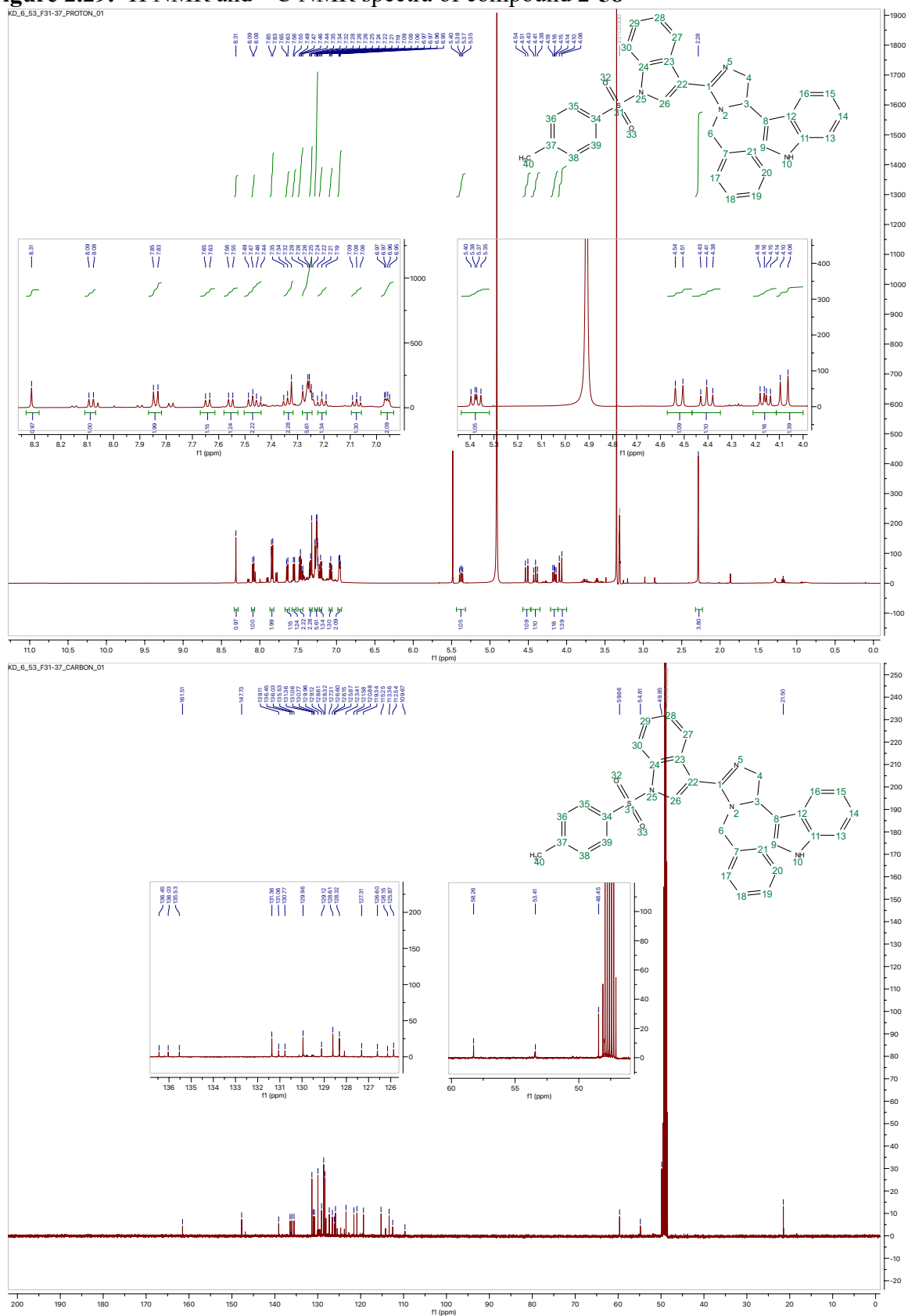


Figure 2.31. ^1H NMR and ^{13}C NMR spectra of compound **2-60**.

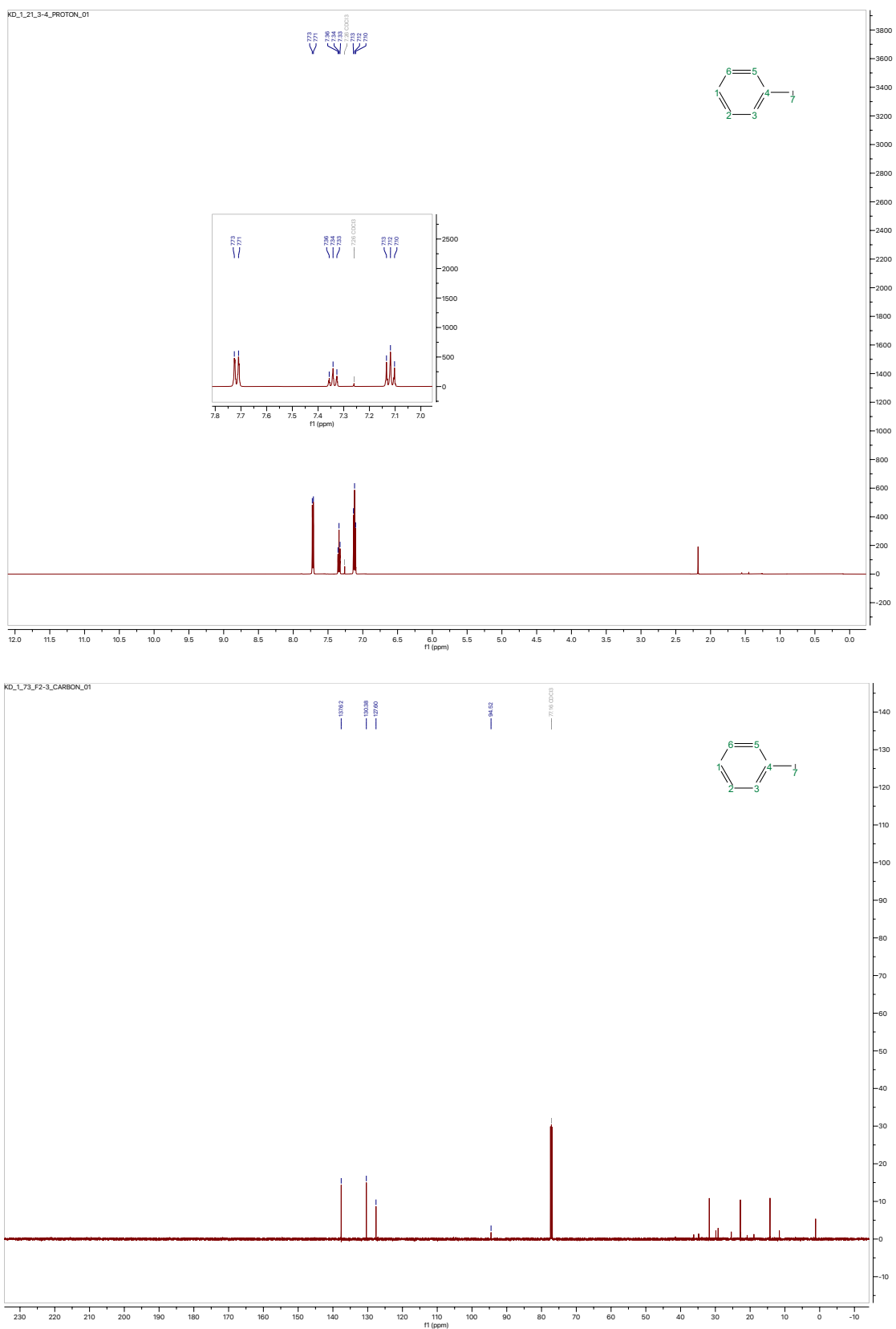


Figure 2.32. ^1H NMR and ^{13}C NMR spectra of compound **2-63**.

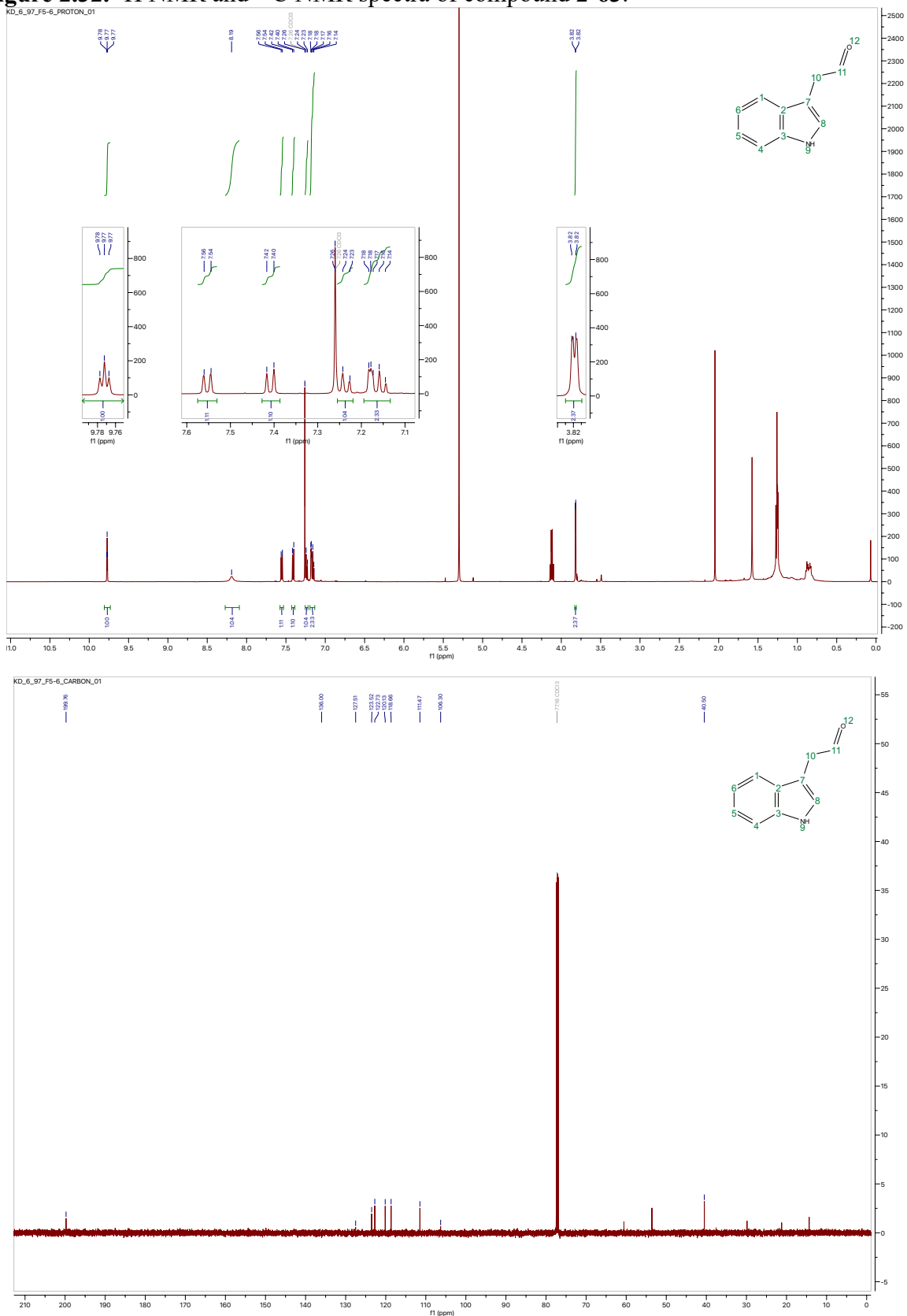


Figure 2.33. ^1H NMR and ^{13}C NMR spectra of compound **2-67**.

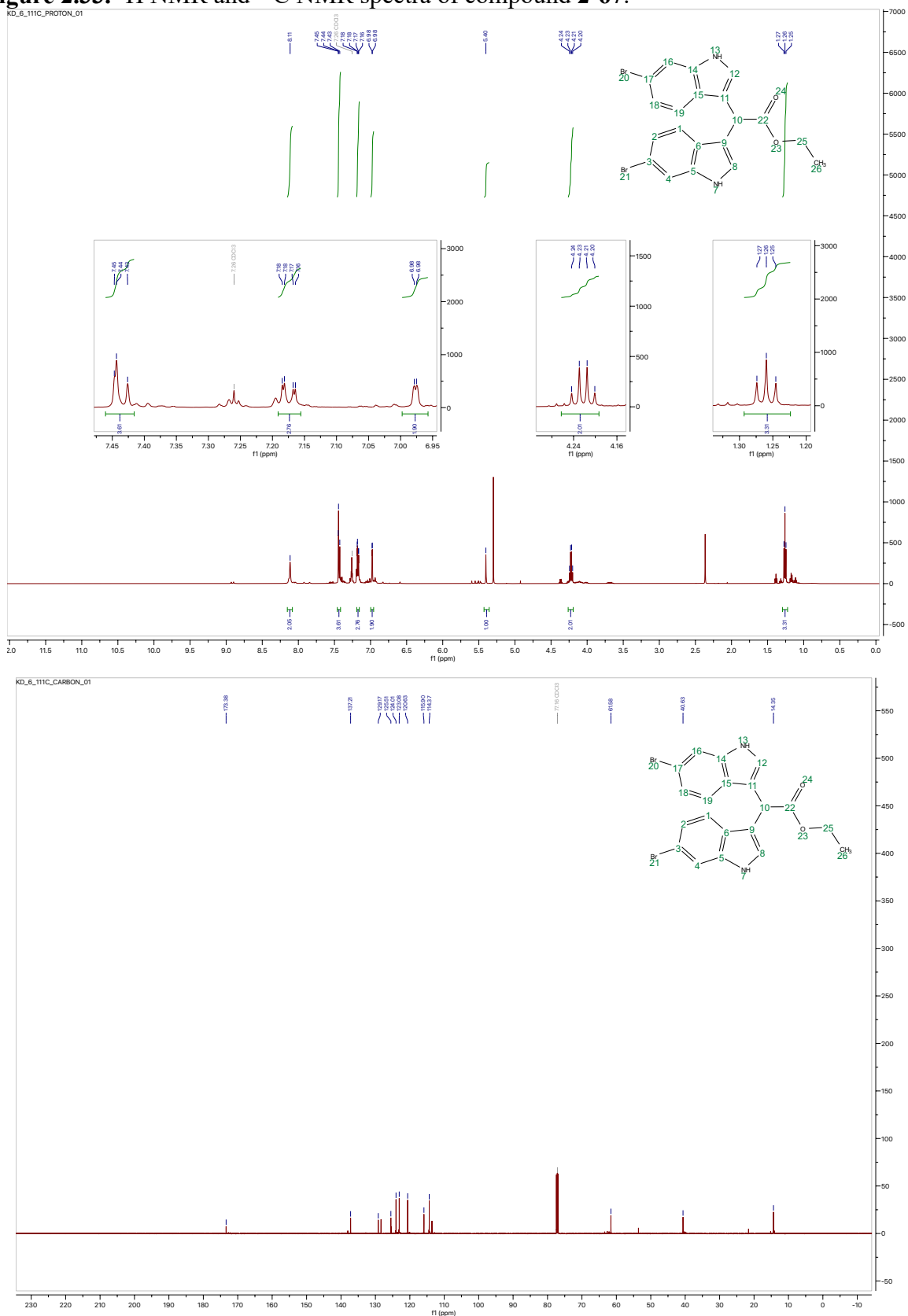


Figure 2.34. ^1H NMR and ^{13}C NMR spectra of compound **2-66**.

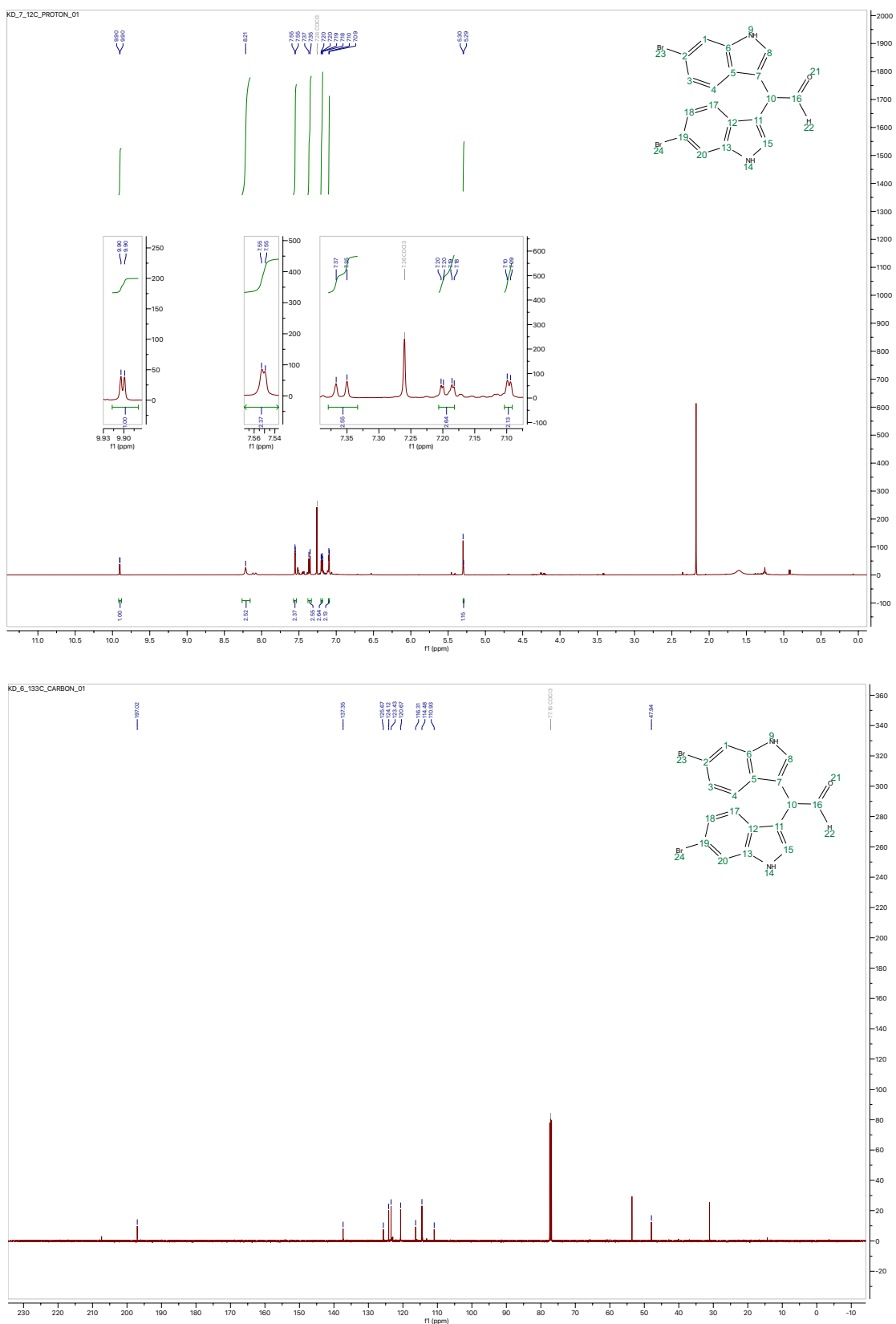


Figure 2.35. ^1H NMR and ^{13}C NMR spectra of compound **2-19**.

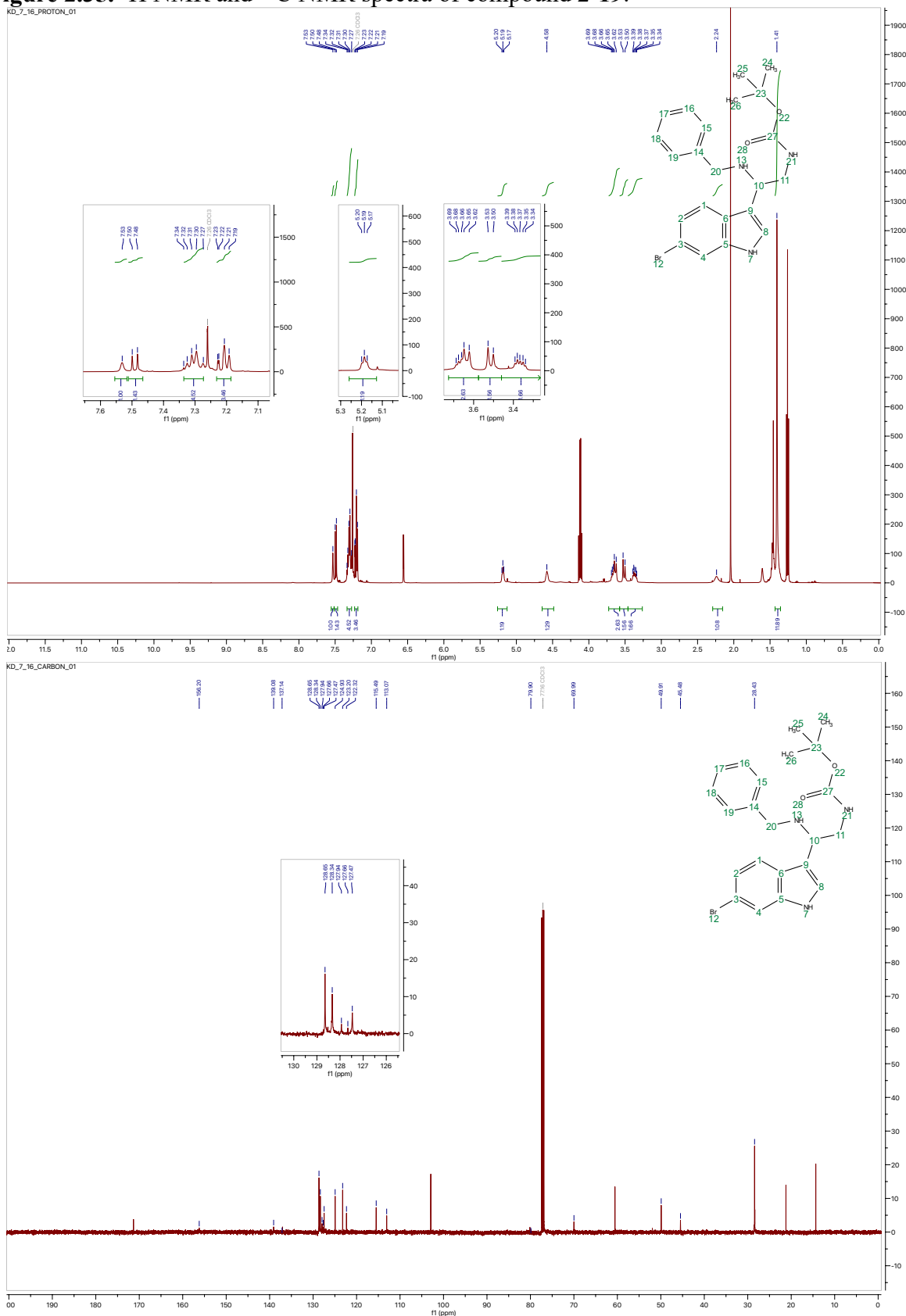
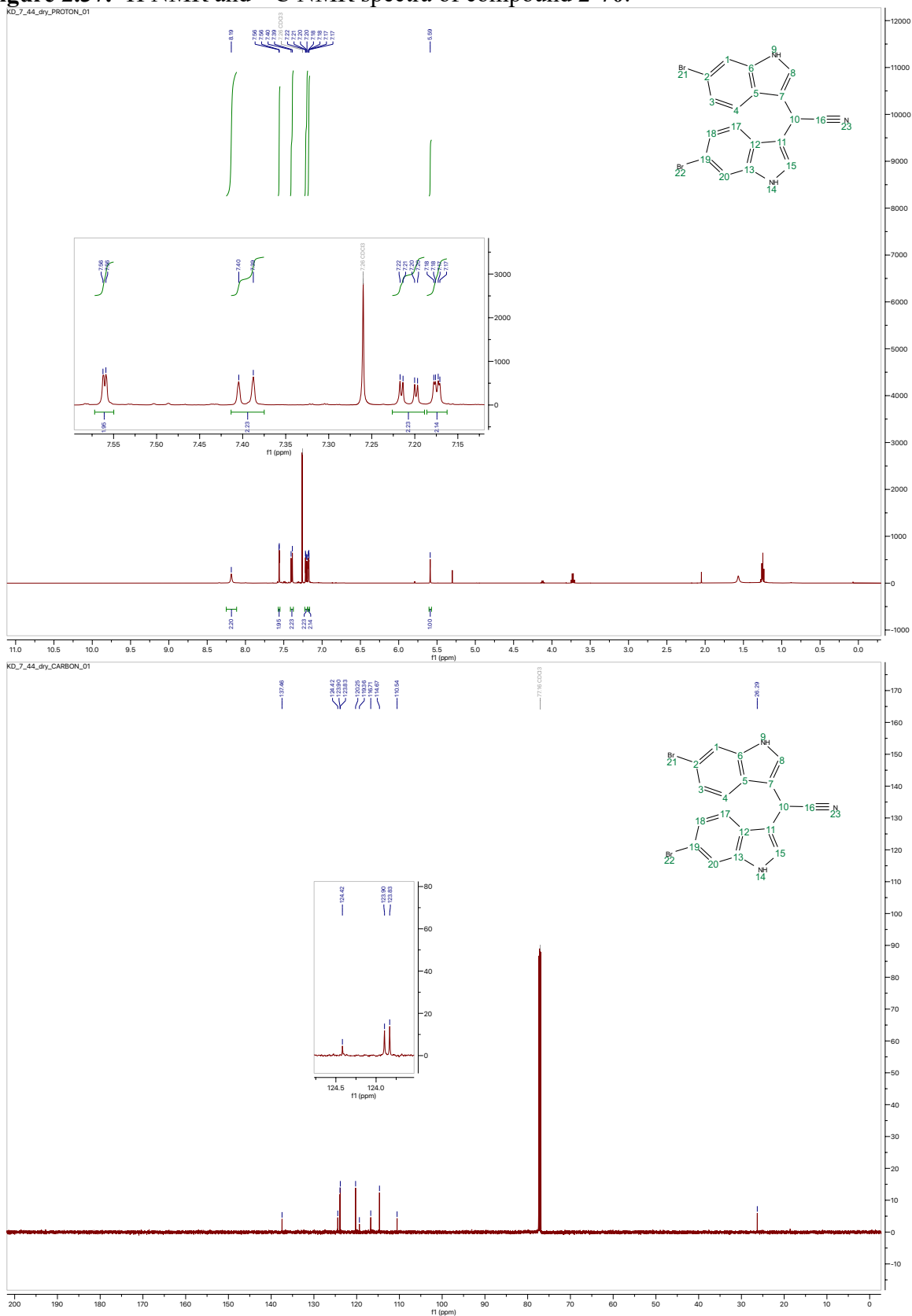


Figure 2.37. ^1H NMR and ^{13}C NMR spectra of compound **2-70**.

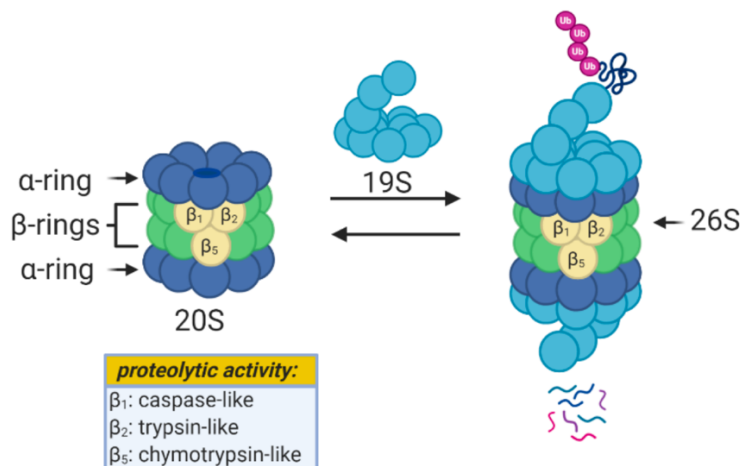


Chapter 3: Synthesis of Small Molecule Acyl-Astemizole Analogues as Activators of the 20S Proteasome

3.1 Introduction

The 26S proteasome is a protein complex in the body that is responsible for the proteolysis of redundant proteins into recyclable peptide fragments.^{1,2,3} As shown in **Figure 3.1**, the 26S proteasome is comprised of one or two 19S regulatory particles which associate with the barrel-shaped 20S core particle. This 20S core particle (also referred to as the 20S proteasome) is comprised of two stacked heptameric beta rings, which are sandwiched between two heptameric alpha rings.¹ The beta rings are responsible for the catalytic proteolytic activity of the proteasome, as they contain the three unique catalytic sites (the chymotrypsin-like (CT-L), trypsin-like (T-L), and caspase-like (Casp-L) sites), and the alpha rings serve as a “gate,” which opens and is activated upon association with the 19S regulatory particle.^{1,2} The 19S regulatory particle not only activates the proteasome by opening the gate, but it also facilitates recognition of “tagged” (ubiquitinated) proteins followed by their subsequent, de-ubiquitination, unfolding, and translocation of the substrate through the gate of the 20S core particle.⁴ The 20S proteasome lacks this 19S regulatory particle and is, therefore, considered the latent state of the proteasome with predominantly closed gates, preventing the degradation of folded proteins. However, it has been shown that the 20S proteasome is able to degrade intrinsically disordered proteins (IDPs) via a ubiquitin-independent mechanism^{5,6} Unfortunately, this IDP proteolysis via the 20S proteasome is hindered by the fact that the 20S proteasome exists primarily in the closed-gate conformation.

Figure 3.1. General diagram of 26S and 20S proteasomes and a ubiquitinated protein substrate.

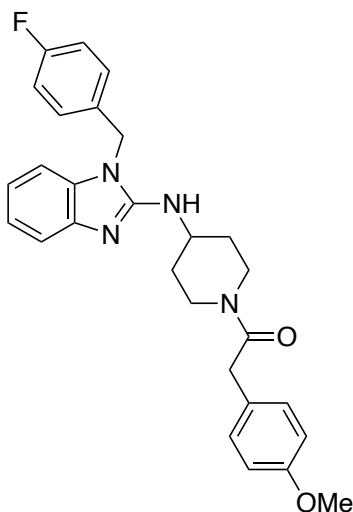


Enhancing the IDP proteolysis would have significant therapeutic implications, as the accumulation of IDPs in the body has been associated with the progression of many neurodegenerative diseases, such as Alzheimer's and Parkinson's disease.⁷ As many neurodegenerative diseases, such as Alzheimer's and Parkinson's disease, have very few FDA approved therapeutics, the development of novel 20S proteasome activators that can facilitate the open-gate conformation of the 20S proteasome and enhance IDP proteolysis has been a primary focus of the Tepe lab.

A potent 20S proteasome activator that has been identified in the Tepe lab is acyl Astemizole, whose structure is shown in **Scheme 3.1**. Dr. Allison Vanecek found that acyl Astemizole displayed an EC_{200} value of 4.6 μ M when probed for enhancement of the 20S proteasome. In addition, acyl Astemizole has drug-like physical properties, with a molecular weight just under 500 g/mol (472.6 g/mol) and a cLogP value of 3.32, in accordance with Lipinski's Rule of Five.^{8,9} Although acyl Astemizole has been shown to display potent proteasome activity, its structure-activity relationship remains largely unexplored. Considering this, acyl Astemizole was identified as a promising target for analogue development. My goal in

this project, in collaboration with Dr. Allison Vanecek, was to design and synthesize acyl Astemizole analogues with improved potency, while maintaining drug-like properties. This chapter will discuss the proteasome activation studies of a small library of synthesized acyl Astemizole analogues.

Scheme 3.1. Chemical structure of acyl Astemizole.



Acyl Astemizole (3-1)

MW: 472.56 g/mol

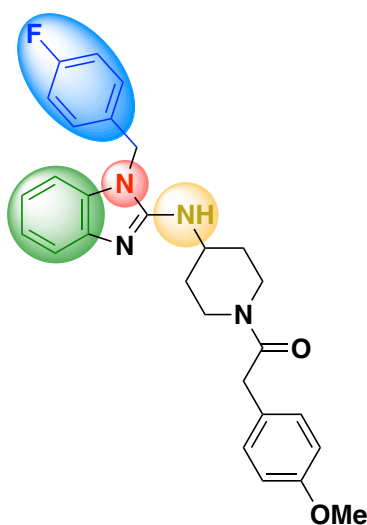
cLog P: 3.32

3.2. Results and Discussion

It was hypothesized that ideal analogues would have comparable or lower molecular weights and comparable cLogP values to that of acyl Astemizole (**3-1**). This would allow for additional modifications to be made to analogues to increase potency, without violating the Lipinski's rule of five.⁹ To begin exploring which structural moieties of acyl Astemizole are necessary for 20S proteasome activation and/or where other structural modifications could be incorporated without decreasing the 20S proteasome activity, initial acyl Astemizole analogues were designed in which portions of the compound were removed to see how the activity was affected. In the first step of analogue design, several key moieties of acyl Astemizole's chemical

structure were identified as potential areas to probe in structure activity relationship studies. As shown in **Scheme 3.2**, the 4-fluoro benzyl protecting group, the fused benzene ring of the benzimidazole core, the nitrogen atom of the benzimidazole core, and the amino linker group were identified as chemical moieties to be probed.

Scheme 3.2 Chemical structure of acyl Astemizole and highlighted functionality to be probed during analogue exploration.



Acyl Astemizole (3-1)

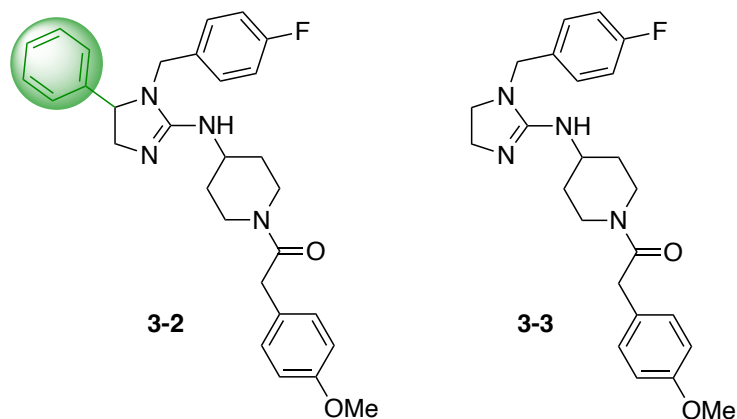
3.2.1. Acyl Astemizole analogue development

3.2.1.1. Class one analogues

The first moiety of acyl Astemizole's chemical structure that was probed via analogue development was the fused benzene ring of the benzimidazole core (green, **Scheme 3.2**). This is a very interesting moiety to investigate because if analogues lacking this fused benzene ring are found to maintain 20S proteasome modulation activity, this would allow for active, significantly lower molecular weight acyl Astemizole analogues. As shown in **Scheme 3.3**, in this first class of analogues, two initial acyl Astemizole imidazoline analogues (**3-2** and **3-3**) were designed for synthesis and biological analysis. To explore the importance of the fused benzene ring of acyl

Astemizole (**3-1**) with respect to its 20S proteasome activity, this moiety was analyzed in stages. The first imidazoline analogue (**3-2**) maintains the benzene ring as a substituent, rather than a fused ring, and the second imidazoline analogue (**3-3**) does not contain the benzene moiety (**Scheme 3.3**).

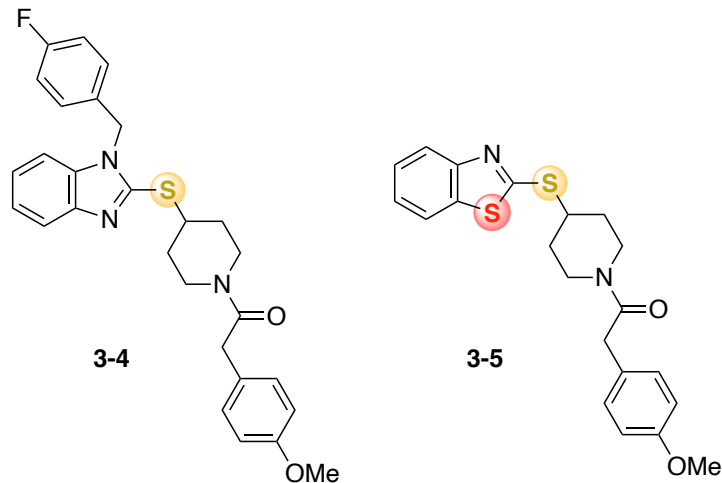
Scheme 3.3. Initial class one acyl Astemizole analogues (**3-2** and **3-3**).



3.2.1.2. Class two analogues

The second class of acyl Astemizole analogues that was developed was focused on probing acyl Astemizole's nitrogen linker atom (yellow, **Scheme 3.2**) and the nitrogen atom of the benzimidazole core (red, **Scheme 3.2**). These analogues were designed to explore the scope of the structure-activity relationship of the linker atom and heterocyclic core of acyl Astemizole. As shown in **Scheme 3.4**, initially, two thio-linker analogues were developed. To study these structural changes in a stepwise manner, a thio-linker acyl Astemizole was designed (**3-4**), as well as a thio-linker analogue with a benzimidazole core (**3-5**) (**Scheme 3.4**). Analogue **3-5** was particularly interesting as its synthesis would not only allow for investigation into the scope of the heterocyclic core of acyl Astemizole (**3-1**), but it would also allow for initial exploration of the importance of the 4-fluorobenzyl moiety.

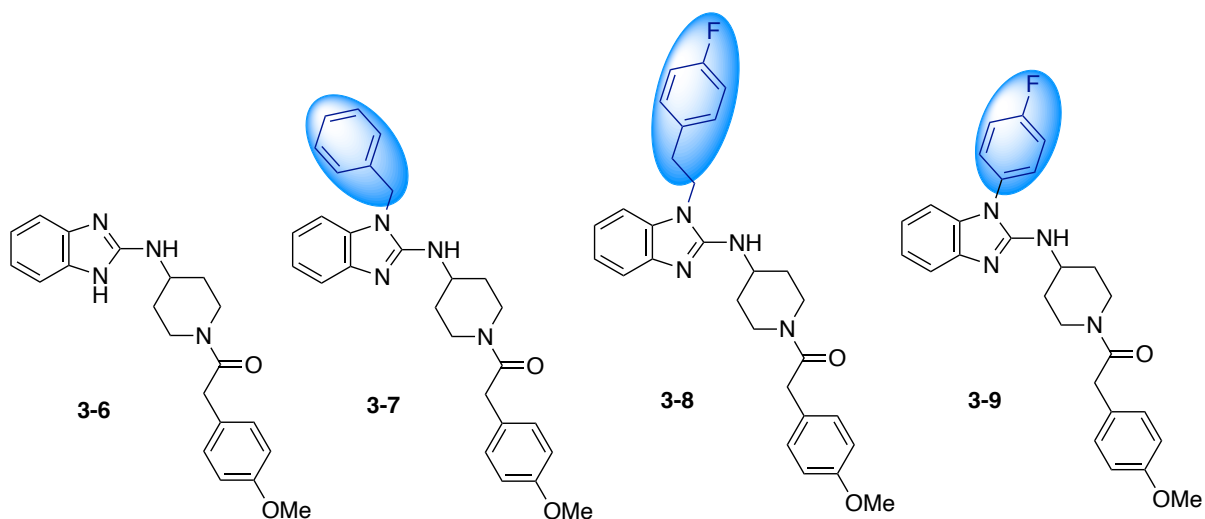
Scheme 3.4. Initial class two acyl Astemizole analogues (**3-4** and **3-5**).



3.2.1.3. Class three analogues

The third class of acyl Astemizole analogues that was developed was aimed at probing the 4-fluorobenzyl group (blue, **Scheme 3.2**) of acyl Astemizole (**3-2**). Similar to class one, this aryl moiety would be interesting to probe because if analogues lacking this aryl ring are found to maintain 20S proteasome modulation activity, this would allow for active, significantly lower molecular weight acyl Astemizole analogues. Therefore, as shown in **Scheme 3.5**, the first class three analogue that was designed was debenzylated acyl Astemizole (**3-6**) to determine if this aryl ring was necessary for 20S proteasome activity. On the other hand, in exploration of different aryl groups, three additional analogues were designed. As shown in **Scheme 3.5**, the first was an analogue bearing a benzyl group (**3-7**) in order to explore the importance of the fluoro-substituent on biological activity. Then, two analogues exploring aryl moiety linker length were also designed: one with one additional methylene (**3-8**) and one with one less methylene (**3-9**) (**Scheme 3.5**).

Scheme 3.5. Initial class three acyl Astemizole analogues (**3-6**, **3-7**, **3-8**, and **3-9**).



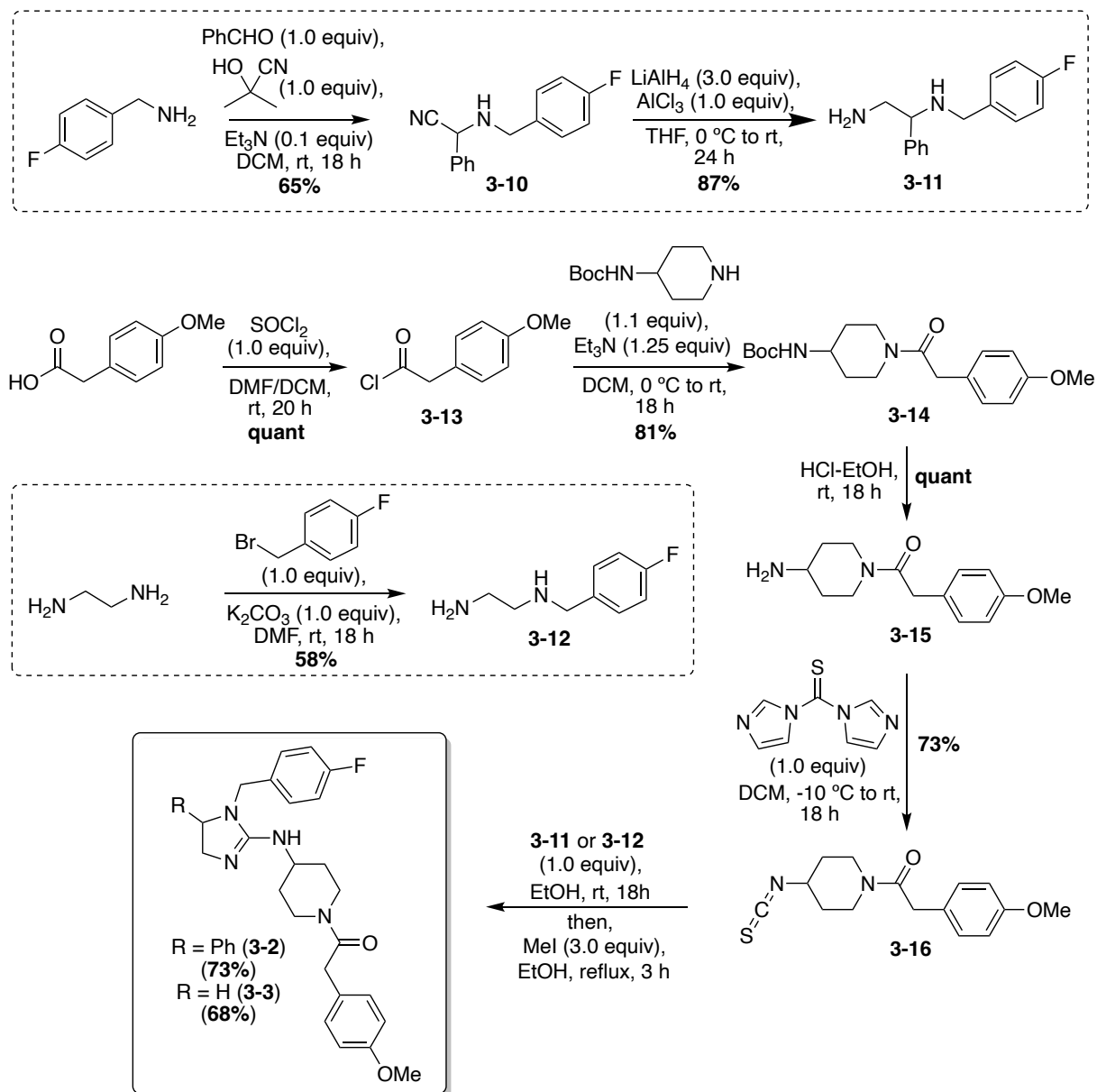
3.2.2. Acyl Astemizole analogue synthesis

3.2.2.1. Class one acyl Astemizole analogue syntheses

The first class one acyl Astemizole analogue to be synthesized was the imidazoline analogue bearing the phenyl substituent (**3-2**). It was hypothesized that this imidazoline analogue could be accessed via a late stage imidazoline cyclization of a diamine fragment with an isothiocyanate intermediate. Similar cyclizations have been reported in literature.¹⁰ As shown in **Scheme 3.6**, first, the diamine intermediate (**3-11**) was synthesized in two steps from the commercially available 4-fluorobenzylamine via a Strecker reaction and a subsequent cyanide reduction in high yields. Then, the commercially available 2-(4-methoxyphenyl)acetic acid was quantitatively converted to the respective acyl chloride (**3-13**) and this acyl chloride intermediate (**3-13**) was used to acylate the commercially available *tert*-butyl piperidin-4-ylcarbamate to access the protected amino-piperidine intermediate (**3-14**) in 81% yield. This piperidine intermediate (**3-14**) was then quantitatively deprotected and subsequently underwent isothiocyanate formation via 1,1'-thiocarbonyldiimidazole (TCDI) to access the isothiocyanate

intermediate (**3-16**) in 73% yield. The last step of this synthesis was the imidazoline cyclization in which the diamine intermediate (**3-11**) was condensed with the isothiocyanate intermediate (**3-16**) to the corresponding thiourea, followed by methylation, cyclization, and loss of a thiol group to form the desired imidazoline analogue (**3-2**) in 73% yield.

Scheme 3.6. Synthesis of initial class one acyl Astemizole imidazoline analogues (**3-3** and **3-4**).



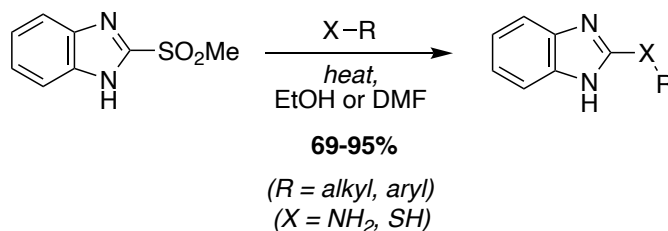
As shown in **Scheme 3.6**, the imidazoline analogue lacking the phenyl substituent (**3-3**) was synthesized in the same manner as **3-2**. The only difference was the structure of the diamine intermediate (**3-12**). This diamine intermediate (**3-12**) was synthesized in one step via mono-4-fluorobenylation of the commercially available ethylenediamine to access **3-12** in 58% yield. This diamine intermediate then underwent the same condensation/methylation/cyclization sequence with the isothiocyanate intermediate (**3-16**) to access the desired acyl Astemizole imidazoline analogue (**3-3**) in 68% yield.

3.2.2.2. Class two acyl Astemizole analogue syntheses

3.2.2.2.1. Thio-linker analogue synthesis

It was hypothesized that the thio-linker analogue (**3-4**) could be accessed via a late-stage oxidative nucleophilic displacement of a sulfone group as a good leaving group. Similar transformations have been previously reported in literature for the synthesis of 2-amino and 2-thio benzimidazoles from 2-methylsulfonyl benzimidazole, as shown in **Scheme 3.7**.¹¹ The 2-methylsulfonyl benzimidazole starting material can be readily synthesized via a mild oxidation of 2-methylthio-benzimidazole via *meta*-chloroperoxybenzoic acid (*m*-CPBA) following literature procedures.¹²

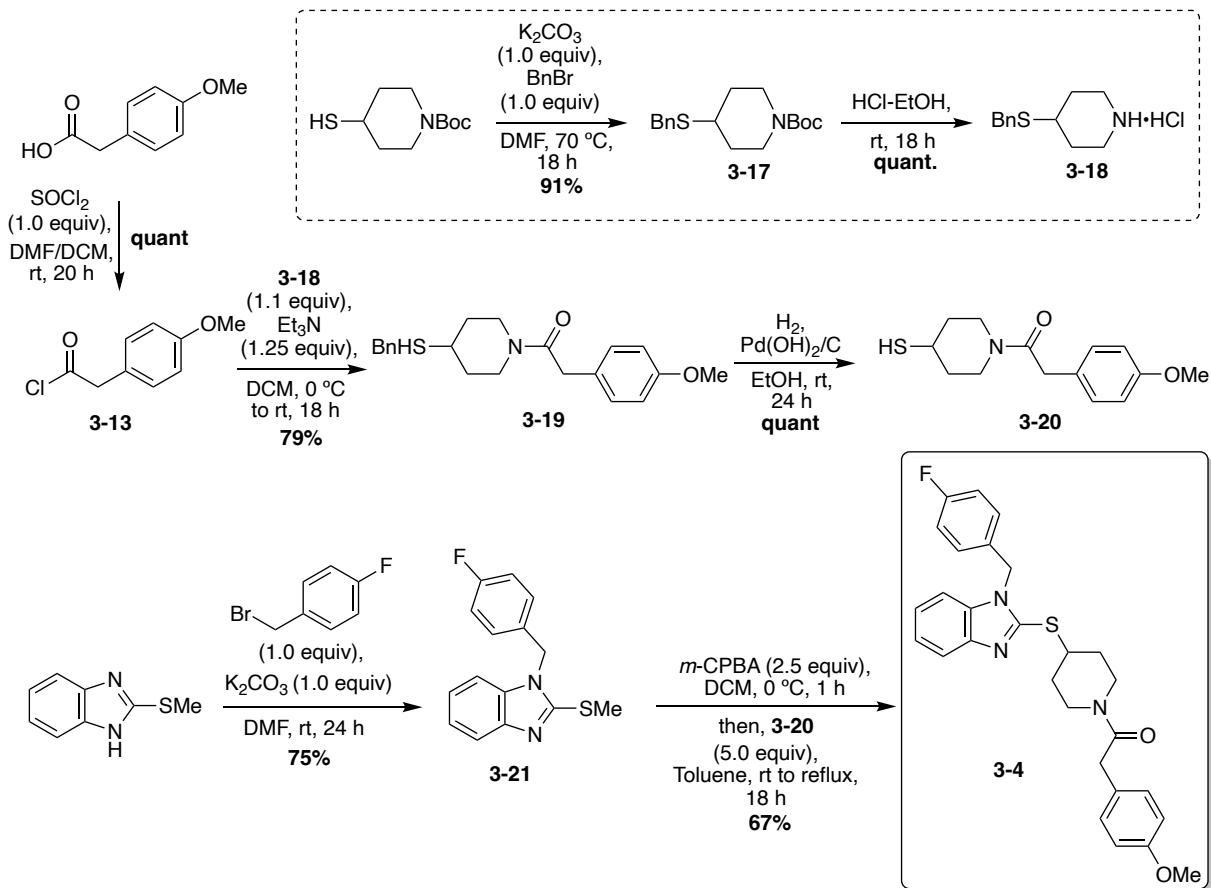
Scheme 3.7. Previous work reported for the synthesis of 2-amino and 2-thio benzimidazoles from 2-methylsulfonyl benzimidazole.



Application of this methodology was used for the synthesis of the thio-linker acyl Astemizole analogue (**3-4**) using a complex sulfur nucleophile (**3-20**), as shown in **Scheme 3.8**.

In the synthesis of **3-4**, the 4-benzylthiopiperidine intermediate (**3-18**) was first achieved via benzylation and subsequent acid-mediated Boc-deprotection in very high yields. Next, the *N*-acylated 4-thio piperidine nucleophile (**3-20**) was synthesized in three steps from the commercially available 2-(4-methoxyphenyl)acetic acid via acid chloride formation, acylation of the piperidine intermediate (**3-18**), and subsequent de-benzylation in high yields (**Scheme 3.8**). With the sulfur nucleophile (**3-20**) in hand, the key late-stage oxidative nucleophilic displacement of the sulfone group could be explored. After 4-fluorobenylation of 2-(methylthio)-1*H*-benzo[*d*]imidazole to access **3-21**, the resulting protected 2-methylthio-benzimidazole intermediate (**3-21**) was subjected to oxidative conditions via *m*-CPBA to install the sulfone moiety. Immediately after oxidation, the recently formed sulfone intermediate was subjected to nucleophilic attack by **3-20** to displace the sulfone group, accessing the desired thio-linker analogue (**3-4**) in 67% yield (**Scheme 3.8**).

Scheme 3.8. Synthesis of thio-linker acyl Astemizole analogue (**3-4**).

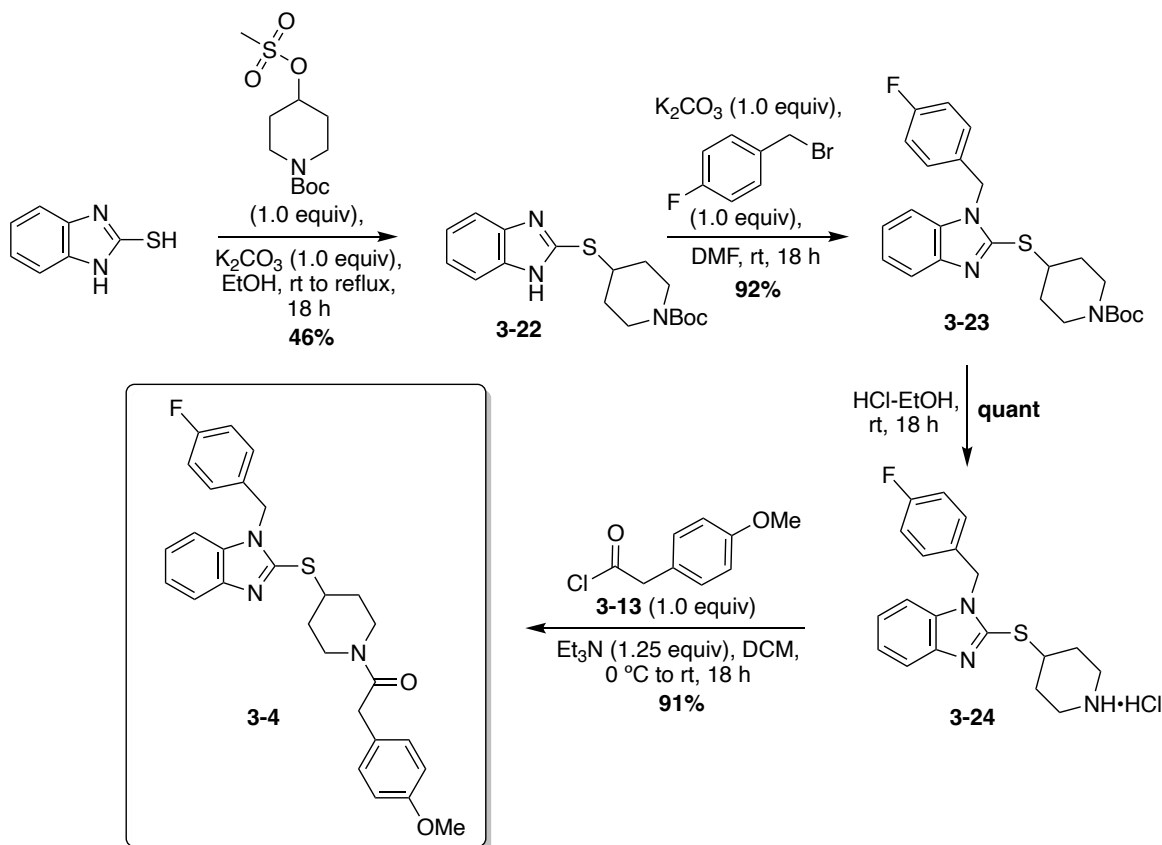


To design a more expeditious synthetic route toward acyl Astemizole analogues that structurally resemble **3-4**, an additional approach was explored. Instead of going through step-intensive synthesis of the *N*-acylated 4-thiopiperidine nucleophile (**3-20**), this process was expedited by installing the piperidine moiety at an earlier stage. As shown in **Scheme 3.9**, 2-thiobenzimidazole underwent base-mediated nucleophilic attack on the commercially available *N*-Boc-4-mesyloxypiperidine, as has been reported in literature for similar transformations.¹³ After this nucleophilic attack to displace the mesyloxy moiety, the piperidine substituted intermediate (**3-22**) was accessed in 46% yield. Intermediate **3-22** then underwent 4-fluorobenzoylation and subsequent Boc deprotection to access intermediate **3-24** in very high yields. The last step was acylation of the piperidine intermediate (**3-24**) via the same acyl

chloride intermediate (**3-13**) to access the thio-linker analogue (**3-4**) in 91% yield (**Scheme 3.9**).

This adapted approach, including the aforementioned single step to access the acyl chloride intermediate (**3-13**), was five steps overall. This was significantly more expedited than the previous approach, which consisted of seven steps overall (**Scheme 3.8**).

Scheme 3.9. Expedited synthesis of the acyl Astemizole thio-linker analogue (**3-4**).



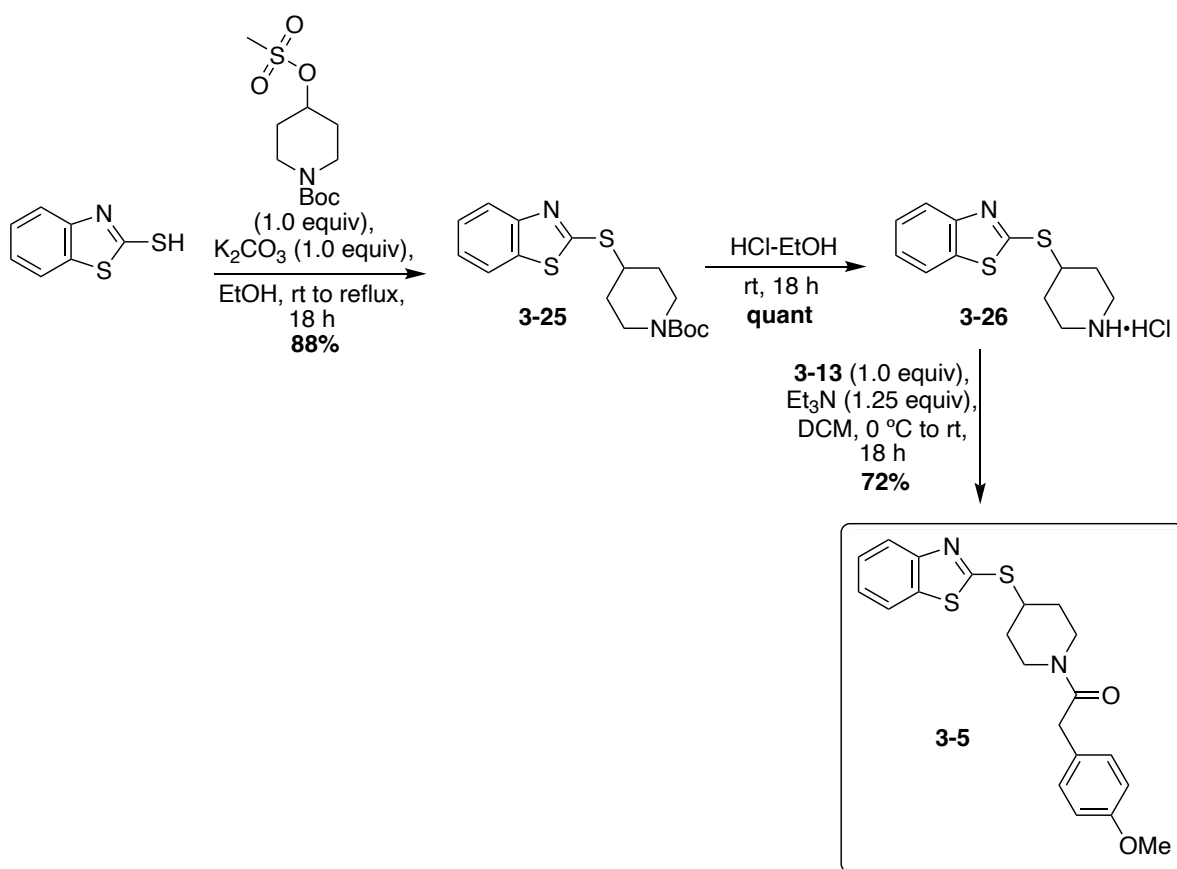
3.2.2.2.1. Thio-linker benzothiazole analogue synthesis

The thio-linker benzothiazole analogue (**3-5**) was synthesized via the same procedure as was previously discussed for the expedited synthesis of **3-4**. As shown in **Scheme 3.10**, the commercially available 2-mercaptobenzothiazole was reacted with the commercially available N -Boc-4-mesyloxypiperidine to undergo nucleophilic displacement of the mesyloxy group, accessing the desired piperidine-substituted intermediate (**3-25**) in 88% yield. This yield was

significantly higher than that of the previously discussed **3-22** (Scheme 3.9). It is noteworthy to mention that the conversion in both nucleophilic displacement reactions was high. Therefore, the isolation method was likely the cause of these significantly different yields, as **3-22** was isolated via filtration of the formed precipitate and **3-25** was isolated via column chromatography.

Column chromatography appeared to be the superior form of isolation for this reaction. The protected piperidine intermediate (**3-25**) was quantitatively Boc-protected and subsequently underwent acylation via the acyl chloride intermediate (**3-13**) to access the desired thio-linker benzothiazole analogue (**3-5**) in 72% yield.

Scheme 3.10. Synthesis of the thio-linker benzothiazole analogue (**3-5**).

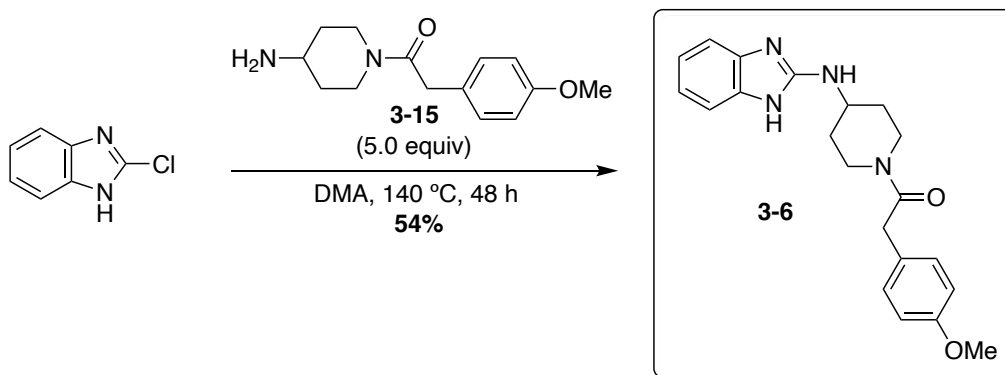


3.2.2.3. Class three acyl Astemizole analogue syntheses

3.2.2.3.1. Debenzylated acyl Astemizole analogue synthesis

In the synthesis of the debenzylated acyl Astemizole analogue (**3-6**), a different synthetic route was devised in order to allow for the synthesis of the free benzimidazole core. It was hypothesized that this analogue (**3-6**) could be expeditiously synthesized via a thermal coupling of the commercially available 2-chlorobenzimidazole and the previously synthesized *N*-acylated 4-amino piperidine tail (**3-15**). Similar thermal couplings have been reported in literature in the synthesis of Astemizole and related analogues.¹⁴ As shown in **Scheme 3.11**, commercially available 2-chlorobenzimidazole underwent thermal coupling with an excess of the *N*-acylated 4-aminopiperidine tail to afford the debenzylated acyl Astemizole analogue (**3-6**) in 54% yield.

Scheme 3.11. Synthesis of the debenzylated acyl Astemizole analogue (**3-6**).

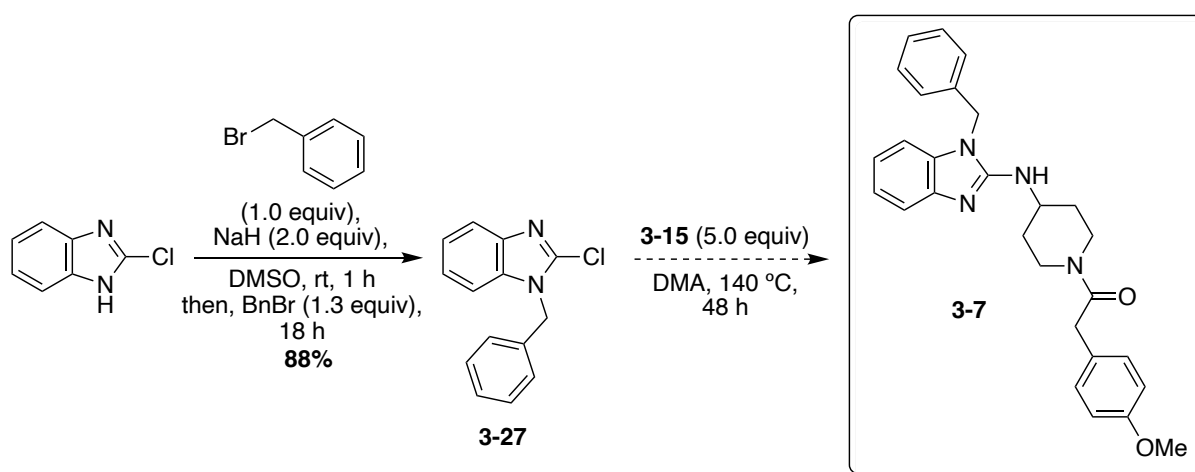


3.2.2.3.2. Progress toward synthesis of the benzylated analogue

It was proposed that the benzylated acyl Astemizole analogue (**3-7**) could be synthesized via the same thermal coupling approach as was previously used in the synthesis of **3-6**. Contrary to this, the previously discussed approach to the thio-linker analogues (**3-4** and **3-5**, **Scheme 3.9** and **3.10**) was identified as potentially problematic for the nitrogen linker analogues due to possible regioselectivity issues that could arise with the late-stage acylation. Therefore, the thermal coupling method was identified as the most favorable approach for synthesis of acyl

Astemizole analogues containing nitrogen linker atoms. As shown in **Scheme 3.12**, in the synthesis of **3-7**, commercially available 2-chlorobenzimidazole was benzylated to access the benzylated 2-chlorobenzimidazole intermediate (**3-27**) in 88% yield. The next proposed step in this synthesis was the thermal coupling of **3-27** and **3-15** to access the benzylated acyl Astemizole analogue (**3-7**). This last thermal coupling step remains a point of focus for the future.

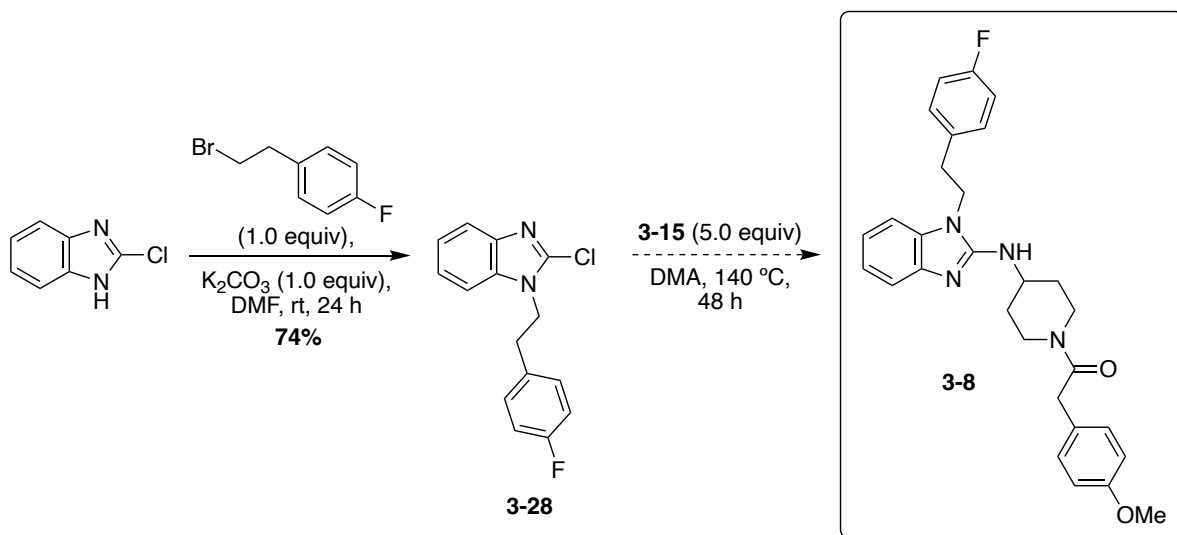
Scheme 3.12. Synthesis of the benzylated acyl Astemizole analogue (**3-7**).



3.2.2.3.3. Progress toward synthesis of the two methylene aryl linker analogue

It was proposed that the acyl Astemizole analogue containing an extra aryl linker methylene (**3-8**) could be synthesized via the same thermal coupling approach as was previously used in the synthesis of **3-6** and **3-7**. As shown in **Scheme 3.13**, the commercially available 2-chlorobenzimidazole was first alkylated with the commercially available 1-(2-bromoethyl)-4-fluorobenzene to access the desired alkylated intermediate (**3-28**) in 74% yield. The next proposed step in this synthesis was the thermal coupling of **3-28** and **3-15** to access the acyl Astemizole analogue containing an extra aryl linker methylene (**3-8**). This last thermal coupling step remains a point of focus for the future.

Scheme 3.13. Synthesis of the acyl Astemizole analogue containing an extra aryl linker methylene (**3-8**).

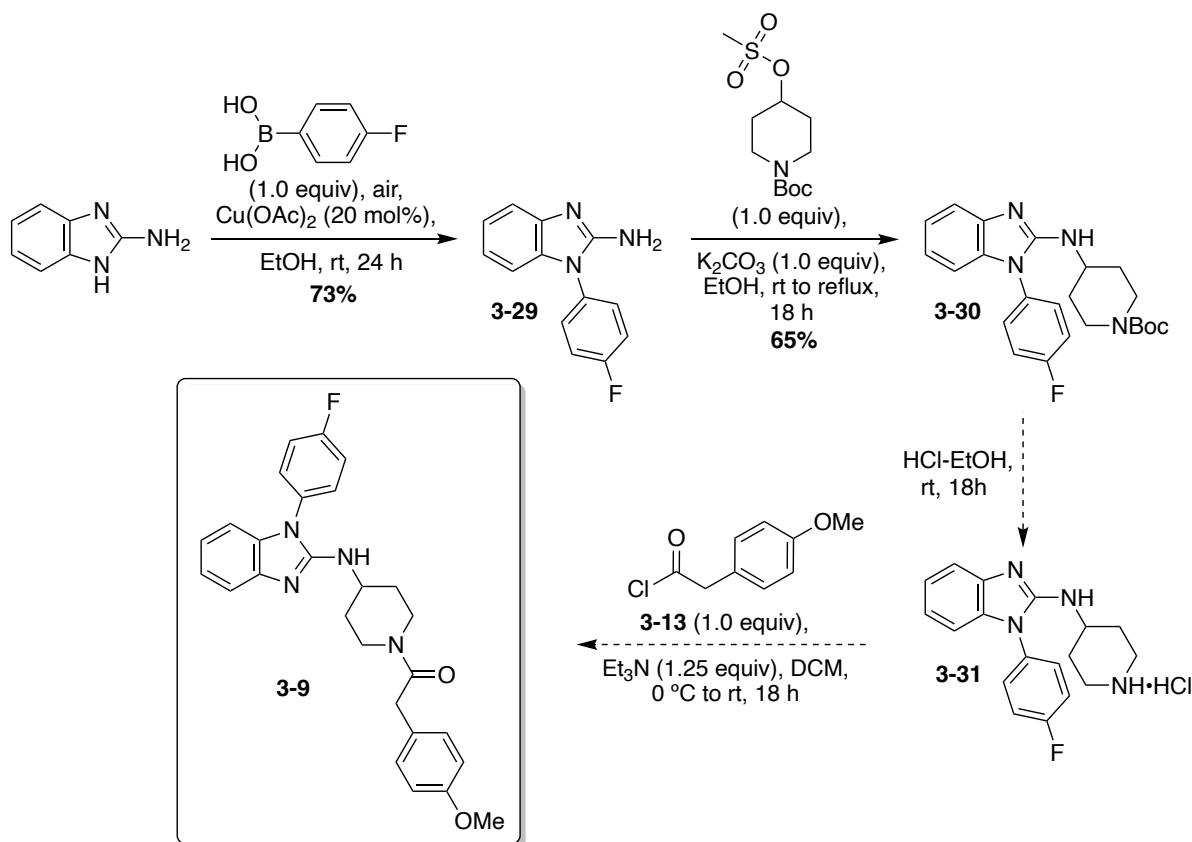


3.2.2.3.4. Progress toward synthesis of the 4-fluorophenyl substituted analogue

Due to synthetic limitations in the formation of 2-chloro-1-(4-fluorophenyl)-benzimidazole as an intermediate, unfortunately, the thermal coupling approach was not viable for the synthesis of the 4-fluorophenyl substituted analogue (**3-9**). Therefore, despite the aforementioned potential regioselectivity issues with the late-stage acylation, the same method that was used in the synthesis of the thio-linker analogues (**3-4** and **3-5**, **Scheme 3.9**) was proposed for the synthesis of **3-9**. As shown in **Scheme 3.14**, first, commercially available 2-aminobenzimidazole underwent a Chan-Lam coupling reaction to afford the 4-fluorophenyl intermediate (**3-29**) in 73% yield, following literature procedures.¹⁵ Then, **3-29** was reacted with the commercially available *N*-Boc-4-mesyloxypiperidine to undergo nucleophilic displacement of the mesyloxy group, accessing the desired piperidine-substituted intermediate (**3-30**) in 65% yield. The last two proposed steps for the synthesis of **3-9** include acid-mediated Boc-deprotection and subsequent late-stage acylation of the piperidine (**3-31**) with the acyl chloride

intermediate (**3-13**) to access the 4-fluorophenyl substituted analogue (**3-9**). These last two steps remain a point of future exploration and optimization.

Scheme 3.14. Synthesis of the 4-fluorophenyl substituted acyl Astemizole analogue (**3-9**).

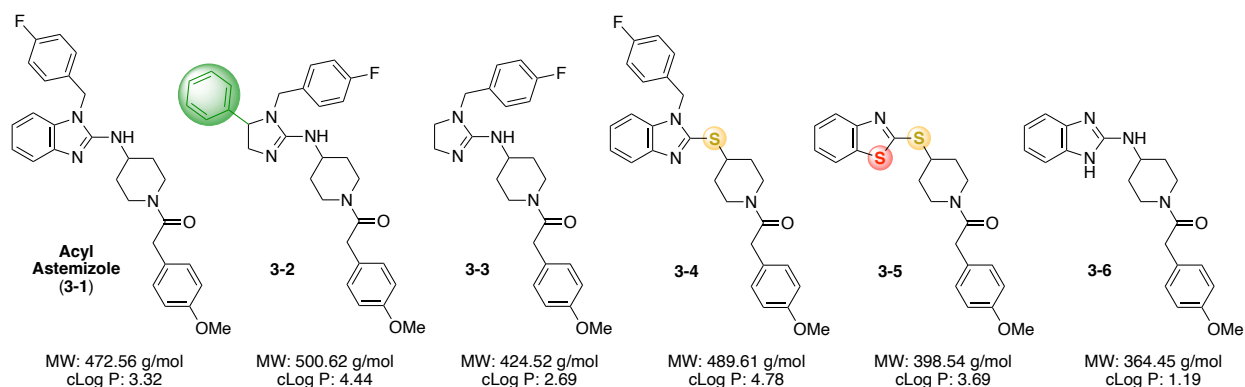


3.2.3. Initial acyl Astemizole analogue 20S proteasome activity studies

The 20S proteasome activity of these synthesized acyl Astemizole analogues was explored in collaboration with Dr. Allison Vanecek. Dr. Vanecek tested these analogues via a fluorogenic peptide degradation assay which utilized short peptide substrates conjugated to the fluorophore 7-amino-4-methylcoumarin (AMC). The three fluorogenic substrate probes Suc-LLVY-AMC, Boc-LRR-AMC, and Z-LLE-AMC were used to test for the activity of the 20S proteasome's three unique catalytic sites, the chymotrypsin-like (CT-L), trypsin-like (T-L), and

caspase-like (Casp-L) sites, respectively. To explore the ability of these synthesized acyl Astemizole analogues to enhance 20S proteasome activity, purified human 20S proteasome was pretreated with varying concentrations of the acyl Astemizole analogue, followed by addition of the fluorogenic substrate probe(s). Proteolytic cleavage of the peptide results in the release of AMC. The resulting fluorescence from the release of this AMC is measured as a rate over time to quantify 20S proteolytic activity. As shown in **Figure 3.2**, the calculated max fold increase and EC_{200} values were calculated. All biological data was collected in triplicate (n=3).

Figure 3.2. Chemical structures of acyl Astemizole analogues and exploration of their 20S proteasome modulation activity.



Enhancement of 20S Proteasome Activity		
	Max Fold Increase	EC_{200} (μ M)
Acyl Astemizole (3-1)	8.3 ± 1.0	4.6 ± 1.2
3-2	2.9 ± 0.5	2.7 ± 0.7
3-3	5.5 ± 1.4	8.4 ± 1.1
3-4	4.2 ± 1.1	3.7 ± 0.6
3-5	6.2 ± 0.7	8.1 ± 1.2
3-6	1.8 ± 0.5	>80.0

The imidazoline acyl Astemizole analogues (**3-2** and **3-3**) were studied to explore the importance of the fused benzene ring of acyl Astemizole's benzimidazole core. As shown in **Figure 3.2**, the 20S proteasome activity assay results for the phenyl imidazoline analogue (**3-2**)

showed maximum fold enhancement of 2.9-fold (i.e. 290%) over the vehicle at the highest concentration tested and an EC₂₀₀ value of 2.7 μM. It is notable to mention that the EC₂₀₀ value represents the concentration of the drug, or analogue, required to increase the activity by 200%. Compared to acyl Astemizole (**3-1**), **3-2** showed a large decrease in the maximum fold increase compared to acyl Astemizole, but an almost two-fold increase in potency, emphasizing the importance of this aryl ring for 20S proteasome modulation activity. This also indicated that the phenyl ring did not have to be fused to the benzimidazole core to allow for activity but could also be present as a substituent. To further study the relationship of this benzene moiety to the 20S proteasome activity, the imidazoline analogue lacking the phenyl substituent (**3-3**) was also analyzed. The results showed lower maximum fold increase and an almost two-fold loss in potency, with an EC₂₀₀ of 8.5 μM, compared to acyl Astemizole (**3-1**) (**Figure 3.2**). Overall, these findings emphasize the importance of this benzene ring moiety to the 20S proteasome activity.

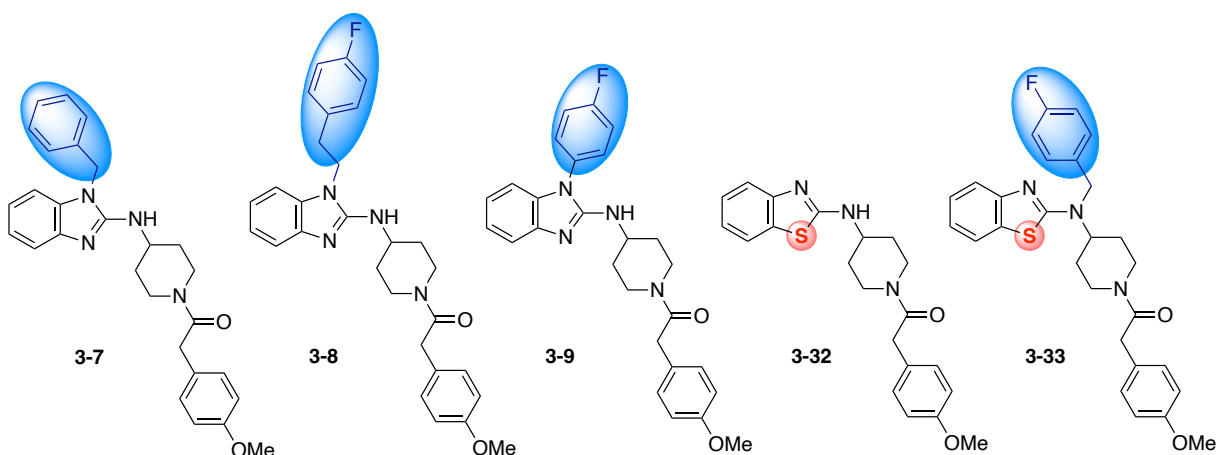
To explore if the incorporation of a thio-linker, rather than an amino-linker, in the 2-position of the benzimidazole core would maintain activity, analogue **3-4** was studied. As shown in **Figure 3.2**, although the maximum fold increase in activity over the vehicle was decreased, the EC₂₀₀ value was comparable to that of acyl Astemizole, suggesting replacement of the amine with a sulfur atom maintains 20S proteasome activity and is a feasible option for future analogues. Another thio-linker analogue with a benzothiazole core (**3-5**) was also analyzed and was found to be moderately active (EC₂₀₀ = 8.1 μM). However, since analogue **3-5** had two scaffold changes compared to **3-4**, additional analogues are required to determine whether the leap this moderately active is due to the benzothiazole core, or loss of the 4-fluorobenzyl moiety.

To explore the effect of the 4-fluorobenzyl group on 20S proteasome activity, the debenzylated acyl Astemizole analogue (**3-6**) was studied. As shown in **Figure 3.2**, **3-6** was

shown to be unable to enhance 20S proteasome activity, demonstrating the great importance of the 4-fluorobenzyl group. Considering the debenzylated analogue's lack of reactivity, the previously discussed moderate activity ($EC_{200} = 8.1 \mu\text{M}$) of **3-5** was even more intriguing, as it lacks the 4-fluorobenzyl moiety but still maintains a some 20S proteasome activity. The design and synthesis of additional analogues, such as a benzothiazole with an amino linker atom or additional 4-fluoroaryl moieties, is needed to study this activity further and remains a focus for the future.

3.3. Conclusions

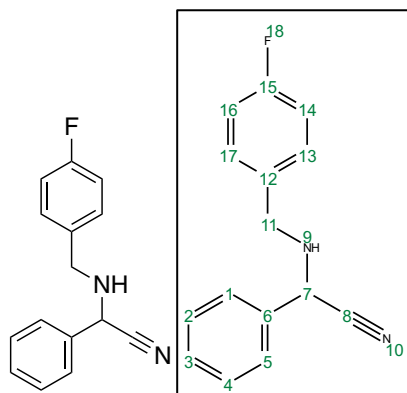
Scheme 3.15. Future acyl Astemizole analogues to be synthesized and studied.



In summary, several acyl Astemizole analogues have been synthesized which have given valuable insights into the relationship between several structural moieties of acyl Astemizole and its 20S proteasome modulation activity. However, some structure activity relationship questions remain regarding these aforementioned synthesized analogues, specifically focusing on the activities of **3-5** and **3-6**. As was previously mentioned, the 4-fluorobenzyl group of acyl Astemizole (**3-1**) was identified as very important for biological activity as it was found that the debenzylated acyl Astemizole analogue (**3-6**) lacked 20S proteasome activity. Interestingly,

though, **3-5** was found to have moderate 20S proteasome activity even though it lacked the 4-fluorobenzyl moiety. The synthesis of additional analogues to explore these findings, such as a benzothiazole analogue with an amino linker (**3-32**) and a benzothiazole analogue with the 4-fluorobenzyl group on the amino linker (**3-33**) were identified as a point of focus for future studies (**Scheme 3.15**). In addition, as shown in **Scheme 3.15**, to further explore the scope of the 4-fluorobenzyl aryl moiety with respect to 20S proteasome activity, the completion of the previously discussed aryl analogue syntheses (**3-7**, **3-8**, and **3-9**) were also identified as a point of focus for future studies. Overall, the design, synthesis, and biological studies of these acyl Astemizole analogues have provided valuable insights into the structure-activity relationship of acyl Astemizole (**3-1**). As acyl Astemizole (**3-1**) remains a promising target in the Tepe lab, and these findings will be of great use for future analogue development.

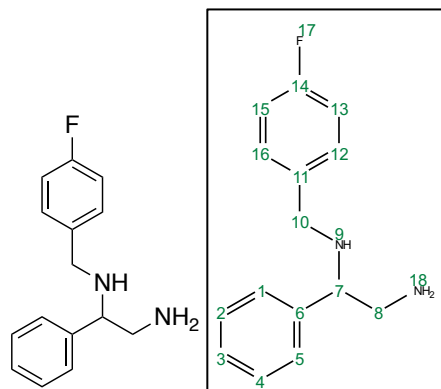
3.4 Experimental



2-((4-fluorobenzyl)amino)-2-phenylacetonitrile (3-10)

To a mixture of benzaldehyde (0.20 mL, 2.0 mmol, 1.0 equiv), 4-fluorobenzylamine (0.23 mL, 2.0 mmol, 1.0 equiv), and acetone cyanohydrin (0.18 mL, 2.0 mmol, 1.0 equiv) in anhydrous MeCN (10 mL) in an oven dried flask, was added Et₃N (0.01 mL, 0.1 mmol, 0.05 equiv) at room temperature, under an atmosphere of N₂ gas. This resulting solution was then allowed to stir for 18 hours at room temperature under N₂. After 18 hours, the reaction was quenched with H₂O (5 mL), extracted with ethyl acetate (3x30mL), dried over Na₂SO₄, filtered, and concentrated in vacuo. The resulting crude residue was then purified via silica gel column chromatography (hexanes/ethyl acetate) to yield the desired product as a yellow oil that crystallized to a yellowish, clear, crystalline solid (0.31 g, 65%). **M.P.:** 39-40°C, **¹H NMR** (500 MHz, CDCl₃) δ 7.54 (d, *J* = 7.0 Hz, 2H, (**H1**, **H5**)), 7.46 – 7.33 (m, 5H, (**H2**, **H3**, **H4**, **H13**, **H17**)), 7.04 (t, *J* = 8.7 Hz, 2H, (**H14**, **H16**)), 4.74 (s, 1H, (**H7**)), 4.03 (d, *J* = 13.0 Hz, 1H, (**H11**)), 3.93 (d, *J* = 13.0 Hz, 1H, (**H11**)). **¹³C NMR** (126 MHz, CDCl₃) δ 162.38 (d, *J* = 245.6 Hz, (**C15**)), 134.67 (**C6**), 133.90 (d, *J* = 2.9 Hz, (**C12**)), 130.13 (d, *J* = 8.1 Hz, (**C13**, **C17**)), 129.21 (**C3**), 129.11 (**C2**, **C4**), 127.38 (**C1**, **C5**), 118.74 (**C8**), 115.58 (d, *J* = 21.0 Hz, (**C14**, **C16**)), 53.49 (**C7**), 50.60 (**C11**).

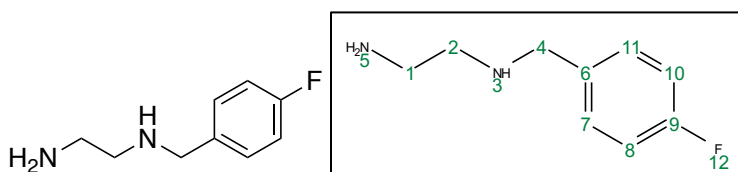
FTIR (cm⁻¹): 3314, 3069, 2896, 2254, 1503. **HRMS-ESI (m/z):** Calculated for C₁₅H₁₃FN₂
(M+H)⁺: 241.1141, Found: 241.1147.



***N*¹-(4-fluorobenzyl)-1-phenylethane-1,2-diamine (3-11)**

An oven-dried rb flask was purged with Argon gas for 5 min. To this was then added LiAlH₄ (0.23 g, 6.0 mmol, 3.0 equiv), which was then purged again with Ar gas for another 5 min. This rb was then cooled to 0°C and then anhydrous THF (3 mL) was then added. After 10 minutes, a solution of AlCl₃ (0.27 g, 2.0 mmol, 1.0 equiv) in THF (10 mL) was added at 0°C, under Ar. This was allowed to stir for 15 minutes to allow for formation of the active catalyst. Then, the mono-*p*-fluoro-benzylated amino nitrile intermediate (**3-10**) (0.48 g, 2.0 mmol, 1.0 equiv) was added dropwise in anhydrous THF (3 mL) at 0°C. The reaction was then allowed to warm to rt and was stirred for 24 hours under an atmosphere of Ar gas. After completion, the reaction was then quenched slowly (dropwise) with 2M aqueous NaOH solution until the bubbling stopped. The organic layer was then extracted with ethyl acetate (3x30mL), dried over Na₂SO₄, filtered, and concentrated in vacuo. The resulting crude residue was then purified via silica gel column chromatography (MeOH (1% Et₃N)/DCM) to yield the desired product as a clear, colorless oil (0.43 g, 87%). ¹H NMR (500 MHz, CD₃OD) δ 7.44 – 7.35 (m, 4H, (**H1**, **H2**, **H4**, **H5**)), 7.34 –

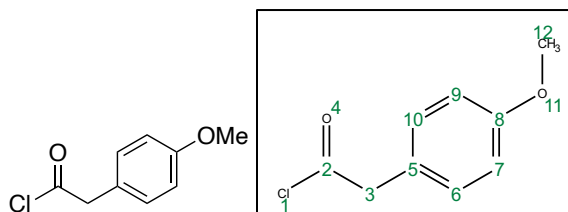
7.26 (m, 3H, (**H3**, **H12**, **H16**)), 7.01 (t, $J = 8.8$ Hz, 2H, (**H13**, **H15**)), 3.73 (dd, $J = 8.4, 5.6$ Hz, 1H, (**H7**)), 3.64 (d, $J = 13.2$ Hz, 1H, (**H10**)), 3.49 (d, $J = 13.2$ Hz, 1H, (**H10**)), 2.98 (dd, $J = 12.8, 5.5$ Hz, 1H, (**H8**)), 2.92 (dd, $J = 12.8, 5.5$ Hz, 1H, (**H8**)). ^{13}C NMR (126 MHz, CD_3OD) δ 163.25 (d, $J = 243.2$ Hz, (**C14**)), 141.76 (**C6**), 137.04 (d, $J = 2.9$ Hz, (**C11**)), 131.23 (d, $J = 8.1$ Hz, (**C12**, **C16**)), 129.89 (**C2**, **C4**), 128.92 (**C3**), 128.47 (**C1**, **C5**), 115.89 (d, $J = 21.5$ Hz, (**C13**, **C15**)), 63.17 (**C7**), 50.93 (**C10**), 47.35 (**C8**). FTIR (cm^{-1}): 3374, 3352, 3311, 3055, 2886, 1508. HRMS-ESI (m/z): Calculated for $\text{C}_{15}\text{H}_{17}\text{FN}_2$ ($\text{M}+\text{H}$) $^+$: 245.1454, Found: 245.1475.



*N*¹-(4-fluorobenzyl)ethane-1,2-diamine (3-12)

To an oven-dried round bottom flask was added ethylenediamine (0.67 mL, 10.0 mmol, 1.0 equiv) dissolved in anhydrous DMF (15 mL) at 20°C under an atmosphere of N_2 gas. To this was then added K_2CO_3 (1.38 g, 10.0 mmol, 1.0 equiv) and 4-fluoro benzyl bromide (1.24 mL, 10.0 mmol, 1.0 equiv) sequentially at 20°C under N_2 gas. The resulting reaction mixture was then allowed to stir at 20°C for 18 hours under N_2 gas. After 18 hours, the reaction was quenched with deionized H_2O (20 mL), washed with saturated aqueous LiCl solution (3x50 mL), extracted with EtOAc (3x50 mL), dried over Na_2SO_4 , filtered, and concentrated in vacuo. The resulting crude residue was then purified via silica gel column chromatography (DCM/MeOH (2% TEA)) to yield the desired product as a clear pale-yellow oil. (0.97 g, 58%). ^1H NMR (500 MHz, CD_3OD) δ 7.36 (dd, $J = 8.6, 5.4$ Hz, 2H, (**H7**, **H11**)), 7.05 (t, $J = 8.8$ Hz, 2H, (**H8**, **H10**)), 3.74 (s, 2H, (**H4**)), 2.75 (t, $J = 6.3$ Hz, 2H, (**H2**)), 2.65 (t, $J = 6.3$ Hz, 2H, (**H1**)). ^{13}C NMR (126 MHz,

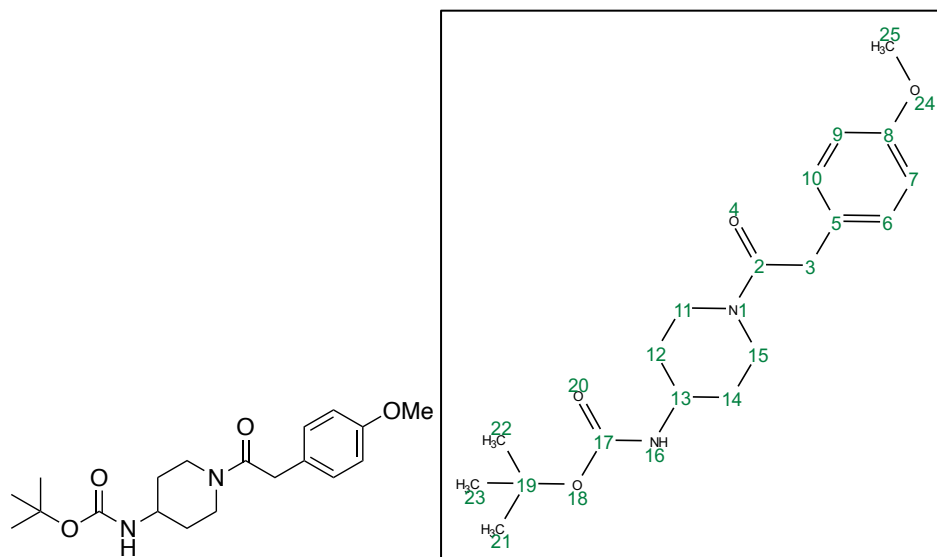
CD₃OD) δ 163.48 (d, J = 243.7 Hz, (C9)), 136.82 (d, J = 2.9 Hz, (C6)), 131.37 (d, J = 8.1 Hz, (C7, C11)), 116.04 (d, J = 21.5 Hz, (C8, C10)), 53.64 (C4), 52.07 (C2), 41.75 (C1). FTIR (cm⁻¹): 3356, 3301, 3279, 3021, 2891, 1515. HRMS-ESI (m/z): Calculated for C₉H₁₃FN₂ (M+H)⁺: 169.1441, Found: 169.1467.



2-(4-methoxyphenyl)acetyl chloride (3-13)

4-methoxyphenyl acetic acid (1.66 g, 10.0 mmol, 1.0 equiv) was first dissolved in anhydrous DCM (20mL) in an oven-dried flask at room temperature under an atmosphere of N₂ gas. SOCl₂ was then added (1.1 mL, 15.0 mmol, 1.5 equiv), followed by DMF (4 drops, 0.01 mmol, 0.001 equiv). The resulting solution was then allowed to stir at room temperature, under an atmosphere of N₂ gas for 20 hours. After 20 hours, the reaction was then concentrated in vacuo to afford the desired product as an orange oil (1.85 g, Quantitative).

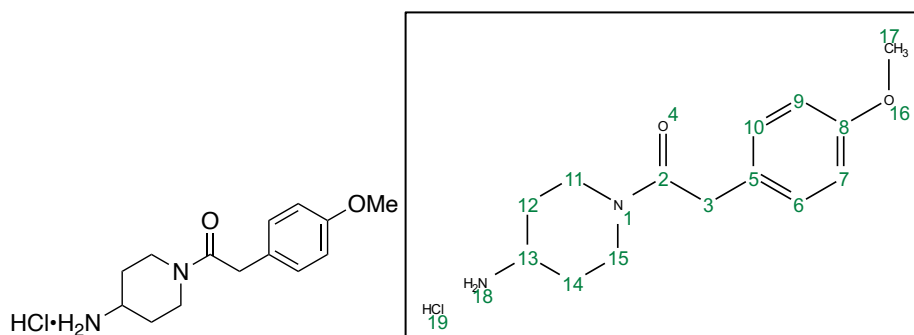
¹H NMR (500 MHz, DMSO) δ 7.16 (d, J = 8.7 Hz, 2H, (H6, H10)), 6.86 (d, J = 8.7 Hz, 2H, (H7, H9)), 3.72 (s, 3H, (H12)), 3.48 (s, 2H, (H3)). ¹³C NMR (126 MHz, DMSO) δ 173.00 (C2), 158.06 (C8), 130.42 (C6, C10), 126.99 (C5), 113.69 (C7, C9), 55.06 (C12), 39.81 (C3). FTIR (cm⁻¹): 3037, 2836, 1779, 1503, 1249, 1041. HRMS-ESI (m/z): Calculated for C₉H₉ClO₂ (M+H)⁺; (M+2)²⁺: 185.0369; 187.0377, Found: 185.0372; 187.0381.



***tert*-butyl (1-(2-(4-methoxyphenyl)acetyl)piperidin-4-yl)carbamate (3-14)**

To an oven-dried flask was added acyl chloride intermediate (0.55 g, 3.0 mmol, 1.0 equiv) in anhydrous DCM (2mL). (*N*-Boc-4-amino)piperidine (0.66 g, 3.3 mmol, 1.1 equiv) in anhydrous DCM (3mL) was then added dropwise to the solution at 0°C under an atmosphere of N₂ gas. Et₃N (0.41 mL, 2.75 mmol, 1.25 equiv) was then also added dropwise at 0°C under N₂. The reaction was then allowed to warm to room temperature and was stirred for 18 hours at room temperature under N₂ gas. The reaction was then quenched with H₂O (10 mL), washed with saturated NaHCO₃ solution (10 mL), extracted with DCM (3x30mL), dried over Na₂SO₄, filtered, and concentrated in vacuo. The resulting crude residue was then purified via silica gel column chromatography (DCM/MeOH) to yield the desired product as a pale yellow, crystalline solid (0.85 g, 81%). **M.P.:** 128-129°C. ¹H NMR (500 MHz, CD₃OD) δ 7.16 (d, *J* = 8.6 Hz, 2H, (**H7**, **H9**)), 6.88 (d, *J* = 8.7 Hz, 2H, (**H6**, **H10**)), 4.43 – 4.34 (m, 1H, (**H11** or **H15^(A)**)), 3.97 – 3.89 (m, 1H, (**H11** or **H15^(B)**)), 3.77 (s, 3H, (**H25**)), 3.70 (d, *J* = 4.6 Hz, 2H, (**H3**)), 3.57 – 3.47 (m, 1H, (**H13**)), 3.12 (t, *J* = 12.9 Hz, 1H, (**H11** or **H15^(B)**)), 2.82 (t, *J* = 12.9 Hz, 1H, (**H11** or

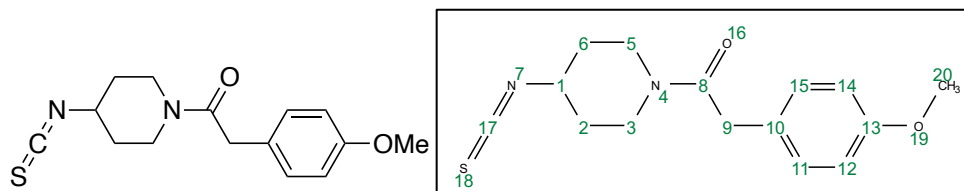
H15^(A)), 1.87 – 1.80 (m, 1H, (**H12 or H14^(A)**)), 1.79 – 1.68 (m, 1H, (**H12 or H14^(B)**)), 1.42 (s, 9H, (**H21, H22, H23**)), 1.33 – 1.21 (m, 1H, (**H12 or H14^(A)**)), 1.16 – 1.05 (m, 1H, (**H12 or H14^(B)**)). ¹³C NMR (126 MHz, CD₃OD) δ 172.33 (**C2**), 160.03 (**C17**), 157.71 (**C8**), 130.67 (**C7, C9**), 128.27 (**C5**), 115.18 (**C6, C10**), 80.11 (**C19**), 55.69 (**C25**), 54.82 (**C13**), 46.23 (**C11 or 15^(B)**), 42.02 (**C11 or 15^(A)**), 40.59 (**C3**), 33.37 (**C12 or 14^(B)**), 32.65 (**C12 or 14^(A)**), 28.73 (**C21, C22, C23**). FTIR (cm⁻¹): 3321, 3022, 2875, 1686, 1662, 1503, 1250, 1225, 1041. HRMS-ESI (**m/z**): Calculated for C₁₉H₂₈N₂O₄ (M+H)⁺: 349.2127, Found: 349.2132.



1-(4-aminopiperidin-1-yl)-2-(4-methoxyphenyl)ethan-1-one hydrochloride (3-15)

To an oven-dried flask was added the acylated Boc-amino piperidine intermediate (0.35 g, 1.0 mmol, 1.0 equiv) dissolved in anhydrous EtOH (3 mL). To this was then added HCl solution (4M in EtOH, 3.3 mL) at room temperature, under an atmosphere of N₂ gas. The resulting reaction mixture was then stirred for 18 hours at rt under N₂ gas. After 18 hours, the reaction was then concentrated in vacuo to afford the desired product as a yellow foaming solid (0.28 g, Quantitative). ¹H NMR (500 MHz, CD₃OD) δ 7.19 (d, *J* = 7.0 Hz, 2H, (**H7, H9**)), 6.89 (d, *J* = 6.9 Hz, 2H, (**H6, H10**)), 4.60 (d, *J* = 11.7 Hz, 1H, (**H11 or H15^(A)**)), 4.15 – 4.07 (m, 1H, (**H11 or H15^(B)**)), 3.79 – 3.75 (m, 5H, (**H3, H17**)), 3.38 – 3.35 (m, 1H, (**H13**)), 3.17 – 3.14 (m, 1H, (**H11**

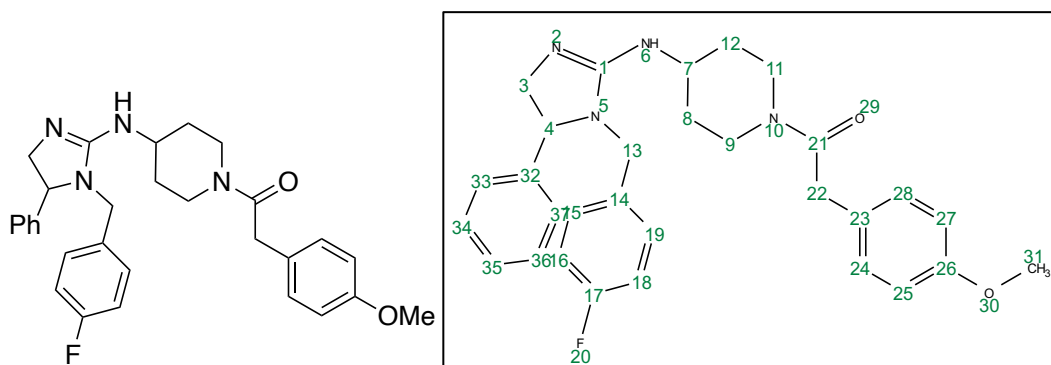
or **H15^(B)**)), 2.81 – 2.73 (m, 1H, (**H11** or **H15^(A)**)), 2.08 – 2.02 (m, 1H, (**H12** or **H14^(A)**)), 2.01 – 1.94 (m, 1H, (**H12** or **H14^(B)**)), 1.49 – 1.42 (m, 1H, (**H12** or **H14^(A)**)), 1.35 – 1.30 (m, 1H, (**H12** or **H14^(B)**)). ¹³C NMR (126 MHz, CD₃OD) δ 172.57 (**C2**), 160.02 (**C8**), 130.75 (**C7**, **C9**), 127.79 (**C5**), 115.24 (**C6**, **C10**), 55.78 (**C17**), 49.40 (**C13**), 45.65 (**H11** or **H15^(B)**), 41.42 (**H11** or **H15^(A)**), 40.38 (**C3**), 31.20 (**H12** or **H14^(B)**), 30.58 (**H12** or **H14^(A)**). FTIR (cm⁻¹): 3445, 3362, 3023, 2879, 1659, 1522, 1253, 1042. HRMS-ESI (m/z): Calculated for C₁₇H₂₆N₂O₂ (M+H)⁺: 249.1603, Found: 249.1629.



1-(4-isothiocyanatopiperidin-1-yl)-2-(4-methoxyphenyl)ethan-1-one (3-16)

To an oven-dried round bottom flask was added the neutralized 2-amino piperidine intermediate (**3-15**) (0.57 g, 2.0 mmol, 1.0 equiv) dissolved in anhydrous DCM (15 mL) at room temperature under an atmosphere of N₂ gas. The resulting solution was then cooled to -10°C. Then, di(1*H*-imidazol-1-yl)methanethione (392.1 mg, 2.2 mmol, 1.1 equiv) was added at -10°C under N₂ gas. The resulting solution was then allowed to warm to room temperature and was stirred for 18 hours. After 18 hours, the reaction was quenched with H₂O (25 mL), extracted with EtOAc (3x30mL), dried over Na₂SO₄, filtered, and concentrated in vacuo to yield the desired product as a pale-yellow oil (0.42 g, 73%). ¹H NMR (500 MHz, CDCl₃) δ 7.15 (d, *J* = 8.7 Hz, 2H, (**H11**, **H15**)), 6.86 (d, *J* = 8.7 Hz, 2H, (**H12**, **H14**)), 3.95 – 3.88 (m, 1H, (**H1**)), 3.80 (s, 3H, (**H20**)), 3.71 – 3.68 (m, 2H, (**H3** or **H5^(A)**)), 3.67 (s, 2H, (**H9**)), 3.61 – 3.53 (m, 1H, (**H3** or **H5^(B)**)), 3.44

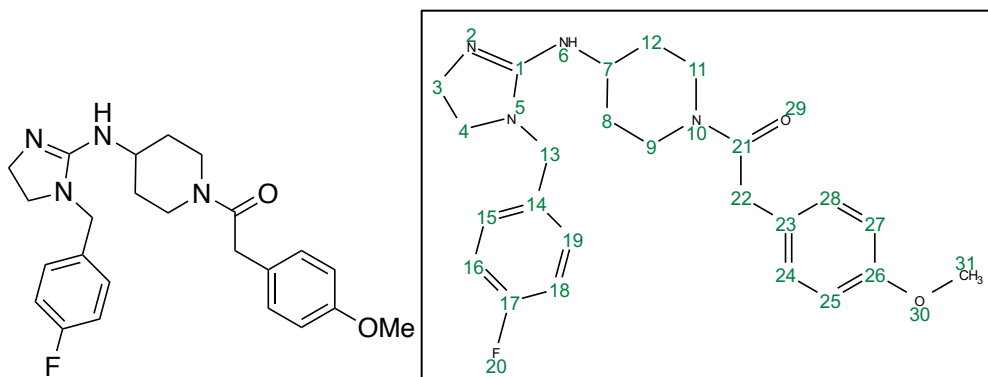
– 3.30 (m, 1H, (**H3 or H5^(B)**)), 1.91 – 1.86 (m, 1H, (**H2 or H6^(A)**)), 1.81 – 1.70 (m, 1H, (**H2 or H6^(A)**)), 1.68 – 1.61 (m, 1H, (**H2 or H6^(B)**)), 1.60 – 1.52 (m, 1H, (**H2 or H6^(B)**)). ¹³C NMR (126 MHz, CDCl₃) δ 169.85 (**C8**), 158.65 (**C13**), 137.09 (**C17**), 129.60 (**C11, C15**), 126.85 (**C10**), 114.40 (**C12, C14**), 55.42 (**C20**), 53.06 (**C1**), 43.03 (**C3 or C5^(B)**), 40.42 (**C9**), 38.69 (**C3 or C5^(A)**), 32.49 (**C2 or C6^(B)**), 31.93 (**C2 or C6^(A)**). FTIR (cm⁻¹): 3023, 2887, 2101, 1685, 1255, 1224, 1045. HRMS-ESI (m/z): Calculated for C₁₅H₁₈N₂O₂S (M+H)⁺: 291.1167, Found 291.1179.



1-(4-((1-(4-fluorobenzyl)-5-phenyl-4,5-dihydro-1H-imidazol-2-yl)amino)piperidin-1-yl)-2-(4-methoxyphenyl)ethan-1-one (3-2)

To an oven-dried round bottom flask was added the diamine intermediate (**3-11**) (0.48 g, 2.0 mmol, 1.0 equiv) dissolved in anhydrous EtOH (10mL). At 20°C, under an atmosphere of N₂, was then added the isothiocyanate intermediate (**3-16**) (0.58 g, 2.0 mmol, 1.0 equiv). The resulting solution was then allowed to stir for 18 hours at room temperature, under N₂ gas. After 18 hours, the reaction mixture was heated to reflux (80°C) and was stirred at reflux for 3 hours under an atmosphere of N₂ gas. Upon heating, methyl iodide (0.37 mL, 6.0 mmol, 3.0 equiv) was added in three batches (one per hour). After the 3 hours, the reaction mixture was allowed to cool to room temperature and then the solvent was removed in vacuo. The resulting crude residue was

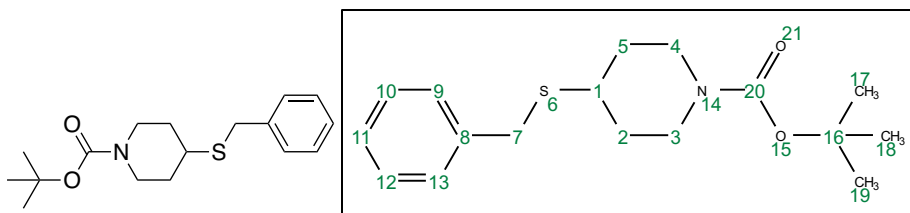
then purified via silica gel column chromatography (DCM/MeOH) to yield the desired product as a yellow oil. (0.73 g, 73%). $^1\text{H NMR}$ (500 MHz, CD_3OD) δ 7.44 – 7.38 (m, 3H, (**H33**, **H35**, **H37**)), 7.32 – 7.25 (m, 2H, (**H15**, **H19**)), 7.20 (d, $J = 8.6$ Hz, 2H, (**H24**, **H28**)), 7.11 – 7.06 (m, 4H, (**H16**, **H18**, **H34**, **H36**)), 6.89 (d, $J = 8.8$ Hz, 2H, (**H25**, **H27**)), 4.85 (dd, $J = 9.8, 8.2$ Hz, 1H, (**H4**)), 4.74 (dd, $J = 16.3, 4.3$ Hz, 1H, (**H3**)), 4.69 – 4.61 (m, 1H, (**H9 or 11**^(A))), 4.18 – 4.07 (m, 2H, (**H8 or 12**^(A), **H9 or 11**^(B))), 3.94 (dd, $J = 16.3, 3.3$ Hz, 1H, (**H3**)), 3.82 – 3.77 (m, 1H, (**H13**)), 3.77 (s, 3H, (**H31**)), 3.76 (s, 2H, (**H22**)), 3.73 – 3.65 (m, 2H, (**H7**, **H13**)), 3.62 – 3.57 (m, 1H, (**H9 or 11**^(B))), 3.20 – 3.10 (m, 1H, (**H8 or 12**^(A))), 2.79 – 2.70 (m, 1H, (**H9 or 11**^(A))), 2.17 – 2.01 (m, 1H, (**H8 or 12**^(B))), 1.56 – 1.43 (m, 1H, (**H8 or 12**^(B))). $^{13}\text{C NMR}$ (126 MHz, CD_3OD) δ 174.03 (**C21**), 166.49 (**C17**), 160.15 (**C26**), 158.26 (**C1**), 143.02 (**C32**), 138.22 (**C14**), 130.81 (**C34**, **C36**), 130.70 (**C24**, **C28**), 130.45 (**C33**, **C37**), 130.07 (**C35**), 128.69 (**C15**, **C19**), 128.50 (**C23**), 116.76 (**C16**, **C18**), 115.26 (**C25**, **C27**), 64.04 (**C4**), 59.99 (**C22**), 55.67 (**C31**), 52.91 (**C7**), 51.00 (**C9 or C11**^(B)), 46.36 (**C3**), 46.16 (**C8 or C12**^(A)), 41.90 (**C9 or C11**^(A)), 40.66 (**C13**), 33.06 (**C8 or C12**^(B)). **FTIR** (cm^{-1}): 3352, 3009, 2886, 1655, 1639, 1512, 1248, 1039. **HRMS-ESI** (m/z): Calculated for $\text{C}_{30}\text{H}_{33}\text{FN}_4\text{O}_2$ ($\text{M}+\text{H}$)⁺: 501.2666, Found: 501.2690.



1-(4-((1-(4-fluorobenzyl)-4,5-dihydro-1H-imidazol-2-yl)amino)piperidin-1-yl)-2-(4-methoxyphenyl)ethan-1-one (3-3)

To an oven-dried round bottom flask was added mono 4-fluorobenzylated ethylenediamine intermediate (**3-12**) (0.34 g, 2.0 mmol, 1.0 equiv) dissolved in anhydrous EtOH (10mL). At 20°C, under an atmosphere of N₂, was then added the isothiocyanate intermediate (**3-16**) (0.58 g, 2.0 mmol, 1.0 equiv). The resulting solution was then allowed to stir for 18 hours at room temperature, under N₂ gas. After 18 hours, the reaction mixture was heated to reflux (80°C) and was stirred at reflux for 3 hours under an atmosphere of N₂ gas. Upon heating, methyl iodide (0.37 mL, 6.0 mmol, 3.0 equiv) was added in three batches (one per hour). After the 3 hours, the reaction mixture was allowed to cool to room temperature and then the solvent was removed in vacuo. The resulting crude residue was then purified via silica gel column chromatography (DCM/MeOH) to yield the desired product as a clear, colorless oil. (0.58 g, 68%). ¹H NMR (500 MHz, CD₃OD) δ 7.52 – 7.43 (m, 2H, (**H15**, **H19**)), 7.30 (d, *J* = 8.5 Hz, 2H, (**H24**, **H28**)), 7.24 (d, *J* = 8.6 Hz, 2H, (**H25**, **H27**)), 6.97 (t, *J* = 8.7 Hz, 2H, (**H16**, **H18**)), 5.47 (s, 2H, (**H13**)), 5.08 – 4.95 (m, 1H, (**H7**)), 4.87 – 4.78 (m, 1H, (**H9** or **H11**^(A))), 4.29 – 4.23 (m, 1H, (**H9** or **H11**^(B))), 3.88 – 3.77 (m, 2H, (**H4**)), 3.76 (s, 3H, (**H31**)), 3.75 – 3.69 (m, 4H, (**H3**, **H22**)), 3.30 – 3.23 (m, 1H, (**H9** or **H11**^(B))), 2.90 – 2.81 (m, 1H, (**H9** or **H11**^(A))), 2.54 – 2.43 (m, 1H, (**H8** or **H12**^(A))),

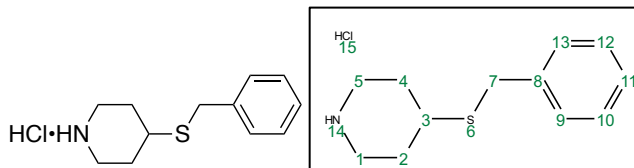
2.35 – 2.25 (m, 1H, (**H8 or H12^(B)**)), 2.11 – 2.05 (m, 1H, (**H8 or H12^(B)**)), 1.99 – 1.93 (m, 1H, (**H8 or H12^(A)**)). ¹³C NMR (126 MHz, CD₃OD) δ 166.85 (**C21**), 162.49 (d, *J* = 54.3 Hz, (**C17**)), 160.15 (**C26**), 153.50 (**C1**), 131.66 (d, *J* = 3.4 Hz, (**C14**)), 130.79 (**C24, C28**), 130.14 (d, *J* = 8.1 Hz, (**C15, C19**)), 128.16 (**C23**), 116.72 (d, *J* = 22.4 Hz, (**C16, C18**)), 115.33 (**C25, C27**), 55.72 (**C31**), 54.55 (**C4**), 53.36 (**C13**), 50.93 (**C3**), 49.28 (**C9 or C11^(B)**), 46.76 (**C9 or C11^(A)**), 42.59 (**C7**), 40.75 (**C22**), 35.23 (**C8 or C12^(A)**), 31.17 (**C8 or C12^(B)**). FTIR (cm⁻¹): 3344, 3011, 2882, 1659, 1638, 1506, 1255, 1042. HRMS-ESI (m/z): Calculated for C₂₄H₂₉FN₄O₂ (M+H)⁺: 425.2347, Found: 425.2361.



***tert*-butyl 4-(benzylthio)piperidine-1-carboxylate (3-17)**

To an oven-dried flask purged with N₂ gas was added *tert*-butyl 4-mercaptopiperidine-1-carboxylate (0.65 g, 3.0 mmol, 1.0 equiv) dissolved in anhydrous DMF (5mL). To this was then added K₂CO₃ (0.41 g, 3.0 mmol, 1.0 equiv) and benzyl bromide (0.36 mL, 3.0 mmol, 1.0 equiv) sequentially at room temperature under an atmosphere of N₂ gas. The resulting mixture was then heated to 70°C and was allowed to stir under N₂ gas for 18 hours. After 18 hours, the reaction was cooled to room temperature, then diluted with H₂O (10mL) and ethyl acetate (30mL) and was washed with saturated aqueous LiCl solution (3x30mL). Then organic layer was then extracted with ethyl acetate (3x30mL), dried over Na₂SO₄, filtered, and concentrated in vacuo. The resulting crude residue was then purified via silica gel column chromatography

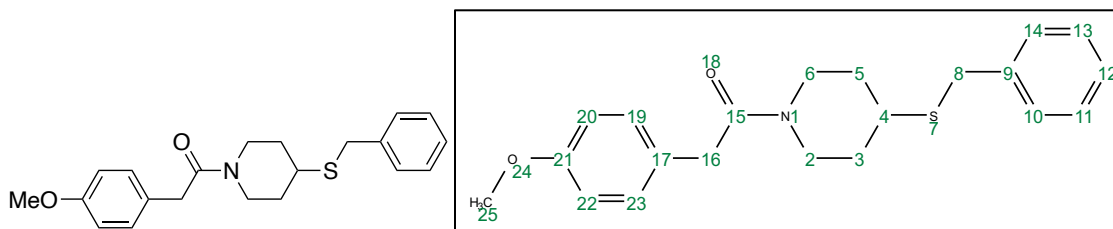
(Hexanes/ethyl acetate) to yield the desired product as a clear, colorless oil (0.84 g, 91%). ^1H NMR (500 MHz, CDCl_3) δ 7.34 – 7.27 (m, 4H, (**H9**, **H10**, **H12**, **H13**)), 7.26 – 7.20 (m, 1H, (**H11**)), 4.00 – 3.84 (m, 2H, (**H3** or **H4**)), 3.75 (s, 2H, (**H7**)), 2.86 (t, $J = 11.3$ Hz, 2H, (**H3** or **H4**)), 2.88-2.65 (m, 1H, (**H1**)), 1.95 – 1.79 (m, 2H, (**H2** or **H5**)), 1.57 – 1.45 (m, 2H, (**H2** or **H5**)), 1.44 (s, 9H, (**H17**, **H18**, **H19**)). ^{13}C NMR (126 MHz, CDCl_3) δ 154.80 (**C20**), 138.50 (**C8**), 128.84 (**C9**, **C13**), 128.66 (**C10**, **C12**), 127.12 (**C11**), 79.64 (**C16**), 43.27 (**C3**, **C4**), 40.60 (**C1**), 34.69 (**C7**), 32.29 (**C2**, **C5**), 28.54 (**C17**, **C18**, **C19**). FTIR (cm^{-1}): 3004, 2878, 1678, 1556, 1255, 1052. HRMS-ESI (m/z): Calculated for $\text{C}_{17}\text{H}_{25}\text{NO}_2\text{S}$ ($\text{M}+\text{H}$) $^+$: 309.1762, Found: 309.1789.



4-(benzylthio)piperidine hydrochloride (3-18)

To an oven-dried flask was added *tert*-butyl 4-(benzylthio)piperidine-1-carboxylate intermediate (0.84 g, 2.7 mmol, 1.0 equiv) dissolved in anhydrous EtOH (5 mL). To this was then added HCl solution (4M in EtOH, 4.5 mL) at room temperature, under an atmosphere of N_2 gas. The resulting reaction mixture was then stirred for 18 hours at rt under N_2 gas. After 18 hours, the reaction was then concentrated in vacuo to afford the desired product as a pink crystalline solid (0.66 g, Quantitative). **M.P.:** 145-146°C, ^1H NMR (500 MHz, CD_3OD) δ 7.38-7.33 (m, 2H, (**H9**, **H13**)), 7.30 (t, $J = 7.5$ Hz, 2H, (**H10**, **H12**)), 7.23 (t, $J = 7.3$ Hz, 1H, (**H11**)), 3.83 (s, 2H, (**H7**)), 3.40 – 3.35 (m, 2H, (**H1** or **H5**)), 3.06 – 2.98 (m, 2H, (**H1** or **H5**)), 2.93 – 2.84 (m, 1H, (**H3**)), 2.18 – 2.10 (m, 2H, (**H2** or **H4**)), 1.81 – 1.70 (m, 2H, (**H2** or **H4**)). ^{13}C NMR (126 MHz,

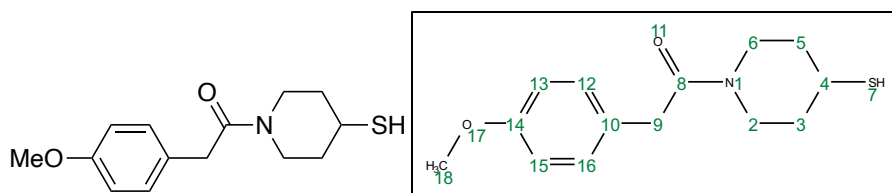
CD₃OD) δ 139.67 (C8), 129.92 (C9, C13), 129.57 (C10, C12), 128.11 (C11), 49.85 (C1 or C5), 45.18 (C1 or C5), 44.26 (C3), 38.75 (C7), 35.59 (C2 or C4), 30.25 (C2 or C4). FTIR (cm⁻¹): 3332, 3032, 2836, 1509. HRMS-ESI (m/z): Calculated for C₁₂H₁₇NS (M+H)⁺: 208.1160, Found: 208.1180.



1-(4-(benzylthio)piperidin-1-yl)-2-(4-methoxyphenyl)ethan-1-one (3-19)

To an oven-dried flask was added acyl chloride intermediate (0.18 g, 1.0 mmol, 1.0 equiv) in anhydrous DCM (2 mL). 4-(benzylthio)piperidine (0.23 g, 1.1 mmol, 1.1 equiv) in anhydrous DCM (3 mL) was then added dropwise to the solution at 0°C under an atmosphere of N₂ gas. Et₃N (0.18 mL, 1.25 mmol, 1.25 equiv) was then also added dropwise at 0°C under N₂. The reaction was then allowed to warm to room temperature and was stirred for 18h at room temperature under N₂ gas. The reaction was then quenched with H₂O (10 mL), washed with saturated NaHCO₃ solution (10 mL), extracted with DCM (3x30mL), dried over Na₂SO₄, filtered, and concentrated in vacuo. The resulting crude residue was then purified via silica gel column chromatography (DCM/MeOH) to yield the desired product as a clear, colorless oil (0.28 g, 79%). ¹H NMR (500 MHz, CD₃OD) δ 7.33 – 7.24 (m, 4H, (H10, H11, H13, H14)), 7.23 – 7.17 (m, 1H, (H12)), 7.14 (d, *J* = 8.7 Hz, 2H, (H19, H23)), 6.87 (d, *J* = 8.7 Hz, 2H, (H20, H22)), 4.26 – 4.18 (m, 1H, (H2 or H6^(A))), 3.88 – 3.80 (m, 1H, (H2 or H6^(B))), 3.75 (s, 3H, (H25)), 3.73

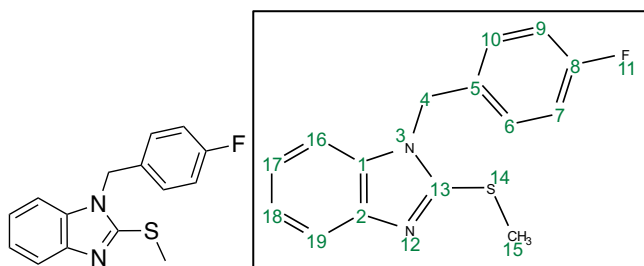
(s, 2H, **(H8)**), 3.67 (s, 2H, **(H16)**), 3.09 (td, $J = 12.2, 3.1$ Hz, 1H, **(H2 or H6^(B))**), 2.89 (td, $J = 12.1, 3.1$ Hz, 1H, **(H2 or H6^(B))**), 2.78 – 2.69 (m, 1H, **(H4)**), 1.93 – 1.84 (m, 1H, **(H3 or H5^(A))**), 1.79 – 1.70 (m, 1H, **(H3 or H5^(B))**), 1.43 – 1.31 (m, 1H, **(H3 or H5^(A))**), 1.24 – 1.13 (m, 1H, **(H3 or H5^(B))**). ¹³C NMR (126 MHz, CD₃OD) δ 172.18 (**(C15)**), 160.04 (**(C21)**), 140.04 (**(C9)**), 130.64 (**(C19, C23)**), 129.89 (**(C11, C13)**), 129.47 (**(C10, C14)**), 128.25 (**(C17)**), 127.94 (**(C12)**), 115.16 (**(C20, C23)**), 55.67 (**(C25)**), 46.83 (**(C2 or C6^(B))**), 42.56 (**(C2 or C6^(A))**), 41.24 (**(C4)**), 40.62 (**(C16)**), 35.26 (**(C8)**), 33.69 (**(C3 or C5^(B))**), 33.16 (**(C3 or C5^(A))**). FTIR (cm⁻¹): 3013, 2882, 1654, 1515, 1252, 1039. HRMS-ESI (m/z): Calculated for C₂₁H₂₅NO₂S (M+H)⁺: 356.1684, Found: 356.1701.



1-(4-mercaptopiperidin-1-yl)-2-(4-methoxyphenyl)ethan-1-one (**3-20**)

To an oven-dried flask was added 1-(4-(benzylthio)piperidin-1-yl)-2-(4-methoxyphenyl)ethan-1-one (0.37 g, 1.0 mmol, 1.0 equiv) dissolved in EtOH (5mL). To this was then added Pd(OH)₂/C (10 wt%, 1 scoop) at rt, under an atmosphere of H₂ gas (utilizing an H₂ balloon). The reaction was then allowed to stir for 24 hours under H₂ gas. After 24 hours, the reaction was then worked up via filtration through a celite pad and washed with MeOH (400mL) to remove the excess Pd(OH)₂/C. The resulting filtrate was then concentrated in vacuo to afford the desired product as a clear, pale-yellow oil (0.27 g, Quantitative). ¹H NMR (500 MHz, CD₃OD) δ 7.17 (d, $J = 7.8$ Hz, 2H, **(H12, H16)**), 6.88 (d, $J = 7.6$ Hz, 2H, **(H13, H15)**), 3.77 (s, 3H, **(H18)**), 3.70 (s, 2H, **(H9)**), 3.57 – 3.52 (m, 2H, **(H2 or H6)**), 3.53 – 3.43 (m, 2H, **(H2 or H6)**), 3.22 – 3.18 (m, 1H,

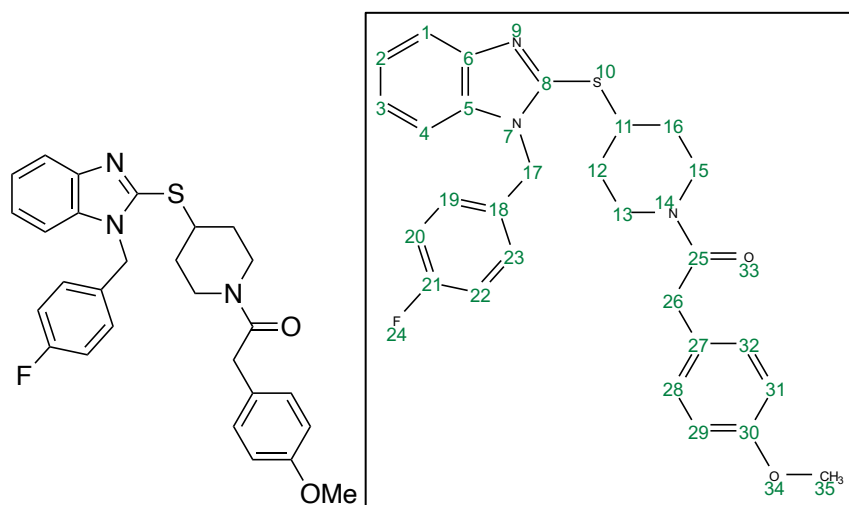
(H4)), 1.65 – 1.44 (m, 2H, (H3 or H5)), 1.39 – 1.27 (m, 2H, (H3 or H5)). ¹³C NMR (126 MHz, CD₃OD) δ 172.15 (C8), 159.96 (C14), 130.61 (C12, C16), 128.39 (C10), 115.09 (C13, C15), 58.30 (C25), 55.69 (C2 or C6), 48.52 (C2 or C6), 44.11 (C4), 40.68 (C9), 27.20 (C3 or C5), 26.62 (C3 or C5). FTIR (cm⁻¹): 3050, 2885, 2575, 1653, 1511, 1244, 1048. HRMS-ESI (m/z): Calculated for C₁₄H₁₉NO₂S (M+H)⁺: 266.1215, Found: 266.1233.



1-(4-fluorobenzyl)-2-(methylthio)-1H-benzo[d]imidazole (3-21)

To an oven-dried flask purged with N₂ gas was added 2-(methylthio)-1H-benzo[d]imidazole (0.82 g, 5.0 mmol, 1.0 equiv) dissolved in anhydrous DMF (5mL). To this was then added K₂CO₃ (0.69 g, 5.0 mmol, 1.0 equiv) and 4-fluorobenzyl bromide (0.62 mL, 5.0 mmol, 1.0 equiv) sequentially at room temperature under an atmosphere of N₂ gas. The resulting mixture was then allowed to stir at room temperature under N₂ gas for 24 hours. After 24 hours, the reaction was then diluted with H₂O (10 mL) and ethyl acetate (30 mL) and was washed with saturated aqueous LiCl solution (3x30mL). Then organic layer was then extracted with ethyl acetate (3x30mL), dried over Na₂SO₄, filtered, and concentrated in vacuo. The resulting crude residue was then purified via silica gel column chromatography (MeOH (1% Et₃N)/DCM) to yield the desired product as a white, crystalline solid (1.02 g, 75%). **M.P.:** 99-100°C, ¹H NMR (500 MHz, CD₃OD) δ 7.59 (d, *J* = 6.8 Hz, 1H, (H16)), 7.33 (d, *J* = 6.9 Hz, 1H, (H19)), 7.25 –

7.15 (m, 4H, **(H6, H10, H17, H18)**), 7.03 (t, $J = 8.8$ Hz, 2H, **(H7, H9)**), 5.34 (s, 2H, **(H4)**), 2.75 (s, 3H, **(H15)**). ^{13}C NMR (126 MHz, CD_3OD) δ 163.75 (d, $J = 245.6$ Hz, **(C8)**), 154.71 (**(C13)**), 144.21 (**(C2)**), 137.27 (**(C1)**), 133.29 (d, $J = 2.9$ Hz, **(C5)**), 130.10 (d, $J = 8.1$ Hz, **(C6, C10)**), 123.58 (**(C17)**), 123.40 (**(C18)**), 118.44 (**(C19)**), 116.58 (d, $J = 21.9$ Hz, **(C7, C9)**), 110.65 (**(C16)**), 47.62 (**(C4)**), 14.98 (**(C15)**). FTIR (cm^{-1}): 3052, 2867, 1501. HRMS-ESI (m/z): Calculated for $\text{C}_{15}\text{H}_{13}\text{FN}_2\text{S}$ ($\text{M}+\text{H}$) $^+$: 273.0862, Found: 273.0887.



1-(4-((1-(4-fluorobenzyl)-1H-benzo[d]imidazol-2-yl)thio)piperidin-1-yl)-2-(4-methoxyphenyl)ethan-1-one (3-4)

Procedure A

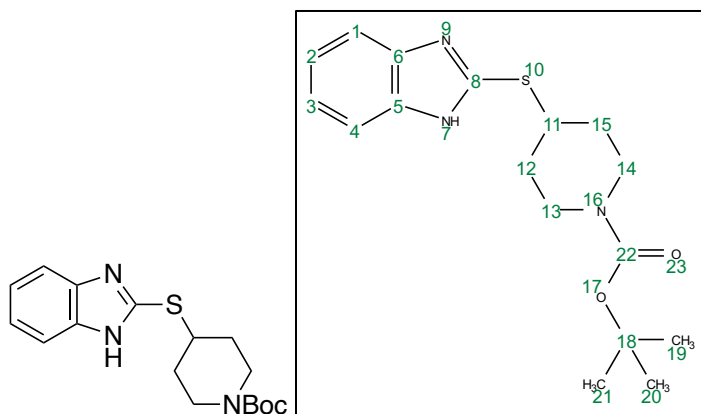
To an oven-dried flask was added the 1-(4-fluorobenzyl)-2-(methylthio)-1H-benzo[d]imidazole intermediate (**3-21**) (54.5 mg, 0.2 mmol, 1.0 equiv) dissolved in anhydrous DCM (3mL). This solution was then cooled to 0°C. At 0°C, under an atmosphere of N_2 gas was added *m*-CPBA (75% mixture, 0.11 g, 0.50 mmol, 2.5 equiv), portion-wise. This was then allowed to stir for one hour at 0°C under N_2 gas. After 1h, the reaction mixture was then quenched with saturated

aqueous NaHCO₃ solution (5mL), extracted with DCM (3x20mL), dried over Na₂SO₄, filtered, and concentrated in vacuo. The resulting yellowish crude product was then immediately dissolved in a mixture of anhydrous toluene (5mL). To this was then added the acylated thio-piperidine tail intermediate (**3-20**) (0.27 g, 1.0 mmol, 5.0 equiv) at room temperature, under an atmosphere of N₂ gas. The resulting solution was then heated to reflux (~110°C) and was allowed to stir for 18 hours under N₂ gas. After 18 hours, the reaction was allowed to cool to room temperature and was quenched with H₂O (1mL), then was diluted in MeOH (100mL) and concentrated in vacuo. The resulting crude residue was then purified via silica gel column chromatography (DCM/MeOH) to yield the desired product as a pale yellowish/off-white semi-solid (0.066 g, 67%).

Procedure B

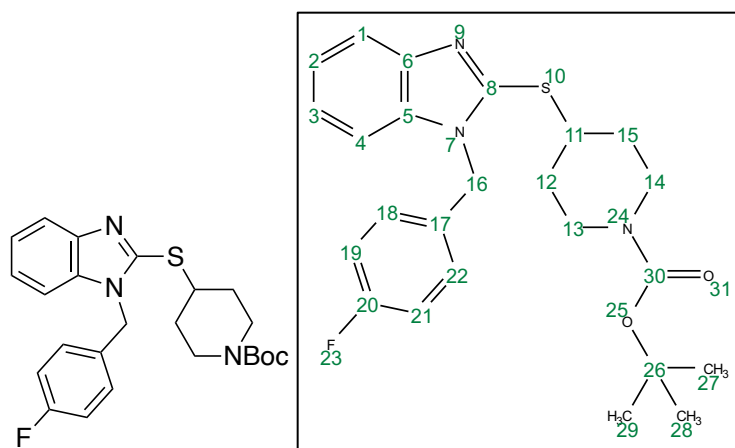
To an oven dried round bottom flask was added 1-(4-fluorobenzyl)-2-(piperidin-4-ylthio)-1*H*-benzo[*d*]imidazole hydrochloride intermediate (**3-24**) (0.38 g, 1.0 mmol, 1.0 equiv) dissolved in anhydrous DCM (10 mL). This solution was first neutralized to pH~7 using anhydrous Et₃N. The resulting solution was then cooled to 0°C. Then, at 0°C under an atmosphere of N₂ gas, was added Et₃N (0.17 mL, 1.25 mmol, 1.25 equiv). Next, at 0°C, under N₂ gas, was added 2-(4-methoxyphenyl)acetyl chloride (**3-13**) (0.18 g, 1.0 mmol, 1.0 equiv) dropwise in anhydrous DCM (3 mL). The resulting solution was then allowed to warm to 20°C and was stirred for 18 hours at 20°C under N₂ gas. After 18 hours, the reaction was then quenched with H₂O (20 mL), extracted with DCM (3x30mL), dried over Na₂SO₄, filtered, and concentrated in vacuo. The resulting crude residue was then purified via silica gel column chromatography (DCM/MeOH) to yield the desired product as a yellowish semi-solid. (0.45 g, 91%). ¹H NMR (500 MHz, CD₃OD) δ 7.60 (dd, *J* = 7.2, 1.6 Hz, 1H, (**H4**)), 7.34 (dd, *J* = 7.2, 1.6 Hz, 1H, (**H1**)), 7.23 (ddd, *J* = 7.4,

6.2, 1.5 Hz, 1H, (**H3**)), 7.20 (ddd, $J = 7.4, 6.2, 1.5$ Hz, 1H, (**H2**)), 7.17 – 7.10 (m, 4H, (**H19**, **H23**, **H28**, **H32**)), 7.00 (t, $J = 8.7$ Hz, 2H, (**H20**, **H22**)), 6.84 (d, $J = 8.7$ Hz, 2H, (**H29**, **H31**)), 5.35 (s, 2H, (**H17**)), 4.33 – 4.25 (m, 1H, (**H13**, **H15^(A)**)), 3.97 – 3.82 (m, 2H, (**H11**, **H13**, **H15^(B)**)), 3.73 (s, 3H, (**H35**)), 3.67 (d, $J = 5.7$ Hz, 2H, (**H26**)), 3.26 – 3.17 (m, 1H, (**H13**, **H15^(B)**)), 3.04 – 2.95 (m, 1H, (**H13**, **H15^(A)**)), 2.12 – 2.03 (m, 1H, (**H12**, **H16^(A)**)), 1.99 – 1.90 (m, 1H, (**H12**, **H16^(B)**)), 1.60 – 1.49 (m, 1H, (**H12**, **H16^(A)**)), 1.39 – 1.25 (m, 1H, (**H12**, **H16^(B)**)). ^{13}C NMR (126 MHz, CD_3OD) δ 172.21 (**C25**), 163.66 (d, $J = 245.1$ Hz, (**C21**)), 160.00 (**C30**), 151.22 (**C8**), 144.14 (**C6**), 136.83 (**C5**), 133.38 (d, $J = 3.3$ Hz, (**C18**)), 130.65 (**C28**, **C32**), 129.97 (d, $J = 8.1$ Hz, (**C19**, **C23**)), 128.12 (**C27**), 124.01 (**C3**), 123.70 (**C2**), 118.85 (**C4**), 116.58 (d, $J = 21.9$ Hz, (**C20**, **C22**)), 115.04 (**C29**, **C31**), 111.07 (**C1**), 55.66 (**C35**), 47.74 (**C17**), 46.76 (**C13**, **C15^(B)**), 44.98 (**C11**), 42.55 (**C13**, **C15^(A)**), 40.60 (**C26**), 33.67 (**C12**, **C16^(B)**), 33.04 (**C12**, **C16^(A)**). FTIR (cm^{-1}): 3027, 2893, 1658, 1517, 1243, 1042. HRMS-ESI (m/z): Calculated for $\text{C}_{28}\text{H}_{28}\text{FN}_3\text{O}_2\text{S}$ ($\text{M}+\text{H}$) $^+$: 490.1964, Found: 490.1979.



***tert*-butyl 4-((1*H*-benzo[*d*]imidazol-2-yl)thio)piperidine-1-carboxylate (3-22)**

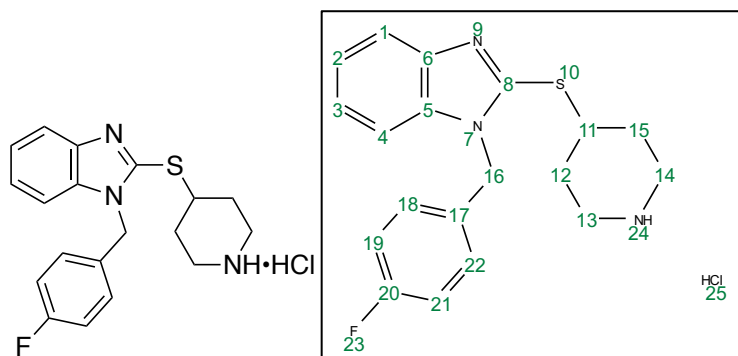
To an oven-dried round bottom flask was added containing a solution of *tert*-butyl 4-((methylsulfonyl)oxy)piperidine-1-carboxylate (0.56 g, 2.0 mmol, 1.0 equiv) and 2-mercapto-benzimidazole (0.30 g, 2.0 mmol, 1.0 equiv) in anhydrous EtOH (10 mL) was added K₂CO₃ (0.28 g, 2.0 mmol, 1.0 equiv) at room temperature, under an atmosphere of N₂ gas. The resulting reaction mixture was then heated to reflux (80°C) and was allowed to stir for 18 hours under an atmosphere of N₂ gas. After 18 hours, the reaction was allowed to cool to room temperature and was poured into saturated aqueous NH₄Cl solution (30 mL), followed by extraction with EtOAc (3x30mL). The extract was then washed with brine (25 mL), dried over Na₂SO₄ and concentrated in vacuo. The resulting precipitate was then collected via filtration after suspension in a mixed solvent of EtOAc/MeOH to afford the desired product as a white solid. (0.31 g, 46%). **M.P.:** 240°C (decomp.), **¹H NMR** (500 MHz, CDCl₃) δ 9.08 (s, 1H, **(H7)**), 7.69 (d, *J* = 7.2 Hz, 1H, **(H1)**), 7.35 (d, *J* = 7.4 Hz, 1H, **(H4)**), 7.26 – 7.17 (m, 2H, **(H2, H3)**), 4.06 – 3.99 (m, 1H, **(H11)**), 3.97 – 3.94 (m, 2H, **(H13, H14)**), 3.10 – 3.01 (m, 2H, **(H13, H14)**), 2.19 – 2.08 (m, 2H, **(H12, H15)**), 1.74 – 1.63 (m, 2H, **(H12, H15)**), 1.46 (s, 9H, **(H19, H20, H21)**). **¹³C NMR** (126 MHz, CDCl₃) δ 159.35 (**(C22)**), 154.83 (**(C8)**), 148.41 (**(C6)**), 145.52 (**(C5)**), 122.96 (**(C2)**), 122.30 (**(C3)**), 118.70 (**(C1)**), 114.91 (**(C2)**), 79.92 (**(C18)**), 44.17 (**(C13, C14)**), 43.84 (**(C11)**), 32.56 (**(C12, C15)**), 28.57 (**(C19, C20, C21)**). **FTIR (cm⁻¹):** 3423, 3051, 2890, 1688, 1244. **HRMS-ESI (m/z):** Calculated for C₁₇H₂₃N₃O₂S (M+H)⁺: 334.1589, Found: 334.1595.



***tert*-butyl 4-((1-(4-fluorobenzyl)-1*H*-benzo[*d*]imidazol-2-yl)thio)piperidine-1-carboxylate (3-23)**

To an oven-dried round bottom flask was added *tert*-butyl 4-((1*H*-benzo[*d*]imidazol-2-yl)thio)piperidine-1-carboxylate (0.67 g, 1.5 mmol, 1.0 equiv) dissolved in anhydrous DMF (10 mL) at 20°C under an atmosphere of N₂ gas. To this was then added K₂CO₃ (0.21 g, 1.5 mmol, 1.0 equiv) and 4-fluoro benzyl bromide (0.18 mL, 1.5 mmol, 1.0 equiv) sequentially at 20°C under N₂ gas. The resulting reaction mixture was then allowed to stir at 20°C for 18 hours under N₂ gas. After 18 hours, the reaction was quenched with DI H₂O (20 mL), washed with saturated aqueous LiCl solution (3x30 mL), extracted with EtOAc (3x30 mL), dried over Na₂SO₄, filtered, and concentrated in vacuo. The resulting crude residue was then purified via silica gel column chromatography (DCM/MeOH) to yield the desired product as a clear pale-yellow oil. (0.81 g, 92%). ¹H NMR (500 MHz, CD₃OD) δ 7.61 (d, *J* = 6.6 Hz, 1H, (**H4**)), 7.40 (d, *J* = 6.6 Hz, 1H, (**H1**)), 7.27 – 7.22 (m, 2H, (**H2**, **H3**)), 7.20 (dd, *J* = 8.8, 5.3 Hz, 2H, (**H19**, **H21**)), 7.04 (t, *J* = 8.7 Hz, 2H, (**H18**, **H22**)), 5.43 (s, 2H, (**H16**)), 3.99 – 3.90 (m, 3H, (**H11**, **H13**, **H14**)), 3.16 – 2.94 (m, 2H, (**H13**, **H14**)), 2.13 – 2.05 (m, 2H, (**H12**, **H15**)), 1.65 – 1.56 (m, 2H, (**H12**, **H15**)), 1.45 (s, 9H, (**H27**, **H28**, **H29**)). ¹³C NMR (126 MHz, CD₃OD) δ 163.73 (d, *J* = 245.1 Hz, (**C20**)),

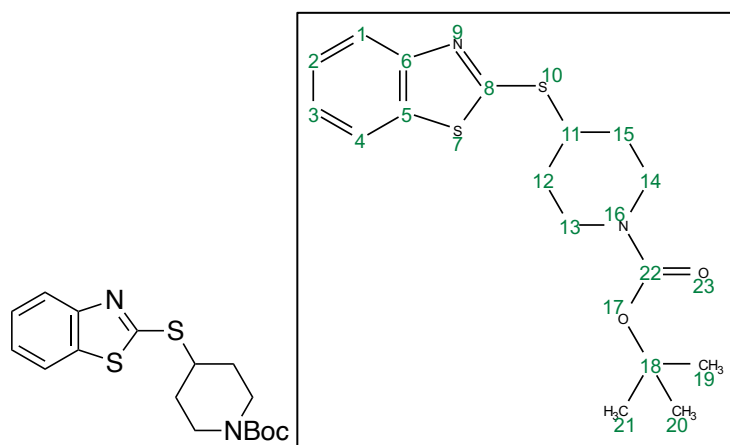
156.26 (C30), 151.46 (C8), 144.20 (C6), 136.91 (C5), 133.56 (d, $J = 3.3$ Hz, (C17)), 130.05 (d, $J = 8.1$ Hz, (C19, C21)), 124.01 (C3), 123.70 (C2), 118.85 (C1), 116.61 (d, $J = 21.9$ Hz, (C18, C22)), 111.11 (C4), 81.22 (C26), 54.84 (C16), 47.78 (C11), 45.33 (C13, C14), 33.08 (C12, C15), 28.64 (C27, C28, C29). FTIR (cm^{-1}): 3076, 2899, 1685, 1237. HRMS-ESI (m/z): Calculated for $\text{C}_{24}\text{H}_{28}\text{FN}_3\text{O}_2\text{S}$ ($M+H$) $^+$: 442.1964, Found: 442.1978.



1-(4-fluorobenzyl)-2-(piperidin-4-ylthio)-1H-benzo[d]imidazole hydrochloride (3-24)

To an oven-dried flask was added *tert*-butyl 4-((1-(4-fluorobenzyl)-1H-benzo[d]imidazol-2-yl)thio)piperidine-1-carboxylate (0.44 g, 1.0 mmol, 1.0 equiv) and ethanolic HCl (3.3M in EtOH, 5 mL). This was stirred at 20°C under an atmosphere of N_2 gas for 18 hours. After completion, as indicated by TLC, the reaction mixture was concentrated in vacuo to obtain a semi-solid. This semi-solid was triturated with Et_2O (5 mL) and concentrated in vacuo to afford the crude product as a yellow-red foaming solid. This was used in subsequent steps without any further purification (>99% determined by NMR, Quantitative). ^1H NMR (500 MHz, CD_3OD) δ 7.72 – 7.64 (m, 1H, (H4)), 7.51 – 7.39 (m, 1H, (H1)), 7.26 – 7.18 (m, 2H, (H2, H3)), 7.02 – 6.99 (m, 2H, (H19, H21)), 6.79 – 6.69 (m, 2H, (H18, H22)), 5.37 (s, 2H, (H16)), 4.03 – 3.76 (m, 1H, (H11)), 3.13 – 3.01 (m, 2H, (H13, H14)), 2.88 – 2.77 (m, 2H, (H13, H14)), 2.03 – 1.99 (m, 2H, (H12, H15)),

1.71 – 1.68 (m, 2H, **(H12, H15)**). ^{13}C NMR (126 MHz, CD_3OD) δ 164.21 (d, $J = 240.3$ Hz, **(C20)**), 149.63 **(C8)**, 134.28 **(C6)**, 133.33 **(C5)**, 131.09 (d, $J = 8.6$ Hz, **(C17)**), 129.77 **(C3)**, 128.14 (d, $J = 31.9$ Hz, **(C19, C21)**), 126.91 **(C2)**, 117.20 (d, $J = 21.9$ Hz, **(C18, C22)**), 115.17 **(C1)**, 114.12 **(C4)**, 50.49 **(C16)**, 44.76 **(C13, C14)**, 37.85 **(C11)**, 32.36 **(C12, C15)**. FTIR (cm^{-1}): 3331, 3032, 2883, 1517. HRMS-ESI (m/z): Calculated for $\text{C}_{19}\text{H}_{20}\text{FN}_3\text{S}$ ($\text{M}+\text{H}$) $^+$: 342.1440, Found: 342.1466.

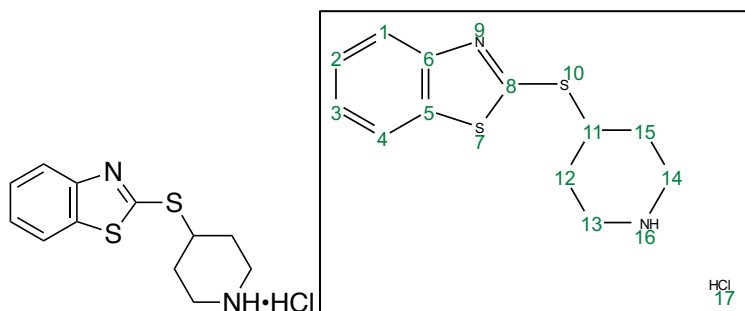


tert-butyl 4-(benzo[*d*]thiazol-2-ylthio)piperidine-1-carboxylate (3-25)

To an oven-dried round bottom flask was added containing a solution of *tert*-butyl 4-((methylsulfonyl)oxy)piperidine-1-carboxylate (0.56 g, 2.0 mmol, 1.0 equiv) and 2-mercapto-benzothiazole (0.33 g, 2.0 mmol, 1.0 equiv) in anhydrous EtOH (15 mL) was added K_2CO_3 (0.28 g, 2.0 mmol, 1.0 equiv) at room temperature, under an atmosphere of N_2 gas. The resulting reaction mixture was then heated to reflux (80°C) and was allowed to stir for 18 hours under an atmosphere of N_2 gas. After 18 hours, the reaction was allowed to cool to room temperature and was poured into saturated aqueous NH_4Cl solution (30 mL), followed by extraction with EtOAc (3x30mL). The extract was then washed with brine (20 mL), dried over Na_2SO_4 and concentrated

in vacuo. The resulting crude residue was then purified via silica gel column chromatography (DCM/MeOH) to yield the desired product as a clear pale orange-pink solid. (0.62 g, 88%).

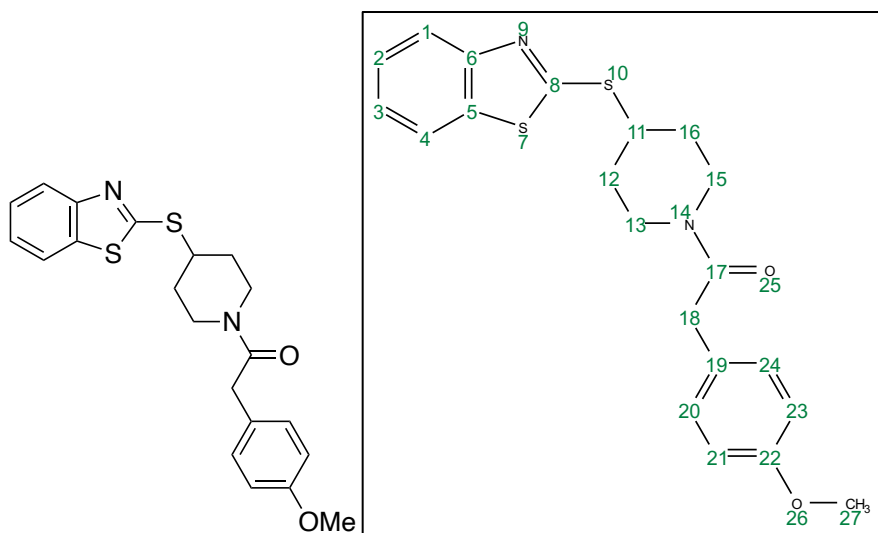
M.P.: 148 – 150°C. **¹H NMR** (500 MHz, CDCl₃) δ 7.88 (d, *J* = 8.1 Hz, 1H, **(H4)**), 7.76 (d, *J* = 8.0 Hz, 1H, **(H1)**), 7.42 (td, *J* = 8.3, 7.2, 1.3 Hz, 1H, **(H2)**), 7.31 (td, *J* = 8.2, 7.2, 1.2 Hz, 1H, **(H3)**), 4.16 – 4.05 (m, 1H, **(H11)**), 3.96 (s, 2H, **(H13, H14)**), 3.16 – 3.08 (m, 2H, **(H13, H14)**), 2.23 – 2.14 (m, 2H, **(H12, H15)**), 1.79 – 1.68 (m, 2H, **(H12, H15)**), 1.47 (s, 9H, **(H19, H20, H21)**). **¹³C NMR** (126 MHz, CDCl₃) δ 165.26 (**(C8)**), 154.80 (**(C22)**), 153.41 (**(C6)**), 135.43 (**(C5)**), 126.21 (**(C2)**), 124.56 (**(C3)**), 121.79 (**(C1)**), 121.13 (**(C4)**), 79.93 (**(C18)**), 44.74 (**(C13, C14)**), 32.20 (**(C11)**), 28.63 (**(C12, C15)**), 28.57 (**(C19, C20, C21)**). **FTIR (cm⁻¹):** 3021, 2893, 1672, 1505, 1221. **HRMS-ESI (m/z):** Calculated for C₁₂H₂₂N₂O₂S₂Na (M+H)⁺: 374.1099, Found: 374.1102.



2-(piperidin-4-ylthio)benzo[d]thiazole hydrochloride (3-26)

To an oven-dried flask was added *tert*-butyl 4-(benzo[d]thiazol-2-ylthio)piperidine-1-carboxylate (0.60 g, 1.8 mmol, 1.0 equiv) and ethanolic HCl (3.3M in EtOH, 5 mL). This was stirred at 20°C under an atmosphere of N₂ gas for 18 hours. After completion, as indicated by TLC, the reaction mixture was concentrated in vacuo to obtain a semi-solid. This semi-solid was triturated with Et₂O (5 mL) and concentrated in vacuo to afford the crude product quantitatively as an off-white foaming solid. This was used in subsequent steps without any further purification (>99%

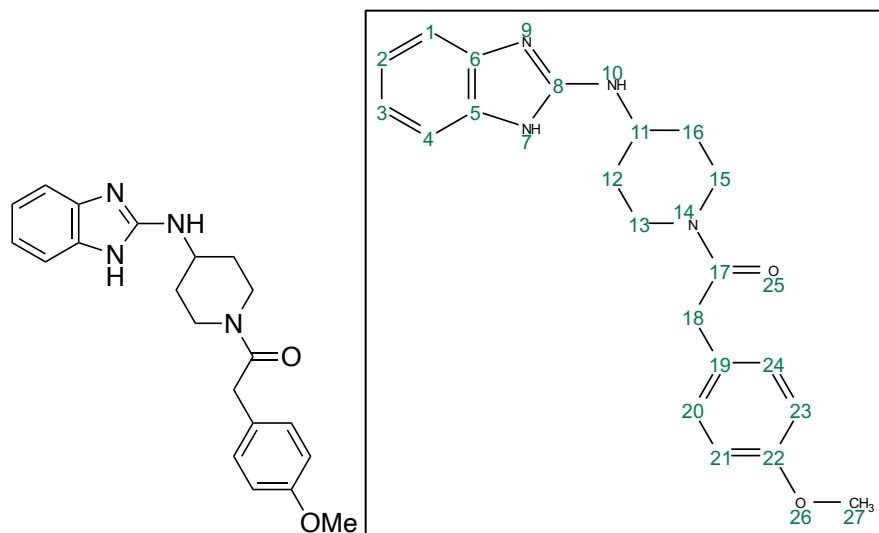
determined by NMR, Quantitative). ^1H NMR (500 MHz, CD_3OD) δ 7.90 (d, $J = 8.0$ Hz, 1H, **(H4)**), 7.86 (d, $J = 8.1$ Hz, 1H, **(H1)**), 7.48 (td, $J = 8.2, 7.2, 1.3$ Hz, 1H, **(H2)**), 7.38 (td, $J = 8.3, 7.4, 1.3$ Hz, 1H, **(H3)**), 4.32 – 4.16 (m, 1H, **(H11)**), 3.54 – 3.44 (m, 2H, **(H13, H14)**), 3.29 – 3.25 (m, 2H, **(H13, H14)**), 2.54 – 2.45 (m, 2H, **(H12, H15)**), 2.15 – 2.03 (m, 2H, **(H12, H15)**). ^{13}C NMR (126 MHz, CD_3OD) δ 165.88 (**(C8)**), 154.35 (**(C6)**), 136.44 (**(C5)**), 127.53 (**(C2)**), 126.03 (**(C3)**), 122.51 (**(C1)**), 122.48 (**(C4)**), 44.50 (**(C13, 14)**), 42.54 (**(C11)**), 30.03 (**(C12, C15)**). FTIR (cm^{-1}): 3311, 3002, 2875, 1505. HRMS-ESI (m/z): Calculated for $\text{C}_{12}\text{H}_{14}\text{N}_2\text{S}_2$ ($\text{M}+\text{H}$) $^+$: 251.0677, Found: 251.0686.



1-(4-(benzo[*d*]thiazol-2-ylthio)piperidin-1-yl)-2-(4-methoxyphenyl)ethan-1-one (**3-5**)

To an oven dried round bottom flask was added 2-(piperidin-4-ylthio)benzo[*d*]thiazole hydrochloride intermediate (**3-26**) (0.49 g, 1.8 mmol, 1.0 equiv) dissolved in anhydrous DCM (10 mL). This solution was first neutralized to pH~7 using anhydrous Et_3N . The resulting solution was then cooled to 0°C . Then, at 0°C under an atmosphere of N_2 gas, was added Et_3N (0.31 mL, 2.3 mmol, 1.25 equiv). Next, at 0°C , under N_2 gas, was added 2-(4-

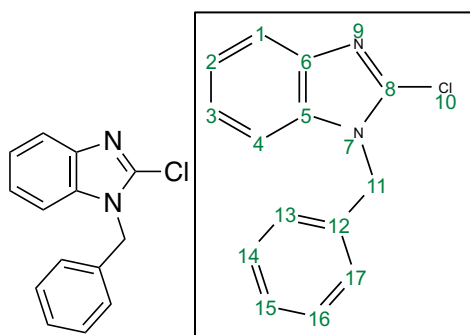
methoxyphenyl)acetyl chloride (**3-13**) (0.32 g, 1.8 mmol, 1.0 equiv) dropwise in anhydrous DCM (1 mL). The resulting solution was then allowed to warm to 20°C and was stirred for 18 hours at 20°C under N₂ gas. After 18 hours, the reaction was then quenched with H₂O (20 mL), extracted with DCM (3x30mL), dried over Na₂SO₄, filtered, and concentrated in vacuo. The resulting crude residue was then purified via silica gel column chromatography (DCM/MeOH) to yield the desired product as a white semi-solid. (0.49 g, 72%). ¹H NMR (500 MHz, CD₃OD) δ 7.85 (d, *J* = 8.0 Hz, 1H, **(H4)**), 7.82 (d, *J* = 8.1 Hz, 1H, **(H1)**), 7.45 (t, *J* = 7.6 Hz, 1H, **(H2)**), 7.35 (t, *J* = 7.6 Hz, 1H, **(H3)**), 7.17 (d, *J* = 8.3 Hz, 2H, **(H21, H23)**), 6.88 (d, *J* = 8.4 Hz, 2H, **(H20, H24)**), 4.38 – 4.29 (m, 1H, **(H13 or H15^(A))**), 4.13 – 4.05 (m, 1H, **(H11)**), 3.99 – 3.92 (m, 1H, **(H13 or H15^(B))**), 3.76 (s, 3H, **(H27)**), 3.72 (d, *J* = 2.6 Hz, 2H, **(H18)**), 3.35 – 3.29 (m, 1H, **(H13 or H15^(B))**), 3.15 – 3.01 (m, 1H, **(H13 or H15^(A))**), 2.25 – 2.16 (m, 1H, **(H12 or H16^(A))**), 2.12 – 2.04 (m, 1H, **(H12 or H16^(B))**), 1.72 – 1.59 (m, 1H, **(H12 or H16^(A))**), 1.52 – 1.41 (m, 1H, **(H12 or H16^(B))**). ¹³C NMR (126 MHz, CD₃OD) δ 172.38 (**(C17)**), 166.83 (**(C8)**), 160.12 (**(C22)**), 154.37 (**(C6)**), 136.37 (**(C5)**), 130.70 (**(C21, C23)**), 128.19 (**(C19)**), 127.45 (**(C2)**), 125.86 (**(C3)**), 122.38 (**(C1)**), 122.36 (**(C4)**), 115.21 (**(C20, C24)**), 55.68 (**(C27)**), 46.87 (**(C13 or C15^(B))**), 45.35 (**(C11)**), 42.64 (**(C13 or C15^(A))**), 40.62 (**(C18)**), 33.53 (**(C12 or C16^(B))**), 32.97 (**(C12 or C16^(A))**). FTIR (cm⁻¹): 3076, 2893, 1656, 1510, 1255, 1044. HRMS-ESI (m/z): Calculated for C₂₁H₂₂N₂O₂S₂ (M+H)⁺: 399.1201, Found: 399.1221.



1-(4-((1*H*-benzo[*d*]imidazol-2-yl)amino)piperidin-1-yl)-2-(4-methoxyphenyl)ethan-1-one – (3-6)

In an oven-dried flask, 2-chloro-1*H*-benzo[*d*]imidazole (0.15 g, 1.0 mmol, 1.0 equiv) was dissolved in anhydrous dimethylacetamide (DMA) (5 mL). To this was then added the neutralized acylated 4-amino piperidine tail (**3-15**) (1.24 g, 5.0 mmol, 5.0 equiv). The resulting mixture was then heated to 140°C and was allowed to stir for 48 hours under an atmosphere of nitrogen gas. After 48 hours, the solution was allowed to cool to room temperature and was diluted with EtOAc (30 mL), washed with saturated aqueous LiCl solution (2x30mL), extracted with EtOAc (3x30mL), dried over Na₂SO₄, filtered, and concentrated in vacuo. The resulting crude residue was then purified via silica gel column chromatography (DCM/MeOH) to yield the desired product as a clear, colorless oil. (0.20 g, 54%). ¹H NMR (500 MHz, CD₃OD) δ 7.40 – 7.33 (m, 2H, (**H1**, **H4**)), 7.27 – 7.22 (m, 2H, (**H2**, **H3**)), 7.20 (d, *J* = 8.0 Hz, 2H, (**H21**, **H23**)), 6.89 (d, *J* = 8.1 Hz, 2H, (**H20**, **H24**)), 4.56 – 4.50 (m, 1H, (**H13** or **H15**^(A))), 4.15 – 4.00 (m, 1H, (**H13** or **H15**^(B))), 3.91 – 3.80 (m, 1H, (**H11**)), 3.79 – 3.74 (m, 5H, (**H18**, **H27**)), 3.31 – 3.23 (m, 1H, (**H13** or **H15**^(B))), 2.98 – 2.86 (m, 1H, (**H13** or **H15**^(A))), 2.02 – 1.95 (m, 1H, (**H12** or

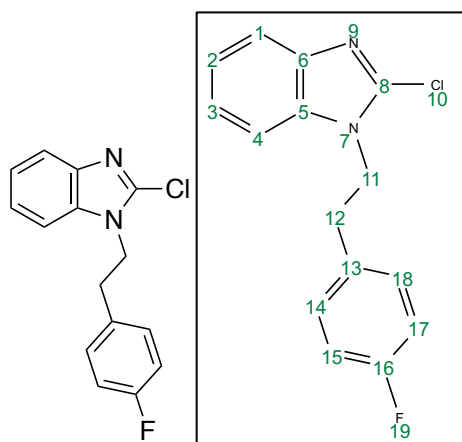
H16^(A)), 1.89 – 1.80 (m, 1H, (**H12 or H16^(B)**)), 1.53 – 1.41 (m, 1H, (**H12 or H16^(A)**)), 1.36 – 1.32 (m, 1H, (**H12 or H16^(B)**)). ¹³C NMR (126 MHz, CD₃OD) δ 172.42 (**C17**), 160.09 (**C22**), 150.80 (**C8**), 131.75 (**C5, C6**), 130.74 (**C21, C23**), 128.21 (**C19**), 124.50 (**C2, C3**), 115.22 (**C20, C24**), 112.42 (**C1, C4**), 55.70 (**C27**), 51.91 (**C11**), 45.97 (**C13 or C15^(B)**), 41.59 (**C13 or C15^(A)**), 40.64 (**C18**), 33.02 (**C12 or C16^(B)**), 32.44 (**C12 or C16^(A)**). FTIR (cm⁻¹): 3422, 3348, 3025, 2879, 1661, 1530, 1252, 1040. HRMS-ESI (m/z): Calculated for C₂₁H₂₄N₄O₂ (M+H)⁺: 365.1978, Found: 365.1998.



1-benzyl-2-chloro-1*H*-benzo[*d*]imidazole (3-27)

To an oven-dried round bottom flask was added 2-chloro-1*H*-benzimidazole (0.50 g, 3.3 mmol, 1.0 equiv) dissolved in anhydrous DMSO (3 mL). Then NaH (0.25 g (60 wt% in mineral oil), 6.6 mmol, 2.0 equiv) at room temperature. The resulting reaction mixture was then allowed to stir for one hour at room temperature under an atmosphere of N₂ gas. After one hour, benzyl bromide (0.51 mL, 4.3 mmol, 1.3 equiv) was added at room temperature under N₂ gas and the reaction was allowed to stir for 18 hours. After 18 hours the reaction was then quenched slowly with ice cold H₂O (20 mL) and a white precipitate then formed. The white precipitate was then collected via vacuum filtration to afford the desired product as a white solid (0.70 g, 88%). **M.P.:** 106-

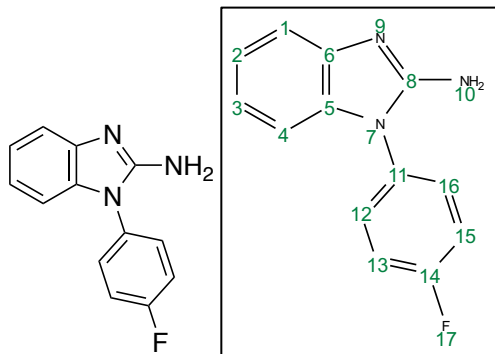
108°C, $^1\text{H NMR}$ (500 MHz, CD_3OD) δ 7.61 (dd, $J = 6.2, 3.1$ Hz, 1H, (**H4**)), 7.44 (dd, $J = 6.1, 3.2$ Hz, 1H, (**H1**)), 7.37 – 7.23 (m, 5H, (**H2**, **H3**, **H14**, **H15**, **H16**)), 7.19 (d, $J = 7.1$ Hz, 2H, (**H13**, **H17**)), 5.49 (s, 2H, (**H11**)). $^{13}\text{C NMR}$ (126 MHz, CD_3OD) δ 142.26 (**C6**), 141.98 (**C8**), 136.83 (**C12**), 136.34 (**C5**), 130.01 (**C14**, **C16**), 129.17 (**C15**), 127.96 (**C13**, **C17**), 124.85 (**C3**), 124.33 (**C2**), 119.51 (**C4**), 111.74 (**C1**), 48.73 (**C11**). **FTIR** (cm^{-1}): 3009, 2875, 1508. **HRMS-ESI** (m/z): Calculated for $\text{C}_{14}\text{H}_{11}\text{ClN}_2$ ($\text{M}+\text{H}$) $^+$, (Cl^{35}); (Cl^{37}): 243.0689; 245.0663, Found: 243.0705; 245.0683.



2-chloro-1-(4-fluorophenethyl)-1H-benzo[d]imidazole (3-28)

In an oven dried flask, 2-chloro-1H-benzimidazole (0.31 g, 2.0 mmol, 1.0 equiv) was dissolved in anhydrous DMF (5 mL). To this was then sequentially added K_2CO_3 (0.28 g, 2.0 mmol, 1.0 equiv) and 1-(2-bromoethyl)-4-fluorobenzene (0.41 g, 2.0 mmol, 1.0 equiv) at room temperature. This resulting solution was allowed to stir for 24 hours at room temperature, under an atmosphere of nitrogen gas. After 24 hours, the reaction mixture was diluted in EtOAc (30 mL), washed with saturated aqueous LiCl solution (2x30mL), extracted with EtOAc (3x30mL), dried over Na_2SO_4 , filtered, and concentrated in vacuo. The resulting crude residue was then purified

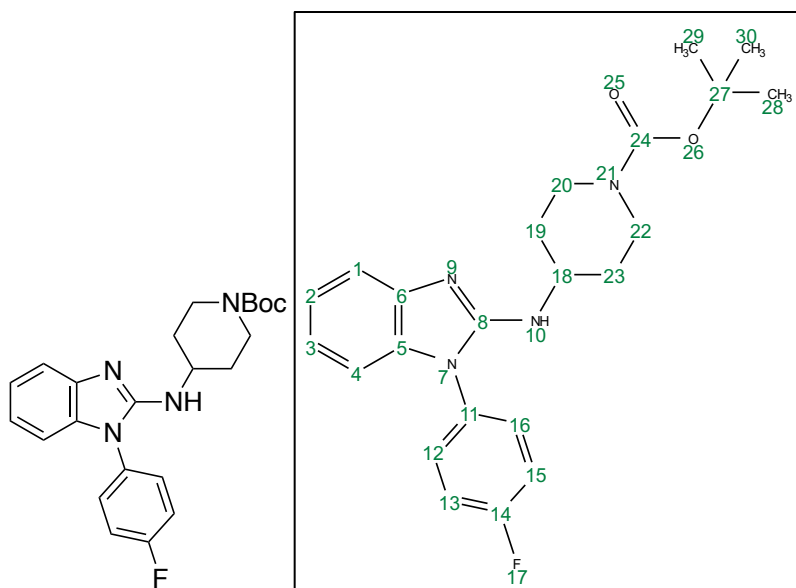
via silica gel column chromatography (DCM/MeOH) to yield the desired product as a white solid. (0.41 g, 74%). **M.P.:** 70 - 71°C, **¹H NMR** (500 MHz, CDCl₃) δ 7.72 – 7.67 (m, 1H, **(H4)**), 7.30 – 7.24 (m, 2H, **(H2, H3)**), 7.20 – 7.17 (m, 1H, **(H1)**), 7.01 (dd, *J* = 8.5, 5.5 Hz, 2H, **(H15, H17)**), 6.94 (t, *J* = 8.6 Hz, 2H, **(H14, H18)**), 4.38 (t, *J* = 7.2 Hz, 2H, **(H11)**), 3.08 (t, *J* = 7.2 Hz, 2H, **(H12)**). **¹³C NMR** (126 MHz, CDCl₃) δ 162.12 (d, *J* = 245.6 Hz, **(C16)**), 141.77 (**(C6)**), 140.61 (**(C8)**), 134.84 (**(C5)**), 132.89 (d, *J* = 3.3 Hz, **(C13)**), 130.40 (d, *J* = 8.1 Hz, **(C15, C17)**), 123.30 (**(C3)**), 122.84 (**(C2)**), 119.68 (**(C4)**), 115.80 (d, *J* = 21.5 Hz, **(C14, C18)**), 109.36 (**(C1)**), 46.09 (**(C11)**), 34.90 (**(C12)**). **FTIR (cm⁻¹):** 3022, 2884, 1514. **HRMS-ESI (m/z):** Calculated for C₁₅H₁₂ClFN₂ (M+H)⁺, (Cl³⁵); (Cl³⁷): 275.0751; 277.0762, Found: 275.0758; 277.0770.



1-(4-fluorophenyl)-1*H*-benzo[*d*]imidazol-2-amine (3-29)

To an oven-dried round bottom flask was added 1*H*-benzo[*d*]imidazol-2-amine (0.40 g, 3.0 mmol, 1.0 equiv) at room temperature in anhydrous EtOH (5 mL). To this was then added (4-fluorophenyl)boronic acid (0.42 g, 3.0 mmol, 1.0 equiv) and Cu(OTf)₂ (0.22 g, 0.6 mmol, 0.2 equiv) under an atmosphere of air (air balloon). The resulting reaction mixture was then allowed to stir for 24 hours at room temperature under an atmosphere of air. After 24 hours, the reaction mixture was concentrated in vacuo and then was immediately purified via silica gel column

chromatography (DCM/MeOH (2% Et₃N)) to yield the desired product an off-white solid (0.50 g, 73%). **M.P.:** 125-127°C, **¹H NMR** (500 MHz, CD₃OD) δ 7.52 (dd, *J* = 8.9, 4.9 Hz, 2H, (**H13**, **H15**)), 7.38 (t, *J* = 8.7 Hz, 2H, (**H12**, **H16**)), 7.30 (d, *J* = 7.8 Hz, 1H, (**H4**)), 7.10 (t, *J* = 7.6 Hz, 1H, (**H2**)), 6.99 (t, *J* = 7.6 Hz, 1H, (**H3**)), 6.87 (d, *J* = 7.9 Hz, 1H, (**H1**)). **¹³C NMR** (126 MHz, CD₃OD) δ 164.04 (d, *J* = 247.5 Hz, (**C14**)), 155.57 (**C8**), 143.58 (**C6**), 141.91 (**C5**), 132.03 (d, *J* = 3.0 Hz, (**C11**)), 130.60 (d, *J* = 9.1 Hz, (**C13**, **C15**)), 123.32 (**C2**), 121.41 (**C3**), 118.25 (d, *J* = 22.9 Hz, (**C12**, **C16**)), 115.86 (**C4**), 109.27 (**C1**). **FTIR (cm⁻¹):** 3377, 3315, 3041, 2881, 1524. **HRMS-ESI (m/z):** Calculated for C₁₃H₁₀FN₃ (M+H)⁺: 228.0937, Found: 228.0954.



***tert*-butyl 4-((1-(4-fluorophenyl)-1*H*-benzo[*d*]imidazol-2-yl)amino)piperidine-1-carboxylate (3-30)**

To an oven-dried round bottom flask was added containing a solution of *tert*-butyl 4-((methylsulfonyl)oxy)piperidine-1-carboxylate (0.14 g, 0.5 mmol, 1.0 equiv) and 1-(4-fluorophenyl)-1*H*-benzo[*d*]imidazol-2-amine (**3-29**) (0.11 g, 0.5 mmol, 1.0 equiv) in anhydrous

EtOH (10 mL) was added K₂CO₃ (69.1 mg, 0.5 mmol, 1.0 equiv) at room temperature, under an atmosphere of N₂ gas. The resulting reaction mixture was then heated to reflux (80°C) and was allowed to stir for 18 hours under an atmosphere of N₂ gas. After 18 hours, the reaction was allowed to cool to room temperature and was poured into saturated aqueous NH₄Cl solution (30 mL), followed by extraction with EtOAc (3x30mL). The extract was then washed with brine (20 mL), dried over Na₂SO₄ and concentrated in vacuo. The resulting crude residue was then purified via silica gel column chromatography (DCM/MeOH) to yield the desired product as an off-white foaming solid. (0.27 g, 65%). ¹H NMR (500 MHz, CD₃OD) δ 7.53 (dd, *J* = 8.9, 4.8 Hz, 2H, **(H13, H15)**), 7.39 (t, *J* = 8.7 Hz, 2H, **(H12, H16)**), 7.31 (d, *J* = 7.8 Hz, 1H, **(H4)**), 7.13 (td, *J* = 7.6, 1.2 Hz, 1H, **(H2)**), 7.01 (td, *J* = 7.6, 1.2 Hz, 1H, **(H3)**), 6.89 (d, *J* = 7.9 Hz, 1H, **(H1)**), 4.89 – 4.85 (m, 1H, **(H18)**), 3.76 – 3.61 (m, 2H, **(H20, H22)**), 3.40 – 3.26 (m, 2H, **(H20, H22)**), 2.03 – 1.92 (m, 2H, **(H19, H23)**), 1.88 – 1.70 (m, 2H, **(H19, H23)**), 1.46 (s, 9H, **(H28, H29, H30)**). ¹³C NMR (126 MHz, CD₃OD) δ 164.14 (d, *J* = 248.0 Hz, **(C14)**), 156.33 (**(C24)**), 155.25 (**(C8)**), 140.90 (**(C6)**), 135.85 (**(C5)**), 131.72 (d, *J* = 3.2 Hz, **(C11)**), 130.67 (d, *J* = 9.1 Hz, **(C13, C15)**), 123.54 (**(C2)**), 121.73 (**(C3)**), 118.31 (d, *J* = 23.4 Hz, **(C12, C16)**), 115.59 (**(C4)**), 109.44 (**(C1)**), 81.35 (**(C27)**), 78.96 (**(C18)**), 46.45 (**(C20, C22)**), 32.64 (**(C19, C23)**), 28.61 (**(C28, C29, C30)**). FTIR (cm⁻¹): 3339, 3021, 2883, 1680, 1528, 1233. HRMS-ESI (*m/z*): Calculated for C₂₃H₂₇FN₄O₂ (M+H)⁺: 411.2196, Found: 411.2221.

REFERENCES

- (1) Tanaka, K., The Proteasome: Overview of Structure and Functions, *Proc. Jpn. Acad., Ser. B*, **2009**, 85 (1), 12–36. <https://doi.org/10.2183/pjab.85.12>.
- (2) Jones, C. L.; Tepe, J. J., Proteasome Activation to Combat Proteotoxicity, *Molecules*, **2019**, 24 (15), 2841. <https://doi.org/10.3390/molecules24152841>.
- (3) George, D. E.; Tepe, J. J., Advances in Proteasome Enhancement by Small Molecules, *Biomolecules*, **2021**, 11 (12), 1789. <https://doi.org/10.3390/biom11121789>.
- (4) Da Fonseca, P. C. A.; Morris, E. P., Structure of the Human 26S Proteasome, *Journal of Biological Chemistry*, **2008**, 283 (34), 23305–23314. <https://doi.org/10.1074/jbc.M802716200>.
- (5) Ben-Nissan, G.; Sharon, M., Regulating the 20S Proteasome Ubiquitin-Independent Degradation Pathway, *Biomolecules*, **2014**, 4 (3), 862–884. <https://doi.org/10.3390/biom4030862>.
- (6) Asher, G.; Reuven, N.; Shaul, Y., 20S Proteasomes and Protein Degradation “by Default”, *BioEssays*, **2006**, 28 (8), 844–849. <https://doi.org/10.1002/bies.20447>.
- (7) Uversky, V. N., Intrinsically Disordered Proteins and Their (Disordered) Proteomes in Neurodegenerative Disorders, *Front. Aging Neurosci.*, **2015**, 7 (18), 1–6. <https://doi.org/10.3389/fnagi.2015.00018>.
- (8) Mikitsh, J. L.; Chacko, A. M., Pathways for Small Molecule Delivery to the Central Nervous System across the Blood-Brain Barrier, *Perspect Medicin Chem*, **2014**, 6, PMC.S13384. <https://doi.org/10.4137/PMC.S13384>.
- (9) Lipinski, C. A.; Lombardo, F.; Dominy, B. W.; Feeney, P. J., Experimental and Computational Approaches to Estimate Solubility and Permeability in Drug Discovery and Development Settings 1PII, *Advanced Drug Delivery Reviews*, **2001**, 46 (1–3), 3–26. [https://doi.org/10.1016/S0169-409X\(00\)00129-0](https://doi.org/10.1016/S0169-409X(00)00129-0).
- (10) Du, D.; Xu, D.; Zhu, L.; Stazi, G.; Zwergel, C.; Liu, Y.; Luo, Z.; Li, Y.; Zhang, Y.; Zhu, K.; Ding, Y.; Liu, J.; Fan, S.; Zhao, K.; Zhang, N.; Kong, X.; Jiang, H.; Chen, K.; Zhao, K.; Valente, S.; Min, J.; Duan, W.; Luo, C., Structure-Guided Development of Small-Molecule PRC2 Inhibitors Targeting EZH2–EED Interaction, *J. Med. Chem.*, **2021**, 64 (12), 8194–8207. <https://doi.org/10.1021/acs.jmedchem.0c02261>.
- (11) Lan, P.; Romero, F. A.; Malcolm, T. S.; Stevens, B. D.; Wodka, D.; Makara, G. M., An Efficient Method to Access 2-Substituted Benzimidazoles under Solvent-Free Conditions, *Tetrahedron Letters*, **2008**, 49 (12), 1910–1914. <https://doi.org/10.1016/j.tetlet.2008.01.100>.

- (12) Dong, Y.; Roberge, J. Y.; Wang, Z.; Wang, X.; Tamasi, J.; Dell, V.; Golla, R.; Corte, J. R.; Liu, Y.; Fang, T.; Anthony, M. N.; Schnur, D. M.; Agler, M. L.; Dickson, J. K.; Lawrence, R. M.; Prack, M. M.; Seethala, R.; Feyen, J. H. M., Characterization of a New Class of Selective Nonsteroidal Progesterone Receptor Agonists, *Steroids*, **2004**, *69* (3), 201–217. <https://doi.org/10.1016/j.steroids.2003.12.007>.
- (13) Imamura, S.; Hashiguich, S.; Hattori, T.; Nishimura, O.; Kanzaki, N.; Baba, M.; Sugihara, Y., Cyclic Amine Compounds as CCR5 Antagonists, *U.S. Patent 6562978 B1*, **2003**.
- (14) Kumar, M.; Okombo, J.; Mambwe, D.; Taylor, D.; Lawrence, N.; Reader, J.; Van Der Watt, M.; Fontinha, D.; Sanches-Vaz, M.; Bezuidenhout, B. C.; Lauterbach, S. B.; Liebenberg, D.; Birkholtz, L.-M.; Coetzer, T. L.; Prudêncio, M.; Egan, T. J.; Wittlin, S.; Chibale, K., Multistage Antiplasmodium Activity of Astemizole Analogues and Inhibition of Hemozoin Formation as a Contributor to Their Mode of Action, *ACS Infect. Dis.*, **2019**, *5* (2), 303–315. <https://doi.org/10.1021/acsinfecdis.8b00272>.
- (15) Nageswar R., D.; Rasheed, Sk.; Vishwakarma, R. A.; Das, P. Copper-Catalyzed Sequential N-Arylation of C-Amino-NH-Azoles, *Chem. Commun.*, **2014**, *50* (85), 12911–12914. <https://doi.org/10.1039/C4CC05628K>.

Figure 3.5. ^1H NMR and ^{13}C NMR spectra of compound **3-12**.

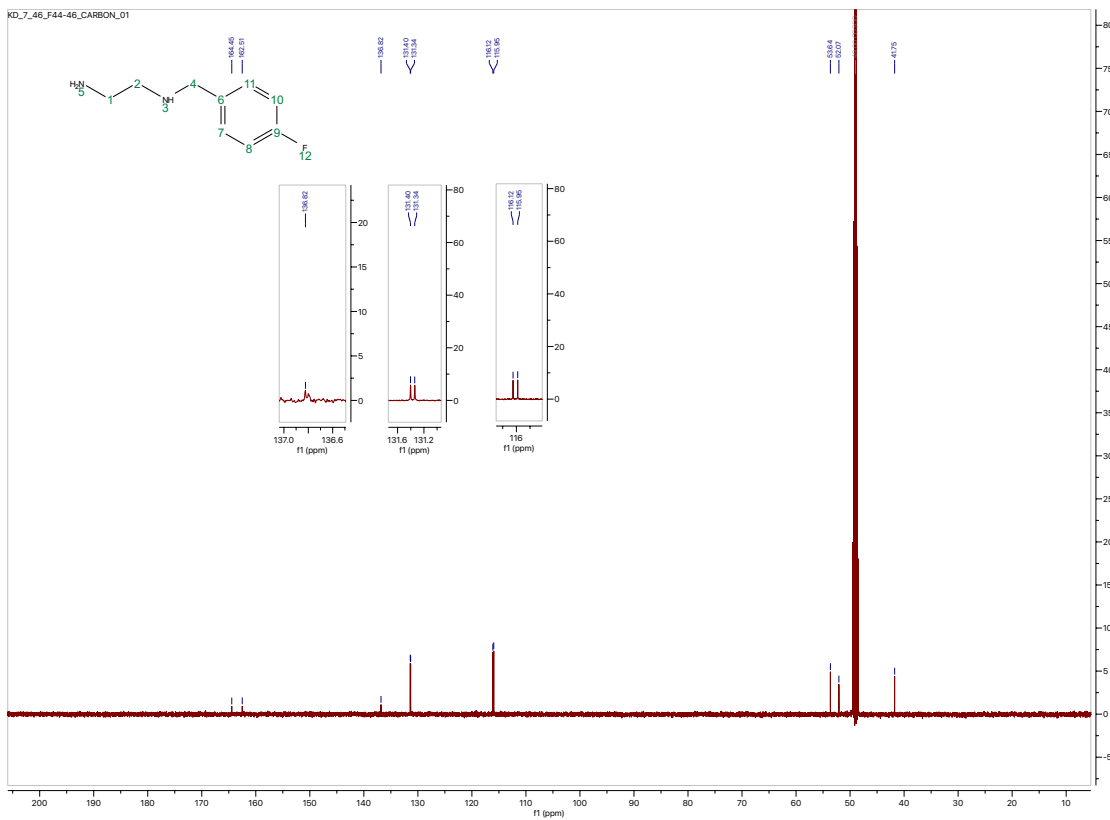
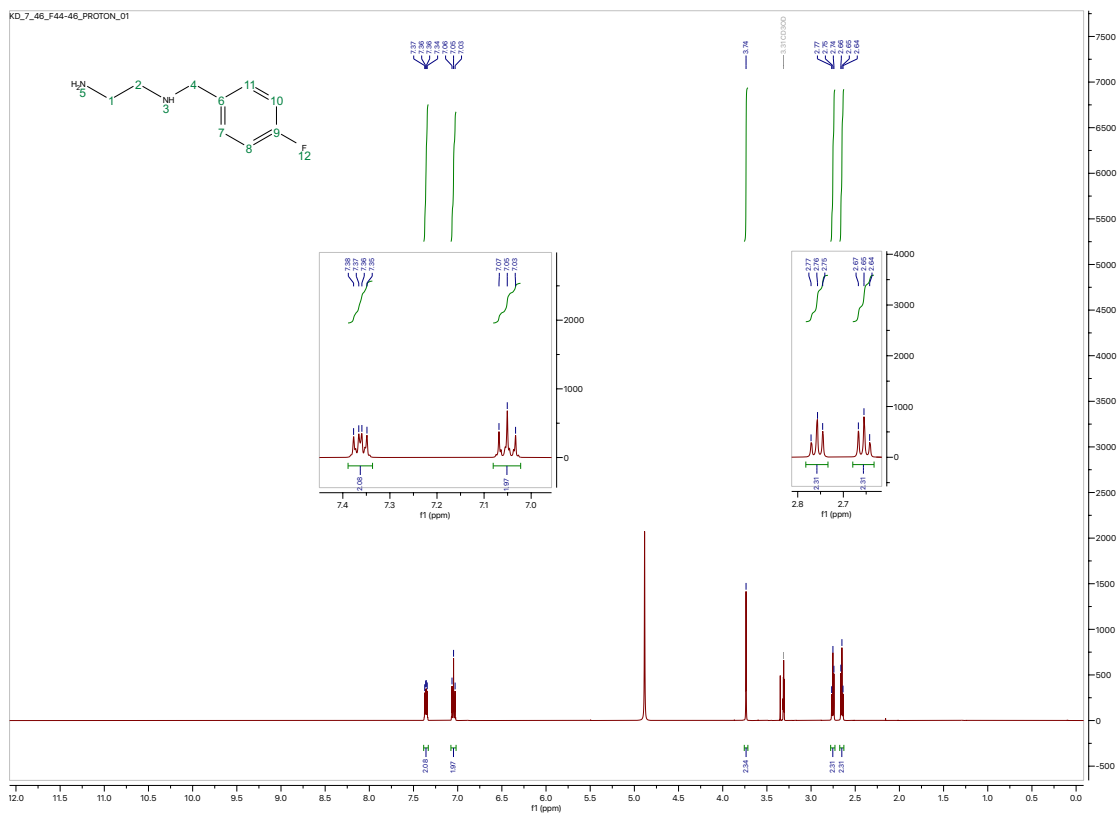


Figure 3.6. ^1H NMR and ^{13}C NMR spectra of compound **3-13**.

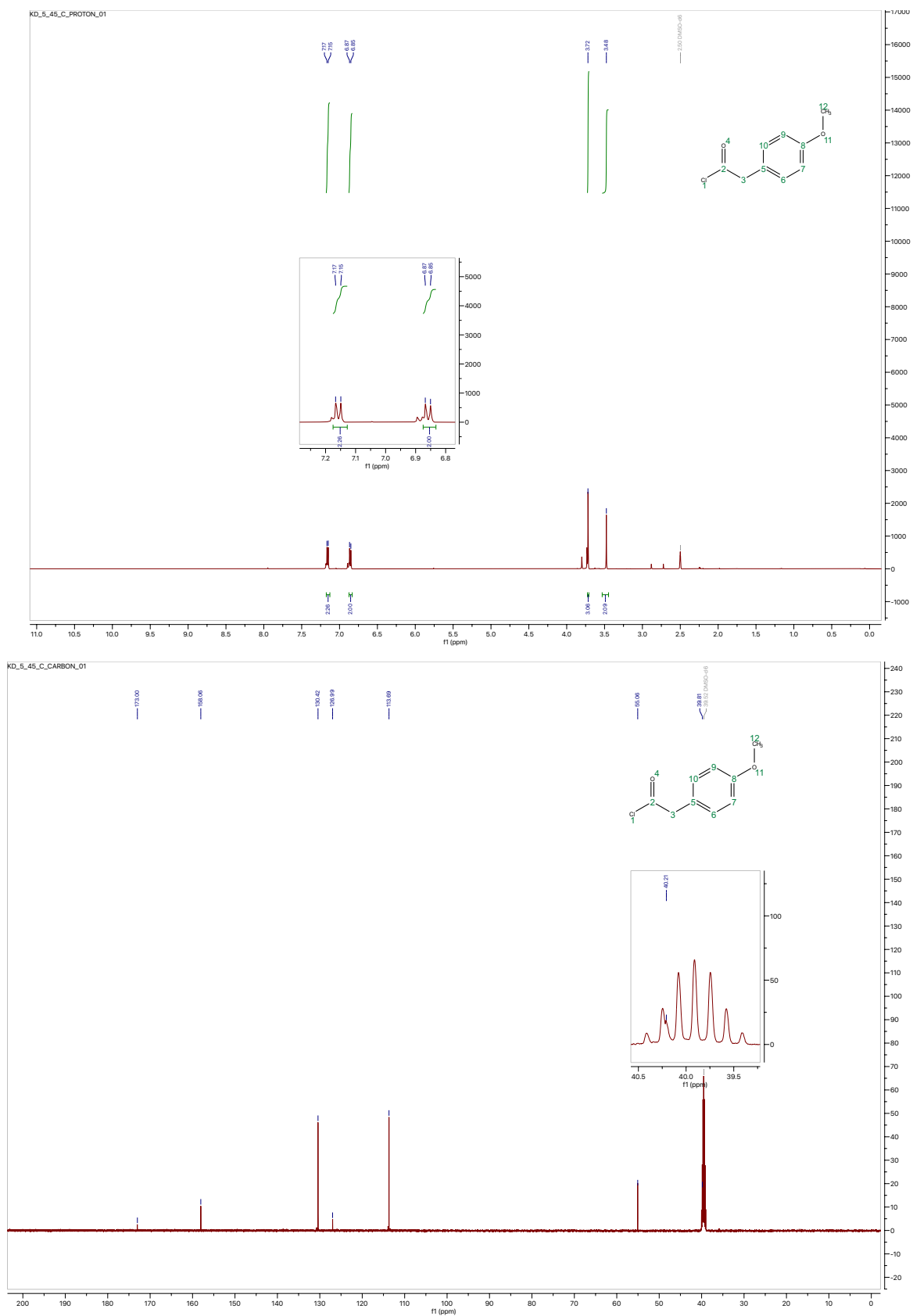


Figure 3.7. ^1H NMR and ^{13}C NMR spectra of compound 3-14.

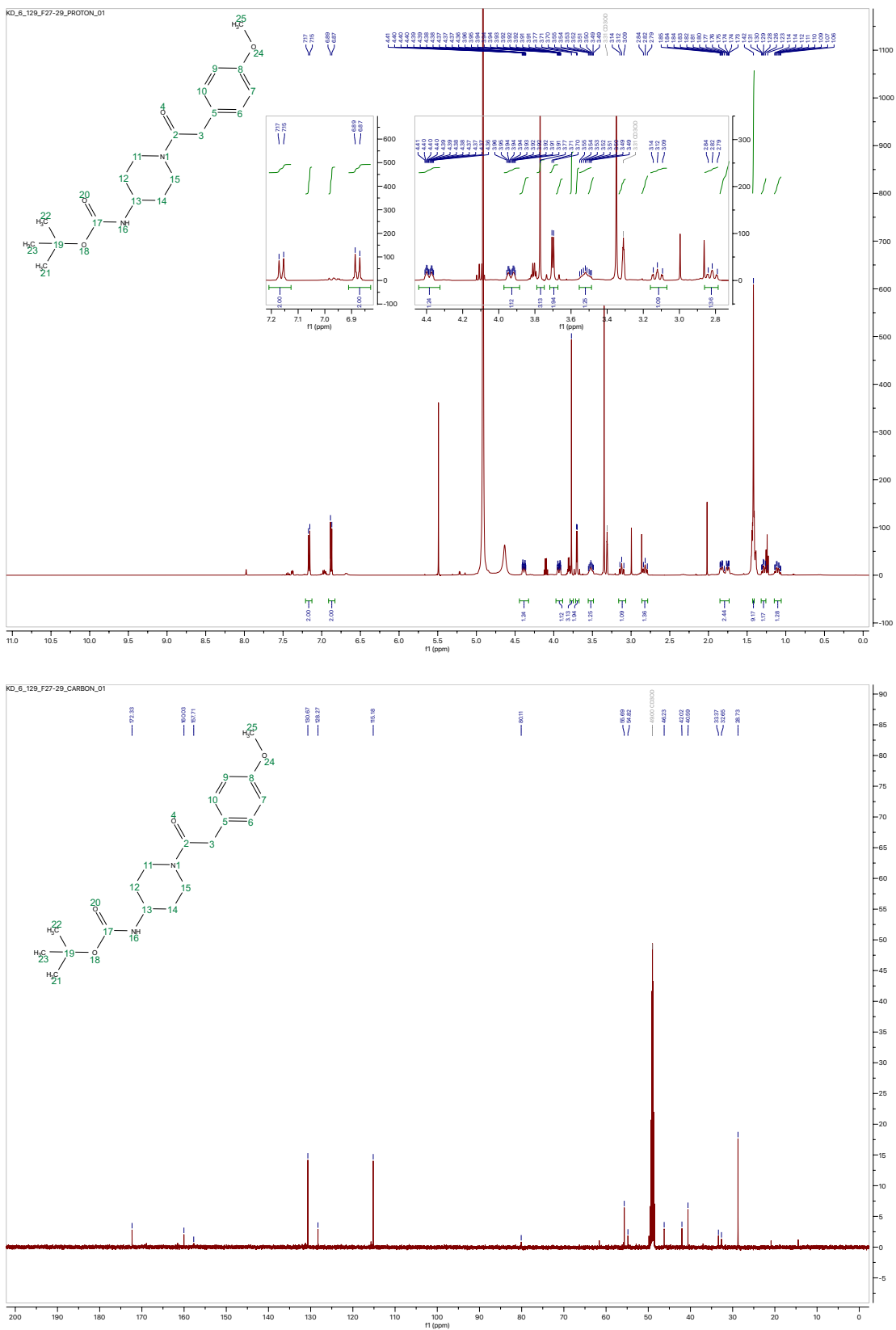


Figure 3.8. ^1H NMR and ^{13}C NMR spectra of compound 3-15.

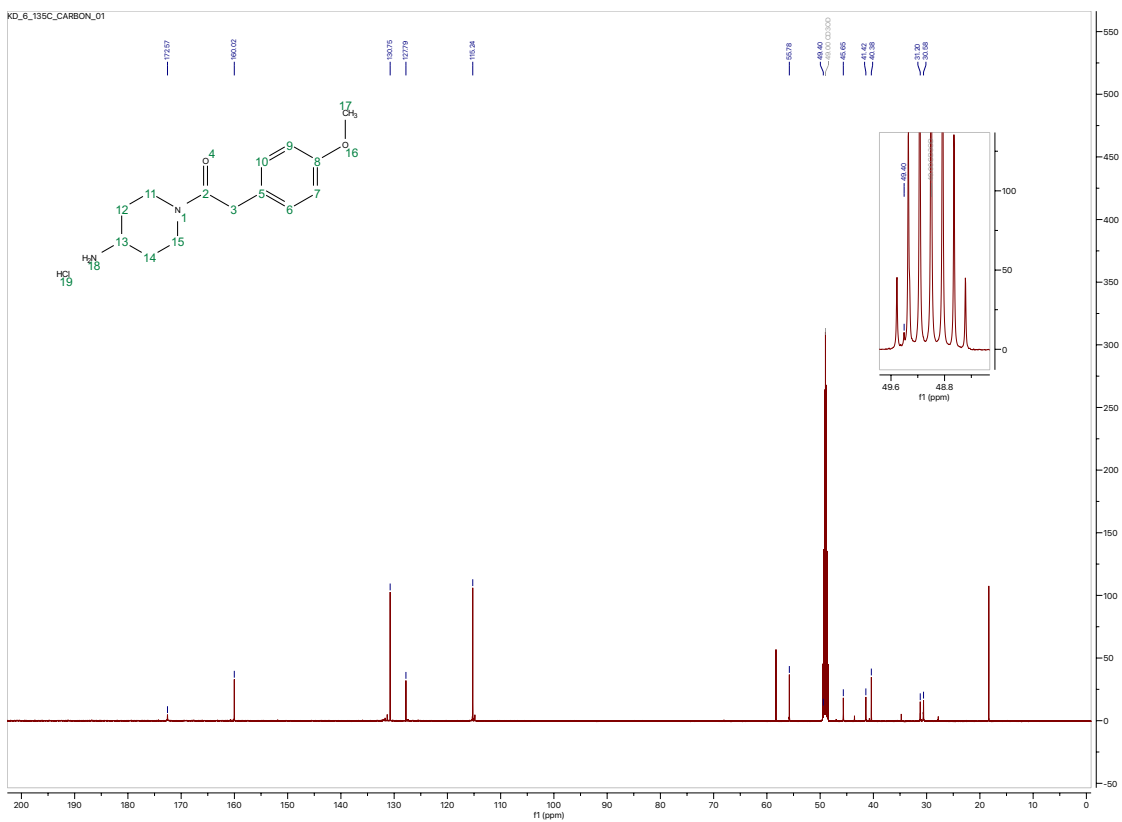
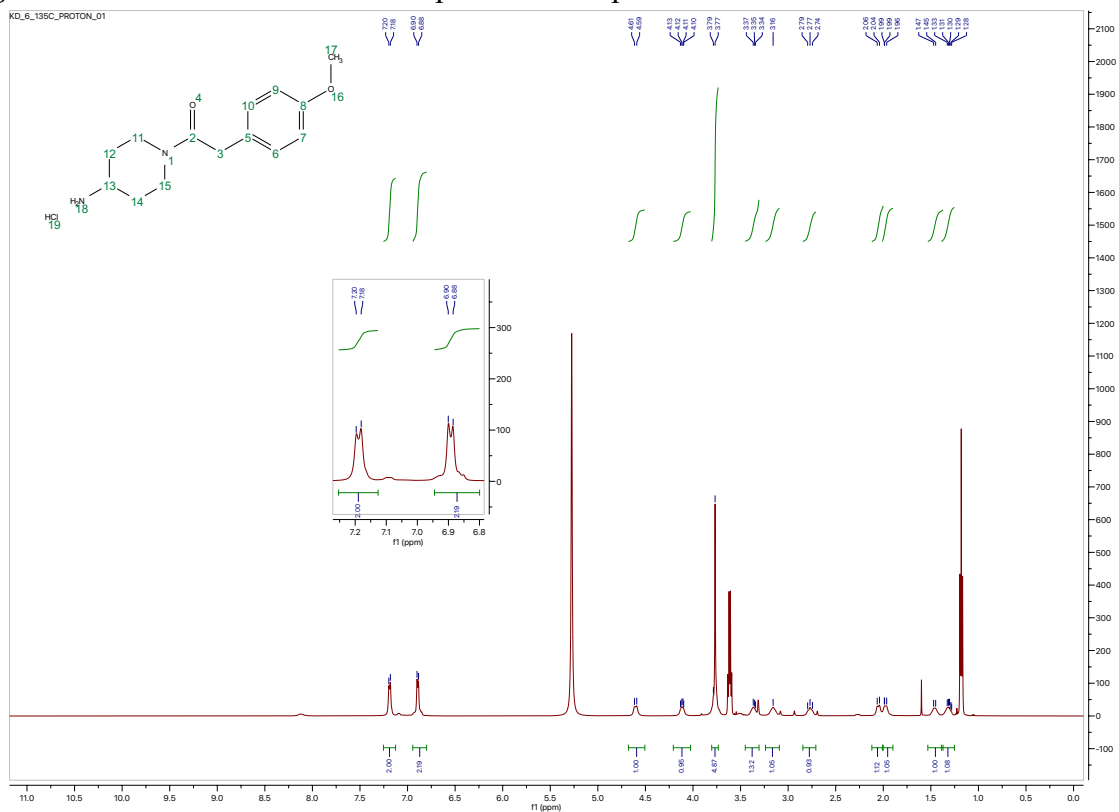


Figure 3.9. ^1H NMR and ^{13}C NMR spectra of compound 3-16.

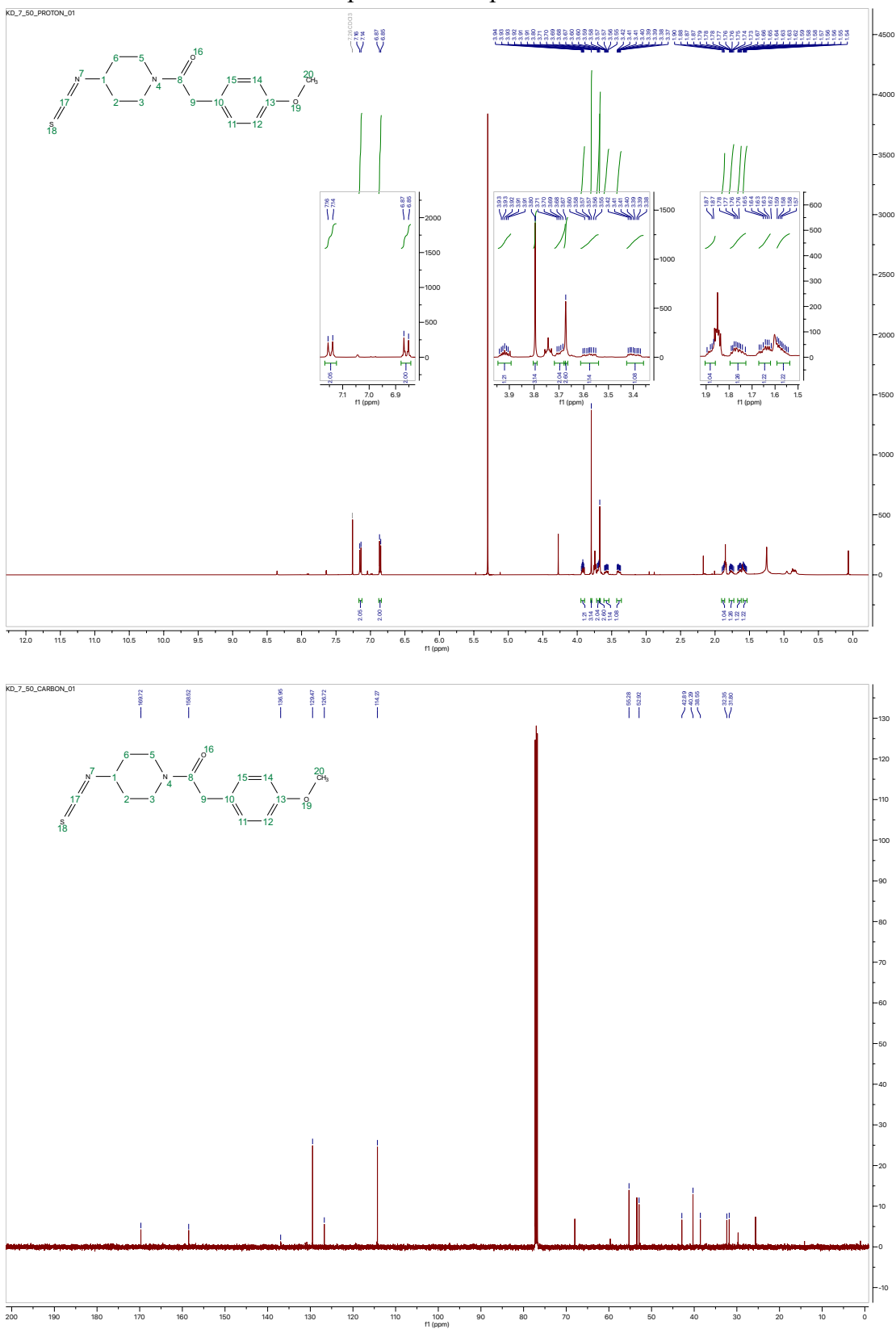


Figure 3.12. ^1H NMR and ^{13}C NMR spectra of compound 3-17.

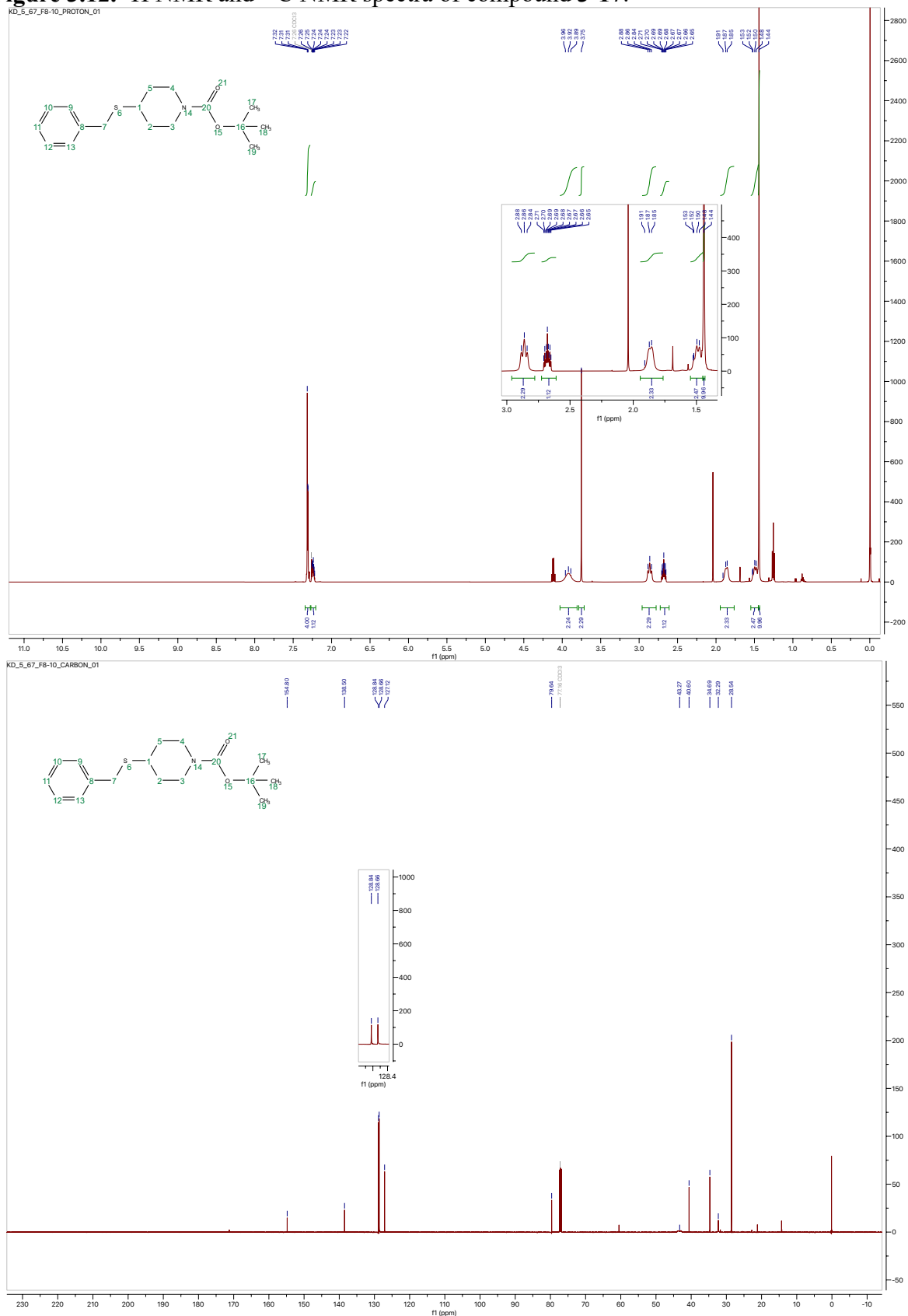


Figure 3.13. ^1H NMR and ^{13}C NMR spectra of compound 3-18.

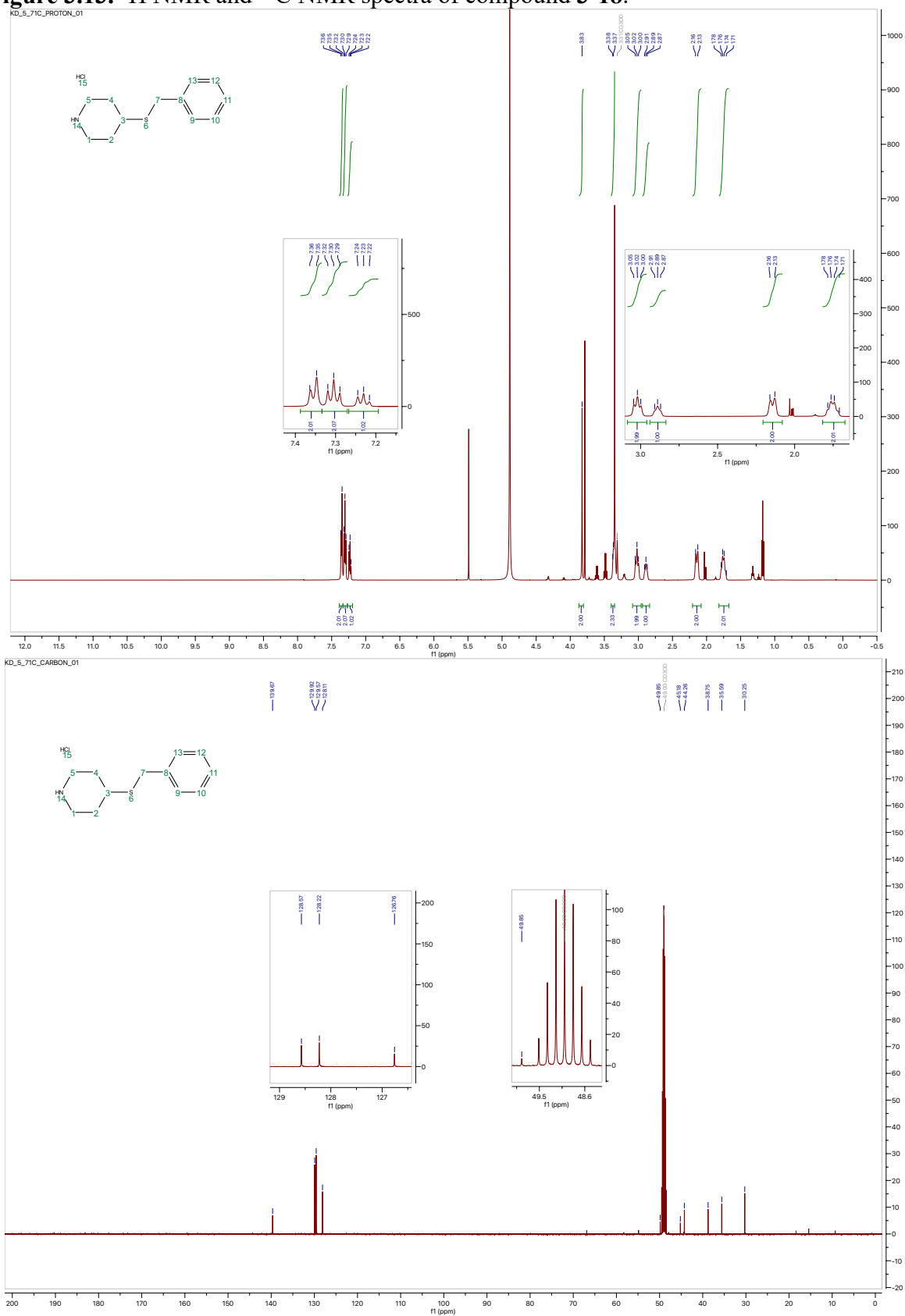


Figure 3.16. ^1H NMR and ^{13}C NMR spectra of compound 3-21.

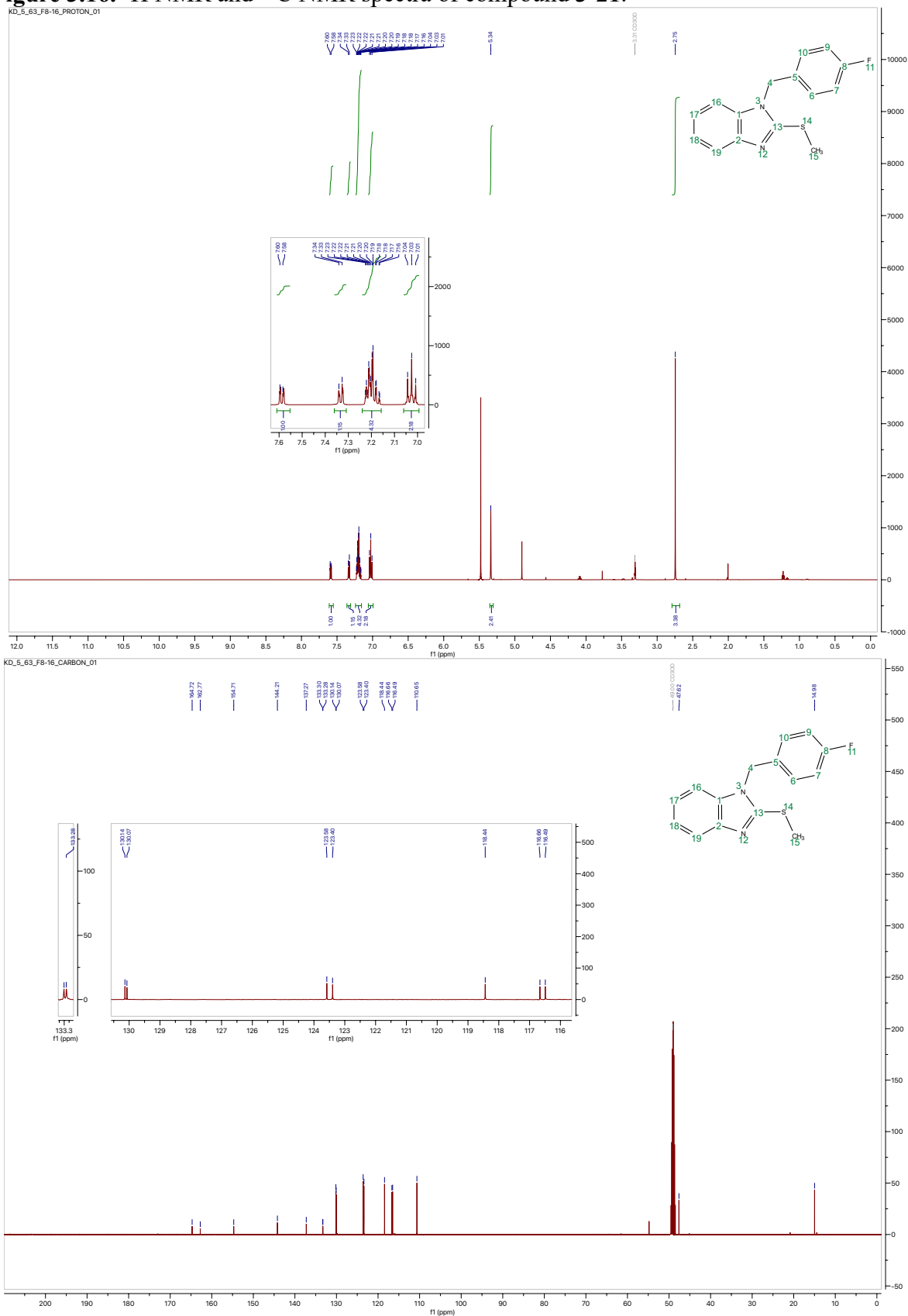


Figure 3.18. ^1H NMR and ^{13}C NMR spectra of compound 3-22.

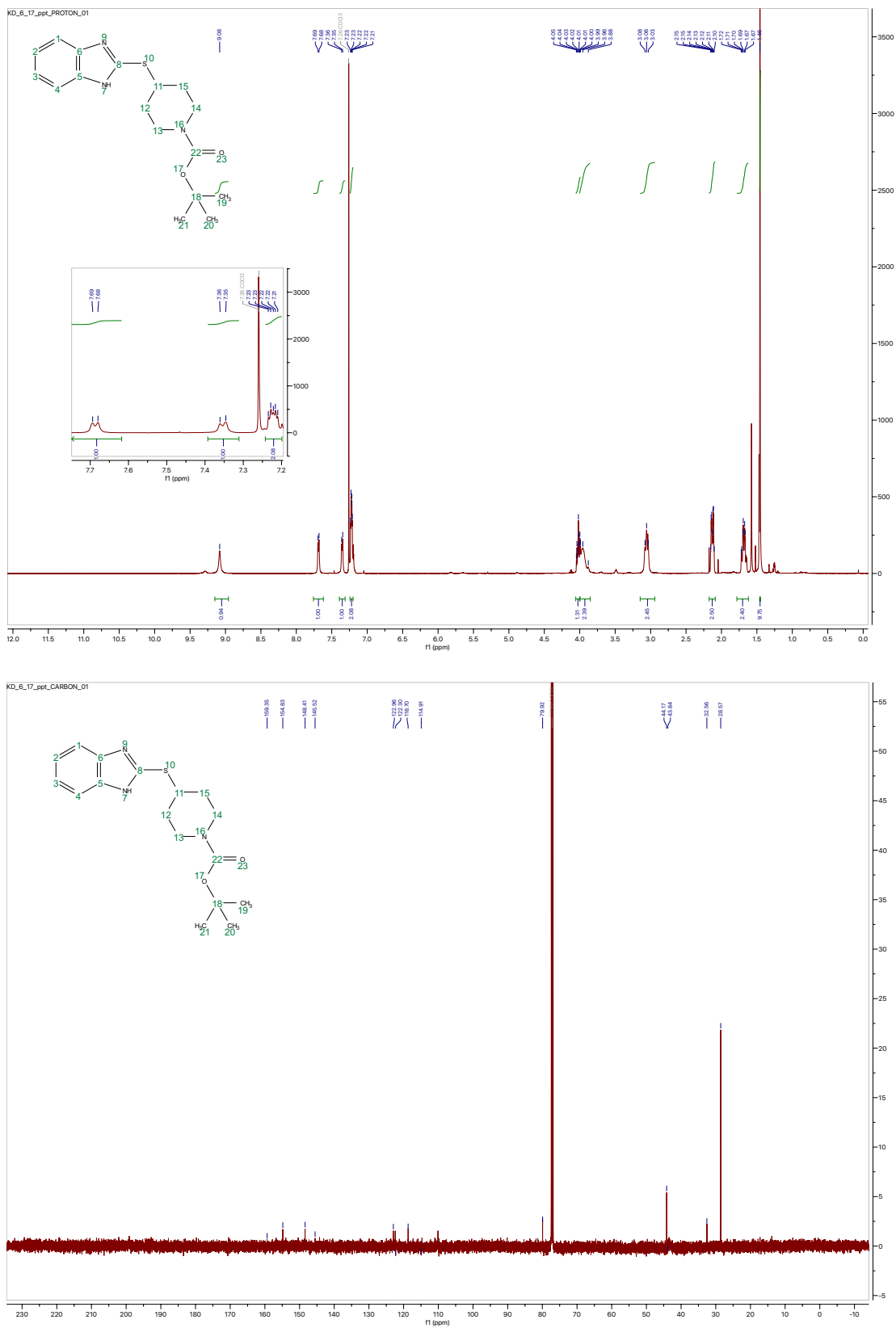


Figure 3.19. ^1H NMR and ^{13}C NMR spectra of compound 3-23.

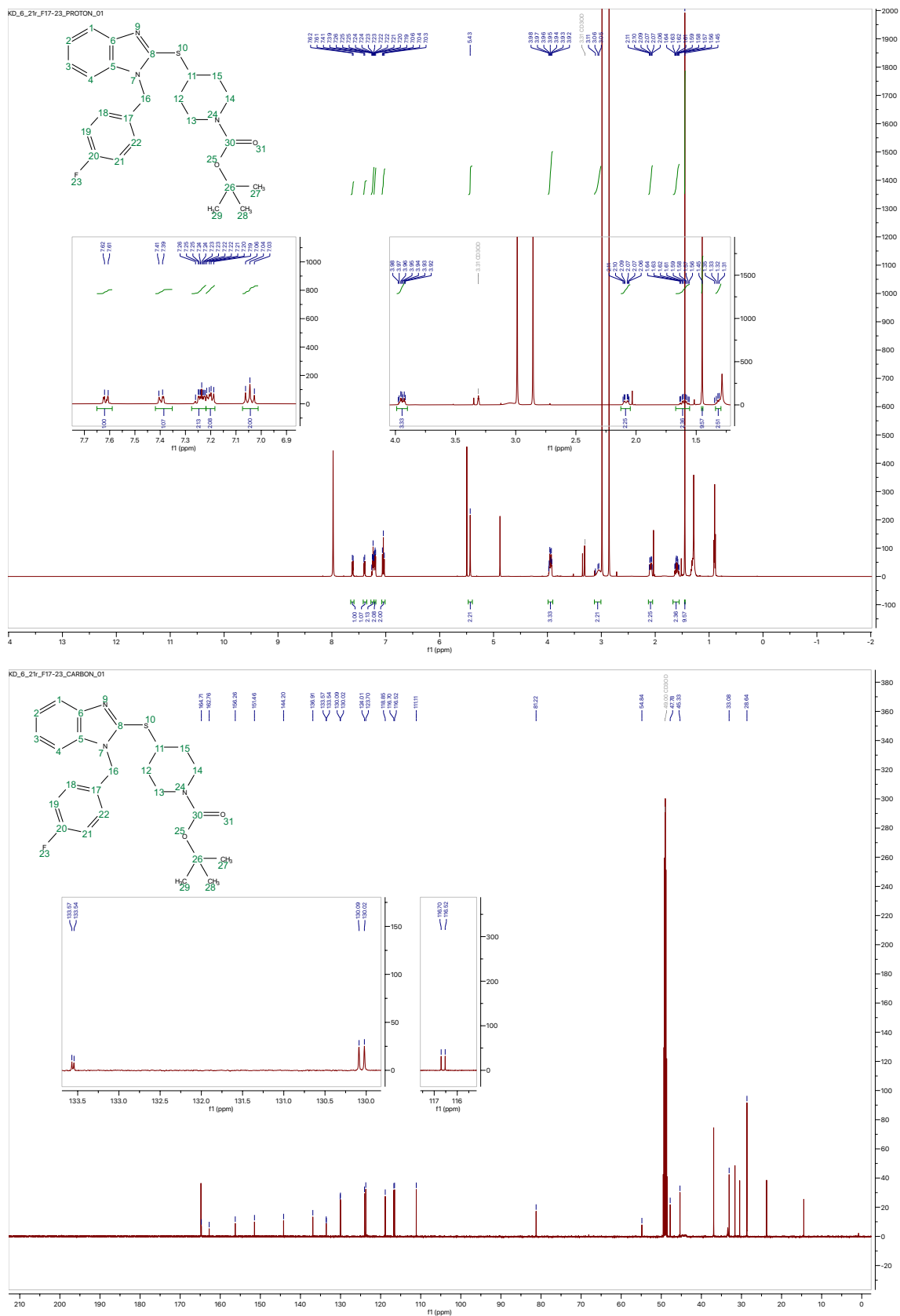


Figure 3.20. ^1H NMR and ^{13}C NMR spectra of compound 3-24.

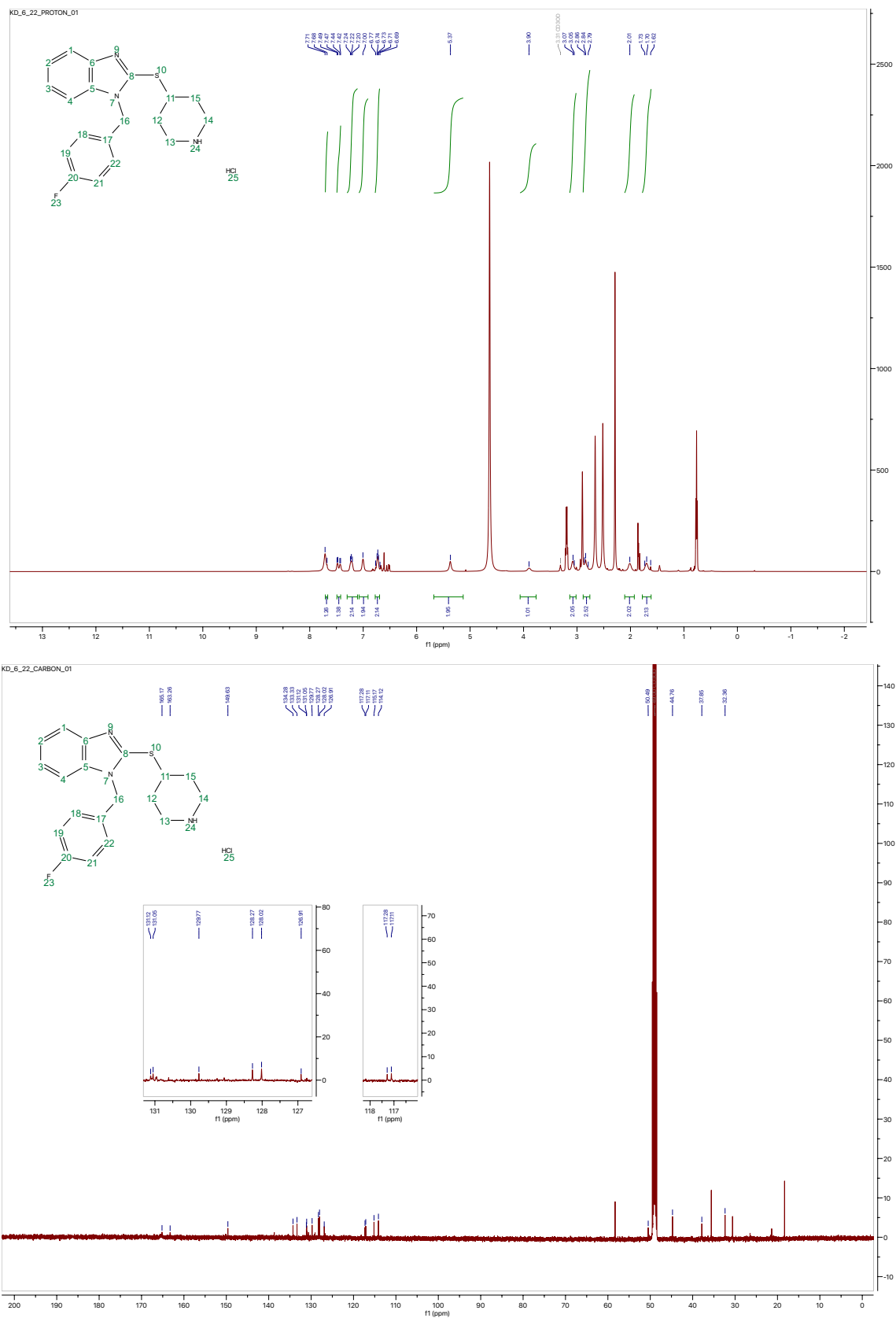


Figure 3.21. ^1H NMR and ^{13}C NMR spectra of compound 3-25.

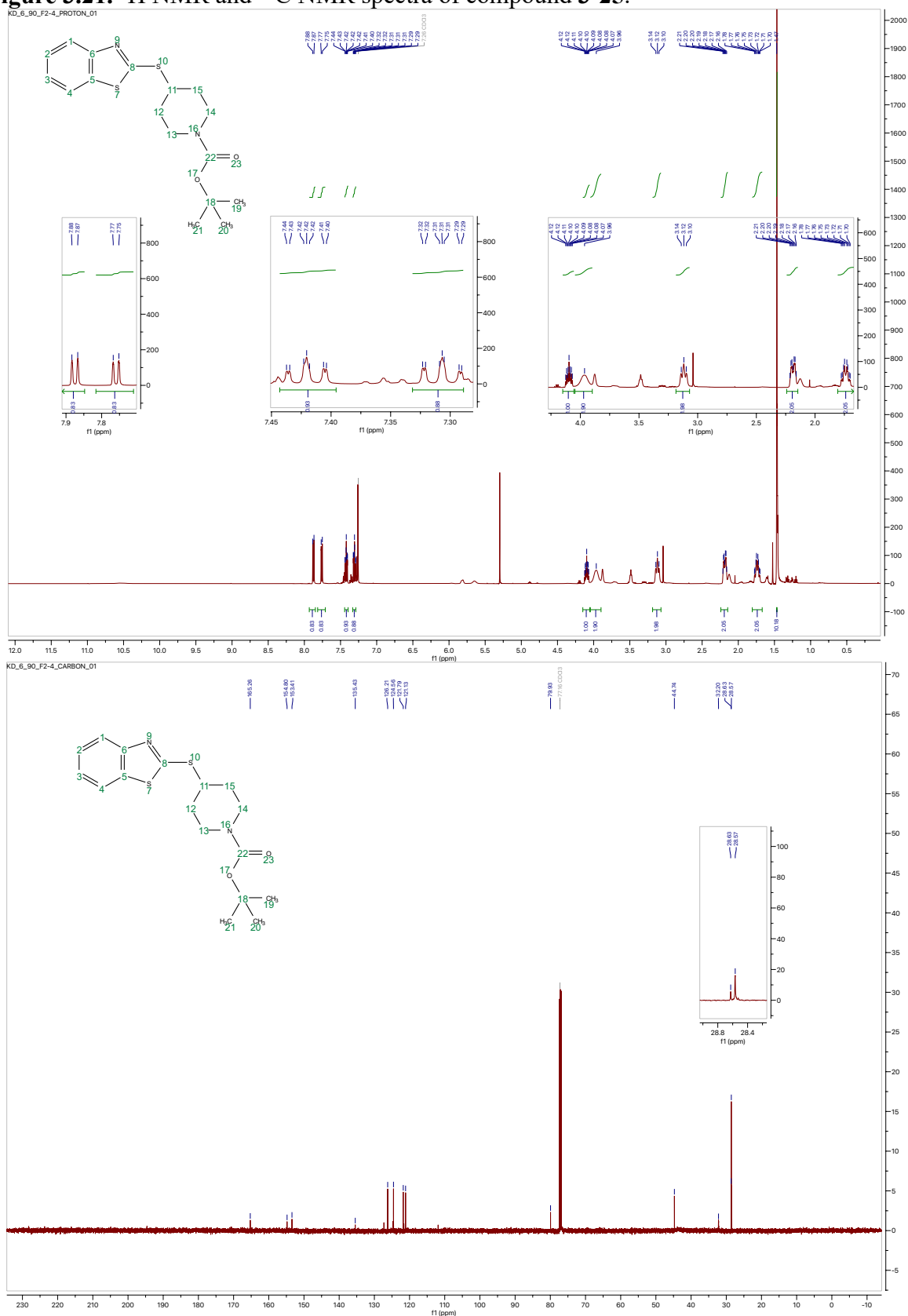


Figure 3.23. ^1H NMR and ^{13}C NMR spectra of compound 3-5.

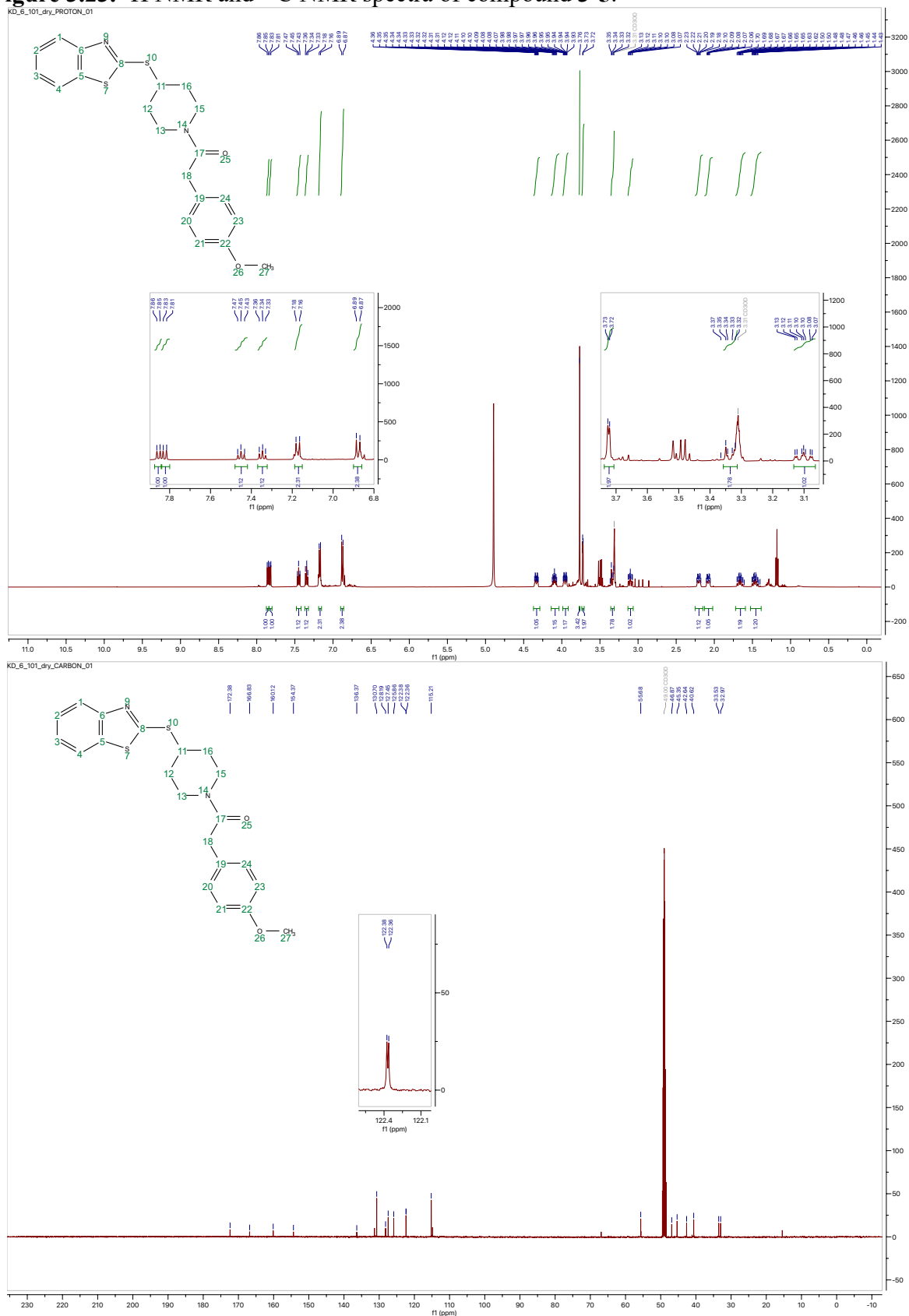


Figure 3.26. ^1H NMR and ^{13}C NMR spectra of compound 3-28.

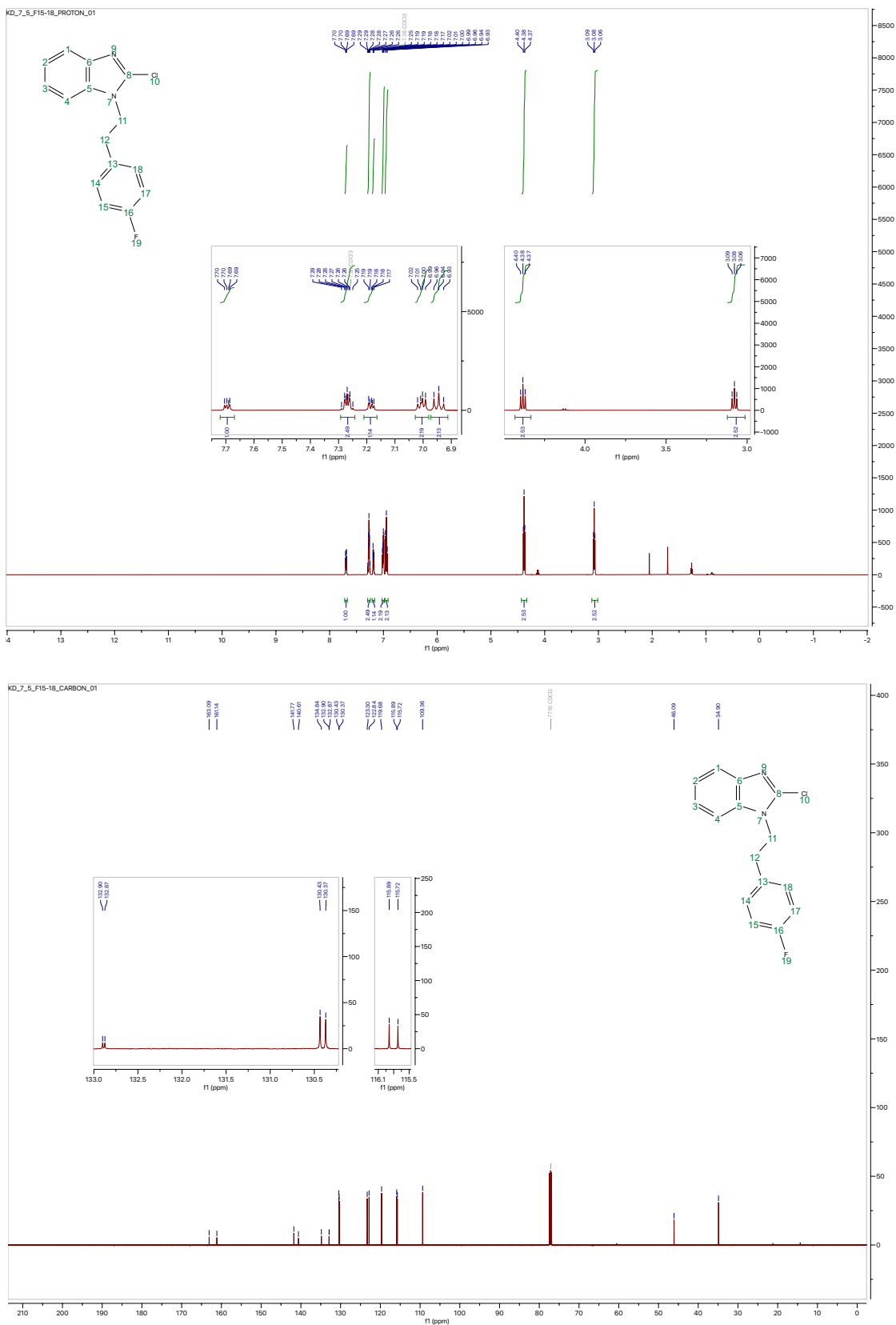


Figure 3.27. ^1H NMR and ^{13}C NMR spectra of compound 3-29.

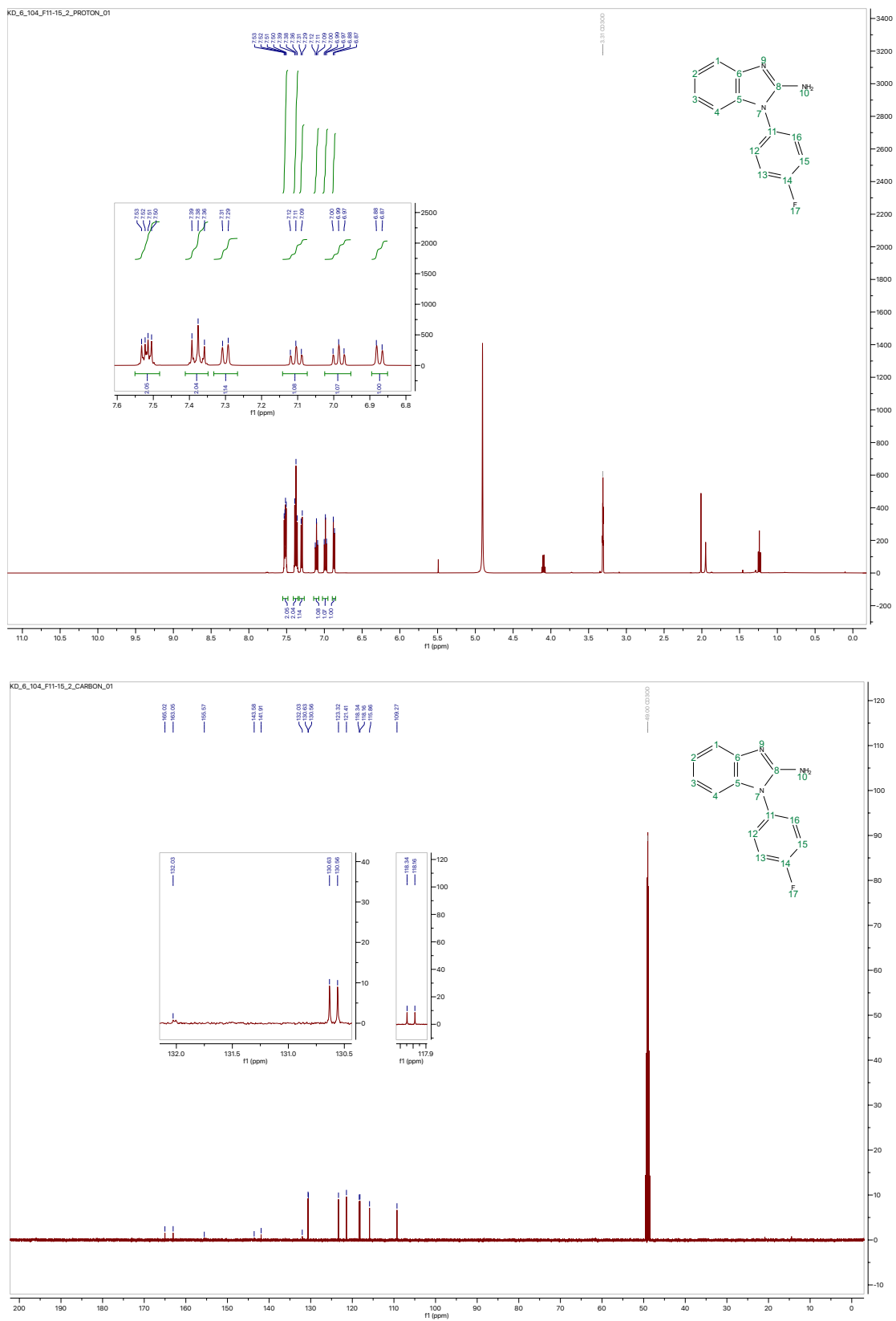
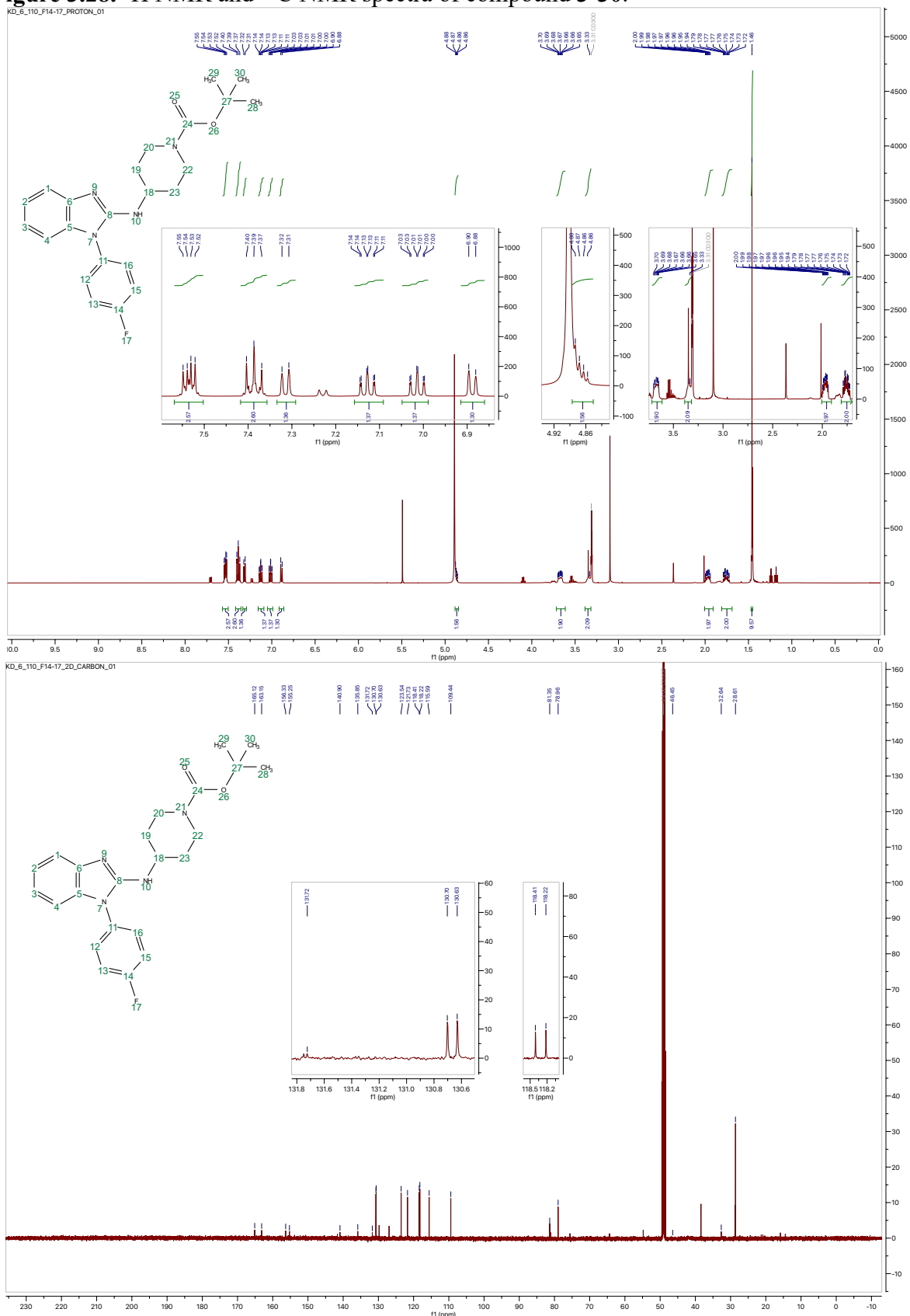


Figure 3.28. ^1H NMR and ^{13}C NMR spectra of compound 3-30.



Chapter 4: Conclusions and Future Works

To conclude, this thesis covers the work that I completed while in the graduate program in Dr. Jetze Tepe's lab at Michigan State University. My work has focused on the application of nitrogen-containing heterocycles in the total synthesis of bis- and tris-indole natural products and in the design and synthesis of small molecule acyl Astemizole analogues to be explored as 20S proteasome modulators.

Progress toward the total synthesis of Tulongicin and its related bis-indole natural product analogues, including the associated challenges of various synthetic approaches, were discussed. Though incomplete, the results of these studies have provided valuable insights to, hopefully, allow for future achievement in the total syntheses of Tulongicin and its related analogues. Currently, further research building upon these findings toward the first total synthesis of Tulongicin is underway in the Tepe lab. Future work for the potential continuation of this project would not only include the synthesis of Tulongicin and its related Bis-indole natural products but would also include further exploration of their biological activities, which remain largely unknown.

Lastly, the design and synthesis of a small library of acyl Astemizole analogues, in collaboration with Dr. Allison Vanecek, was discussed. Several of these analogues displayed potent 20S proteasome activity, which has provided valuable insight into the relationship between multiple structural moieties of acyl Astemizole and its biological activity. The findings of these studies will be useful in future analogue development, as acyl Astemizole remains a promising target in the Tepe lab. In particular, the 4-fluorobenzyl group of acyl Astemizole was identified as very important for its biological activity. These findings inspired the design of several novel acyl Astemizole analogues. As future work for this project, these novel analogues

could be synthesized and tested for 20S proteasome activity to further explore the structure-activity relationship of acyl Astemizole.